2012

Lipid Production from a Louisiana Native Chlorella vulgaris/ Leptolyngbya sp. Co-culture for Biofuel Applications

Rong Bai
Louisiana State University and Agricultural and Mechanical College

LIPID PRODUCTION FROM A LOUISIANA NATIVE *CHLORELLA VULGARIS*/ *LEPTOLYNGBYA SP.*CO-CULTURE FOR BIOFUEL APPLICATIONS

A Dissertation

Submitted to the Graduate Faculty of the
Louisiana State University and
Agricultural and Mechanical College
in partial fulfillment of the
requirements for the degree of
Doctor in Philosophy

in

The Department of Chemical Engineering

by
Rong Bai
B.S., Dalian University of Technology, 2007
May 2013

ACKNOWLEDGEMENTS

First and foremost, I would like to thank my advisor Dr. Michael Benton and co-advisor Dr. Kelly Rusch for giving me a great opportunity to work on this project. I would also like to thank Dr. Maria Teresa Gutierrez-Wing. These three professors provided me with the guidance, encouragement and support I needed in my graduate studies as well as the completion of this dissertation. I also want to thank my advisory committee members, Dr. Martin Hjortsø, Dr. Ioan Negulescu, Dr. Padmanabhan Sundar and Dr. James Henry for their time and valuable suggestions in my academic research. I would like to thank National Science Foundation (NSF – CBET #0853483) for supporting this research.

I greatly appreciate the help from Dr. Kerry Dooley for offering the gas chromatograph and the untiring guidance while using gas chromatography. I also want to thank Dr. Joan King for offering another gas chromatograph and Dr. Alfredo Prudente for his help to set up the machine. My sincere thanks also go to Dr. Ying Xiao from Department of Biology, LSU for her help in taking SEM, TEM images for the biological samples, Dr. Dongmei Cao from Material Characterization Center for her help in XPS and SEM characterization of the nano-materials and Dr. Lee Madsen from LSU AgCenter for the assistance in using the calorimeter.

I would also like to thank my lab mates Athens Silaban, Marjan Mohtashamian and fellow graduate students John Tate, Zenghui Zhang, Barrett Ainsworth, Courtney Lane and Kevin Chenier for their help and encouragement throughout my graduate study. Many thanks to the undergraduate students and student workers: Scott McLennan, Jonathan Delatte, Diana Osorio, Aaron Smith, Daniel Sobie, Olivia LeBlanc and Todd Crawford for their help with the lab work.

I am greatly appreciative of all the help from the supporting staff in Department of Chemical Engineering: Paul Rodriguez, Joe Bell, Darla Dao, Melanie McCandless, Melissa Fay, Danny Fontenot and Robert Willis.

Last but not the least, many thanks go to my parents for their unconditional love and support. I cannot imagine completing the graduate study and dissertation without their encouragement. My thanks also go to my good friends Shivkumar Bale, Imran Chiragh and my roommate Qiang Sheng for their support and friendship throughout the six years of my graduate study.

TABLE OF CONTENTS

LIST OF FIGURES

LIST OF TABLES

ABSTRACT

Over the last several decades, microalgae have garnered great interest for biofuel production mainly due to the high lipid productivity and minimum land competition with food crops. In this research, a Louisiana native *Chlorella vulgaris*/*Leptolyngbya sp.* co-culture was selected for lipid production. The goal of this work is to improve the lipid productivity and lipid composition of this co-culture via optimizing irradiance and nitrogen levels, lipid extraction method and modeling of pilot photobioreactor (HISTAR). Effects of irradiance and nitrate nitrogen levels on total lipid yield, neutral lipid portion, and fatty acid profile of non-aerated and aerated co-cultures were investigated in bench top scale experiments. The maximum lipid productivities were ~17 and 116 mg $L^{-1}d^{-1}$ for non-aerated and aerated cultures respectively. The optimal nitrogen level was 2.94 mM and the optimal irradiance was in the range of 400 and 800 μmol m^{-2} s^{-1}. Neutral lipids comprised approximately 75% of total lipids for non-aerated culture and 89% for aerated cultures. The major fatty acid components were 16- and 18-carbon fatty acids, and ~35% are saturated fatty acids. The fatty acid profiles did not vary significantly with the irradiance and nitrate nitrogen levels. A method using silver nanofibers to enhance the lipid extraction efficiency was investigated. Silver nanoparticles were added to disrupt microalgal cell walls to improve the lipid extraction efficiency of Folch's method and microwave assisted lipid extraction. The results showed that 1000 μg g^{-1} silver nanofibers had the most significant improvement in the efficiency of lipid extraction (~30% and 50% increase in efficiency for Folch's method and microwave assisted lipid extraction respectively). Microwave assisted lipid extraction was the optimal method, considering both fatty acid profile and lipid extraction efficiency. For the modeling of HISTAR system, Steele's model was used for impact of irradiance and Monod model was used for the effects of nitrogen. The final model was able to

predict the trend of lipid percentage increase with limited nitrogen level. The results of the simulations indicated the limited nitrogen constrained the lipid productivity despite of a higher lipid percentage. The results matched the conclusions of the experiments in bench top scale.

1. INTRODUCTION

1.1. Background of Microalgal-based Biofuels

On December 19 2007, the Energy Independence and Security Act of 2007 (EISA 2007) was signed into the law. Under the management goals of EISA 2007, the Renewable Fuel Standard (RFS) requires 136 billion liters of renewable fuel, including 79.5 billion liters of advanced biofuel (i.e., non-corn ethanol), to be produced in the U.S. by 2022. For several reasons, microalgae are considered one of the most promising advanced biofuel feedstocks for meeting the RFS (DOE, 2010). First, microalgae theoretically exhibit 10-100 times higher energy yield per unit area than traditional oil plants (Greenwell et al., 2010; Chisti, 2007) (Table 1.1). Second, microalgae are able to be cultivated on non-arable land, thus avoiding land competition with food crops (Johnson and Wen, 2010). Third, microalgae-based biofuel

Table 1.1. Productivity comparison of some biodiesel feedstock sources from (Chisti 2008).

Crop	Oil yield (L ha^{-1})	Land area needed (M ha)[a]	Percent existing US cropping area
Corn	172	1540	846
Soybean	446	594	326
Canola	1190	223	122
Jatropha	1892	140	77
Coconut	2689	99	54
Oil Palm	5950	45	24
Microalgae[b]	136,900	2	1.1
Microalgae[c]	58,700	4.5	2.5

[a] For meeting 50% of all transport fuel needs of the United States
[b] 70% oil (by wt) in biomass
[c] 30% oil (by wt) in biomass

production is environmentally friendly (Ahmad et al., 2011) because of low carbon emission (Chisti, 2007) and minimal sulphur dioxide and nitrous oxide emissions in comparison to petroleum-based diesel (Mutanda et al., 2011; Li et al., 2008a). Last, other valuable bio-products

such as bioplastics (Samantaray and Mallick, 2012; Sharma et al., 2007; Wu et al., 2002), pigments (Bai et al., 2011; Del Campo et al., 2007; Chaumont and Thepenier, 1995) and omega-3 fatty acids (Adarme-Vega et al., 2012; Chi et al., 2009; Singh et al., 2005) can be obtained from microalgal biomass, partially offsetting the biofuel production cost.

The idea of using algal fuel first arose in the 1950s (DOE, 2010). The U.S. Department of Energy has invested $25 million on the "Aquatic Species Program" (1978-1996) since the 1970s to develop algal based transportation fuels (Sheehan et al., 1998). Over the last several decades, microalgae have been converted into various types of biofuels, such as biodiesel, bio-hydrogen, methanol etc. (not at the industrial level) (Ghasemi et al., 2012). Numerous studies have been carried out on almost all aspects of microalgal biofuel production (Figure1.1), including strain selection (e.g., Mata et al., 2010; Yoo et al., 2010; Rodolfi et al., 2009; Chisti, 2007), cultivation design (e.g., Ketheesan and Nirmalakhandan, 2011; Zimmerman et al., 2011; Posten, 2009; Rusch and Christensen, 2003; Sukenik et al., 1991), biomass dewatering and harvesting (e.g., Pearsall et al., 2011; Vandamme et al., 2011; Uduman et al., 2010), and lipid extraction (Cooney et al., 2009; Cheung et al., 1998). However, technical issues, which are mainly divided into three categories including feedstock (algal biology, algal cultivation and harvesting and dewatering),

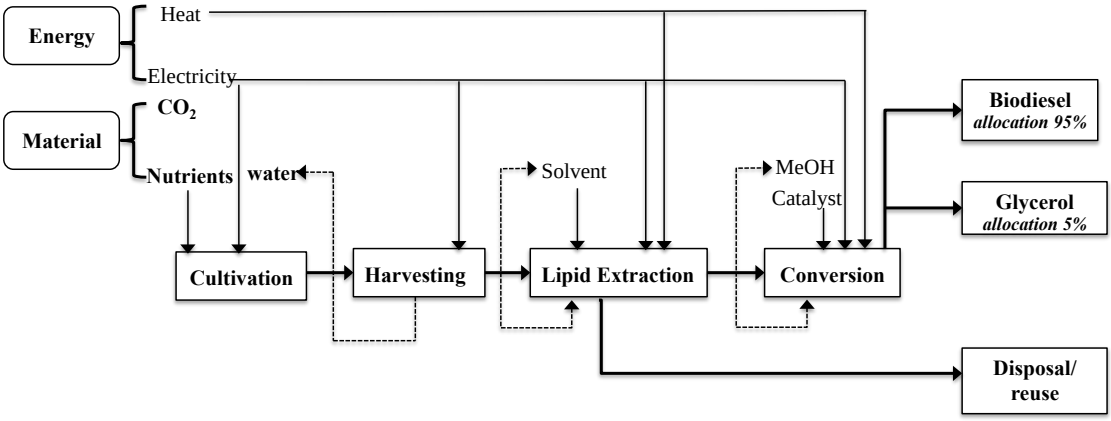

Figure 1.1. System flow-chart of a potential microalgal biofuel production, adapted from Brentner et al. (2011).

conversion (extraction and fractionation, fuel conversion and co-products) and infrastructure (distribution and utilization, resourcing and siting) remain significant and prevent microalgal biofuel from commercial feasibility (Davis et al., 2012; DOE, 2010).

The cost of microalgal biodiesel production is projected at \$2.60 L^{-1} (\$9.84 gal^{-1}) for open ponds and \$5.42 L^{-1} (\$20.53 gal^{-1}) for closed photobioreactors (Davis et al., 2011), far more expensive than the petro-based fossil fuels. To compete with the fossil fuels, the production cost and energy consumption for microalgal biofuel production has to be reduced and long-term research effort will be required (Pienkos and Darzins, 2009). Nevertheless, concerns of integrating the fuels especially into existing infrastructure is another factor limiting the economic viability of microalgal biofuels. Compared to petrodiesel, which is mainly comprised of saturated hydrocarbons, biodiesel usually contains higher percentage of unsaturated fatty acids (Tyson, 2001). Higher unsaturated fatty acid content has been reported to induce the corrosion behavior on metals, such as those comprising current fossil fuel distribution infrastructures due to moisture absorption, microbial oxidation and other contamination (Lee et al., 2010a; Kaul et al., 2007). Therefore, the fatty acid profile of microalgae should be investigated. Prevention and control strategies have to be prepared to reduce the impact of microalgal biofuels on the existing infrastructure. Market demand can significantly influence the economic viability of microalgal biofuels (Oltra, 2011). Similar to the first generation biofuels (i.e., biofuels from food crops such as corns, soybeans etc.) governmental tax policies and incentives are expected to play a critical role in expanding the market for microalgal biofuels (Oltra, 2011; Walls et al., 2011).

1.2. Literature Review

A brief review of the research that is relevant to microalgal biofuel production is presented in the following subsections. Additional literature review and discussion is included in each subsequent chapter.

1.2.1. Photosynthesis in Microalgae and Cyanobacteria

Microalgae and cyanobacteria are photosynthetic organisms that are capable of utilizing solar energy and converting water and CO_2 into biomass (Chisti, 2008). Thus, a fundamental understanding of photosynthesis is critical for microalgal biofuel production viability. Photosynthesis in plant cells is comprised of a series of reactions that occur mainly in the chloroplast (Nelson and Yocum, 2006). These reactions are divided into the light and dark reactions (stages). The light reactions mainly occur on thylakoid membranes, where H_2O is oxidized and ATP and NADPH synthesized. The dark reactions take place in stroma, in which ATP and NADPH are utilized to reduce CO_2 into organic carbon (Horton et al., 2002).

Five major complexes are involved in light reactions: light-harvesting antennae, photosystem II (PS II), photosystem I (PS I), cytochrome b6/f and ATP synthase (Richmond, 2004). The light-harvesting antenna is a pigment-protein complex captures light and transfers energy to photosystem I and II (PSI and PSII). For microalgae, the pigments presented in light-harvesting antenna include chlorophyll-a, chlorophyll-b and carotenoids. For cyanobacteria, additional accessory pigments including phycocyanin and phycoerytherin are presented. PSI and PSII are connected by a series of electron carriers to form the so-called "Z scheme" (Figure 1.2) (Horton et al., 2002). Cytochrome b6/f, which serves as an intermediary for the electron transport between the two photosystems, converts of redox energy into proton gradient used for ATP synthesis (Nelson and Yocum, 2006).

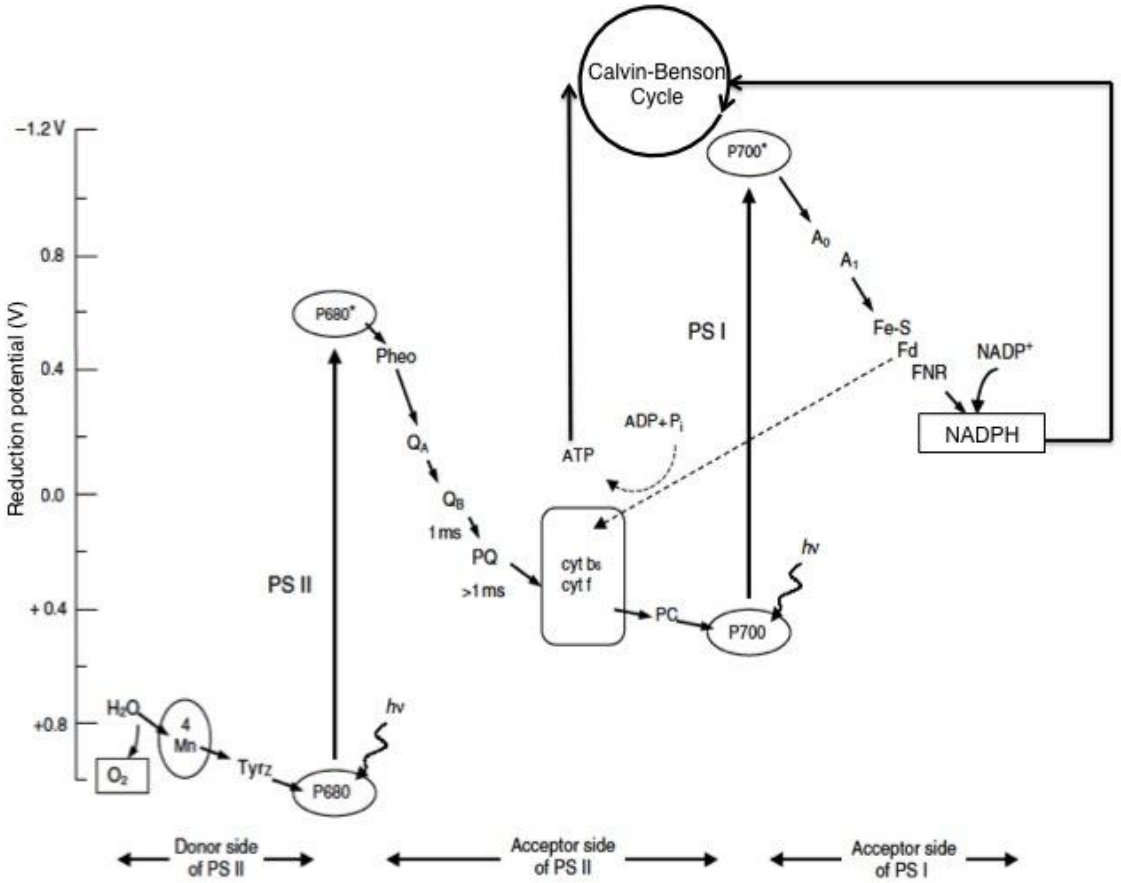

Figure 1.2. The Z scheme for photosynthetic electron flow from H_2O to NADPH from (Richmond, 2004).

When the photons are captured, the energy transferred to photosystem II reaction center (P680), which has an absorption maximum at 680 nm, and excites the P680 to the form with higher reductive energy level (P680*). P680* donates an electron to the electron carriers and becomes the oxidized form of P680 called $P680^+$. The reduction the strong oxidative agent P680 drives the water oxidation reaction, which provides the electrons for the light reactions. The donated electron goes through a series of electron carriers to produce ATP, which provides energy for dark reactions. Then the electron is passed to the reaction center of photosystem I (P700), which has a maximum absorption at 700 nm, and again gets excited by photons absorbed by PSI, resulting in the P700 of higher energy level (P700*). The P700* was oxidized by

donating an electron to the electron carriers. The electron was passed through the electron acceptors for PSI and ends up reducing the $NADP^+$ to NADPH, which provides H^+ for CO_2 reduction in the dark reactions.

Throughout photosynthesis, all of the energy accumulated in the cells originally comes from light. However, only the light in the wavelength range of 400-700 nm (photosynthetic available radiation (PAR)) is utilizable for photosynthesis (Richmond, 2004). Irradiance levels vary significantly in outdoor environments. Therefore, microalgal cells have developed several acclimation processes (mainly in photosystem II) to cope with these variations (Falkowski and Raven, 1997). In irradiance limiting situations, microalgal cells increase their photosynthetic efficiency by adjusting the composition and stoichiometry of the light harvesting antenna subunits for photosystem II to capture the photon flux more effectively (Bonente et al., 2012; Walters, 2005). The mobile light harvest complex (LHCII-L) in photosystem II can also migrate to photosystem I under low irradiance conditions to compensate for the imbalance of excitation between the two photosystems, which is caused by the difference of maximum absorption spectra between photosystem II and photosystem I (680 nm for photosystem II and 700 nm for photosystem I) (Wollman, 2001). However, these acclimation mechanisms cannot completely compensate for photon flux under low irradiance levels. The synthesis of NADPH and ATP in the light reactions can be significantly limited due to low excitation energy for photosystem II and photosystem I, resulting in low biomass and lipid productivity.

Cyanobacteria require little energy to maintain cell function and structure (Mur, 1983). Like microalgae, chlorophyll a, which mainly absorb in the red and blue range, is the major pigment for light harvesting in the cyanobacteria. However, the presence of phycobilins (Figure 1.3) in addition to chlorophyll in the light harvest antennae enables cyanobacteria cells to

effectively capture light in the range of 500-650 nm (green, yellow and orange), which is out of the range of absorption peaks of chlorophyll (665 and 465 nm for chlorophyll a; 647 and 460 for chlorophyll b) (Mur et al., 1999). Hence, the additional light energy harvested in the 500-650 nm range allows cyanobacteria to maintain a higher growth rate than microalgae under low irradiance conditions (Mur et al., 1999). Consequently, in a microalgal/cyanobacterial symbiotic co-culture, when the irradiance is significantly limited for the microalgae, cyanobacteria may be able to partially compensate for the decrease in microalgal growth rate and photosynthetic efficiency.

In oversaturated irradiance conditions, the numbers and sizes of light harvest complexes are reduced to prevent the absorption of excess excitation energy. Nevertheless, oversaturated as photon flux leads to the damage of the electron transfer chain in photosystem II and the production of reactive oxygen species (ROS), resulting in decreased photosynthetic rate (known

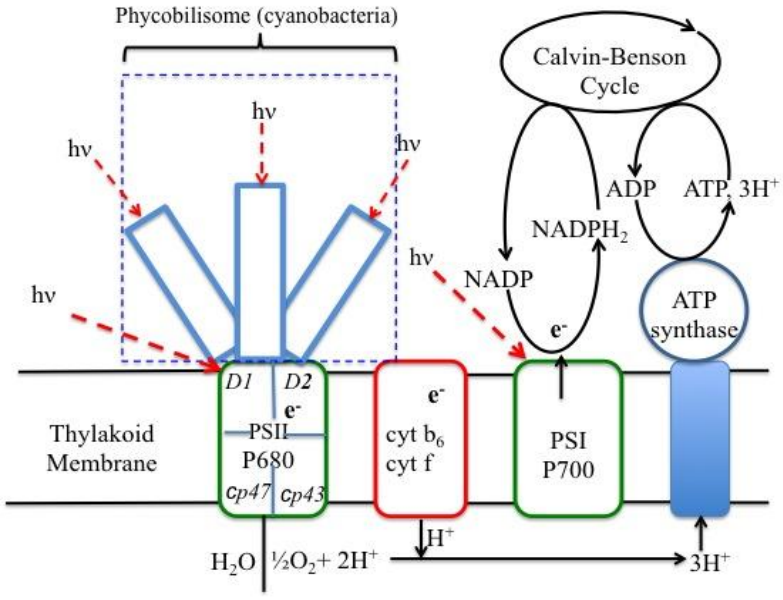

Figure 1.3. Schematic diagrams of light reactions of photosynthesis in microalgae/cyanobacteria. Phycobilisome only exists in cyanobacteria, adapted from (Horton 2002).

photoinhibiton) (Han et al., 2000; Goldman, 1979). Additionally, the recovery from photoinhibition, which involves the constant re-synthesis and replacement process of the D1 subunit for photosystem II (Melis, 1999), is highly energy demanding (Simionato et al., 2011) and may significantly affect the energy availability for biomass and lipid production. Therefore, finding the optimum irradiance level of a culture is critical for microalgal/cyanobacterial biofuel production.

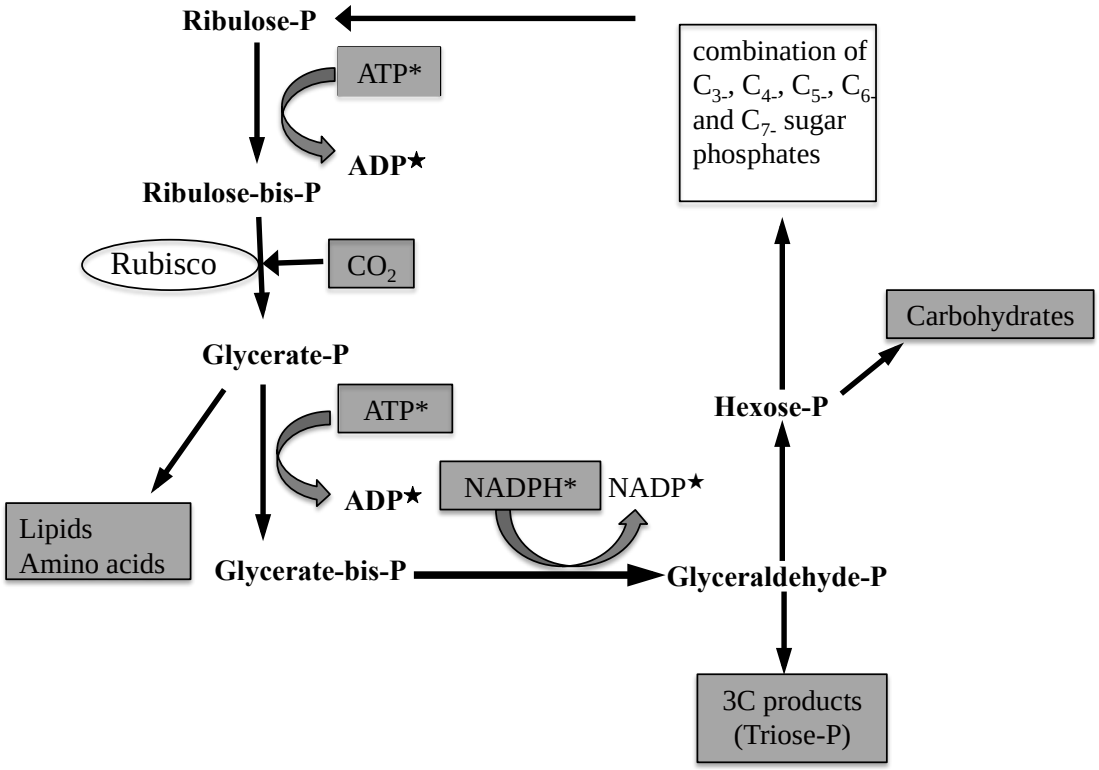

Figure 1.4. Calvin-Benson cycle, adapted from The (*) represents product from light reactions. The (★) represents the products going back to light reactions, from (Richmond, 2004).

The dark reactions are mainly comprised of the Calvin-Benson cycle (carbon assimilation) and photorespiration (Horton et al., 2002). The Calvin-Benson cycle includes four phases: carboxylation, reduction, regeneration and production (Richmond, 2004; Horton et al.,

2002) (Figure 1.4). In the carboxylation phase, one molecule of CO_2 reacts with one molecule of ribulose bisphosphate (Ribulose-bis-P) to form two molecules of phosphoglycerate (Glycerate-P) under the catalysis of ribulose bisphospate carboxylase/oxygenase (Rubisco). In the reduction phase, the Glycerate-P is first converted to Glycerate-bis-P by consuming the energy provided by ATP, and then Glcerate-bis-P is reduced to phosphoglyceraldehyde (Glyceraldehyde-P) by NADPH. Ribulose-P is regenerated through a series of reactions involving 3-, 4-, 5-, 6- and 7-carbon sugar phosphates in the regeneration phase for further CO_2 fixation. Multiple end products, including carbohydrates (primary product), fatty acids, amino acids etc., are generated.

Photorespiration is a process that oxidizes ribulose biphosphate in a series of reactions to generate serine, ammonia and CO_2 without any metabolic gain. In this process, O_2 competes with CO_2 for the same active sites of Rubisco (Horton et al., 2002). The shortage of Rubisco can significantly limit carbon fixation rate (Marcus et al., 2008). Thus, a high O_2/CO_2 ratio in the microalgal culture can suppress the CO_2 fixation and increase the waste of energy and organic carbon. In microalgal cultures, the O_2/CO_2 ratio can be minimized by aeration or mixing to release the accumulated O_2 and directly bubbling CO_2 through the culture.

1.2.2. Lipid Production Pathways

In phototrophic microalgal cells, lipid synthesis starts with the organic carbon generated in Calvin-Benson cycle. CO_2 is considered the sole carbon source for lipid synthesis. A schematic diagram of lipid synthesis was presented in Figure 1.5. In this pathway, there are mainly three precursors that lipid synthesis shares with other metabolic activities: acetyl-CoA, pyruvate and phosphatidic acid. Both acetyl-CoA and pyruvate are used for the citric acid cycle to provide energy for cell metabolism. Phosphatidic acid can be converted to either phospholipids for cell membrane structure or neutral lipids for energy storage.

The impact of nutrient deficiency especially nitrogen deficiency on lipid content in microalgae cells are most likely attributed to effects of nutrient limitation on the lipid synthesis pathway has been reported to significantly affect the lipid content in microalgal cells. When nitrogen is depleted the cell division and cell growth rates inevitably slow down due to the lack of nitrogen to support protein and enzyme synthesis (Sharma et al., 2012). Thus, the energy required for cell division and other metabolic activities decreases, resulting in lower requirements for the citric acid cycle, which provides the metabolic energy for the cells. Hence,

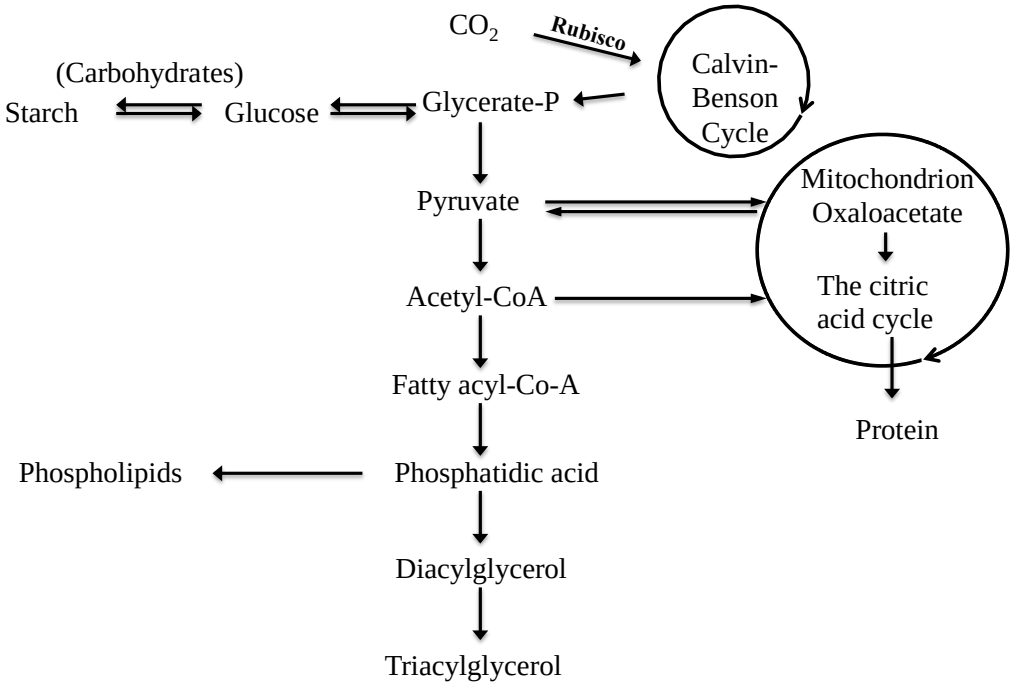

Figure 1.5. The pathways for lipid synthesis adapted from Deng et al. (2011). It starts from Glycerate-P produced in Calvin-Benson cycle. In the process, neutral lipid competes with TCA cycle for Acetyl-CoA and phosphate lipid for phosphatidic acid.

more Acetyl-CoA could be used for lipid production rather than being consumed in TCA cycle. Because of low cell growth and cell division, there is almost no requirement for the synthesis of membrane structures (Sharma et al., 2012), which are mainly comprised of phospholipids. Therefore, more phosphatidic acid is converted to diacylglycerol (DAG) and triacylglycerol

(Ruparelia et al., 2008) as opposed to phosphoslipids (major component of polar lipids), resulting in higher neutral lipid content and lower polar lipid content in the microalgal cells (Deng et al., 2011).

However, nitrogen limitation constrains cell division and biomass productivity, resulting in lower the overall microalgal lipid productivity. The most efficient culture conditions would utilize an optimal nitrogen level promoting maximum lipid productivity by compromising between biomass productivity and total lipid percentage (based on dry biomas, mass/mass). However, the impact of nitrogen limitation/starvation might be alleviated in a microalgal/cyanobacterial co-culture, since many cyanobacterial species have been reported for the ability of nitrogen fixation (Zehr, 2011; Lesser et al., 2007; Vyas and Kumar, 1995).

1.2.3. Impact of Fatty Acid Composition on Biodiesel

To produce biodiesel, the neutral lipids from microalgae are converted into fatty acid methyl ester (FAME) through a reaction known as transesterification. In this reaction, one molecule of triglyceride (main component of neutral lipids) reacts with three molecules of methanol to generate three molecules of FAME, which is the major component of biodiesel (Tyson, 2001). The properties of biodiesel such as cetane number, viscosity, and oxidation stability are determined by the composition of fatty acids that the FAME molecules are comprised of (Ramos et al.; Tyson, 2001). For example, high levels of saturated fatty acids increases the oxidation stability and cetane number for biodiesel (Tyson, 2001). Cardone et al. (2003) reported that the increase of linolenic acid (18:3) content could significantly reduce the oxidation stability of biodiesel.

To ensure the biodiesel produced from neutral lipids complies with the requirement of diesel engine, ASTM D 6751 (specifications for biodiesels blended with middle distillate fuels)

and EN 14214 (Automotive fuels. Fatty acid methyl esters (FAME) for diesel engines. Requirements and test methods) standards are most commonly used. However, these standards present the limits for the properties of biodiesel other than specific requirements for fatty acid profiles of the methyl ester (FAME). To correlated the fatty acid profiles to the technical standards, Ramos et al. (2009) developed a predictive relationship based on the fatty acid profile (% mass of saturated, monounsaturated, polyunsaturated fatty acids) and the EN 14214 standards. Based on Ramos' study, in order to meet the EN 14214 standards, the saturated fatty acids have to be in the range of 30~60% of total fatty acids (mass/mass) and 50% of the unsaturated fatty acids have to be monounsaturated.

The fatty acid profile of neutral lipid from microalgae has been reported to be species dependent (Roncarati et al., 2004; Brown, 1991; Benamotz et al., 1987), but it is also influenced by culture conditions (Rodolfi et al., 2009; Renaud et al., 1991; Piorreck et al., 1984). Rodolfi et al. (2009) reported effects of irradiance level and nitrogen deprivation on the fatty acid profile of *Nannochloropsis sp.* and found that higher irradiance level and low nitrogen level increased the C16 as well as C18 content in the fatty acid profile. Renaud et al. (1991) investigated the fatty acid composition of *Isochrysis sp*. under different irradiance levels, and observed significant changes in fatty acid composition when the irradiance increased from 620 to 1200 μmol m^{-2} s^{-1}. However no significant difference was shown between the irradiance level of 390 and 620 μmol m^{-2} s^{-1} in the study of Renaud et al. (1991). Piorreck et al. (1984) observed that the fatty acid composition of *Chlorella vulgaris* had a significant difference when the nitrate nitrogen level dropped from 10 mM to 0.30 mM. Therefore, investigation of the fatty acid profile of microalgae under various culture conditions should be conducted.

1.2.4. Microalgal Strain Selection

Strain selection is one of the most crucial steps for the commercial feasibility of microalgal biofuel production. Selection criteria include high growth rate, high lipid productivity, adaptability to local climatic conditions etc. (Mutanda et al., 2011). Numerous commercial microalgal strains such as *Botryococcus braunii*, *Nannochloropsis sp.*, and *Scenedesmus sp.*, have been reported to exhibit high lipid productivity under lab conditions (Hempel et al., 2012; Griffiths and Harrison, 2009; Rodolfi et al., 2009; Tran et al., 2009; John Sheehan, 1998). However, these commercially available strains are usually not robust enough to withstand the relatively harsh conditions in a large-scale outdoor culture system, and are often overtaken by invasive species from the local environments (DOE, 2010; Rodolfi et al., 2009; Sheehan et al., 1998). Additionally, the introduction of foreign microalgal strains poses potential risks to local environments (Campbell, 2011), since these strains can alter food webs (Scholin et al., 2000), displacing native phytoplankton and causing local extinction (Hallegreaff et al., 2003).

Genetic engineering has been applied to improve lipid accumulation in microalgal cells by either overexpressing genes involved in neutral lipid biosynthesis or inhibiting the pathways for starch biosynthesis (Li et al., 2010b; Courchesne et al., 2009; Wang et al., 2009). Additionally, random mutagenesis was used to generate microalgal strains with herbicide resistance (Cordero et al., 2011; Cohen et al., 1993). These strains are able to maintain high growth rates in herbicide enriched media, preventing contamination of other algal or cyanobacterial species. However, genetically modified strains are generally considered a potential threat to local ecosystems (Keri Carstens, 2011). Legal and social concerns will likely prevent the large-scale, outdoor culture of genetically modified organisms for biofuel production (de la Vega et al., 2011).

Native microalgal strains pose minimal risk for local environments. They are adapted to local water conditions, withstand local temperature variations, and most importantly, can resist competing microalgal species better than commercially available strains (Mutanda et al., 2011). Bhatnagar et al. (2011) reported the isolation of multiple native strains from industrial wastewater and observed a lipid productivity of 5 g m^{-3} d^{-1} in a 950 L raceway. Zhou et al. (2011) isolated 17 strains from a local water body in Minnesota and found five, *Chlorella sp.*, *Heynigia sp.*, *Hindakia sp.*, *Micractinium sp.*, and *Scenedesmus sp.*, with promising lipid production performance (74.5–77.8 g m^{-3} d^{-1}) in concentrated municipal wastewater. De la Vega et al. (2011) reported 89.7 g m^{-3} d^{-1} lipid productivity from a *Picochlorum sp.*, which was isolated from the Odiel River in southwest Spain. Collectively, these studies imply that isolating microalgal strains with high lipid productivity from local environments might be the optimal approach for strain selection in a large-scale cultivation system.

In natural environments, cyanobacteria are known to form symbiotic associations with a wide variety of organisms including microalgae (Rasmussen and Nilsson, 2003). The cyanobacteria provide multiple benefits to microalgae including lowering oxygen level in the culture, fixing nitrogen, providing growth factors and/or producing Fe, CO_2, NH_4^+, NO_3, or PO_4^{3-} (Graham and Wilcox, 2004). These benefits often induce higher growth rates of microalgae species in the symbiotic associate than in mono algal cultures. Ortiz-Marques et al. (2012) used *Azotobacter vinelandii* (diastrophic bacteria) mutant strain to form "artificial symbiosis" with microalgae. High oil-producing biomass was obtained by nitrogen and carbon fixation (Ortiz-Marquez et al., 2012). Rusch and Gutierrez-Wing (unpublished data) have isolated a Louisiana native *Chlorella vulgaris/Leptolyngbya sp.* co-culture, and discovered that the presence of *Leptolyngbya sp.* increased cell counts of *Chlorella vulgaris* approximately 20 times those of the

Chlorella vulgaris monoculture. Therefore, the idea of selecting naturally or artificially symbiotic microalgal/cyanobacterial (bacterial) co-cultures could be a viable option to enhance microalgal biofuel production.

1.2.5. Cultivation System for Microalgae and Cyanobacteria

The selection of the culture system has a significant effect on the cost effectiveness of microalgal biofuel production (Carvalho et al., 2006; Lee, 2001). A wide variety of microalgal cultivation systems have been reported for mass production (Xu et al., 2012; Barbosa et al., 2004; Morita et al., 2000; Trotta, 1981). These cultivation systems can be divided into three general categories: open ponds/raceway, closed photobioreactors and hybrid systems.

Currently, the mass production of microalgal biomass is usually done in open pond/raceway systems. The most commonly used open pond systems include raceway ponds, unmixed ponds, circulating ponds and thin layer inclined ponds (Singh and Dhar, 2011). Closed photobioreactors are used to minimize contamination and increase productivity (Singh and Dhar, 2011; Rodolfi et al., 2009; Sheehan et al., 1998). The advantages and disadvantages for open ponds and closed bioreactors have been summarized by Ghasemi et al. (2012) (Table 1.2). Although the biomass productivity of closed systems is considered much higher than the open systems, other factors, such as high capital costs, cleaning issues and cooling issues (Ghasemi et al., 2012; DOE, 2010), are preventing scalability of the closed bioreactor system for microalgal mass production. However, one of the most serious issues for open ponds is vulnerability to contamination and culture shift, both of which significantly limit the biomass productivity. The algal strains that have been cultivated successfully in the open ponds systems at industrial scale are limited to *Chlorella, Spirulina, Dunaliella* and *Haematococcus* which can tolerate highly alkaline or saline conditions (Chisti, 2007).

There is no absolute choice between open ponds and closed bioreactor systems. The best way to select a cultivation system is to evaluate it in conjunction with strain selection and other factors such as local weather conditions, water availability, harvesting techniques etc. However, hybrid systems, in which photobioreactor serves as feeder of high density inoculum culture to open pond/raceway, have been reported (DOE, 2010; Benson et al., 2007; Huntley and Redalje, 2007; Ben-Amotz, 1995). This type of systems combines the advantages of photobioreactors and open pond/raceway. In the first stage, microalgae are cultivated in a closed photobioreactor, which provides an enclosed and fully controlled environment to minimize culture contamination. In the second stage, the dense culture provided by the first stage is grown in an open pond/raceway system, which requires minimum capital and maintenance cost. Consequently, the risk for culture overtaking by contaminants is reduced while maintaining a lower production cost.

Rusch and Malone (1998) designed the Hydraulically Integrated Serial Turbidostat Algal Reactor (HISTAR) system for mass production of microalgae. HISTAR is a combination of both sealed (turbidostats) and open topped components (continuous-flow stirred-tank reactor, CFSTR). The two precisely controlled turbidostats produce high quality, concentrated, contaminant-free inoculum microalgal culture and feed it to the first CFSTR (at the flow rate of Q_{tb}) every 10 minutes. The make-up water with nutrients is continuously flushed to the first tank (at the flow rate of Q_f), generating hydraulic gradient and driving the culture flowing through the eight CFSTRs. Although the reactors in HISTAR system are open-top tanks, the system is able to contain and mitigate the contaminants (Theegala et al., 1999; Rusch and Malone, 1998). By adjusting the flow rate of water with nutrients, the local dilution rate for each CFSTR can be

Table 1.2. The advantages and disadvantages of open ponds and closed bioreactors, adapted from Ghasemi et al. (2012).

Factor	Open pond	Closed bioreactor
Required space	High	Low
Water loss	Very high, may also cause salt precipitation	Low
CO_2 loss	High, depending on pond depth	Low
Oxygen concentration	Usually low enough because of continuous spontaneous outgassing	Build up in closed system requires gas exchange devices (O_2 must be removed to prevent inhibition of photosynthesis, photo oxidative damage and photorespiration)
Temperature	Highly variable, some control possible by pond depth	Cooling often required (by spraying water on PBR or immersing tubes in cooling baths)
Shear	Usually low (gentle mixing)	Usually high (fast and turbulent flows required for good mixing, pumping through gas exchange devices)
Cleaning	No issue	Required (wall-growth and dirt reduce light intensity), but causes abrasion, limiting PBR lifetime
Contamination risk	High (limiting the number of species that can be grown)	Medium to low
Biomass quality	Variable	Reproducible
Biomass concentration	Low, between 0.1 and 0.5 g L^{-1}	High, generally between 0.5 and 8.0 g L^{-1}
Production flexibility	Only few species possible, difficult to switch	High, switching possible
Process control and reproducibility	Limited (flow speed, mixing, temperature only by pond depth)	Possible within certain tolerances
Weather dependence	High (light intensity/quality, temperature, rainfall)	Medium (light intensity/quality, cooling required)
Evaporation	High	Low
Capital costs	High ~ $100,000 per ha	Very high ~ $250,000 to 1,000,000 per ha (PBR plus supporting systems)
Operating costs	Low (paddle wheel, CO_2 addition)	Higher (CO_2 addition, oxygen removal, cooling, cleaning, maintenance)
Harvesting costs	High, species dependent	Lower due to high biomass concentration and better control over species and conditions

maintained at a level greater than the specific growth rate of the potential contaminants. Consequently, the contaminants are washed out before they can reach a detrimental concentration (Theegala et al., 1999). Theegala et al. (1999) investigated the ability of mitigationof contaminants for HISTAR via both simulation and experiments. The results simulation demonstrated that the local dilution rate D_n is the most important parameter for contamination mitigation in HISTAR. The contaminants washout experiments proved that 300 million live rotifers in microalgae (*Thalassiosira*) culture was completely washed out after simply increasing the local dilution rate by six fold.

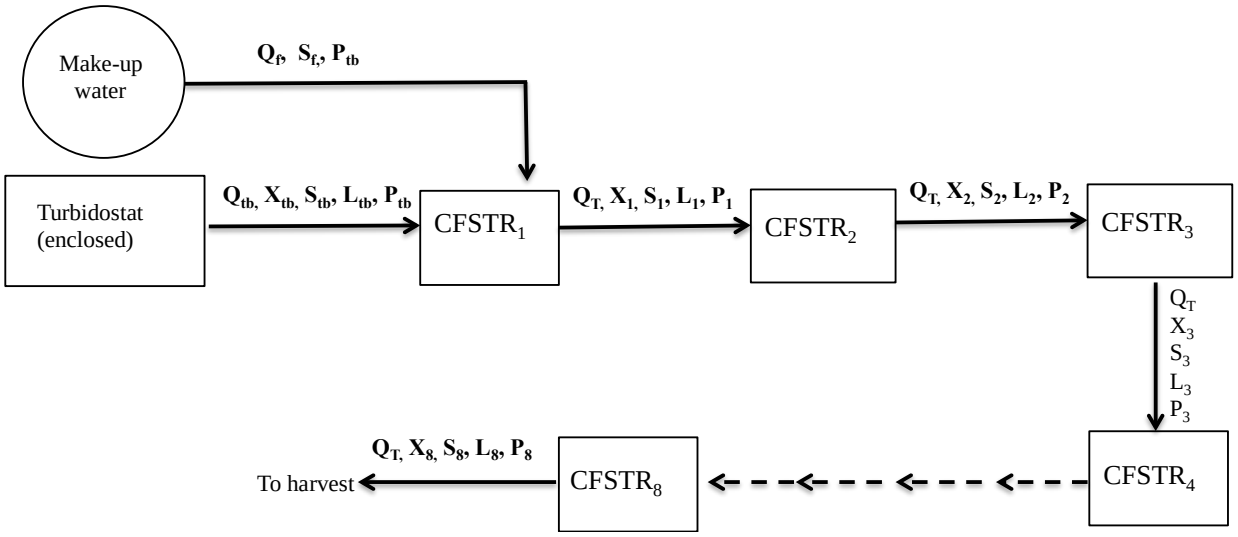

Figure 1.6. The schematic diagram of HISTAR system**.**

To gain a more fundamental understanding of HISTAR system, multiple efforts have been made to construct a mathematical model to optimize the operating parameters and forecast production results. Rusch and Malone (1998) established the first HISTAR model by coupling mass balances with Monod growth kinetics to provide foresight during the design process. The governing equations were eight differential mass balance equations, one for each CFSTR. The

effluent biomass concentration of a $CFSTR_n$ (X_n) was the input biomass concentration of $CFSTR_{n+1}$. The input biomass concentration for the $CFSTR_1$ was calculated based on the following equation:

$$X_i = \frac{(Q_{tb}X_{tb}) + (Q_f X_f)}{Q_{tb} + Q_f} \quad (1)$$

Where Q_{tb} is the flow rate of the turbidostats, X_{tb} is the biomass concentration of the turbidostats, Q_f is the flow rate for makeup water, X_f is the biomass concentration in the makeup water (usually X_f= 0).

The mass balance equation on the first CFSTR is expressed as:

$$\frac{dX_1}{dt}V_n = Q_T X_i - Q_T X_1 + U_1 X_1 V_n \quad (2)$$

Where Q_T is the total flow rate of the system (Q_{tb}+Q_f), V_n is the volume of each CFSTR, X_1 is the biomass concentration of the first CFSTR, U_1 is the net biomass growth rate of first CFSTR.

The differential equation for the other seven CFSTRs is:

$$\frac{dx_n}{dt}V_n = Q_T X_{n-1} - Q_T X_n + U_n X_n V_n \quad (3)$$

where X_n is the biomass concentration of the nt^h CFSTR, U_n is the net growth rate for biomass in n^{th} CFSTR.

Benson et al. (2007) developed a mechanistic model to investigate the impact of the light dynamics on the microalgal productivity in the HISTAR system. Multiple types of light kinetics models (relationship between average internal scalar irradiance level I_{an} and specific growth rate $\mu_{n)}$ were discussed, including an exponential model (Pulz and Scheibenbogen, 1998), a hyperbolic model (Grima et al., 1996) and Steele's model (Steele, 1965). Steele's model was selected for the HISTAR system because it acknowledges photoinhibition, and it proved to be

the best fit for HISTAR in a previous study (Benson and Rusch, 2006). The net microalgal growth rate within $CFSTR_n$ can be calculated as:

$$U_n = \mu_{max} \frac{I_{an}(PAR)}{I_{opt}(PAR)} e^{1-\frac{I_{an}(PAR)}{I_{opt}(PAR)}} - K_e \quad (4)$$

Where I_{opt} is the optimal irradiance level associated with μ_{max}.

Combining the effects of both irradiance and nutrient level should lead to a more robust model to forecast microalgal productivity. The first step in developing such a model is the calculation of specific growth rates relative to maximum rates in terms of irradiance and nutrient levels. Two common approaches are used to combine the effects. The first is "Blackman's law of the minimum", which uses the smaller of the fractional growth rates as the one in the growth model. The second approach multiples the two fractional growth rate to generate a combined growth rate (Haney and Jackson, 1996). Since the relationship (i.e. greater or smaller) between the two fractional growth rates may vary from CFSTR to CFSTR for HISTAR, the growth rate based on the second approach is proposed in this work, multiplying the fractional growth rate of Steele's model and Monod model for light and nutrient limitations, respectively.

$$U_n = \mu_{max} \frac{I_{an}(PAR)}{I_{opt}(PAR)} e^{1-\frac{I_{an}(PAR)}{I_{opt}(PAR)}} \cdot \frac{S}{K_s + S} \cdot \frac{P}{K_p + P} - K_e \quad (5)$$

Where S is the nitrogen concentration (g m^{-3}), K_s is the half saturation coefficient (g m^{-3}) for nitrogen, P is the phosphorus concentration (g m^{-3}), K_p is the half saturation coefficient (g m^{-3}) for phosphorus. Since the N:P ratio of the media used in this work (~6:1) is much lower than the Refield ratio (16:1) (Redfield, 1934) nitrogen can be considered sole rate limiting nutrients.

The biomass yield per gram of nutrients is calculated as:

$$Y = \frac{U_n X}{W_n S} \quad (6)$$

where W_n is the consumption rate of nitrogen (d^{-1}), Y is biomass yield on the nutrient. The governing equation for nitrogen can be written as:

$$\frac{dS_1}{dt}V_1 = Q_T S_i - Q_T S_1 - \frac{U_1 X_1}{Y}V_1 \quad (7)$$

$$\frac{dS_n}{dt}V_n = Q_T S_{n-1} - Q_T S_n - \frac{U_n X_n}{Y}S_n V_n \quad (8)$$

Where S_1 is the concentration of rate limiting nutrient within $CFSTR_1$, S_i is the nutrient concentration for the inoculum (combining both input media and culture from turbidostats), and S_n is the concentration of rate limiting nutrient in $CFSTR_n$.

Recently, a few studies focusing on modeling of microalgal lipid production have been reported. Packer et al. (2011) explained the lipid accumulation in microalgal cells by separating the lipid and the rest part of the biomass. However, the model is based on the assumption that the initial lipid content for the microalgal cells was zero. Thus, not suitable for the *Chlorella vulgaris*/*Leptolyngbya* co-culture in HISTAR system. The Luedeking and Piret equation (Luedeking and Piret, 1959) was used to construct the microalgal lipid production models (Tevatia et al., 2012; Yang et al., 2011). In this equation, the instantaneous production rate of the bio-product is directly proportional to the instantaneous biomass production rate and biomass concentration:

$$\frac{dL}{dt} = \alpha\frac{dX}{dt} + \beta X \quad (9)$$

Where dL/dt is the instantaneous rate of bio-product formation, dX/dt is the instantaneous growth rate of biomass, X is the biomass concentration, α, β are constants which are defined as the lipid formation coefficient (g g^{-1}) and non-growth correlation coefficient (g g^{-1} d^{-1}), respectively. In the exponential growth phase, when the specific growth rate is constant (dX/dt=UX, U is the net specific growth rate of biomass), the equation becomes dL/dt=(αU+β)X,

resulting in a constant lipid and biomass production ratio. When the cells stop growing, the first term of equation 9 goes to zero and all lipid production continues at the rate of βX, resulting an increased lipid percentage. This model matches with reported studies that the found microalgal lipid percentage increases in the late exponential/stationary phase (Nigam et al., 2011; Huerlimann et al., 2010; Zhu et al., 1997). Therefore, Equation (10) could be used to model the lipid production rate for the *Chlorella vulgaris*/*Leptolyngbya* co-culture in HISTAR system. Accordingly, the governing equation for lipid production in each CFSTR could be expressed as:

$$\frac{dL_1}{dt}V_1 = Q_T L_i - Q_T L_1 + (\alpha U_1 X_1 + \beta X_1)V_1 \quad (10)$$

$$\frac{dL_n}{dt}V_n = Q_T L_{n-1} - Q_T L_n + (\alpha U_n X_n + \beta X_n)V_n \quad (11)$$

Where L_1 is the lipid concentration in the first CFSTR (g m^{-3}), p_i is the lipid concentration of the inoculum, L_{n-1} is the lipid concentration in $CFSTR_{n-1}$, L_n is the lipid concentration in the $CFSTR_n$. The six governing equations (Equations 2, 3, 7, 8, 10, 11) will be able to simulate the biomass, lipid production and nitrogen consumption in the HISTAR system. In previous studies on HISTAR, the lighting cost of biomass production was estimated and optimized (optimal lighting cost at \$35 kg^{-1}) (Benson, 2003). In this work, the cost of biomass and lipid production (\$ kg^{-1} lipid), including lighting (electricity), aeration (electricity), nutrients and water, was investigated via simulations.

1.2.6. Lipid Extraction

Life cycle analyses indicate that lipid extraction is one of the most energy demanding processes in microalgal biofuel production (Teixeira, 2012; Brentner et al., 2011; Lardon et al., 2009). Currently, the most commonly used lipid extraction method for commercial application is organic solvent extraction. The principle for organic solvent extraction is based on the concept of

"like dissolves like", i.e., the polar solutes will preferably dissolve in similar polar solvents while non-polar solutes will preferably dissolve in similar non-polar solvents. For the purpose of microalgal biofuel, especially biodiesel production, the target solutes are neutral lipids, thus non-polar solvents, like chloroform, hexane (industrial standard) and petroleum ether, are usually used to extract the neutral lipids. However, in the cytoplasm, some of the neutral lipids are found associated with polar lipids as a complex, which is strongly linked to the cell membranes (Halim et al., 2012). The van der Waal forces between the non-polar solvents and neutral lipids are insufficient to disrupt the lipid-membrane associations (Halim et al., 2012). Therefore, polar solvents, such as methanol, isopropanol, ethanol etc., are added into the nonpolar solvent to disrupt the neutral lipid-membrane complex by forming hydrogen bonds with the membrane associated polar lipids (Medina et al., 1998).

Halim et al. (2012) described microalgal lipid extraction by co-solvents (nonpolar and polar lipid mixture) as a five-step process (Figure 1.5): the polar and nonpolar solvents penetrate the cell wall and cell membrane by diffusion and enter the cytoplasm (step 1). Solvents interact with lipids via van der Waals force (step 2). A solvent-lipid complex is formed (step 3). The solvent-lipid complex diffuses through the cell wall (step 4) and static organic solvent film, which reduces diffusion rate of the lipid, entering the bulk solvent (step 5). Throughout the entire process, the solvent has to diffuse through the cell wall twice to complete the lipid extraction. Therefore, the multi-layer cell wall (Richmond, 2004) for microalgal cells can significantly limit the lipid extraction efficiency. Thus, cell wall disruption could considerably improve the lipid extraction efficiency. The microalgal cell wall is mainly comprised of linear and branched polysaccharides, which form networks of microfibrils with a strong semi-crystalline patterns (Northcote, 1963). The mechanical strength of bacterial polysaccharides with similar crystalline

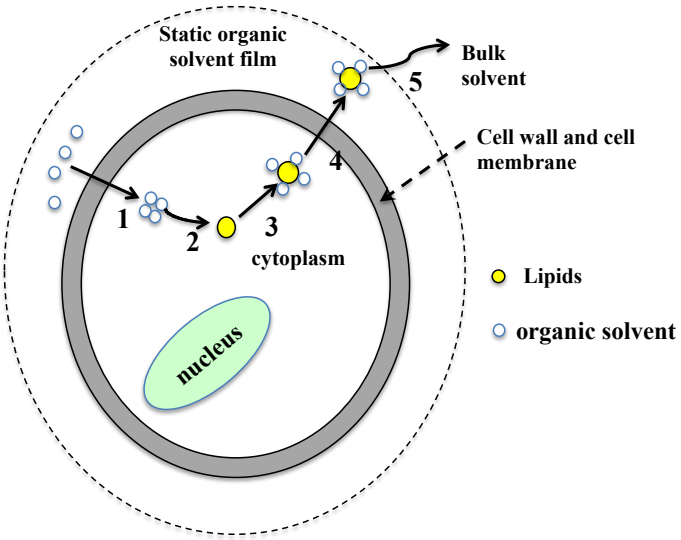

Figure 1.7. Schematic diagram of lipid extraction by organic solvent, adapted from (Halim et al., 2012).

structure has been measured at 9 kJ kg^{-1}, which is close to the 12 kJ kg^{-1} for carbon fibers (Teixeira, 2012). The tensile strength of cell walls have been reported as high as 95~100 atmospheres (Carpita, 1985). Mechanical grinding is usually applied to break the cell wall of oil producing crops (soybean, rapeseed, and canola) before the lipid extraction process. However, microalgal biomass paste usually contains large amount of water (~80%, mass/mass, aftercentrifugation) since the drying process is extremely energy intensive. In addition to creating a great barrier between the solvent and cells, the bulk water in microalgal paste can drastically limit the efficiency of cell disruption by mechanical grinding (pressing). The cells flow through the micro-channels in the bulk water instead of getting disrupted (Cooney et al., 2009). Various methods have been developed to enhance the lipid extraction from microalgal cells including sonication, freeze-drying, microwave etc. (Prabakaran and Ravindran, 2011; Lee et al., 2010b; Cooney et al., 2009).

Sonication has been widely applied in the lipid extraction for microalgal biomass (Cravotto et al., 2008; Borthwick et al., 2005; Pernet and Tremblay, 2003). Basically, the

microalgal suspension is placed into a container, and sonic waves are generated in a high pressure-low pressure oscillation pattern. Vacuum bubbles in the surrounding liquid, formed in the low-pressure period, explode during the high-pressure cycle. This oscillation releases shock waves in the surrounding liquid forming jet streams, and the shear force breaks the cell walls (Onyeche et al., 2002). Cravotto et al. (2008) reported 4.8%~25.9% improvement over traditional Soxhlet extraction. However, sonication assisted lipid extraction is highly energy intensive. Gerde et al. (2012) reported that 80 kJ L^{-1} (based on culture volume) was needed to efficiently disrupt cell walls of *Chlamydomonas reinhardtii* by using sonication.

Cooney et al. (2009) investigated manual grinding-assisted lipid extraction from *Nannochloropsis sp.* The results indicated that grinding freeze-dried sample gives the highest lipid extraction efficiency. Lipid content improved by 45% compared to the freeze-dried samples not ground. However, for the purpose of fuel production from microalgal biomass, grinding combined with freeze-drying is highly energy intensive and time consuming. Wolkers et al. (2011) estimated that cost of freeze-drying one kilogram of microalgae is about $532 to $665 (€ 400 to 500). Therefore, lipid extraction assisted by freeze-drying is not commercially viable.

Microwave assisted solvent extraction changes the electric field along with the wavelength at the frequency of 2450 MHz, generating ionic conduction and dipole rotation of target molecules. The friction between ionic conduction and the solution in conjunction with molecular vibrations leads to solution heating, especially of polar molecules. Water molecules inside the microalgal cells are heated at a high rate while the other components of the sample stay relatively cool. Once the intracellular water is hot enough to evaporate, high pressure points will be formed inside of the cells, eventually causing the cells to rupture (Vivekananda Mandal, 2007). Lee et al. (2010b) reported that lipid percentage from *Chlorella vulgaris* (mass/mass,

based on dry biomass) increased ~5% when using microwave at 100^{o}C for 5 minutes. For *Botryococcus sp.*, an increase of lipid percentage from ~10% to ~30% percent was recorded by using microwave at the same temperature and heating time (Lee et al., 2010b). Prabakaran et al. (2011) found the lipid percentage of *Chlorella vulgaris* increased from ~8% to 18% due to the assistance of microwaves at 100^{o}C for 5 minutes. However, Iqbal (2012) estimated that the cost of microwave assisted lipid extraction from microalgae was in the range \$13.27~21.26 gal^{-1} oil. Thus, this method currently is not commercially feasible.

Silver and copper are known to have antimicrobial activity, which is directly related to their ability to disrupt cell walls (Kora et al., 2009; Ruparelia et al., 2008; Fry et al., 2002). This antimicrobial and cell disruption activity could be significantly enhanced by using nanostructured metal (silver, copper etc.) due to its larger surface area to volume ratio (Ayala-Núñez et al., 2009). Ruparelia et al. (2008) found that the antimicrobial efficiency for silver nanoparticles, which was directly related to cell wall disruption, was almost 40-50% higher than copper nanoparticles. Therefore, nanostructured silver is likely a better choice for microalgal cell disruption than copper is.

The cell wall disruption by silver nanoparticles has been described as a two-phase process (Chwalibog et al., 2010). In the first phase, silver nanoparticles attach and anchor on the surface of cell wall. The electrostatic forces and molecular interactions involved cause structural and morphology changes, damaging the cell wall. In the second phase, the nanoparticles penetrate the damaged area on the cell wall, perforating the cell membrane and releasing the intracellular contents (Díaz-Visurraga et al., 2011). Therefore, the addition of silver nanoparticles in the extraction matrix should considerably improve the lipid extraction efficiency.

As to the recycle strategy, silver nanoparticles synthesized with cobalt seeds could be recovered by applying a magnetic force to take advantage of the magnetic permeability of cobalt. Using silver nanoparticles fixed on the surface of bulk substrate could be another way to simplify the recovering process of silver nanoparticles.

1.3. Goals and Objectives of Research

This research focused on lowering the microalgal lipid production cost via strain selection, cultivation design (nitrogen and irradiance levels, simulations of HISTAR operation) and improved lipid extraction. The impacts of these improvements on the lipid quality (fatty acid profile and neutral lipid fraction) were assessed. The primary objective of the dissertation was to optimize the lighting, nutrients (nitrogen) conditions and lipid extraction methods to maximize the lipid productivity from microalgal/cyanobacterial co-culture.

In this work, a Louisiana *Chlorella vulgaris*/*Leptolyngbya sp.* co-culture was selected for its high lipid content and growth rate (Rusch and Gutierrez-Wing (unpublished data)). The lipid productivity and lipid content (based on the dry biomass) of this co-culture were quantified under five different irradiance, two nitrogen levels and two aeration levels in a bench-top scale experiment conducted with two aeration levels (non-aerated and aeration rate at 0.47 L^{-1} min). The neutral lipid fraction and the fatty acid profile under each condition were quantified. The optimal condition of those tested for biodiesel production was identified.

A novel method of enhanced lipid extraction via silver nanoparticles (Gutierrez-Wing and Rusch, 2011) was investigated. Silver nanoparticles have been shown to damage cell walls, and this damage may be able to increase the lipid extraction efficiency from the algal biomass. The impacts of silver nanofibers on the lipid extraction efficiency of Folch's method and microwave-assisted extraction were evaluated. The fatty acid profile was analyzed to determine the best extraction condition for microalgal biodiesel production.

A mathematical model was expanded based on Benson et al. (2007) to add the impact of nitrogen levels on biomass and lipid productivity from the Louisiana *Chlorella vulgaris*/*Leptolyngbya* co-culture in the HISTAR system. The model included the effects of irradiance and nitrogen levels, following Steele and Monod model respectively. The cost for lipid production was calculated in the model.

2. EFFECTS OF NITROGEN AND IRRADIANCE ON LIPID CONTENT AND FATTY ACID COMPOSITION OF A LOUISIANA NATIVE *CHLORELLA VULGARIS/LEPTOLYNGBYA SP.* CO-CULTURE

2.1. Introduction

The concerns on sustainability of fossil fuel coupled with an increasing global demand for energy has necessitated the search for reliable alternative energy resources. Biofuels will play a crucial role in any alternative energy portfolio. Over the last several decades, first (grain, sugarcane etc.), second (sugarcane bagasse, wood residues etc.) and third (microalgae, bio-waste etc.) generation feedstocks have been converted to biofuels to various degrees of success (Prabakaran and Ravindran, 2011; Atsumi et al., 2008; Fischer et al., 2008; Hill, 2007). As the third generation of biofuel feedstock, microalgae are widely considered one of the most viable biofuel sources (Hu et al., 2008). First, microalgae theoretically exhibit 10-100 times higher energy yield per unit area than traditional terrestrial plants (Greenwell et al., 2010; Dote et al., 1994). Second, microalgae are able to be cultivated on non-arable land, thus avoiding land competition with food crops (Huang et al., 2010b; Johnson and Wen, 2010; Chisti, 2007). Third, microalgae-based biofuel has low carbon emission (Chisti, 2007) and minimal sulphur dioxide, nitrous oxide emissions in comparison to petroleum-based diesel (Mutanda et al., 2011; Li et al., 2008a). Last, other valuable bio-products such as bioplastics (Samantaray and Mallick, 2012; Sharma et al., 2007; Wu et al., 2002), pigments (Bai et al., 2011; Del Campo et al., 2007; Chaumont and Thepenier, 1995) and omega-3 fatty acids (Adarme-Vega et al., 2012; Chi et al., 2009; Singh et al., 2005) can be obtained from microalgal biomass, partially offsetting the biofuel production cost.

While promising, there are still several limitations associated with development of a microalgal-based biofuel production industry. Selecting appropriate microalgal strains for large-scale culture is critical. Numerous commercial microalgal strains such as *Botryococcus braunii*,

Nannochloropsis sp. and *Scenedesmus sp.* have been reported to exhibit high lipid content under lab conditions (Griffiths and Harrison, 2009; Tran et al., 2009; John Sheehan, 1998), but for mass production, maintaining monoalgal cultures for weeks or even months in open systems is extremely difficult (Rodolfi et al., 2009) due to invasive species and limited strain adaptability to local environments. Genetic engineering has been proposed to develop strains more adapted to local environments for large-scale cultivation systems (Wijffels and Barbosa, 2010). However, the introduction of genetically modified strains is risky to the environments (Bakshi, 2003). More realistically, native strains have lower potential risk for local environments. These strains are adapted to the local climatological and water conditions, and most importantly, can resist invasive microalgal species better than introduced strains (Mutanda et al., 2011) Zhou et al. (2011) isolated 17 microalgal strains from local municipal wastewater streams in Minnesota and found five of them with promising lipid production performance (74.5-77.8 g m^{-3} d^{-1}). De la vega et al. (2011) reported a lipid productivity of 89.7 g m^{-3} d^{-1} from a *Picochlorum sp.*, which was isolated from the Odiel River in southwest Spain. Bhatnagar et al. (2011) grew several microalgal strains isolated from local municipal wastewater stream in a 950 L raceway, and the highest lipid productivity reached 5 g m^{-3} d^{-1}. These studies implied that isolating microalgal strains with high lipid productivity from local environments could be a viable approach for large-scale biofuel production.

Several recent studies have investigated utilization of microalgal/bacterial (cyanobacterial) co-culture instead of monoalgal culture for biomass production (Ortiz-Marquez et al., 2012; Imase et al., 2008; Park et al., 2008; de-Bashan et al., 2002). For example, Oritz-Marques et al. (2012) used *Azotobacter vinelandii* mutant strain to form "artificial symbiosis" with *Chlorella sorokiniana*, allowing the co-culture to grow diazotrophically (grow via nitrogen

fixation). Park et al. (2008) discovered that the bacteria naturally grown with *Chlorella ellipsoidea* resulted in 3 times greater algal growth than *Chlorella ellipsoidea* alone. Similarly, Rusch and Gutierrez-Wing (unpublished data) have isolated a Louisiana native *Chlorella vulgaris/Leptolyngbya sp.* co-culture, and discovered that the presence of *Leptolyngbya sp.* increased cell counts of *Chlorella vulgaris* approximately 20 times those of the *Chlorella vulgaris* monoculture. These results implied that selecting naturally or artificially symbiotic microalgal/cyanobacterial (bacterial) co-cultures could be preferential for microalgal biomass or lipid production.

Maximizing lipid productivity of microalgal cultures requires not only the selection of suitable strains but also optimization of growth conditions, which significantly influence both lipid content and lipid compositions (Guschina and Harwood, 2006). Two important growth conditions are culture media nutrients and irradiance. As for all photosynthetic organisms, light is a major factor that impacts biomass and lipid accumulation, since it provide all the energy to generate NADPH and ATP, which are used for CO_2 fixation in the Calvin-Benson cycle. In response to variations of irradiance, microalgal cells adjusting the composition and stoichiometry of light harvesting antenna subunits. to capture photons more efficiently. Under low irradiance conditions, the size and numbers of light harvesting complexes increases to capture photons more efficiently. However, this mechanism cannot completely compensate the insufficient excitation energy induced by low irradiance, resulting in inadequate $NADPH_2$ and ATP production and limited biomass and lipid productivity. Under high irradiance conditions, although both the size and number of light harvest are reduced, excessive irradiance can promote the generation of reactive oxidative species (ROS), resulting in damage the photosystem II. Continuous repairing of photosystem II is highly energy demanding (Simionato et al., 2011) and

may significantly affect the energy availability for biomass and lipid production. Therefore, it is essential to find the optimal irradiance level for microalgal/cyanobacterial biofuel production.

As one of the major nutrients, the effects of nitrogen level on the lipid content have been studied extensively (Widjaja et al., 2009; Chu and Alvarez-Cohen, 1998; Suen et al., 1987). In the pathway of lipid synthesis, three precursors (pyruvate, acetyl-CoA and phosphatidic acid) for neutral lipid production are involved in other metabolic activities. Pyruvate and acetyl-CoA both can be utilized in the citric acid cycle to provide metabolic energy for the cells. Phosphatic acid can be either converted into phospholipids (major composition for polar lipids) for membrane structure or neutral lipids. When the nitrogen is deprived in the culture, the protein and enzyme synthesis is significantly limited, hampering cell division and other metabolic activity (Sharma et al., 2012). Lower cell division and metabolic activity rate lead to lower energy demand from the citric acid. Thus, more pyruvate and acetyl-CoA can be utilized for lipid production. Lower cell division rate also result in lower needs for synthesis of membrane structure. Therefore, the no more phosphate lipids are needed and more phosphatic acid can be converted into neutral lipids (Ruparelia et al., 2008). However, the lack of nitrogen might limit the overall lipid productivity due to the limitation of biomass growth rate (Chen et al., 2011b; Converti et al., 2009; Widjaja et al., 2009). Therefore, the optimal nitrogen level for lipid production should be able to balance lipid content and biomass growth rate.

For bio-oil applications, especially biodiesel production, only neutral lipids are utilized (Chen et al., 2009). The fatty acid profile of the neutral lipids influences several properties of biodiesel including viscosity, gelling point and acidity, has to comply with the requirement of the current diesel engine. Consequently, numerous studies have been implemented to investigate the effects of the culture conditions on the fatty acid compositions of microalgae. Variables such as

temperatures, carbon dioxide and media have been reported to affect the fatty acid profile for microalgal culture (Carvalho and Malcata, 2000; Tsuzuki et al., 1990; Olson and Ingram, 1975). Rodolfi et al. (2009) reported effects of irradiance level and nitrogen deprivation on the fatty acid profile of *Nannochloropsis sp.* and found that higher irradiance level and low nitrogen level increased the C16 as well as C18 content in the fatty acid profile. (Kralova and Sjoblom, 2010). However, the most commonly used standards for biodiesel, including ASTM D 6751 standard (specifications for biodiesels blended with middle distillate fuels) and EN 14214 (Automotive fuels. Fatty acid methyl esters (FAME) for diesel engines. Requirements and test methods) only listed the requirements for fuel properties (viscosity, cetane number, flash point etc.) instead of fatty acid profiles. Ramos et al. (2009) developed correlations to predict whether FAME produced from neutral lipids will meet the EN14214 standards based on the fatty acid profile. According to the correlation developed by Ramos et al. (2009) the saturated fatty acids have to be in the range of 30~60% of total fatty acids (mass/mass) and 50% of the unsaturated fatty acids have to be monounsaturated in order to meet EN 14214 standards.

In this work, the lipid productivity and fatty acid profile of a fresh water *Chlorella vulgaris*/*Leptolyngbya sp.* co-culture isolated from College Lake near Louisiana State University-Baton Rouge was investigated and characterized. The effects of irradiance and nitrogen levels on the lipid content, neutral lipid fraction and fatty acid profile were investigated. While the experiments were conducted at the bench-scale, they could provide the information that can be applied in the mass production of this native co-culture in a large-scale culture system in the future.

2.2. Methods and Materials

2.2.1. Strain Selection

The co-culture investigated in this work contains 97% microalgae cells and 3% cyanobacteria cells the based on cell count analyses conducted with BD Accuri^{TM} C6 flow cytometer (Figures 2.1 and 2.2). The identification analysis of this co-culture was conducted by the Culture Collection of Algae (UTEX) under the direction of Dr. Nobles. The sequence analysis of ITS2 rDNA region indicate the microalgae species was *Chlorella vulgaris* and the cyanobacteria most probably belongs to the genus *Leptolyngbya* based on the sequence analysis of 23S rDNA region. Rusch and Gutierrez-Wing (unpublished data) have found that the co-existence of *Chlorella vulgaris* and the *Leptolyngbya sp.* result in higher growth rate than the *Chlorella vulgaris* alone. Thus, the co-culture had been selected for the research described in this work, and hereto forth is referred to as the Louisiana co-culture.

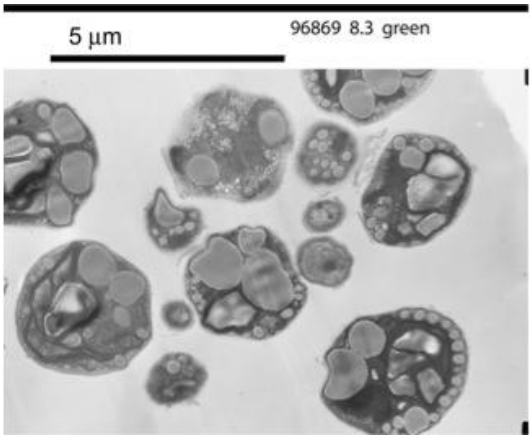

Figure 2.1. TEM image of the Louisiana *Chlorella vulgaris/Leptolyngbya sp.*co-culture.

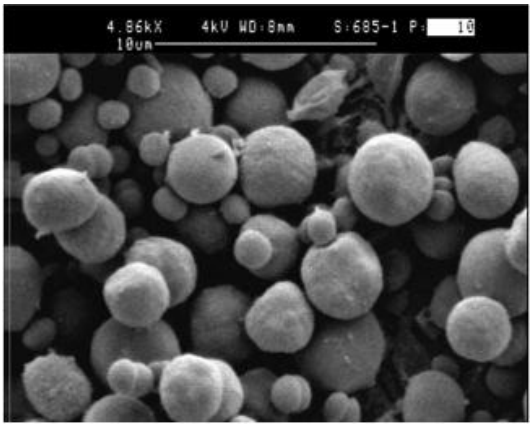

Figure 2.2. SEM image of the Louisiana *Chlorella vulgaris*/*Leptolyngbya sp.* co-culture.

2.2.2. Co-culture Cultivation

Stock Culture

Stock cultures of *Chlorella vulgaris*/*Leptolyngbya sp.* were maintained in Bold's basal medium ($NaNO_3$ 2.94 mM for 100% N and 1.47 mM for 50% N, $CaCl_2 \cdot H_2O$ 0.17 mM, $MgSO_4 \cdot 7H_2O$ 0.3 mM, K_2HPO_4 0.43 mM, KH_2PO_4 1.29 mM, NaCl 0.43 mM, P-IV metal solution which is comprised of $Na_2EDTA \cdot 2H_2O$, $FeCl_3 \cdot 6H_2O$, $MnCl_2 \cdot 4H_2O$, $ZnCl_2$, $CoCl_2 \cdot 6H_2O$, $Na_2MoO_4 \cdot 2H_2O$, vitamin solution which contains vitamin B_{12}, biotin and thiamine). High pressure sodium (HPS) lamp was used to provide continuous surface incident irradiance of 310 µmol m^{-2} s^{-1} to the 1 L stock cultures (in 2L Erlenmeyer flasks). The temperature was maintained at 25±2^{o}C. Continuous aeration at an airflow rate of 0.47 L min^{-1} (1 SCFH) was provided. Carbon dioxide injected in the cultures daily at the flow rate of 0.47 L min^{-1} for 1 minute to control the pH value at 7-8. Approximately one third of the culture was replaced by the Bold's Basal medium each week to maintain the growth.

Experiment Setup

The experiment was conducted in batch model, following a two-factorial (five scalar irradiance levels × two nitrate nitrogen levels), randomized block design. Triplicates were done for each treatment. Continuous illumination was provided by 400 watt high pressure sodium lamps located above the culture. Five scalar irradiance levels (180, 400, 600, 800 and 1200 µmol m^{-2} s^{-1} at culture time t=0, culture concentration x=0) were achieved by adjusting the vertical distance between the HPS lamps and the surface of the culture. The scalar irradiance was measured by completely submerging a Li-193 spherical quantum sensor in blank Bold's basal media in a 2 L Erlenmeyer flask. The corresponding incident irradiance levels (103, 310, 520, 715 and 1078 µmol m^{-2} s^{-1}) were measured using a LI-190 terrestrial flat quantum sensor on the

upper surface of the culture. Scalar irradiance was used since it provides better estimation of light energy input to the culture. The two nitrate nitrogen levels were 2.94 mmol N L^{-1} and 1.47 mmol N L^{-1}, equivalent to 100% (treatment 100%) and 50% (treatment 50%) of the Bold's Basal medium nitrate nitrogen concentration.

The experiments were cultivated in a 2 L Erlenmeyer flasks containing 1 L of culture with the initial concentration of 100 g m^{-3}. The temperature was maintained at 25±1^{o}C by a water bath. No aeration was applied for the culture. CO_2 was bubbled through the culture daily at 0.24 L min^{-1} (0.5 SCFH for 15 seconds) to maintain the pH below 10.0. Cultures were acclimated to the respective irradiance and nitrogen conditions in 0.6 L aliquots in 1.0 L Erlenmeyer for seven days.

Daily optical density (OD) was measured at 664 and 750 nm using a HACH DR/4000 UV/Vis spectrophotometer. Four milliliters of sample from each culture was collected using a 5 mL sterile plastic serological pipette. The OD readings at wavelength of 664 nm estimate the chlorophyll-a content while OD readings at 750 nm estimate the turbidity of the culture. Since optical density at 664 nm has a better correlation with biomass of the co-culture, OD readings at 664 nm were used in this research. After reaching the late exponential/stationary phase (determined by no increase in optical density for two consecutive days), the co-cultures were transferred to 1 L plastic (HDPE) bottle and preserved at -20^{o}C until analyzed.

2.2.3. Biomass Productivity

The protocol of dry biomass analysis followed LSU Civil and Environmental Engineering Water Quality Lab SOP PA 200 adapted from Standard Method 2540D (APHA, 2001). To avoid evaporation of volatile compounds, modification of drying temperature (65^{o}C) and duration (three hours) was applied. GF/C filter paper (1.2 µm pore size) was used instead of the GF/F (0.7 µm) filter paper. The decant liquid after filtration was analyzed using flow

cytometry (BD Accuri^{TM} C6) and the results revealed that no cell loss during the filtration. Ten milliliters initial culture and five milliliter final culture was filtered through a pre-weighed GF/C filter. The filter with biomass was dried at 65 ^{o}C for three hours. The filter was let cool down for one hour in a desiccator. The final mass of the filter was recorded.

For each treatment, a calibration curve was established to convert daily optical density readings to biomass concentration. The final culture for each treatment was diluted into five different biomass concentrations. The optical density at wavelength of 664 nm and corresponding dry biomass concentration were measured for each dilution level. The calibration curve was then fitted by linear regression. Finally, daily biomass concentration was calculated based on the optical density readings and biomass productivity (g m^{-3} d^{-1}) was calculated (only for the exponential growth phase).

2.2.4. Lipid Extraction

Soxhlet has been demonstrated to provide more complete lipid extraction than other methods, such as Folch's method, Bligh and Dyer, etc. (Siddiquee and Rohani, 2011), although it will not be commercially viable. In this work, Soxhlet extraction was chosen to evaluate the total lipid content for the co-culture. For each treatment, 120 mL sample from the 1.0 L co-culture was filtered with the GF/C glass fiber filter. The filter with the biomass was dried at 65^{o}C for 60 minutes. The dried biomass was weighed. Soxhlet extraction with the biomass sample was performed using chloroform: methanol 2:1 (v:v) for four hours. The solvent was evaporated at the temperature of 65 ^{o}C. The lipid fraction was weighed and resuspended in 3 mL of solvent for preservation at -20^{o}C until the fatty acid analysis was performed. The biomass productivity (g m^{-3} d^{-1}) multiplied by the total lipid content (% of the dry biomass, mass/mass) gave the lipid productivity (g m^{-3} d^{-1}).

2.2.5. Lipid Fraction Analysis

Neutral and polar lipid fractions were determined for each lipid sample following the procedure from Pernet et al. (2006). Sep-Pak^{TM} pre-packed columns with Si-NH_2 sorbent were used to separate neutral and polar lipids. The column was first preconditioned with 4 mL of methanol followed by 4 mL of chloroform. The lipid sample was loaded into the column and eluted with chloroform-isopropanol (2:1) to recover the neutral lipid fraction followed by elution of the column with methanol to recover the polar lipids. The solvents were evaporated and each fraction was weighed.

2.2.6. Fatty Acid Analysis

The neutral lipid fraction was transesterified into FAME (fatty acid methyl ester) and prepared for the gas chromatography analysis. The transesterification procedure followed IUPAC Method II. D. 19 (IUPAC, 1979). The samples were boiled with 0.5 M NaOH methanolic solution for 10 minutes. Boron trifluoride (BF_3) methanolic solution was added and then the mixture was boiled for 2 minutes. After adding 1.5 mL heptane and boiling for 1 more minute, 20 mL of saturated NaCl solution was poured into the flask to form a two-phase liquid system (FAME and heptane in the upper phase). About 1 mL upper phase was transferred into a 2 mL vial for gas chromatography analysis.

The fatty acids were determined using gas chromatography (HP 5890 Series II) equipped with an SP^{TM}-2330 column (30 m, 0.25mm ID, 0.20 μm film). The initial oven temperature was kept at 80 ^{o}C for 1 minute and then increased to 220 ^{o}C at a ramp of 4 ^{o}C min^{-1} and maintained at 220 ^{o}C for 5 minutes. Helium was kept at 2.0 mL min^{-1} as the carrier gas. The gas chromatography data were analyzed with Chemstation^{TM} software, and the mass percentage of each fatty acid component was reported. Triplicates were done for each FAME sample.

2.2.7. Estimation of the Energy Return (Lipid Energy) on Light Energy Input

To evaluate the efficiency of the Louisiana co-culture to convert light energy into lipid energy, the energy return (lipid energy) on energy input (light energy) was calculated. The calculation was adapted from the Zijffers et al. (2010), which was used for biomass yield on light energy:

$$Y_{lipid\ ,E} = \frac{P_L}{I_s \times 10^{-6} \times 8.64 \times 10^4} \times \frac{V}{A} \quad (1)$$

where $Y_{lipid,\ E}$ is the lipid per mole photons, P_L (g m^{-3} d^{-1}) is the lipid productivity, I_s is scalar irradiance level (µmol m^{-2} s^{-1}, culture concentration x=0), V/A is the volume to wetted surface area ratio of the culture. For 1.0 L culture in a 2.0 L Erlenmeyer flask used in this work, V/A is 0.023 m^3 m^{-2}.

The lipid caloric content (C_L, kJ g^{-1}) was determined with a Parr 6200 isoperibol calorimeter. The sample of 0.5 g of total lipid in sample cup was installed into the caloric bomb, and a platinum ignition wire was attached to the lipid sample. The caloric bomb was charged with O_2 till the pressure reached 10-35 atm. The platinum wire then was ignited. After the run finished, the caloric content of the lipid was automatically calculated. Duplicates were done. The energy return of lipid on light energy was calculated following the equation:

$$\eta = Y_{\boldsymbol{Lipid,E}} \times \frac{C_L}{E} \quad (2)$$

Where η (%) is the energy return of lipid on the light energy for each irradiance level. E (kJ (mole photon)$^{-1}$) is a parameter to convert the scalar irradiance to energy. For HPS lamps, E is estimated to be 201 kJ (mole photon)$^{-1}$ as reported by Thimijan and Heins (1983). The calculated

η was plotted against each internal scalar irradiance level (where the culture concentration x=0) to investigate the effects of irradiance levels on the energy return (lipid energy) on light energy input.

2.2.8. Data Analysis

For each treatment, the mean and standard deviation of total lipid percentage (% of dry biomass, mass/mass), lipid productivity (g m^{-3} d^{-1}), neutral lipid percentage (% of total lipid, mass/mass), fatty acid percentage (% of total FAME, mass/mass) and energy return on light energy (% of energy for each irradiance level) were reported. Two-way ANOVA (analysis of variance) on these measurements was conducted using SAS^{TM} (9.1.3) to determine whether the effects of the treatments (scalar irradiance and nitrate nitrogen levels) were significant. Turkey test was performed to determine the differences among particular treatments. All statistical analysis was based on α=0.05.

2.3. Results and Discussion

2.3.1. Lipid Content and Productivity

The results of two-way ANOVA analysis showed that both irradiance and nitrate nitrogen levels had significant effects on total lipid content (p<0.0001 for effects of irradiance and p=0.0005 for effects of nitrogen) and lipid productivity (p<0.0001 for effects of irradiance and p=0.0081 for effects of nitrogen). The lipid content of the dry biomass increased from ~22% (100% N) and ~25% (50% N) at 180 μmol m^{-2} s^{-1} to a maximum of ~38% (50% N) and ~31% (100% N) for the 400 μmol m^{-2} s^{-1} irradiance treatments respectively (Table 2.1). However, the lipid content (~26% for 100% N and ~31% for 50% N) at 600 μmol m^{-2} s^{-1} was lower than 400 and 800 μmol m^{-2} s^{-1} (the experiment was repeated for three more replicates). When the irradiance reached 1200 μmol m^{-2} s^{-1}, the lipid content dropped to ~16% (100% N) and ~20%

(50% N), the lowest lipid content for the five irradiance levels tested. The results of lipid productivity showed the same trend as lipid percentages, starting low for 180 μmol m^{-2} s^{-1}, reaching the highest for the 400 and 800 μmol m^{-2} s^{-1} but slightly lower for the 600 μmol m^{-2} s^{-1} and dropping to the lowest at 1200 μmol $m^{-2}s^{-1}$ (Table 2.2).

Table 2.1. Total lipid percentage (based on dry biomass, mass/mass) of the Louisiana *Chlorella vulgaris/Leptolyngbya sp.* co-culture with five scalar PAR irradiance (180, 400, 600, 800 and 1200 μmol m^{-2} s^{-1}) and two nitrate nitrogen levels (100% N and 50% N).

Irradiance	Lipid percentage (%, mass/mass, based on dry biomass)	
(μmol m^{-2} s^{-1})	50% N	100%N
180	24.8%±2.0%^{bcd}	21.6%±3.1%^{cd}
400	37.5%±3.8%^{a}	30.7%±0.9%^{ab}
600	31.2%±2.4%^{ab}	25.5%±3.2%^{bc}
800	35.0%±4.7%^{a}	30.6%±2.5%^{ab}
1200	19.6%±0.8%^{cd}	16.3%±5.8%^{d}

*(*mean±standard deviation*)

a-d Values with different superscript letters indicate a significant difference (p<0.05) while values share same superscript letters indicate no significant difference. Tukey's test was conducted.

Table 2.2. Total lipid productivity (g m^{-3} d^{-1}) of the Louisiana *Chlorella vulgaris/Leptolyngbya sp.*co-culture with five scalar PAR irradiance (180, 400, 600, 800 and 1200 μmol m-2 s-1) and two nitrate nitrogen levels (100% N and 50% N).

Irradiance	Lipid productivity (g m^{-3} d^{-1})	
(μmol m^{-2} s^{-1})	50%N	100%N
180	9.66±1.00^{cd}	10.4±0.29^{cd}
400	13.7±1.27^{abc}	17.0±1.61^{a}
600	12.3±1.73^{abc}	12.0±2.32^{bc}
800	10.8±1.91^{c}	16.1±2.25^{ab}
1200	6.13±0.77^{d}	5.93±2.02^{d}

*(*mean±standard deviation*)

a-d Values with different superscript letters indicate a significant difference (p<0.05) while values share same superscript letters indicate no significant difference, based on Tukey's test.

With respect to nitrogen, the 50% nitrate nitrogen level increased lipid percentage by 3-5% compared to the 100% nitrate nitrogen level for all irradiance levels (Table 2.1), although the increase was not statistically significant. Nitrogen starvation has been reported to increase the lipid content (Chen et al., 2011b; Widjaja et al., 2009; Li et al., 2008b; Chu and Alvarez-Cohen, 1998; Suen et al., 1987; Spoehr and Milner, 1949). In the lipid synthesis pathway, the citric acid cycle, which provide the metabolic energy for cells, consume the precursor (pyruvate and acetyl-CoA) for lipid production. The limited nitrogen source constrains the protein synthesis in the cells and accordingly lowered the rate of cell reproduction, so the energy demand for cell division and other activities decreased. Therefore, more pyruvate and acetyl-CoA are used to produce lipid (Deng et al., 2011). However, the increase of lipid percentage induced by nitrate nitrogen starvation did not compensate for the decrease of total biomass, resulting in a lower net lipid productivity for the 50% nitrate nitrogen treatments (Table 2.1). By combining the effects of irradiance and nitrate nitrogen levels, for all the tested treatments, the optimal condition of the Louisiana co-culture for lipid productivity was 400 μmol m^{-2} s^{-1} at the 100% N level.

The maximum lipid productivity under all treatments was ~17 g m^{-3} d^{-1} at the irradiance of 400 μmol m^{-2} s^{-1} and 100% nitrate nitrogen level. This lipid productivity was almost 2.5 times higher than the lowest one, which was at 1200 μmol m^{-2} s^{-1} irradiance with the 100% nitrate nitrogen level (Table 2.2). The lower lipid productivity for the 180 μmol m^{-2} s^{-1} was probably attributed to insufficient excitation energy from low irradiance, limiting the NADPH and ATP produced in the light reactions. Therefore, in the Calvin-Benson cycle, the energy for CO_2 fixation was limited, resulting a lower biomass and lipid productivity (Beer et al., 2009). The low lipid productivity for the 1200 μmol m^{-2} s^{-1} was likely due to photo-inhibition caused by excessive irradiance, which increase the generation of reactive oxidative species and cause the

damage of photosystem II (Long et al., 1994). The recovering and repairing process of photosystem II is highly energy demanding (Simionato et al., 2011), resulting in insufficient energy in Calvin-Benson cycle. Therefore, the biomass and lipid productivity decreased.

The reason for the lower lipid productivity at 600 μmol m^{-2} s^{-1} (repeated three more times) than 400 and 800 μmol m^{-2} s^{-1} is not clear but might be related to the combined effects of irradiance and the presence of *Leptolyngbya sp.* on *Chlorella vulgaris* cell growth. Rusch and Gutierrez-Wing (unpublished data) found the *Leptolyngbya sp.* in this co-culture significantly increased the growth rate of the *Chlorella vulgaris* cells. The *Chlorella vulgaris* cell growth rate at 400 μmol m^{-2} s^{-1} was probably complimented by the *Leptolyngbya sp.* although the photon energy was less than at 800 μmol m^{-2} s^{-1}. When the irradiance increased to 600 μmol m^{-2} s^{-1}, the growth of *Leptolyngbya sp.* might have been limited since high irradiance level constraint the growth of cyanobacteria (Guven and Howard, 2011). As the irradiance increased to 800 μmol m^{-2} s^{-1}, although the growth of *Leptolyngbya sp.* was further limited, the photon energy was optimal for cell growth and the positive effects of the irradiance overcame the decrease of the effects of *Leptolyngbya sp.* resulting in a higher cell growth rate and lipid productivity than 600 μmol m^{-2} s^{-1}.

The results of lipid productivity for *Chlorella vulgaris* from other researchers vary in the range of 4-78 g m^{-3} d^{-1} (Abou-Shanab et al., 2011; Illman et al., 2000; Lv et al., 2010; Rodolfi et al., 2009; Widjaja et al., 2009; Yeh et al., 2010). The lipid productivity reported in this work (17 g m^{-3} d^{-1}) is higher than several of these studies. Compared to Illman et al. (2000) and Widjaja et al. (2009), which reported lipid productivity of 14.8 and 12.8 g m^{-3} d^{-1}, the higher lipid productivity in this study might be attributed to the high irradiance level applied (400 μmol m^{-2} s^{-1} compared to less than 30 μmol m^{-2} s^{-1} for both of the studies). Most likely the low irradiance

levels reported in Illman et al. (2000) and Widjiaja et al. (2009) caused photolimitation, resulting in lower lipid productivity. The symbiotic relationship between *Chlorella vulgaris* and *Leptolyngbya sp.* in this co-culture could be another factor that induced the high lipid productivity in this study, since Rusch and Gutierrez-Wing (unpublished data) has shown that the cell count of the co-culture can be 20 times as high as that of monoalgal *Chlorella vulgaris* culture.

Others reported higher lipid productivity for *Chlorella vulgaris* than this work. For example, Abou-Shanab et al. (2011) reported a lipid productivity of 20.9 g m^{-3} d^{-1}. Kuei-ling Yeh et al. (2011) reported lipid productivity as high as 78 g m^{-3} d^{-1}. Lv et al. (2010) and Rodolfi et al. (2009) reported lipid productivity of 40.0 and 36.9 g m^{-3} d^{-1} respectively. However, all these studies applied continuous mixing of the culture by aeration or shaking. Aeration can benefit the microalgal culture in several aspects. First aeration can reduced the oxidative stress for the culture by disrupting the oxygen accumulation and physically displacement (Bunt, 1971). Second, aeration can increase the uptake and exudation rate of the metabolic products for the cells (Singh and Dhar, 2011). Finally, via mixing the culture, aeration and shaking can provide uniform light exposure for the culture, preventing photoinhibition for cells close to the light source and photo-limitation for cells far away. Therefore, the lower lipid productivity in this work might be mainly attributed to the lack of aeration or mixing. Additionally, Lv et al. (2010), Kyei-ling Yeh et al. (2011) and Rodolfi et al. (2009) all applied continuous CO_2 (≥1%, v/v) for the culture. Higher CO_2 concentration can increase the rate of CO_2 assimilation in Calvin-Benson cycle and suppress photorespiration (Richmond, 2004), which consume organic carbon without any energy gain, resulting in higher biomass and lipid productivity.

2.3.2. Neutral Lipid Percentage

The results of the two-way ANOVA analysis indicated the irradiance levels had a significant effect on neutral lipid percentage (p=0.0001) while the nitrogen levels (p=0.3027) did not. The neutral lipid percentage of total lipids for this co-culture is ~75% at the lower four irradiance levels, falling to approximately 65% for the 1200 μmol m^{-2} s^{-1} irradiance level. The decrease of neutral lipid percentage at 1200 μmol m^{-2} s^{-1} is most likely due to photoinhibition induced by oversaturated photon energy input. The lack of increase in neutral lipid percentage (on total lipid, mass/mass) at 50% N (1.47 mM) level is most likely attributed to the fact that the 50% N in this research was not low enough to cause a statistically significant increase in neutral lipid percentage. In Piorreck et al. (1984), the highest neutral lipid percentage for *Chlorella vulgaris* did not increase until the nitrogen level dropped from 10 mM to 0.297 mM. Therefore, the neutral lipid percentage under lower nitrogen levels should be investigated for the Louisiana co-culture in the future.

Table 2.3. The neutral lipid percentage over the total lipid (mass/mass) the Louisiana co-culture with five surface scalar irradiance levels (180, 400, 600, 800 and 1200 μmol m^{-2} s^{-1}) and two nitrate nitrogen levels (100% N and 50% N).

Irradiance (μmol m^{-2} s^{-1})	Neutral lipid percentage (%, mass/mass based on total lipid)	
	50% N	100%N
180	74.5±5.17[a]	74.1±5.09[a]
400	77.4±2.83[a]	75.1±3.15
600	73.6±1.32[a]	74.2±1.69[a]
800	74.2±3.07[a]	77.2±0.33[a]
1200	67.9±1.51[ab]	62.0±7.87[b]

[a-b] Values with different superscript letters indicate a significant difference (p<0.05) while values share same superscript letters indicate no significant difference. Tukey's test was conducted.

Researchers have reported higher neutral lipid percentage (on total lipids, mass/mass) for various microalgal strains (Ryckebosch et al., 2012a; Suen et al., 1987; Piorreck et al., 1984). The highest neutral lipid percentage for *Chlorella vulgaris* in Piorereck et al. (1984) was 83.3%

with nitrogen level of 0.1 mM. Ryckebosch et al. (2012) and Suen et al. (1987) reported that ~80% of neutral lipid on total lipids for *Phaeodactylum tricornutum* and *Nannochloropsis sp.* respectively. However, all these reported studies with higher neutral lipid percentages were conducted with aeration. As discussed before, aeration provides multiple benefits to microalgal culture, including reducing oxidative stress, uniform light exposure etc. Therefore, the lack of aeration might be the factor that leads to the lower neutral lipid percentage in this work. In the future, the neutral lipid percentage of this co-culture with aeration should be investigated.

2.3.3. Fatty Acid Compositions

In each sample, 14 fatty acids were identified. Neither the irradiance nor nitrate nitrogen levels influenced the composition of the fatty acids generated by this native co-culture (the $p>0.05$ in Tukey's test for all fatty acids). Since the properties of the biodiesel were determined by fatty acid profiles, these results implied the properties (acidity, chemical stability and gelling point) of the biodiesel made from the Louisiana co-culture most likely would be relatively consistent with respect to irradiance and nitrogen levels.

The major fatty acids (Figure 2.3) for this Louisiana co-culture were 16-carbon and 18-carbon fatty acids, approximately 40% and 55%, respectively. Palmitic acid (C16:0) comprises the highest portion of all the components, around 30%. The fatty acids smaller than 14 carbons were undetectable. Overall, the saturated fatty acids proportion was approximately 39%. Although the fatty acid profile for microalgae is species dependent (Roncarati et al., 2004; Brown, 1991; Benamotz et al., 1987), other studies on the fatty acid profile of *Chlorella vulgaris* reported fatty acid profiles that are different from this work. For example, In Ryckebosch et al. (2012), the C18:3 content of the *Chlorella vulgaris* culture was ~30.2% compared to 17.94% in

this work. The saturated fatty acid content for a *Chlorella vulgar*is culture was only 16.5% in Piorreck et al. (1984) compared to 35% for the Louisiana co-culture. Most likely, these differences in fatty acids profiles were caused by biological variances.

Comparing the fatty acid profile of the co-culture to the components of petro-diesel, several significant differences can be recognized. The average chain length of petro-diesel is C12, but all the components of the FAME from this co-culture were more than fourteen carbons. Thus, the viscosity of the FAME will be higher than the petro-diesel. Petro-diesel normally contains 25% unsaturated hydrocarbons (Risher and Rhodes, 1995) while the percentage of unsaturated fatty acids for this *Chlorella vulgaris/Leptolyngbya sp.* co-culture was 35%. This might result the biodiesel derived from the co-culture exhibits lower oxidation stability. Similar to FAME from other feedstocks based biofuel (Bannister et al., 2011), the biodiesel produced from the Louisiana co-culture has higher oxygen content comparing the petro-diesel that is mainly paraffin, thus the energy content of the FAME is slightly lower than the petro-diesel (Tyson, 2001). However, the FAME based biofuels, will have much lower aromatic hydrocarbon content and sulfur content, which makes the FAME based biofuel more environmental friendly (Risher and Rhodes, 1995).

However, based on Ramos et al. (2009), in order to meet the EN 14214 standards (Automotive fuels. Fatty acid methyl esters (FAME) for diesel engines. Requirements and test methods.) the monounsaturated fatty acids percentage on total unsaturated fatty acids (mass/mass) had to be greater than 50% compared to 41.35% in this work (Table 2.4). High percentage of polyunsaturated fatty acids not only reduce the cetane number and oxidation stability of the biodiesel (Tyson, 2001), it also promote the corrosive behavior of the biodiesel on the current infrastructure for fuel distritubtion (e.g. pipe line, storage tank etc.) (Wang et al.,

2011). Currently, the most commonly used method to overcome this problem is to blend the biodiesel with petrol diesel (Tyson, 2001). The cetane number and oxidation stabilities of the biodiesel produced from this co-culture can be compensated by petrol diesel with higher saturated hydrocarbons.

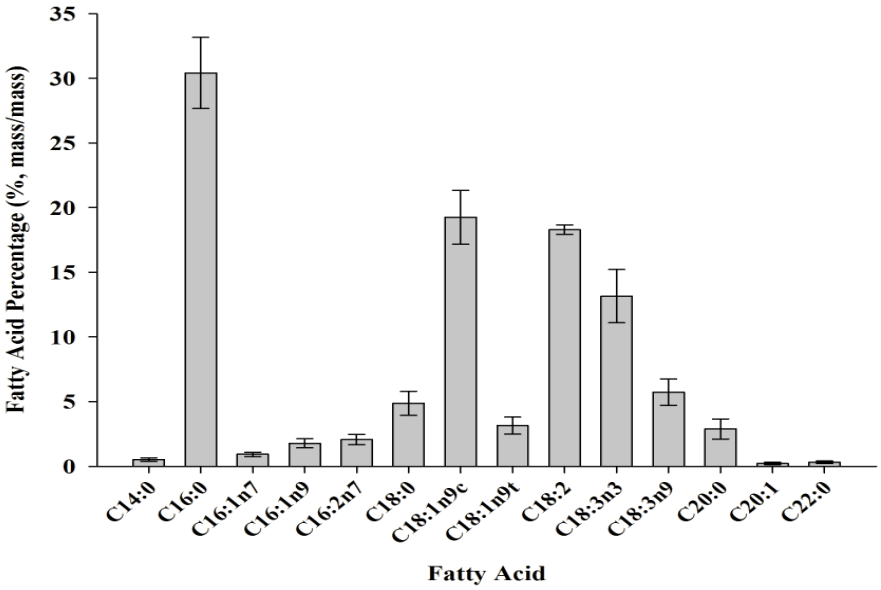

Figure 2.3. Fatty acid compositions percentage (*mean±standard error*, based on the mass of total fatty acid, mass/mass) of the Louisiana *Chlorella vulgaris/Leptolyngbya sp.* co-culture (180 µmol m^{-2} s^{-1} irradiance and 100% nitrogen). (Example of the nomenclature: C18:1n9c means the fatty acid has 18 carbon atoms with one C=C bond. The first double bond is located at the 9^{th} carbon. The "c" at the end of the name indicates it is cis-structure).

Table 2.4. The categorized fatty acid profile of the Louisiana co-culture *Chlorella vulgaris/ Leptolyngbya* co-culture (mean±standard error).

Category	Percentage (%, mass/mass)
Saturated FA	38.97±2.27
Monounsaturated FA (MUFA)	25.31±1.26
Polyunsaturated FA (PUFA)	36.02±2.16
MUFA/(MUFA+PUFA)	41.35±2.00

2.3.4. Estimation of the Energy Efficiency for Irradiance

The caloric content of the lipid produced from the Louisiana co-culture was 29.91±1.17 kJ g^{-1}. The highest energy return on light energy (based on the light energy at each scalar irradiance level) was approximately 0.23% (Figure 2.4). An exponential decay in energy return on light energy (y) with increasing irradiance level (x) was observed ($y=0.38\%e^{-0.002x}$, $R^2=0.953$ for 100% N; $y=0.33\%e^{-0.002x}$, $R^2=0.999$ for 50% N). With respect to the nitrate nitrogen, the lower nitrogen level (50% N of Bold's Basal media) generated lower energy return (of lipid energy) on light energy than the 100% N level ($p<0.0075$). Based on these results, for the indoor

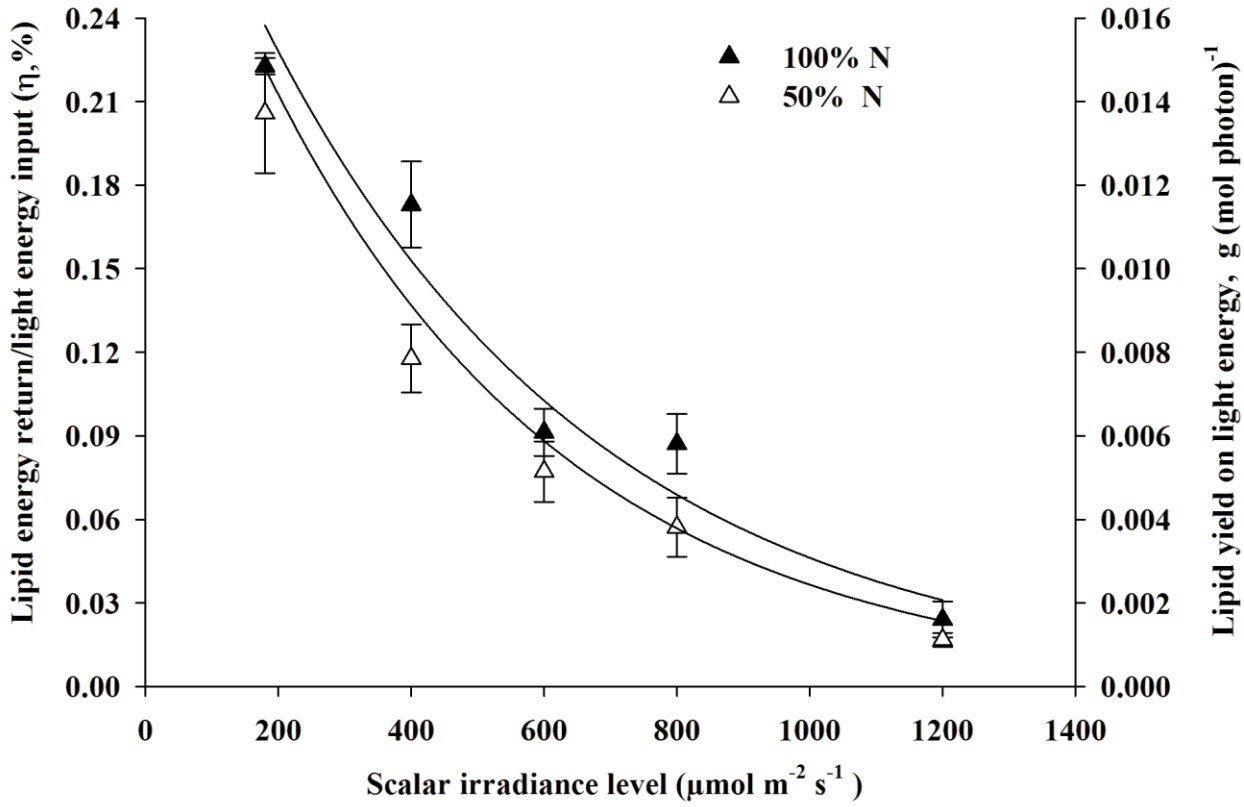

Figure 2.4. Oil energy produced by the algae versus the energy input from the irradiance *Chlorella vulgaris*/*Leptolyngbya sp.* co-culture with five scalar PAR irradiance (180, 400, 600, 800 and 1200 µmol m^{-2} s^{-1}) and two nitrate nitrogen levels (100% N and 50% N).

culture system the lower irradiance (180 μmol $m^{-2}s^{-1}$) with 100% nitrate nitrogen level is more energy efficient than other conditions considering only light energy input for the Louisiana co-culture. However, the lipid productivity was limited at 180 μmol m^{-2} s^{-1} compared to higher irradiance level (400, 800 μmol m^{-2} s^{-1}). For outdoor culture systems, in which the cost of the light source is minimized, the optimal point is the irradiance level with highest lipid productivity (400, 800 μmol m^{-2} s^{-1}). More specifically, for the most commonly used outdoor open pond culture systems, the depth of the culture could be adjusted to get an average irradiance level of 400 ~ 800 μmol m^{-2} s^{-1} to maximize the lipid productivity.

Silaban et al. (under review) reported a highest photosynthetic efficiency of 0.99% for biomass production of the Louisiana co-culture under the same irradiance and nitrogen levels as this work. This value is much lower than other studies on microalgal photosynthetic efficiency. For example, Doucha and Livansky (2009) and Morita et al. (2002) and reported photosynthetic efficiency of 9% and 7.25% respectively. However, these studies are conducted in photobioreactors that have high surface area to volume ratios (153.8 and 101.5 m^2 m^{-3} respectively compared to 44 m^2 m^{-3} in this study), which might be attributed to the high photothynthetic efficiency values in these studies.

The lack of aeration is most likely another factor for the low photosynthetic efficiency in this work. As discussed before, aeration can increase microalgal biomass and lipid productivityby providing uniformed light exposure and lower oxidation stress in the culture. In order to improve the photosynthetic efficiency and energy return (lipid energy) on light energy, the culture surface area to volume ratio need to be increased and aeration has to be applied. However, in a large-scale culture system, the cost of using photobioreactors with large surface area to volume ratios and aeration should be evaluated.

2.4. Conclusions

This work characterized the effects of irradiance and nitrate levels on lipid productivity, neutral lipid percentage and fatty acid profile for a native *Chlorella vulgaris/Leptolyngbya sp.*co-culture. The results indicate this Louisiana native co-culture exhibited high lipid productivity (maximum ~17 g m^{-3} d^{-1}). Neutral lipids comprise ~75% of total lipids, 16- and 18-carbon components dominate the fatty acid profile and approximately 39% of the fatty acids are saturated.

The irradiance affected the lipid percentage (lipid/dry biomass; mass/mass), total lipid productivity and the neutral lipid percentage for this co-culture. For all tested conditions, the optimal irradiance levels were 400 μmol m^{-2} s^{-1}, corresponding to the highest total lipid percentage, total lipid productivity and neutral lipid percentages. The lower lipid productivity for 180 μmol m^{-2} s^{-1} was due to the insufficient energy input while for 1200 μmol m^{-2} s^{-1}, the irradiance energy induced photoinhibition that prevent the lipid production for the Louisiana co-culture. Further study is needed to investigate the reason of lower lipid productivity at 600 μmol m^{-2} s^{-1} than 400 and 800 μmol m^{-2} s^{-1}. Based on these results, the optimal irradiance levels that could be applied in a large-scale culture system to maximize the biodiesel productivity from the biomass feedstock of this native co-culture are 400 μmol m^{-2} s^{-1}. Nitrogen starvation promoted lipid percentage but limited the total lipid productivity and thus should not be applied in the mass production system. The optimum nitrate nitrogen level was 100%. Neither irradiance nor nitrate levels had significant effects on the fatty acid profile of the co-culture, which implied possible consistency of the biodiesel produced from the Louisiana co-culture.

3. LIPID PRODUCTIVITY AND FATTY ACID COMPOSITIONS OF AN AERATED *CHLORELLA VULGARIS/LEPTOLYNGBYA SP*. CO-CULTURE ISOLATED FROM SOUTHERN LOUISIANA

3.1. Introduction

Microalgae have been promoted as one of the most promising feedstocks for biofuel production. Over several decades, numerous studies have been carried out on several aspects of microalgal biofuel production, including strain selection (i.e., Mata et al., 2010; Yoo et al., 2010; Rodolfi et al., 2009; Chisti, 2007), cultivation design (i.e., Ketheesan and Nirmalakhandan, 2011; Zimmerman et al., 2011; Posten, 2009; Rusch and Christensen, 2003; Sukenik et al., 1991), biomass dewatering (i.e., Pearsall et al., 2011; Vandamme et al., 2011; Uduman et al., 2010), and lipid extraction (i.e., Cooney et al., 2009; Cheung et al., 1998). However, there are still some technical issues, which were summarized in the Department of Energy's *National Algal Biofuels Technology Roadmap* (DOE, 2010), which currently inhibit the commercial viability of microalgal biofuels (Davis et al., 2012; Singh and Cu, 2010).

With respect to strain selection, results form previous bench scale studies have indicated that many commercial microalgal strains, including *Chlorella vulgaris*, *Nannochloropsis sp.*, and *Scenedesmus sp.*, exhibit lipid productivities as high as 178 g m^{-3} d^{-1} (Mutanda et al., 2011; Gouveia and Oliveira, 2009; Rodolfi et al., 2009; Chiu et al., 2008; Takagi et al., 2000). Unfortunately, these commercially available strains are usually not robust enough to withstand the conditions in a large-scale outdoor culture system (Sheehan et al., 1998). Recent thought processes (de la Vega et al., 2011; Zhou et al., 2011; Sheehan et al., 1998) consider native microalgae superior to introduced strains as they are already adapted to local climatological conditions and resistant to competing strains (Mutanda et al., 2011). Many recent studies have focused on the use of native strains. For example, after culturing strains originally isolated from local municipal wastewater in a 950 L raceway, Bhatnagar et al. (2011) observed lipid

productivity of 5 g m^{-3} d^{-1}. Likewise, Zhou et al. (2011) isolated five native strains from local municipal wastewater streams, which demonstrated strong adaptability to the wastewater and local environments, and the lipid productivity reached 74.5–77.8 g m^{-3} d^{-1}. De la Vega et al. (2011) identified a *Picochlorum sp.* from the Odiel River in Spain and reported a lipid productivity of 89.7 g m^{-3} d^{-1}. Collectively, these studies suggest that native strains with high lipid productivity can be a viable feedstock source of strains for microalgal biofuels in industrial culture systems.

Fewer documented studies exist detailing the selection of natural cyanobacterial species. In their natural environments, cyanobacteria are often found in symbiosis or symbiosis-like relationships with algae and many other organisms. The cyanobacteria benefit the microalgae in multiple ways, including lowering oxygen levels/stress in the culture, nitrogen fixation, providing growth factors and/or producing Fe, CO_2, NH_4^+, NO_3, or PO_4^{3-} (Graham and Wilcox, 2004). These benefits may enable much higher microalgal growth rates than those observed in monoalgal cultures. Therefore, microalgal/cyanobacterial co-cultures can be advantageous for biofuel production, particularly if such a co-culture is native to the local environment. Rusch and Gutierrez-Wing (unpublished data) have isolated a Louisiana native *Chlorella vulgaris/Leptolyngbya sp.*co-culture native to southern Louisiana and discovered that the presence of *Leptolyngbya sp.* induced higher biomass growth rate of *Chlorella vulgaris* compared to a monoalgal culture of *Chlorella vulgaris*.

Even with ideal species/strain selection, culture system design and operational conditions have to be matched with the species physiology to optimize growth and lipid production. For example, irradiance levels (Bonente et al., 2012; Khoeyi et al., 2012; Benson et al., 2007) and nitrogen concentration (Widjaja et al., 2009; Chu and Alvarez-Cohen, 1998; Suen et al., 1987)

significantly affect the lipid productivity of microalgal cultures. Clearly, a better understanding of how these parameters affect the selected strain's productivity and behavior is a fundamental requirement for economically viable biofuel production.

For phototrophic microalgal cultures, photons provide energy for the light reactions of photosynthesis to synthesize NADPH and ATP (H in light reactions are from oxidation of water), which are used to power the reductive conversion of CO_2 to carbohydrates in the Calvin-Benson cycle. Irradiance levels fluctuate significantly in natural outdoor environments, thus several light acclimation processes have been developed (mainly in photosystem II) to allow microalgal cells to cope with these variations (Falkowski and Raven, 1997). Under irradiance limiting situations, microalgal cells increase their photosynthetic efficiency by regulating the composition and stoichiometry of the peripheral light harvesting antenna subunits (Lhcb) for photosystem II to capture the photon flux more effectively (Bonente et al., 2012; Walters, 2005). The mobile light harvest complex (LHCII-L) in photosystem II can also migrate to photosystem I under low irradiance conditions to compensate for the imbalance of excitation between the two photosystems, which is caused by the difference of maximum absorption spectra between photosystem II and photosystem I (680 nm for photosystem II and 700 nm for photosystem I) (Wollman, 2001). However, it is impossible for these acclimation mechanisms to completely compensate for photon flux under low irradiance levels. Thus, synthesis of NADPH and ATP can be significantly limited due to low excitation energy for photosystem II and photosystem I, resulting in low biomass and lipid productivity. Compared to microalgae, cyanobacteria require little energy to maintain cell function and structure (Mur, 1983). Hence, cyanobacteria are able to maintain a relatively higher growth rate than microalgae under low irradiance conditions (Mur et al., 1999). The presence of phycobilins in the light harvest antennae enables cyanobacteria to

capture light in the range of 500-650 nm (green, yellow and orange), which is hardly absorbed by chlorophyll (Mur et al., 1999). Subsequently, in a microalgal/cyanobacterial co-culture, when the irradiance is significantly limited for the microalgae, the increase of growth rate for cyanobacteria may be able to partially compensate the decrease of growth rate for microalgal cells.

Under oversaturated irradiance conditions (i.e. photoinhibition), for both microalgae and cyanobacteria, the numbers and sizes of the light harvest complexes are reduced to prevent the absorption of excess excitation energy. Nevertheless, oversaturated photon flux leads to the production of reactive oxygen species (ROS), resulting in increased oxidative stress in the culture. Additionally, the recovery from photoinhibition, which involves constant re-synthesis and replacement process of the D1 subunit for photosystem II (Melis, 1999), is highly energy demanding (Simionato et al., 2011) and may significantly affect the energy availability for biomass and lipid production. Therefore, finding the optimum irradiance level of a culture is essential for microalgal/cyanobacterial biofuel production.

Nitrogen availability influences biomass and lipid accumulation in microalgal cultures (Widjaja et al., 2009; Chu and Alvarez-Cohen, 1998; Suen et al., 1987). Within the lipid synthesis pathway, both the citric acid cycle and phospholipids compete with neutral lipids (triacylglycerol and diacylglycerol) for precursors (i.e., pyruvate and acetyl-CoA for the citric acid cycle and phosphatidic acid for phospholipids). When nitrogen is depleted, the cell division and cell growth rates inevitably slow down due to the lack of nitrogen to support protein and enzyme synthesis (Sharma et al., 2012). Thus, the energy required for cell division and other metabolic activities decreases. The demand for the citric acid cycle, the chief energy source for

most metabolic activities, decreases causing more triose phosphate to be utilized for lipid synthesis.

Because of low cell growth and cell division, there is almost no requirement for the synthesis of membrane compounds (Sharma et al., 2012), which are mainly comprised of phospholipids. Therefore, more phosphatidic acid is converted to diacylglycerol (DAG) and triacylglycerol (Ruparelia et al., 2008) as opposed to phosphoslipids, resulting in higher neutral lipid content and lower polar lipid content in the microalgal cells. However, the limited nitrogen level constrains cell division and biomass productivity, which could considerably lower the overall microalgal lipid productivity (Chen et al., 2011b; Converti et al., 2009; Widjaja et al., 2009). The most efficient culture conditions would utilize an optimal nitrogen level promoting maximum lipid productivity by compromising between biomass productivity and total lipid percentage (based on dry biomass, mass/mass). However, the impact of nitrogen limitation/starvation might be alleviated in a microalgal/cyanobacterial co-culture, since many cyanobacterial species have been reported for the ability of nitrogen fixation (Zehr, 2011; Lesser et al., 2007; Vyas and Kumar, 1995).

Manipulating culture conditions for maximum lipid productivity may not produce the best culture conditions for biofuel production, since the neutral lipid percentage may not be optimized. For biofuel production (especially biodiesel), only neutral lipids are converted into fatty acid methyl esters (FAME) (Chen et al., 2009). Fatty acids profiles of microalgae are important because several key properties of biodiesel such as gelling point, viscosity and acidity depend on the fatty acid composition (Kralova and Sjoblom, 2010). In order to use biodiesel in diesel engine, the fuel properties have to comply with the standards such as ASTM D 6751 (specifications for biodiesels blended with middle distillate fuels) and EN 14214 (Automotive

fuels. Fatty acid methyl esters (FAME) for diesel engines. Requirements and test methods). Therefore, fatty acid profile of neutral lipids produced from microalgae has to be investigated. Fatty acid composition for microalgae is species specific (Roncarati et al., 2004; Brown, 1991; Benamotz et al., 1987), but it is influenced by culture conditions (Carvalho and Malcata, 2000; Olson and Ingram, 1975). Irradiance levels are known to affect the ratio of saturated/unsaturated fatty acids (Su et al., 2011; Guedes et al., 2010; Rodolfi et al., 2009; Tsuzuki et al., 1990). Therefore, monitoring the fatty acids profiles associated with different culture conditions and utilizing these conditions to obtain a more desirable fatty acid profile (i.e., close to petro-diesel, chain length of C12 and highly saturated) for biodiesel production is highly recommended.

In this work, an aerated Louisiana native *Chlorella vulgaris*/*Leptolyngbya sp.* co-culture was grown under multiple irradiance and nitrogen levels to provide fundamental data on its potential for biofuels production. The effects of irradiance and nitrogen levels on total lipid percentage (mass/mass, based on dry biomass), lipid productivity, neutral lipid percentage (mass/mass, based on total lipid) and fatty acids profile were assessed.

3.2. Methods and Materials

3.2.1. Strain Selection

The co-culture investigated in this work was a 97%:3% (based on cell count analyses conducted with BD Accuri^{TM} C6 flow cytometer) microalgae:cyanobacteria mixture (Figures 3.1 and 3.2) originally isolated from College Lake near Louisiana State University, Baton Rouge, Louisiana. The identification analysis of this co-culture was done by the Culture Collection of Algae, University of Texas (UTEX) under the direction of Dr. Nobles. The microalgal species was identified as *Chlorella vulgaris* by sequence analysis of ITS2 rDNA region. The cyanobacteria most probably belongs to the genus *Leptolyngbya*, according to sequence analysis

of 23S rDNA region. Throughout this paper, this mixture will be referred as the "Louisiana co-culture".

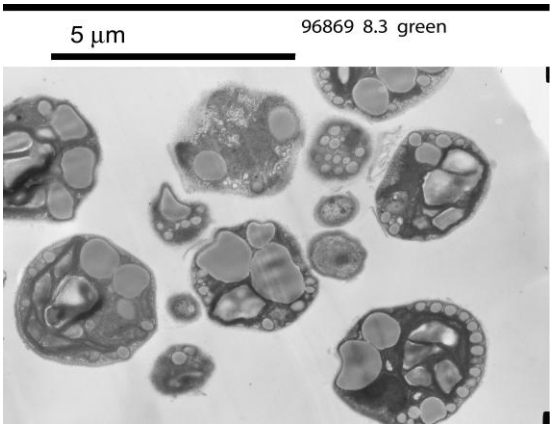

Figure 3.1. TEM image of the *Chlorella vulgaris/Leptolyngbya* in the Louisiana co-culture.

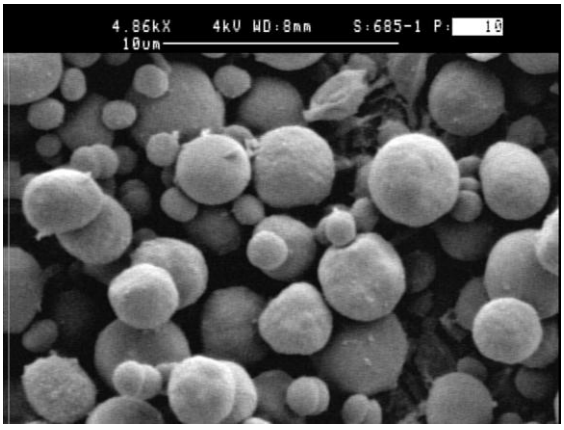

Figure 3.2. SEM image of the *Chlorella vulgaris/Leptolyngbya* in the Louisiana co-culture.

3.2.2. Co-culture Cultivation

Stock Culture

Stock cultures of *Chlorella vulgaris*/*Leptolyngbya sp.* were maintained in Bold's basal medium ($NaNO_3$ 2.94 mM for 100% N and 1.47 mM for 50% N, $CaCl_2 \cdot H_2O$ 0.17 mM, $MgSO_4 \cdot 7H_2O$ 0.3 mM, K_2HPO_4 0.43 mM, KH_2PO_4 1.29 mM, NaCl 0.43 mM, P-IV metal solution comprised of $Na_2EDTA \cdot 2H_2O$, $FeCl_3 \cdot 6H_2O$, $MnCl_2 \cdot 4H_2O$, $ZnCl_2$, $CoCl_2 \cdot 6H_2O$, $Na_2MoO_4 \cdot 2H_2O$, vitamin solution which contains vitamin B_{12}, biotin and thiamine). Continuous surface incident irradiance of 310 µmol m^{-2} s^{-1} was to provided to the 1 L stock cultures (in 2L Erlenmeyer flasks) by 400 watt HPS (High Pressure Sodium) lamps. The temperature was maintained at 25±2^{o}C. Continuous aeration was maintained at an airflow rate of 0.47 L min^{-1}. Carbon dioxide was bubbled through the cultures at an flow rate of 0.47 L min^{-1} for 1 minute every day to maintain the pH at 7-8. One third of the culture was removed and replaced by the Bold's Basal medium each week.

Experiment Setup

A two-factorial, randomized block design (five internal scalar irradiance levels × two nitrate nitrogen levels) was used in this work. The experiment was performed in sequential triplicates. The two nitrate nitrogen levels (culture time t=0) were 2.94 mM N and 1.47 mM N, equivalent to 100% (treatment 100%) and 50% (treatment 50%) of the Bold's Basal medium nitrate nitrogen concentration. The five internal scalar irradiance levels (I_s) (culture time t=0 and culture concentration x=0) were 180, 400, 600, 800 and 1200 µmol m^{-2} s^{-1} (equivalent to incident irradiance level of 103, 310, 520, 715 and 1078 µmol m^{-2} s^{-1}). The internal scalar irradiance levels were measured by completely submerging a LI-193 spherical quantum irradiance sensor in the culture media. The incident irradiance sensor was measured with a LI-190 flat quantum sensor by inserting the sensor into a 2 L Erlenmeyer flask through a hole at the bottom. The varying levels were achieved by adjusting the vertical distance between the HPS (High Pressure Sodium) lamps and the surface of the cultures. Scalar irradiance level was used in this study because it provides a better estimate of the light energy input for the glass Erlenmeyer flask. Since the studies were conducted in a volume of 1 liter, the internal scalar irradiance was also approximately the surface irradiance.

The experiments were conducted in batch mode using 2 L Erlenmeyer flasks containing 1 L of culture with the initial concentration of 100 g m^{-3}. The phosphorus concentration was maintained at 1.72 mM for all the cultures (Bold's Basal media level). The nitrogen and phosphorus level were determined according to Standard Method 4110 (Ion Chromatography using Dionex™ IC25). An air pump was connected to a 5 mL sterile serological pipette via silicone tubing, and the end of pipette was submerged in each to maintain a continuous airflow rate of 0.47 L min^{-1}. Every 72 minutes, carbon dioxide was added at 0.24 L min^{-1} for 2 minutes,

resulting a carbon dioxide concentration of 2% v/v (based on the aeration flow rate) and a pH at 7.0±0.5. The culture temperature was maintained at 25±1^{o}C by a water bath. Sterile, deionized water was added to each flask daily to compensate for evaporation losses.

Four milliliters of sample were collected daily from each flask and optical density was measured at wavelength 664 nm and 750 nm with a HACH DR/4000 UV/Vis spectrophotometer. The optical density at 664 nm is correlated to chlorophyll-a content while the measurement at 750 nm estimate the turbidity of the culture. When the optical density readings stopped increasing for two consecutive days (two days into stationary phase), the culture from each flask was transferred into a one-liter plastic (HDPE) bottle and stored in a freezer at -20^{o}C until analyzed.

3.2.3. Biomass Productivity

Dry biomass analysis followed LSU Civil and Environmental Engineering Water Quality Lab SOP PA 200, which was adapted from Standard Method 2540D (Total suspended solids, APHA, 2001). Instead of GF/F filters (0.7 μm pore size), GF/C filters (1.2 μm pore size) were used in this protocol due to prolonged filtration time by using GF/F filters with smaller pore size. Flow cytometry (BD Accuri^{TM} C6) analyses on decant liquid revealed no cell loss through the GF/C filter during the filtration process. GF/C filters were washed and ashed at 550^{o}C for 30 minutes. Ten milliliters of initial (t=0) and five milliliters of the final Louisiana co-culture from each flask was filtered through a pre-weighed GF/C filter. The filter and microalgal biomass were dried at 65^{o}C for three hours, cooled in a desiccator for one hour and the final mass of the sample recorded. For each culture conditions, one sample from each culture was analyzed.

A calibration curve for each treatment was prepared to convert daily optical density readings into daily biomass concentration. Only the optical density readings at the wavelength of 664 nm are used since the chlorophyll-a has better correlation with the biomass concentration of

the co-culture. At the end of the experiment, the culture was collected and diluted to five different biomass concentrations. The optical density at wavelength 664 nm and actual dry biomass were measured for each dilution level. Finally, the calibration curve was fitted by linear regression to correlate the daily optical density readings and daily biomass concentrations. The daily biomass concentrations (in the exponential growth phase) were used to calculate the biomass productivity (g m^{-3} d^{-1}).

3.2.4. Lipid Extraction

Soxhlet extraction was used to evaluate the total lipid percentage for the co-culture. Although Soxhlet extraction will not be commercially feasible for large scale lipid extraction due to prolonged heating duration, it is considered to provide more complete lipid extraction than other methods (i.e. Foch's or Bligh and Dyer methods) (Siddiquee and Rohani, 2011; Bligh and Dyer, 1959; Folch et al., 1957). The biomass of 120 mL co-culture sample from each flask was filtered through the GF/C filter and dried at 65^{o}C for one hour. The total lipid content was extracted over four hours using chloroform:methanol 2:1 (v:v). Finally, the solvent was evaporated using a rotary evaporator, and the final mass of lipid was recorded. The lipid productivity (Díaz-Visurraga et al.) (g m^{-3} d^{-1}) was calculated by multiplying the total lipid percentage (% of the dry biomass, mass/mass) by the biomass productivity (g m^{-3} d^{-1}).

3.2.5. Lipid Fraction Analysis

The neutral lipid content as a percent of total lipids (mass/mass) was analyzed to provide a better estimate of lipids available for conversion into biodiesel. The neutral and polar fractions of total lipid samples were determined as described by Pernet et al. (2006) and summarized here. The polar and neutral lipids were separated by Sep-Pak^{TM} pre-packed columns with Si-NH_2 sorbent. The column was first preconditioned by eluting methanol followed by chloroform. The total lipid samples were dissolved in chloroform and loaded in the sorbent. Neutral lipids were

eluted by a chloroform:isopropanol 2:1 (v:v) solution. Subsequently, polar lipids were eluted by methanol. The solvents were evaporated and the mass of polar and neutral portions was determined.

3.2.6. Fatty Acid Analysis

The neutral lipid fraction was converted into fatty acid methyl esters (FAMEs) via transesterification, and the fatty acid composition was analyzed by gas chromatograph. The transesterification procedure followed IUPAC Method II.D.19 (IUPAC, 1979). Ten milliliters of 0.5 M NaOH methanolic solution was added into the neutral lipid sample, and the mixture was boiled for 10 minutes. Boron trifluoride (BF_3) methanolic solution was then added into the mixture and boiled for two minutes. After adding 1.5 mL heptane and boiling for one minute, 20 mL of saturated NaCl solution was slowly added into the flask to form a two-phase liquid system (FAME and heptane in the upper phase). About 1 mL upper phase was transferred into a 2 mL vial. Finally, 0.03g of $NaSO_4$ was added into the vial to remove trace water.

An HP 5890 Series II gas chromatograph with SP^{TM}-2380 column (30 m, 0.25mm ID, 0.20μm film) was utilized to determine the fatty acids composition. The flow rate of the carrier gas (helium) was 2 mL min^{-1}. The initial oven temperature was set at 80^{o}C. After 1 minute, the temperature was increased by 4^{o}C min^{-1} until a final temperature of 220^{o}C was achieved. This temperature was maintained for 5 minutes. The gas chromatography data were analyzed with Chemstation^{TM} software, and the mass percentage of each fatty acid component was reported. Triplicates were done for each FAME sample.

3.2.7. Estimation of the Energy Return (Lipid Energy) on Light Energy Input

To evaluate the ability of the Louisiana co-culture to convert light energy into lipid energy, the energy return (lipid energy) on energy input (light energy) was calculated. Since energy return on investment (EROI) evaluates the energy efficiency for the culture system,

which is not emphasized in a bench-top scale experiment, EROI was not used. The calculation of lipid yield per mole photons was adapted from the work of Zijffers et al. (2010) on biomass yield:

$$Y_{lipid\ ,E} = \frac{P_L}{I_s \times 10^{-6} \times 8.64 \times 10^4} \times \frac{V}{A} \quad (1)$$

Where $Y_{lipid,\ E}$ is the lipid yield per mole photons, P_L (g m^{-3} d^{-1}) is the lipid productivity, V/A is the volume to wetted surface area (excluding the bottom) ratio of the culture (0.023 m^3 m^{-2} for the 1 L cultures in 2 L Erlenmeyer flasks).

The lipid caloric content (C_L, kJ g^{-1}) was determined with a Parr 6200 isoperibol calorimeter. The sample of 0.5 g of total lipid in sample cup was installed into the caloric bomb, and a platinum ignition wire was attached to the lipid sample. The caloric bomb was charged with O_2 till the pressure reached 10-35 atm. The platinum wire then was ignited. After the run finished, the caloric content of the lipid was automatically calculated. Duplicates were done. The energy return of lipid on light energy was calculated following the equation:

$$\eta = Y_{\boldsymbol{Lipid,E}} \times \frac{C_L}{E} \quad (2)$$

Where η (%) is the energy return of lipid on the light energy for each irradiance level. E (kJ (mole photon)$^{-1}$) is a parameter to convert the scalar irradiance to energy. For HPS lamps, E is estimated to be 201 kJ (mole photon)$^{-1}$ as reported by Thimijan and Heins (1983). The calculated η was plotted against each internal scalar irradiance level (where the culture concentration x=0) to investigate the effects of irradiance levels on the energy return (lipid energy) on light energy input.

3.2.8. Data Analyses

The mean and standard deviation of the triplicates under each treatment on the total lipid percentage (% of dry biomass, mass/mass), lipid productivity (g m^{-3} d^{-1}), neutral lipid percentage (% of total lipid, mass/mass), energy return on light energy (% of energy for each scalar irradiance level) were reported. For fatty acid percentage (% of total FAME, mass/mass) mean and standard error was calculated. The statistical significance of the treatment effects (scalar irradiance and nitrate nitrogen levels) on all measurements was determined by two-way ANOVA using SAS^{TM} (9.1.3). Tukey's test was used for multiple comparisons. Significance was determined at an α=0.05.

3.3. Results and Discussion

3.3.1. Total Lipid Percentage and Productivity

The nitrate nitrogen levels had no significant effects on total lipid percentage (p=0.0928) but had significant impacts on lipid productivity (p=0.0003) (Tables 3.1 and 3.2). The 50% nitrogen level resulted in lower lipid productivity. At the same scalar irradiance level, biomass and lipid productivity ratios of 50% and 100% nitrogen levels (biomass productivity at 50% N divided by biomass productivity at 100% N; lipid productivity at 50% N divided by lipid productivity at 100% N) had no significant difference (Table 3.1), indicating that the decrease of lipid productivity at 50% N level was mainly caused by constraining biomass productivity.

The total lipid percentage (Table 3.1) was approximately 35% (26.8% at t=0) for all tested conditions, similar to other works on *Chlorella vulgaris* (Bai et al., (under review); Abou-Shanab et al., 2011; Lv et al., 2010; Yeh et al., 2010; Liang et al., 2009; Rodolfi et al., 2009; Widjaja et al., 2009; Illman et al., 2000). However, the nutrients limitation did not increase total lipid percentage (on dry biomass, mass/mass) (Table 3.1). This result differs from other researchers (Bai et al., (under review); Widjaja et al., 2009; Suen et al., 1987) that showed an

increase in total lipid percentage with decreased nitrogen availability. Bai et al. (under review)) applied nitrogen starvation (50% nitrogen of Bold's Basal medium level) to the same Louisiana co-culture without extra CO_2 addition, and found the lipid percentage increased about 5%. Widjaja et al. (2009) reported a 10~20% increase of lipid percentage for *Chlorella vulgaris* with nitrogen depletion. Illamn et al. (2000) increased lipid content of *Chlorella sp.* by 23% by applying 50% nitrogen of the Watanbe medium. The lack of significant difference in maximum total lipid percentage between 50% and 100% nitrogen at all tested scalar irradiance levels may be due to over-saturation with CO_2, allowing for copious carbon uptake (stored as lipids) after the depletion of the nitrogen.

Table 3.1. Total lipid percentage (based on dry biomass, mass/mass) of the Louisiana *Chlorella vulgaris/Leptolyngbya* co-culture with five scalar irradiance and two nitrogen levels.

Irradiance ($\mu mol\ m^{-2}\ s^{-1}$)	Lipid percentage (%, mass/mass, based on dry biomass)	
	50% N	100%N
180	37.1±2.26	30.6±3.73
400	34.2±2.53	33.7±5.58
600	38.8±0.89	37.5±1.03
800	33.1±4.31	36.3±3.26
1200	36.6±4.22	32.4±2.40

* *mean±standard deviation*

The irradiance levels did not have significant impacts on total lipid percentage (p=0.1021) (based on dry biomass, mass/mass) (Table 3.1) or productivity (p=0.0676) (Table 3.2). However, the higher mean values of lipid productivity at 800 $\mu mol\ m^{-2}\ s^{-1}$ and 100% N indicated the optimal irradiance level for biomass accumulation of this co-culture was most likely close to 800 $\mu mol\ m^{-2}\ s^{-1}$, which matched the results of Silaban et al. ((under reivew)) for the same co- culture. The highest lipid productivity of the Louisiana co-culture in this study was significantly higher than other reported studies on *Chlorella vulgaris* (Bai et al., (under review); Abou-Shanab et al., 2011; Lv et al., 2010; Yeh et al., 2010; Liang et al., 2009; Rodolfi et al.,

2009; Widjaja et al., 2009; Illman et al., 2000) (Table 3.3). All these studies were conducted with the irradiance levels below 100 µmol m^{-2} s^{-1} (Table 3.3), compared to 800 µmol m^{-2} s^{-1} for the highest lipid productivity in this study. Lower irradiance might induce photolimitation, which could limit the lipid productivity. Therefore, the high lipid productivity in this study might be attributed to the higher irradiance levels.

Table 3.2. Total lipid productivity (g m^{-3} d^{-1}) of the Louisiana *Chlorella vulgaris*/*Leptolyngbya* co-culture with five scalar irradiance and two nitrogen levels; Biomass productivity ratio and lipid productivity ratio of the co-culture with 50%N and 100%N under five scalar irradiance levels.

Irradiance	Lipid productivity (g m^{-3} d^{-1})		Biomass productivity ratio	Lipid productivity ratio
(µmol m^{-2} s^{-1})	50%N	100%N	50%N/100%N	50%N/100%N
180	72.6 ± 16.7^{abc}	76.7 ± 13.6^{abc}	$0.785\pm0.176_{AB}$	$0.941\pm0.050_{A}$
400	72.5 ± 20.3^{abc}	96.1 ± 2.9^{abc}	$0.720\pm0.048_{ABC}$	$0.753\pm0.200_{AB}$
600	95.8 ± 12.8^{abc}	111 ± 34.8^{ab}	$0.895\pm0.297_{A}$	$0.928\pm0.315_{A}$
800	59.2 ± 16.0^{c}	116 ± 18.6^{a}	$0.556\pm0.038_{BC}$	$0.508\pm0.071_{C}$
1200	68.7 ± 10.3^{bc}	99.0 ± 22.6^{abc}	$0.622\pm0.016_{BC}$	$0.702\pm0.067_{ABC}$

* *mean±standard deviation*

[a-c] Values with different superscript letters indicate a significant difference ($p<0.05$) while values share same superscript letters indicate no significant difference, based on Tukey's test.

[A-C] Values with different subscript letters indicate a significant difference ($p<0.05$) while values share same superscript letters indicate no significant difference, based on Tukey's test.

The presence of *Leptolyngbya sp.* in this co-culture could be another factor that induced the high lipid productivity. In these studies that reported lower lipid productivities (4-78 g m^{-3} d^{-1}) (Bai et al., (under review); Abou-Shanab et al., 2011; Lv et al., 2010; Yeh et al., 2010; Liang et al., 2009; Rodolfi et al., 2009; Widjaja et al., 2009; Illman et al., 2000), mono-algal *Chlorella vulgaris* culture was utilized, while this work studied on *Chlorella vulgaris*/*Leptolyngbya* co-culture. It has been showed that the *Leptolyngbya sp.* could increase the cell counts of *Chlorella vulgaris* to approximately 20 times those of mono-algal *Chlorella vulgaris* culture (Rusch and Gutierrez-Wing (unpublished data)). Most likely, the increase of cell counts of *Chlorella*

vulgaris cells resulted in higher biomass and lipid productivity. This high productivity of the Louisiana co-culture implied the possible advantages of using microalgal/cyanobacterial co-culture and its potential as a biodiesel producer.

Higher CO_2 concentrations were likely another factor in the high lipid productivity. Abou-shanab et al. (2011) and Liang et al. (2009) reported lipid productivity of 20.9 and 4 g m^{-3} d^{-1} respectively from *Chlorella vulgaris* culture without CO_2 addition. Other studies, such as Bai et al. (under review), Lv et al. (2010) and Widjaja et al. (2009) applied CO_2 with lower concentrations (daily injection, 1% and 0.3% compared to 2% in this study) also reported significnatly lower lipid productivity (Table 3.3). In photosynthesis, CO_2 was assimilated via carboxylation under the catalysis of Rubisco (Ribulose-1,5-bisphosphate carboxylase oxygenase). However, O_2 competes with CO_2 for the same active sites of Rubisco (Horton et al., 2002) for photorespiration, which consumes organic carbon without any energy gain. High CO_2 concentrations might be able to increase the carboxylation rate and suppress photorespiration simultaneously. Consequently, more 3-phosphoglycerate was produced via carboxylation and less energy was consumed in photorespiration, resulting in high lipid productivity.

Aeration might also contribute to high lipid productivity in this work, especially when it is compared to Bai et al. (under review) that reported lipid productivity of 17 g m^{-3} d^{-1} for the *Chlorella vulgaris*/*Leptolyngbya sp.* co-ctulture without applying any agitation or mixing. By disrupting the accumulation of oxygen in the culture through physical displacement (Bunt, 1971), aeration significantly increased carboxylation while suppressing photorespiration (as discussed in the preceding paragraph). Additionally, aeration could improve the uptake and exudation rate of the metabolic products for the microalgal cells (Singh and Dhar, 2011). Finally, by mixing the culture (Wang et al., 2005), aeration provided uniform light exposure for all cells,

Table 3.3. The lipid productivity of *Chlorella vulgaris* from other studies.

Author	Irradiance ($\mu mol\ m^{-2}\ s^{-1}$)	Nitrogen	Aeration	Lipid productivity ($g\ m^{-3}\ d^{-1}$)
This work	800	2.94 mM	Continuous aeration at 0.47 L min^{-1} with 2% CO_2	116
Bai et al. (under review)	800	2.94 mM	No aeration, CO_2 0.47 L min^{-1} for 20 seconds daily	18
Abou-Shanab et al. (2011)	N/A	2.94 mM	Shaking at 150 rpm, no CO_2	20.9
Illman et al. (2000)	76	3.08 mM	Continuous aeration at 1 L min^{-1} with 5% CO_2 v/v	14.8
Liang et al. (2009)	N/A	2.94 mM	Continuous aeration at 0.2 L min^{-1} without CO_2	4
Lv et al. (2010)	60	0.99 mM	Continuous aeration with 1% CO_2 v/v	40
Kuei-ling Yeh et al. (2011)	60	3.09 mM	Continuous aeration at 0.2 L min^{-1} with 2% CO_2 v/v	78
Kuei-ling Yeh et al. (2010)	60	2.94 mM	Continuous aeration with 2% CO_2, v/v	56
Widjaja et al. (2009)	30	5.01 mM	Continuous aeration at 6 L min^{-1} with 0.3% CO_2, v/v	14
Rodolfi et al. (2009)	100	17.6 mM	Continuous aeration with 5% CO_2, v/v	36.9

preventing both irradiance oversaturation for cells close to the light source and photo-limitation for cells far away.

Interestingly, in the previous work conducted on the same strain (without aeration and excess CO_2), there was a considerable decrease in lipid productivity caused by photoinhibition at

the scalar irradiance level of 1200 µmol m^{-2} s^{-1} (Bai et al., (under review)). The lack of photoinhibition in this work at 1200 µmol m^{-2} s^{-1} (Table 3.3) is likely due to the additional CO_2 used to control the culture pH. When the irradiance is oversaturated, the electrons provide by the donor side in photosystem II cannot keep up with the oxidation rate of P680, resulting in the accumulation of $P680^+$ (Klimov et al., 1997). The high oxidative ability of $P680^+$ can cause irreversible damage of proteins and pigment (Klimov et al., 1990). Others have observed that under high irradiance conditions bicarbonate in the culture medium can stabilize the Mn center, which functions on the electron donor side of the photosystem II (Zharmukhamedov et al., 2007; Klimov et al., 1997), enabling the donor side of photosystem II to function normally under high irradiance. The excess CO_2 bubbled through the culture presumably led to an increase in dissolved CO_2 (0.16 g L^{-1}, estimation based on Henry's law) and ultimately a consistent supply of bicarbonate in the medium, preventing the photoinhibition effects.

3.3.2. Neutral Lipid Percentage

A high concentration of neutral lipids is desirable as it is the only portion of the total lipids used to produce biodiesel. Approximately 87.0% of the total lipid content of the Louisiana co-culture was neutral lipids (Table 3.4). This percentage is the highest compared to values previously reported for microalgal strains (Bai et al., (under review); Ryckebosch et al., 2012b; Zhu et al., 1997; Suen et al., 1987; Piorreck et al., 1984). Piorreck et al. (1984) reported a neutral lipid percentage of 83.3% for *Chlorella vulgaris* when nitrogen level was 0.1 and 0.03 mM, but the neutral lipid percentage dropped to 66.7% when nitrogen level was increase to about 0.3 mM. Ryckebosch et al. (2012) reported ~80% neutral lipid percentage for *Phaeodactylum tricornutum* without addition of CO_2 in the aeration. The highest neutral lipid percentage reported in Zhu et al. (1997) was ~60% for *Isochrysis galbana* with continuous aeration at irradiance level of 200 µmol m^{-2} s^{-1}. Suen et al. (1987) was able to get ~80% neutral lipids over total lipids from

Nannochloropsis sp. with low nitrogen media. Bai et al. (under review) reported ~75% neutral lipids from the *Chlorella vulgaris*/*Leptolyngbya sp.* co-culture without continuous aeration and CO_2 addition under the same nitrogen and irradiance levels tested in this work. Compared to this study, none of these reported studies applied CO_2 addition. It is highly likely that the low CO_2 concentration limited neutral lipid production in these reported studies and the 2% CO_2 in aeration in this work was the main factors that attributed to the high neutral lipid percentage. Higher CO_2 concentration in the culture would increase carboxylation rate (as discussed earlier) and provide sufficient CO_2 supply for Calvin-Benson cycle, which produces precursors for lipids (such as 3-phosphoglycerate). When microalgal culture entered late exponential/stationary phase, cell division ceased. The requirement to produce new membrane structure diminished. Thus, phospholipids, the major polar lipids source, are no longer necessary and no longer produced (Sharma et al., 2012). The 3-phosphoglycerate, which is the precursor for both phospholipids and neutral lipids, is preferentially converted to neutral lipids (Deng et al., 2011). Higher CO_2 supply in late exponential/stationary phase will more likely ensure sufficient 3-phosphoglycerate productions, resulting in higher neutral lipid percentage than carbon limited microalgal cultures.

Neither the scalar irradiance levels (p=0.6422) nor the nitrogen levels (p=0.7644) tested in this work had significant impact on the neutral lipid percentage. However, in Bai et al. (under

Table 3.4. Neutral lipid percentage over the total lipid (mass/mass) for the Louisiana co-culture with five scalar irradiance and two nitrogen levels.

Irradiance (μmol m^{-2} s^{-1})	Neutral lipid percentage (%, mass/massbased on total lipid) 50% N	100%N
180	87.2±4.14	87.9±3.33
400	88.7±1.01	87.8±2.53
600	88.5±1.91	86.0±2.85
800	88.0±1.33	89.4±0.94
1200	87.4±0.71	89.7±0.70

[*] *mean±standard deviation*

review), a 10% decrease in neutral lipid percentage over total lipid at the scalar irradiance level of 1200 µmol m^{-2} s^{-1} was observed for the Louisiana co-culture without continuous aeration or 2% CO_2 v/v. The absence of the decrease in neutral lipid percentage at 1200 µmol m^{-2} s^{-1} in this work might be attributed to both aeration and higher CO_2 addition. As discussed before, aeration could lower the O_2 concentration by disrupting the O_2 accumulation in the culture, increasing carboxylation and suppressing photorespiration. By mixing the culture, aeration could prevent irradiance oversaturation for cells close to the light source and photo-limitation for cells far away. Higher CO_2 addition most likely resulted in higher bicarbonate concentration protected the photosystem II from photoinhibition. Therefore, the Louisiana co-culture under 1200 µmol m^{-2} s^{-1} scalar irradiance maintained the same neutral lipid productivity as the other irradiance levels.

The 50% nitrate nitrogen (1.47 mM) did not result in higher neutral lipid percentage in this work. It is most likely because this nitrogen level was not low enough to cause a significant increase in neutral lipid accumulation. Piorreck et al. (1984) tested the neutral lipid percentage (based on total lipids) with different nitrogen levels (0.03-10 mM) for *Chlorella vulgaris* cultures. The results showed that the neutral lipid percentage did not have a significant increase until it dropped to 0.297 mM. Most likely, the 50% nitrogen level (1.47 mM) tested in this work was too high to induce higher neutral lipid percentage. Therefore, lower nitrogen level should be tested in the future.

3.3.3. Fatty Acid Compositions

To use the biodiesel in current diesel engines, multiple fuel properties, such as cetane number, oxidation stability, viscosity etc., have to comply with the technical standards. The most commonly used standards for biodiesel include ASTM D 6751 standard (specifications for biodiesels blended with middle distillate fuels) and EN 14214 (Automotive fuels. Fatty acid methyl esters (FAME) for diesel engines. Requirements and test methods.). However, these

standards present the limits for the properties of biodiesel other than specific requirements for fatty acid profiles of the methyl ester (FAME). To correlated the fatty acid profiles to the technical standards, Ramos et al. (2009) developed a predictive relationship based on the fatty acid profile (% mass/mass, of saturated, monounsaturated, polyunsaturated fatty acids) and the EN 14214 standards. Based on Ramos' study, in order to meet the EN 14214 standards, the saturated fatty acids have to be in the range of 30~60% of total fatty acids (mass/mass) and 50% of the unsaturated fatty acids have to be monounsaturated.

In this work, there were 14 types fatty acids identified in each sample. The major fatty acids were 16-carbon (~40%) and 18-carbon (~55%) (Figure 3.3), similar to biodiesels produced from other types of feed stocks, such as rape seeds, soy bean and palm etc. (Tyson, 2001). Compared to the petrol diesel (C12 on average), the chain length of biodiesel is much longer. However, it is reported that the properties of biodiesel that mainly contains C16 and C18 fatty acids was close to the petrol diesel (Tyson, 2001). Therefore, most likely, the longer chain length of the fatty acids produced from the Louisiana co-culture than the petrol diesel should not significantly impacts fuel quality of the biodiesel.

Saturated fatty acids from the Louisiana co-culture in this work accounted for approximately 33.64±0.83% (Table 3.5) of the total fatty acid content, which satisfied the criteria from Ramos et al. (2009). However, the polyunsaturated fatty acids exceeded the limits (50% of total unsaturated fatty acids) (Table 3.5). High polyunsaturated fatty acid content could results in lower cetane number and poor oxidative stability for biodiesels (Rasoul-Amini et al., 2011). Additionally, fuels with high unsaturated fatty acid content are more corrosive to metals (Lee et al., 2010a; Kaul et al., 2007), which could hamper biodiesel integration to the existing fuel distribution infrastructure (transportation pipe, storage tank) (Wang et al., 2011).

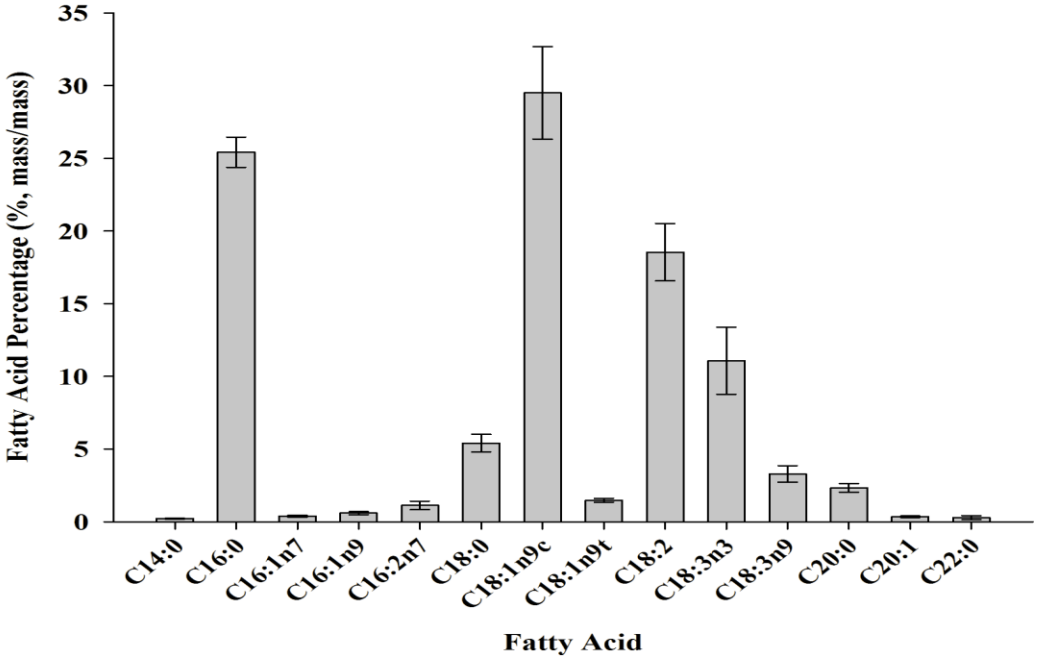

Figure 3.3. Fatty acid compositions percentage (based on the mass of total fatty acid, mass/mass) of the Louisiana *Chlorella vulgaris/Leptolyngbya* co-culture. (Example of the nomenclature: C18:1n9c means the fatty acid has 18 carbon atoms with one C=C bond. The first double bond is located at the 9th carbon. The "c" at the end of the name indicates it is cis-structure).

Table 3.5. The categorized fatty acid profile of the Louisiana co-culture *Chlorella vulgaris/Leptolyngbya* co-culture (*mean±standard error*).

Category	Percentage (%, mass/mass)
Saturated FA	33.64±0.83
Monounsaturated FA (MUFA)	32.30±1.87
Polyunsaturated FA (PUFA)	34.02±2.02
MUFA/(MUFA+PUFA)	48.72±2.86

Currently, there are three methods to increase the saturated fatty acid content in biodiesel: genetic engineering, distillation, and catalytic hydrogenation (Pozdeev et al., 2012). Genetic engineering is advantageous due to its low energy cost. However, many consider genetically modified organisms to be a potential risk to local ecosystems (Keri Carstens, 2011).

Furthermore, legal and social concerns will likely prevent large-scale, transgenic microalgae culture in many countries (de la Vega et al., 2011). Distillation can be useful but the high energy cost (Pozdeev et al., 2012) and waste of unsaturated fatty acids are major concerns for this method. Catalytic hydrogenation could be another option to de-saturate the biodiesel. However, searching for proper catalysts to selectively hydrogenate polyunsaturated fatty acids is still the main challenge (Souza et al., 2012). Besides these methods to lower unsaturated fatty acid content, biodiesel could be blended with petrol diesel to improve the fuel properties (oxidation stability, cetane number etc.).

Bai et al. (under review) investigated the fatty acid profile of the Louisiana co-culture cultivated without aeration and 2% CO_2 addition but under the same irradiance and nitrogen levels as this work. The comparison between this study (Figure 3.3) and Bai et al. (under review) indicated that aeration and 2% CO_2 did not significantly change the fatty acid profile of the Louisiana co-culture. The difference was probably caused by biological variances. However others reported significantly different fatty acid profiles of *Chlorella vulgaris* from the Louisiana co-culture this work (Ryckebosch et al., 2012b; Yusof et al., 2011; Piorreck et al., 1984). Piorreck et al. (1984) reported ~16.5% saturated fatty acid from *Chlorella vulgaris* cultivated with 2.97 mM nitrate nitrogen level, much lower than ~33.6% reported in this work. The saturated fatty acids were ~17.7% (~33.6% in this work) and the C18:3 was ~30.2% (~14.3% in this work) in Ryckebosch et al. (2012). Yusof et al. (2011) reported ~47.1% saturated fatty acids for *Chlorella vulgaris* cultivated under aeration with 1% CO_2. These differences might be attributed to biological variance in the same species. Additionally, the different cultivation conditions in the reported studies might be another factor caused variance of fatty acid profiles.

According to the predictive correlation between fatty acid profile and EN14214 standards developed by Ramos et al. (2009), none of the fatty acid profiles in these reported studies would satisfy EN 14214 standards due to high unsaturated fatty acids or polyunsaturated content. Therefore, the biodiesel produced from *Chlorella vulgaris* in these studies needs to be de-saturated using the methods discussed in preceding paragraph or blend with the petrol diesel to improve the fuel properties.

Neither the scalar irradiance levels nor the nitrogen levels had significant effects on the percentage (mass/mass, based on total fatty acids) of any individual fatty acid (all the p values are greater than 0.05 in Tukey's test). For the impacts of irradiance on fatty acid profile, others reported the irradiance level had no significant effects on fatty acid composition of microalgae until it reached a significantly high level. Tedesco et al. (1989) reported that fatty acid composition of *Spirulina platensis* was not affected by irradiance in the range of 170~870 μmol m^{-2} s^{-1}, but the percentage of γ-linolenic acid increased when the irradiance level reach 1411 μmol m^{-2} s^{-1}. Renaud et al. (1991) investigated the fatty acid composition of *Isochrysis sp*. under different irradiance levels, and observed significant changes in fatty acid composition when the irradiance increased from 620 to 1200 μmol m^{-2} s^{-1}. However, no significant difference was shown between the irradiance level of 390 and 620 μmol m^{-2} s^{-1} in Renaud et al. (1991). These results implied that higher irradiance level (>1200 μmol m^{-2} s^{-1}) might be required in order to induce the variation in fatty acid profiles for the Louisiana co- culture. For the effects of nitrogen concentrations, Piorreck et al. (1984) observed that the fatty acid composition of *Chlorella vulgaris* did not vary until the nitrate nitrogen level drop from 10 mM to 0.30 mM, which was much lower than the nitrogen levels tested in this work (2.94 and 1.47 mM). Thus, it is likely that

the nitrogen levels tested in this work were not low enough to affect the fatty acid compositions for the Louisiana co-culture. Therefore, much lower nitrate nitrogen levels should be tested in the future.

3.3.4. Estimation of the Energy Efficiency for Irradiance

The caloric content of the produced lipids was 29.91±1.17kJ g^{-1}. The highest lipid energy return and lipid yield on light energy was approximately 1.69% and 0.11g (mole photon)$^{-1}$ respectively at 180 μmol m^{-2} s^{-1} irradiance and 100% nitrogen (Figure 3.4), while the lowest (0.24% and 0.02 g (mole photon)$^{-1}$) was observed at 1200 μmol m^{-2} s^{-1} irradiance and 50% nitrate nitrogen level. In Bai et al. (under review), the lipid energy return and lipid yield on light energy for the Louisiana co-culture, which was cultivated under the same nitrogen and irradiance levelsbut without aeration and only daily CO_2 injection, was significantly lower at corresponding scalar irradiance and nitrogen levels than this work (maximum value of 0.24% compared to 1.69% in this work). The higher lipid energy return and lipid yield on light energy in this work most likely was attributed to aeration and 2% CO_2 addition. As discussed before, the aeration could improve lipid productivity by mixing the culture and lowering the oxygen level in the culture. Higher CO_2 level could suppress photorespiration and supply sufficient carbon source for lipid production. Therefore, the lipid energy return on light energy in this work was significantly higher than the non-aerated study.

The highest photosynthetic efficiency for biomass of the Louisiana co-culture under the same culture conditions as this work was 4.10% (0.39 g biomass per mole photon) (Silaban et al., under review). Lipid energy return on light energy in this work counted for ~45% of the photosynthetic efficiency. Others reported that the photosynthetic efficiency for *Chlorella* was in

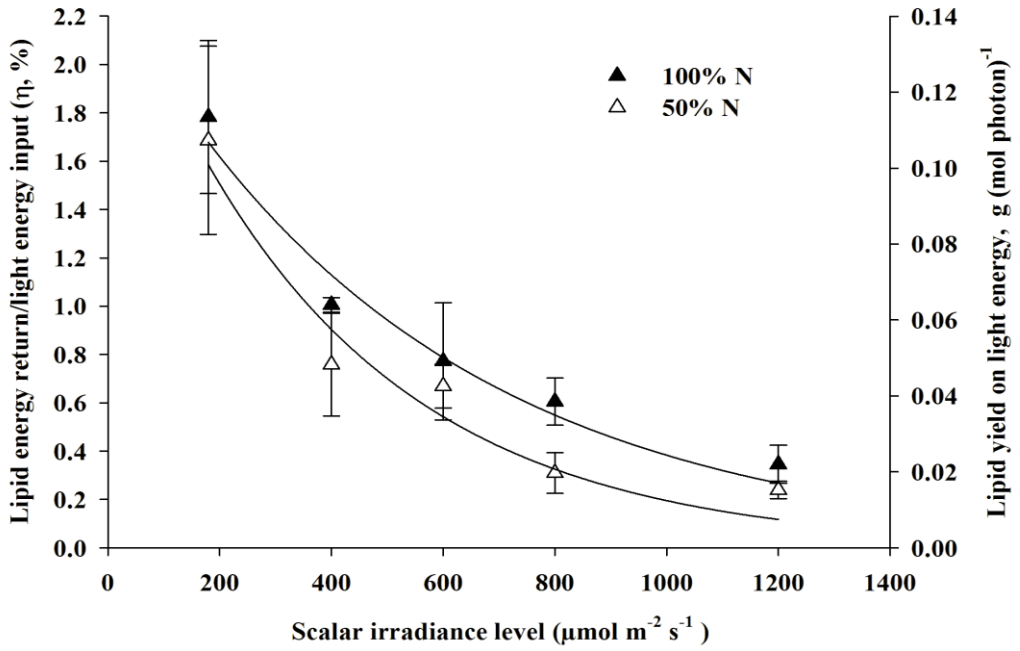

Figure 3.4. Lipid energy return (%) and lipid yield on light energy (g (mole photon)$^{-1}$). *Chlorella vulgaris*/*Leptolyngbya* co-culture with five scalar irradiance (180, 400, 600, 800 and 1200 µmol m^{-2} s^{-1}) and two nitrate nitrogen levels (2.94 mmol N L^{-1} (100% N) and 1.47 mmol N L^{-1} (50% N)).

the range of 4.15~8.66% (Doucha and Livansky, 2009, 2006; Xia and Gao, 2003; Morita et al., 2002; Hase et al., 2000). Although the photosynthetic efficiency in this work fell in the lower end of the range, the higher photosynthetic efficiency values reported were obtained from the culture grown in bioreactors with large surface area to volume ratios, which result in maximum light exposure. For example, Morita et al. (2001) reported photosynthetic efficiency of 7.25% for *Chlorella sorokiniana* culture in a helical tubular reactor with a surface area to volume ratio of 101.5 m^2 m^{-3} compared to 44 m^2 m^{-3} in this work. Doucha and Livansky (2009) observed a peak value of 9% for photosynthetic efficiency of *Chlorella sp.* culture in a thin layer photobioreactor with surface area to volume ratio of 153.8 m^2 m^{-3}. Therefore, the surface area to volume ratio of the Louisiana co-culture could be increased to achieve higher photosynthetic efficiency.

The two-way ANOVA results indicate that both scalar irradiance levels (p<0.0001) and nitrogen levels (p=0.0130) had significant impact on the energy efficiency (the energy content of lipid over the energy from the irradiance). The lipid energy return on irradiance energy (y) followed first order decay with respects of irradiance level (x) ($y = 1.96\%e^{-0.2\%x}$, R^2=0.9766 for 100% N; $y = 1.82\%e^{-0.2\%x}$, R^2=0.9115 for 50% N). This is most likely related to photodamage effect on photosystem II. The D1 subunit of photosystem II is continuously damaged once the cell is exposed to irradiance. The re-synthesis and replacing process of D1 subunit is highly energy demanding (Simionato et al., 2011). The damage effects accelerate with irradiance increases, resulting in higher energy consumption on D1 subunit re-synthesis and replacing process. Thereby, the conversion efficiency of sunlight to lipids decreases. Enhanced thermal dissipation that microalgae utilize under high irradiance levels might be another factor that causes decreased light conversion efficiency (Richmond, 2004). Under high irradiance conditions, microalgal cells can generate a pH gradient in the cells to enhance the thermal dissipation of the photon energy and prevent photoinhibition, resulting lower light energy conversion efficiency.

At each scalar irradiance level, the energy efficiency (lipid energy content over the energy of each scalar irradiance level) decreased with lower nitrogen level due to lower lipid productivity caused by nitrogen limitation. Therefore, the optimal point for the lipid production with respect to irradiance energy efficiency for lipid production should be 180 μmol m^{-2} s^{-1} irradiance and 100% nitrogen level. For outdoor large-scale culture systems, the area of the culture is normally constrained. The solar energy input in the area of microalgal culture is consequently limited. To maximize the conversion efficiency from solar energy to lipid, the depth of the culture can be controlled to reach 180 μmol m^{-2} s^{-1} irradiance level. However, the

increase the depth of the culture might result in over-diluted culture, which can significantly increase the energy cost of the dewater process for the co-culture. Therefore, the conversion efficiency from solar energy to lipid should be balanced with the final culture concentration in order to minimize the production cost.

3.4. Conclusions

This work investigated the effects of scalar irradiance level and nitrogen level on the total lipid percentage, lipid productivity, neutral lipid percentage and fatty acid composition of a Louisiana native *Chlorella vulgaris/Leptolyngbya sp.* co-culture with controlled pH and continuous aeration. The highest lipid productivity for this Louisiana co-culture was 116 g m^{-3} d^{-1} for 800 μmol m^{-2} s^{-1} with 100% nitrogen level and the lowest was 59.2 g m^{-1} d^{-1} for 800 μmol m^{-2} s^{-1} with 50% nitrogen level. In this work, scalar irradiance and nitrogen levels only had significant effect on lipid productivity. The low nitrogen level (50% N) limited the productivity by constraining the biomass productivity. However, in large scale production system, the cost of nitrogen and light energy must be taken into consideration along with lipid productivity. Wastewater with high nitrogen concentration could be used to lower the cost of nitrogen. For outdoor culture systems, the cost for light energy could be considered zero, but indoor culture systems should be designed to maximize the lipid energy return on light energy.

The compositions of the fatty acids profile suggested that the FAME produced from this Louisiana co-culture have to be desaturated or blended with petrol diesel in order to meet the EN 14214 standards. However, the stability of fatty acids profile under various scalar irradiance and nitrogen levels implied that the properties (gelling point, viscosity, acidity, oxidation stability etc.) of the biodiesel produced from this Louisiana *Chlorella vulgaris/Leptolyngbya sp.*co-culture most likely will be relatively consistent.

Although all the experiments in this work were conducted on a bench top scale, the results can provide information for the design of a large culture system. According to the results obtained from this work, the aeration could significantly increase the lipid productivity for the Louisiana co-culture. However, in a large-scale culture system, pumping air through the whole culture can dramatically increase the production cost. Paddlewheels can be used instead of aeration. Although it might not be able to completely compensate the effects of aeration, paddlewheel can significantly lower energy cost. The use of CO_2 should be implemented for the large-scale culture since it had a drastic impact on lipid productivity of the co-culture and generally considered available at no cost (Chisti, 2007; Grima et al., 2003). Nevertheless, the cost of bubbling the CO_2 through the culture should be evaluated depending on the specific design of the culture system (culture depth, surface area etc.). The irradiance level can be adjusted by varying the depth of the culture. In a confined area for microalgal culture, the optimal irradiance for maximum lipid productivity (g m^{-3} d^{-1}) results in low energy conversion efficiency and limited culture volume as discussed earlier, however high energy conversion efficiency lowers the culture concentration and significantly increases the cost for dewater process. Therefore, the optimal irradiance level should be able to balance lipid productivity and the conversion efficiency from solar energy to lipid.

4. SILVER NANOFIBER ASSISTED LIPID EXTRACTION FROM BIOMASS OF A LOUISIANA *CHLORELLA VULGARIS*/*LEPTOLYNGBYA SP.* CO-CULTURE

4.1. Introduction

Over the last several decades, microalgae have garnered significant attention as a feedstock of transportation fuels for the future primarily due to their higher growth rate, photosynthetic efficiency and lipid productivity than first (corn kernels, sugarcane etc.) and second (sugarcane bagasse, wood residues etc.) generation fuel feedstocks (Greenwell et al., 2010; Lehr and Posten, 2009; Rittmann, 2008; Dote et al., 1994). Additionally, microalgae are able to take advantages of non-arable lands, eliminating competition with food crops (Huang et al., 2010a; Johnson and Wen, 2010; Chisti, 2008). Other by-products from microalgal biomass, such as pigments (Chaumont and Thepenier, 1995), omega-3 fatty acids (Singh et al., 2005), biopolymers (Sharma et al., 2007), can partially offset biofuel production costs. Therefore, microalgal biofuels are considered more promising than traditional crop based biofuels.

Microalgal biofuel production is mainly comprised of five steps including strain selection, cultivation, biomass harvesting (dewatering), lipid extraction and transesterification (Mata et al., 2010). Although technical issues remain in almost every of these steps for microalgal biofuel production (Lam and Lee, 2012; Chen et al., 2011a; DOE, 2010), life cycle analyses indicate that lipid extraction is one of the most energy intensive and thus costly processes in the chain (Teixeira, 2012; Brentner et al., 2011; Lardon et al., 2009). Organic solvent based lipid extraction is the most commonly used method for microalgal lipid extraction (Halim et al., 2012).

Halim et al. (2012) have described organic solvent-based lipid extraction from algal cells as a five-step process: (1) the solvent enters the cytoplasm by diffusion through the cell walls and membrane structure; (2) solvent and the lipid interact via van der Waals forces and (3) form a

solvent-lipids complex; (4) the solvent-lipids complex diffuses through the cell wall via a concentration gradient; (5) the solvent-lipid complex passes through a static solvent film surrounding the cells and mixes with the bulk solvent. The process requires solvent to diffuse through the cell wall twice. The multi-layer microalgal cell walls (Richmond, 2004) can significantly limit the diffusion rate of both solvent and lipid. Therefore, disruption of these cell walls would drastically increase the efficiency of solvent-based lipid extraction from microalgae.

Microalgal cell walls are mainly comprised of linear and branched polysaccharides that form networks of microfibrils with strong semi-crystalline patterns (Northcote, 1963). Thus, the tensile strength of cell walls can be as high as 95~100 atmospheres (Carpita, 1985). In order to increase the lipid extraction efficiency, mechanical grinding is usually applied to break the cell wall of oil producing crops (soybean, rapeseed, canola) prior to the lipid extraction process. However, the typical microalgal paste (after centrifugation) contains ~80% (mass/mass) water compared to ~10% for soybean seeds (Wolf et al., 1982). The large amount of bulk water not only generates a barrier between the solvent and the lipid/oil, it also limits the effectiveness of mechanical grinding to break the cell walls. The cells flow through the micro-channels in the bulk water instead of being disrupted (Cooney et al., 2009). Many energy intensive and time-consuming methods have been utilized in an attempt to disrupt microalgal cell walls for increased lipid extraction efficiency, including sonication, manual grinding, and microwaves (Halim et al., 2012; Mercer and Armenta, 2011; Cooney et al., 2009).

Sonication uses the shear force generated by sonic waves to break the cell walls of microalgal cells (Lee et al., 2010b). Cravotto et al. (2008) reported 4.8%~25.9% improvement over traditional Soxhlet extraction without sonication pretreatment on biomass. Lee et al. (Lee et al., 2010b) reported less than 5% increase in lipid percentage by using sonication for 5 minutes

on microalgal cells. Considering the large amount of energy and time it consumes (80 kJ L^{-1} culture (Gerde et al., 2012)), sonication is not ideal for the large-scale lipid extraction from microalgal biomass (Luque-Garcia and de Castro, 2003; Martin, 1993). Cooney et al. (2009) investigated manual grinding-assisted lipid extraction in *Nannochloropsis*, and found grinding freeze-dried sample gives the highest lipid extraction efficiency. Lipid content improved by 45% compared to the unground freeze-dried samples. However, Wolkers et al. (2011) estimated that cost of freeze-drying microalgae is about $532 to $665 per kilogram dry biomass. Thus this method is not commercially viable. Microwave assisted solvent extraction changes the electric field along with the wavelength at high frequency, leading to instantaneous water heating inside the cells. The rapid rise in temperature and pressure causes the rupture of the cell wall structures, facilitating a more rapid diffusion of microalgal lipids into the extracting organic solvent (Halim et al., 2012; Vivekananda Mandal, 2007). A ~200% increase in lipid percentage of *Botryococcus sp.* was reported by applying microwave at 100^{o}C for 10 minutes compared to the original Bligh and Dyer method, however, the lipid percentage only increased ~5% by using the same procedure *on Chlorella vulgaris* and *Scenedesmus sp.* (Lee et al., 2010b). Nevertheless, energy cost for microwave is estimated in the range of $13.27~21.26 gal^{-1} oil (Iqbal et al. 2012). Thus, this method currently was not commercially feasible.

For economic viability, an extraction method requiring less energy input to rupture cell walls in the presence of bulk water is needed. Metals such as copper, cobalt, cadmium, silver etc. have been reported to interact with cell walls and cause structural and morphological changes within cell walls (Macfie et al., 1994; Majidi et al., 1990). Silver and copper have been extensively studied for their antimicrobial activity, which is directly related to the interactions

between the metals and cell walls (Kora et al., 2009; Ruparelia et al., 2008; Fry et al., 2002). This antimicrobial and cell disruption activity could be significantly enhanced by using nanostructured metals due to increased surface to volume ratio (Ayala-Núñez et al., 2009). Ruparelia et al. (2008) found that the antimicrobial efficiency for silver nanoparticles, which was directly related to cell wall disruption, was almost 40-50% higher than copper nanoparticles. Therefore, nanostructured silver could be a better choice for microalgal cell disruption than copper.

The interaction between silver nanoparticles and cell walls for bacteria was separated into two phases. In the first phase, silver nanoparticles attach and anchor on the surface of the cell wall (Chwalibog et al., 2010; Rai et al., 2009). The electrostatic forces and molecular interactions involved are believed to cause structural and morphology changes, damaging the cell wall (Nel et al., 2009). Therefore, the high energy concentration on the surface of silver nanoparticles caused by differential absorption could be another factor that attribute the ability of silver nanoparticles to rupture the cell walls (Adleman et al., 2006). In the second phase, nanoparticles penetrate the cell wall through damaged areas, perforating the cell membranes and releasing intracellular materials (Díaz-Visurraga et al., 2011). Based on the studies above, it is likely the cell disruption activity of silver nanoparticles would significantly increase the lipid extraction efficiency from microalgal cells.

In this study, the ability of silver nanofibers to improve the lipid extraction efficiency of the Folch's method (Folch et al., 1957) and microwave-assisted lipid extraction was assessed for a *Chlorella vulgaris*/*Leptolyngbya sp.* co-culture. The fatty acid profiles of the lipid extracted by each tested method (i.e. silver nanofibers+Folch's method and silver nanofibers+microwave,

Foch's method without silver nanofibers and microwave assited extraction without silver nanofibers) were analyzed to investigate the effects of extraction methods on fatty acid profile from this co-culture.

4.2. Methods and Materials

The impact of silver nanofiber concentrations (0, 50, 200, 500, 1000 μg g^{-1}, mass/mass, based on the solvent-biomass mixture) on the lipid extraction efficiency of the Folch's method and microwave-assisted lipid extraction for a Louisiana *Chlorella vulgaris*/*Leptolyngbya sp.* co-culture was investigated. The fatty acid profiles of the lipids extracted by using each method (i.e. silver nanofibers+Folch's method and silver nanofibers+microwave, Foch's method without silver nanofibers and microwave assisted extraction without silver nanofibers) were determined to provide the information on the effects of the these extraction methods on the compositions of the biodiesel produced from this Louisiana *Chlorella vulgaris*/*Leptolyngbya sp.* co-culture.

4.2.1. Strain Selection and Biomass Production

A *Chlorella vulgaris*/*Leptolyngbya sp.* (97%:3%, by cell counts based on flow cytometer) co-culture was used in this research. This co-culture was isolated from the College Lake on the Louisiana State University campus, Baton Rouge, LA. It is found that the presence of the *Leptolyngbya sp.* in this co-culture could significantly improve the growth rate of the *Chlorella vulgaris* (Rusch and Gutierrez-Wing (unpublished data)). In previous studies, the lipid productivity, lipid percentage (mass/mass, on dry biomass), neutral lipid fraction (mass/mass, on total lipid) and fatty acid profiles of the co-culture under different irradiance and nitrogen levels. The lipid productivity was reported as high as ~116 g m^{-3} d^{-1} with ~89% neutral lipids (Bai et al., (under review). The results of fatty acid analysis of the lipid from this co-culture indicated that the fatty acid profile of this co-culture was similar to other biodiesel feedstocks and the fatty acid

composition did not vary with irradiance and nitrogen levels (Bai et al., (under review)). Therefore, the *Chlorella vulgaris*/*Leptolyngbya sp.* was suitable for biodiesel production and selected for the lipid extraction study in this work.

In this study, the microalgal biomass for this co-culture was produced in a hydraulically integrated serial turbid stat algal reactor (HISTAR) developed by Rusch and Malone (1998). HISTAR is comprised of two enclosed turbidostats and a series of eight open-top, continuous flow stirred-tank reactors (CFSTRs). The inoculum culture was prepared in four 10 L carbons with F/2 media and an irradiance level of 200 μmol m^{-2} s^{-1} with 1 L min^{-1} aeration. When the optical density (OD 664 nm) of the culture reached ~0.5, the co-culture in the carbons was inoculated in the turbidostats with 100 L of F/2 media. The culture grew in the turbidostats in batch mode for 3~4 days until the OD 664 reached 0.6 before it was diluted to 454 L with F/2 media. The HISTAR control system was turned on. Each turbidostat injects high quality inoculum algal culture into the first CFSTR every 20 minutes. Nutrients (F/2 media, Kent Marine, Inc.) mixed with tap water were continuously fed into the first CFSTR at the flow rate of 0.5 L min^{-1}, resulting in a system dilution rate of 0.261 d^{-1} and a local dilution rate of 2.086 d^{-1}. The last CFSTR was connected to a centrifuge to concentrate the microalgal/cyanobacterial co-culture. For the CFSTRs, illumination was provided by the 400 watts high pressure sodium lamps placed ~26.6 cm above each CFSTR. Both metal halide (400 watts) and high pressure sodium (400 watts) lamps were used to provide the illumination for each turbidostats. The aeration rate for each reactor was 21.2 L min^{-1}. The pH was automatically controlled at 7~7.5 by bubbling CO_2 in the culture through air stones. The biomass paste was harvested daily from the centrifuge for the lipid extraction experiments. The operation parameters (i.e. nitrogen level, dilution rate) was optimized for biomass production other than lipid productivities, thus, the lipid

percentage (mass/mass, dry biomass) reported in this work is much lower than the previous studies conducted in batch mode on the same co-culture (Bai et al., (under review)).

4.2.2. Preparations and Characterization of Silver Nanofibers

The silver nanofibers were synthesized based on the protocol by Sun et al. (2002) with the modification of using $CoCl_2$ as seed material. Ethylene glycol (20 mL) was heated to 160^{o}C in a three-neck flask. One milliliter of $CoCl_2$ aqueous solution (1%, mass/mass) was slowly added into the flask. The temperature was maintained at 160^{o}C for 15-60 minutes. When the mixture color changed from pink to lilac, 10 mL of 4% (mass/mass) polyvinyl pyrrolidone (PVP) solution (ethylene glycol as solvent) was slowly added into the flask in order not to change the temperature. Ten mL of $AgNO_3$ (2% mass/mass, in ethylene glycol) solution was added, and the mixture was continuously heated for 1.5 hours at 160^{o}C. The mixture was rinsed with acetone and then centrifuged. The silver nanofibers were suspended in 95% ethanol to prevent agglomeration. Scanning Electron Microscopy was used to determine the approximate length, diameter and surface morphology of the nanofibers synthesized in the experiment. The composition of the nanofibers was determined by XPS.

4.2.3. Lipid Extraction

Folch's Method Assisted by Silver Nanofibers

A two-factorial design was used in this experiment to determine the effects of silver nanofibers on lipid extraction efficiency. Folch's method was performed with two solvent:biomass (wet paste) ratios (20:1 and 10:1, v:v) and five silver nanofiber concentrations (1000, 500, 200, 50, 0 μg g^{-1}, mass/mass, based on the mass biomass/solvent mixture). The lipid extraction without nanofibers (0 μg g^{-1}) was the control for the experiment. chloroform:methanol 2:1 (v:v) was mixed with biomass in a 50 mL centrifuge tube (3 g biomass paste for solvent:biomass ratio of 10:1; 1.5 g biomass paste for solvent:biomass ratio of 20:1). The

moisture content of the biomass paste used was 80.85% (mass/mass, based on the wet paste). The silver nanofibers were added into the biomass/solvent matrix to achieve the desired concentrations. The mixture was agitated in an Innova^{TM} 4340 shaker incubator at 120 rpm and 27^{o}C for 20 minutes. The 0.9% NaCl (mass/mass) solution (0.2 volume of total solvent, v:v) was added to separate the mixture into two phases. The chloroform/lipid phase was recovered and the chloroform was evaporated to obtain the lipid. Triplicates were done for each treatment.

Folch's method with five concentrations of Ag^{+} ($AgNO_3$) (1000, 500, 200, 50, 0 μg g^{-1}) was tested to investigate the effects of Ag^{+} on the lipid extraction efficiency from the Louisiana co-culture biomass pasted. The extraction procedure followed the silver nanofiber assisted lipid extraction except the use of Ag^{+} instead of metal silver. The results were compared with the silver nanofibers assisted Folch's method to determine whether Ag^{+} has the same effects as metal silver nanofibers on lipid extraction. Triplicates were done for each treatment.

Microwave Assisted Lipid Extraction with the Addition of Silver Nanofibers

A three-factor design was utilized in this experiment. Five silver nanofiber concentrations (1000, 500, 200, 50, 0 μg g^{-1}), two heating temperatures (70 and 90^{o}C) and three heating times (2, 5, 10 minutes) were tested to find the optimum conditions for the lipid extraction from the Louisiana native *Chlorella vulgaris*/*Leptolyngbya sp.* biomass paste using microwave assisted lipid extraction.

The biomass paste used in this experiment contains ~80.85% moisture. The co-culture biomass paste and the solvent (chloroform:methanol 2:1, v:v) were mixed in an XP-500^{TM} vessel in a ratio of 1:10 and the silver nanofiber suspension was added. A MARS 5^{TM} laboratory microwave oven was used to heat the sample to the intended temperature (70, 90^{o}C). After the system cooled, 0.2 volume (based on total solvent volume, v/v) of 0.9% NaCl solution was

added and the mixture was centrifuged to separate it into three phases (methanol-water/biomass/ chloroform-lipid). The chloroform-lipid phase was obtained and a rotary evaporator was used to evaporate the solvent. The lipid percentage (based on the mass of dry biomass) was reported for each condition (temperature, nanofiber concentration and heating duration). Triplicates were done for each extraction condition.

4.2.4. Fatty Acid Analysis

The fatty acids profiles of lipids extracted in four different conditions (Folch's method with 0 and 1000 μg g^{-1} silver nanofibers; microwave assisted extraction with 0 and 1000 μg g^{-1} silver nanofibers) were analyzed by gas chromatography to determine the effect of extraction conditions (microwave, silver nanofibers) on the fatty acids profile.

The lipids were first transesterified into fatty acid methyl esters (FAME) following the IUPAC Method II.D.19. Ten milliliters of 0.5 M NaOH methanolic solution was added to the neutral lipid sample, and the mixture was boiled for 10 minutes. Boron trifluoride (BF_3) methanolic solution was then added to the mixture and boiled for two minutes. After adding 1.5 mL heptane and boiling for one minute, 20 mL of saturated NaCl solution was slowly added resulting in a two-phase liquid system (FAME and heptane in the upper phase). About 1 mL upper phase was transferred into a 2 mL vial. Finally, small amount of $NaSO_4$ was added into the vial to remove trace water.

Fatty acid analysis was done in an HP 5890 Series II gas chromatography with SP™-2380 column (30 m, 0.25mm ID, 0.20μm film). The flow rate of the carrier gas (helium) was 2 mL min^{-1}. The initial oven temperature was set at 80°C. After one minute, the temperature was

increased by 4^{o}C min^{-1} until a final temperature of 220^{o}C was achieved. This temperature was maintained for 5 minutes. The gas chromatography data were analyzed with Chemstation^{TM} software, and the mass percentage of each fatty acid component was reported.

4.2.5. Data Analysis

For each treatment, the mean and standard deviation of lipid percentage (based on the dry biomass, mass/mass) was calculated. Two-way ANOVA was conducted using SAS^{TM} (9.3.0) for silver nanofibers assisted lipid extraction to determine whether the effects of silver nanofiber concentrations, solvent:biomass ratios on lipid extraction efficiency were statistically significant. Three-way ANOVA was performed for silver nanofibers and microwave assisted lipid extraction to determine whether the impacts of concentrations of silver nanofibers, heating temperature and heating duration were significant. Tukey's test was performed for multiple comparisons. Significance was determined at an α=0.05.

4.3. Results and Discussion

4.3.1. Characterization of Silver Nanofibers

The characteristic peaks of Ag in XPS analysis (Figures 4.1) at 368 eV (Ag $3d_{5/2}$) and 374 eV (Ag $3d_{3/2}$) revealed that the material synthesized with $AgNO_3$ and $CoCl_2$ were mainly composed of metal silver. The minor peak of binding energy at 780 eV (Figure 4.1) suggested that there was cobalt metal in the nanofibers. The nanofibers comprised of 98% (mass/mass) of silver and about 2% (mass/mass) of cobalt. Characteristic peaks for C_{1s} (284 eV) and O_{1s} (532.4 eV) were detected because of the polyvinylpyrrolidone used to prevent the aggregation of nanofibers. The diameters of the silver nanofibers were around 100 nm. Almost all of the fibers were longer than 5 μm based on the SEM images (Figure 4.2).

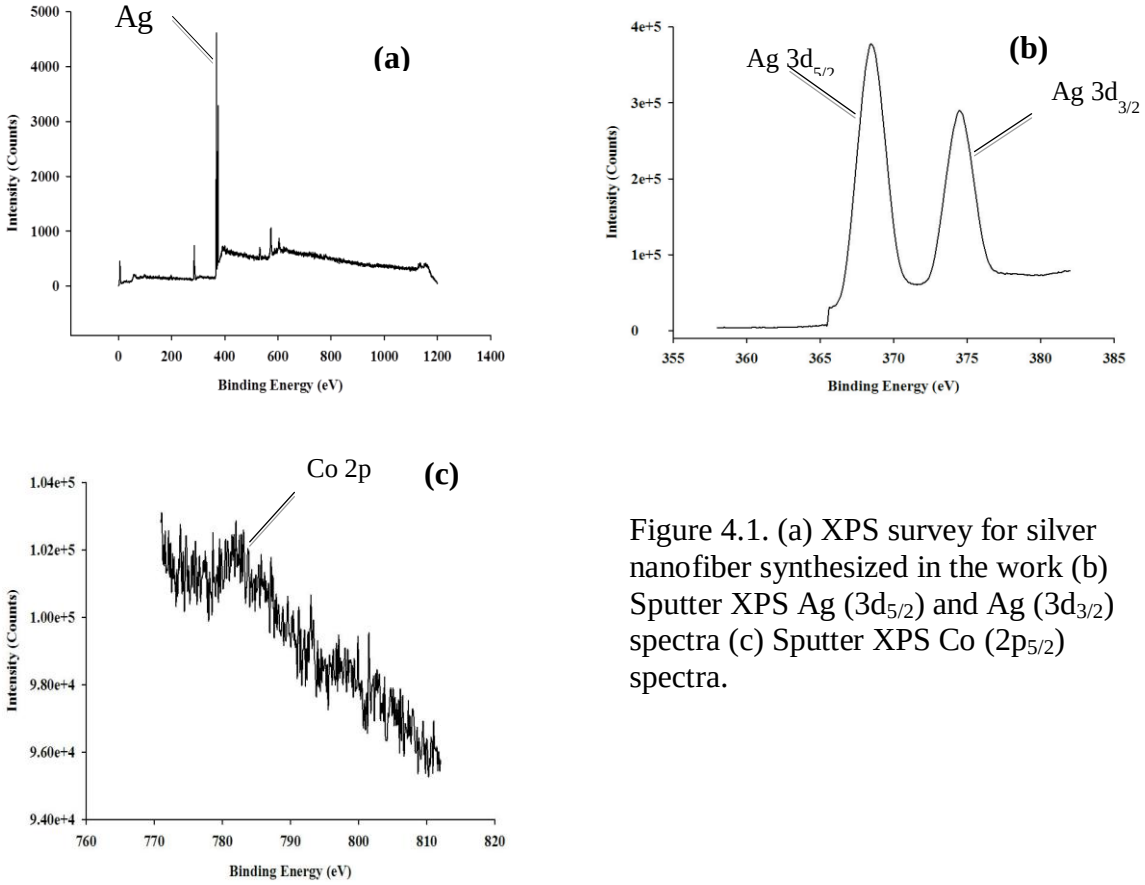

Figure 4.1. (a) XPS survey for silver nanofiber synthesized in the work (b) Sputter XPS Ag ($3d_{5/2}$) and Ag ($3d_{3/2}$) spectra (c) Sputter XPS Co ($2p_{5/2}$) spectra.

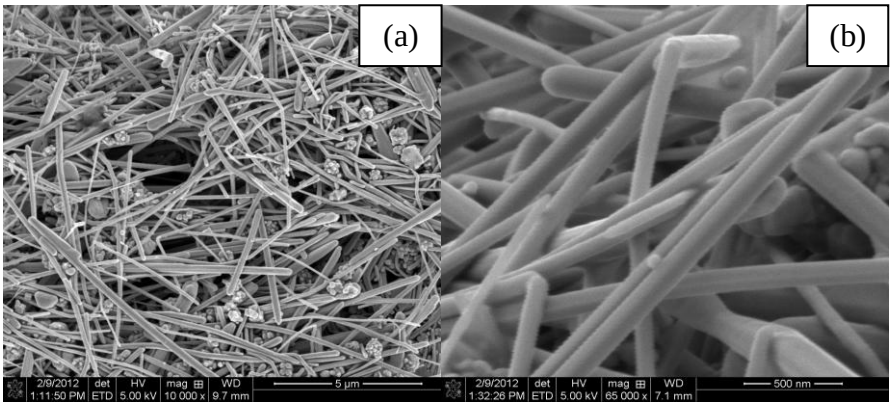

Figure 4.2. (a) SEM image (10,000×) showing the overall dimensions (length and diameter) silver nanofibers (b) SEM image (65,000×) showing detailed the surface morphology of the silver nanofibers.

4.3.2. Folch's Method Assisted by Silver Nanofibers

The results of two-way ANOVA indicated that both silver nanofiber concentrations (p<0.0001) and solvent/biomass ratios (p<0.0001) had significant effects on the lipid extraction efficiency of the Louisiana *Chlorella vulgaris*/*Leptolyngbya sp.* co-culture. The highest lipid percentage (%, mass/mass based on dry biomass) was obtained for the 1000 μg g^{-1} silver nanofibers and solvent:biomass ratio of 20:1 (v:v) (Table 4.1). The results of non-linear regression indicated that the lipid percentage and silver nanofiber concentrations followed an linear relationship for both 20:1 and 10:1 solvent:biomass ratios (Figure 4.3). The equations in Figure 4.3 could provide a great predictive tool to estimate the lipid extraction efficiency for different silver nanofiber concentrations. However, extrapolation for the lipid percentage at silver nanofiber concentrations greater than 1000 μg g^{-1} is not suggested since the actual lipid content in the microalgal cells is limited, and lipid extraction efficiency will reach a saturation value where the lipid percentage stops increase as nanofiber concentration increases. The lipid percentage of biomass samples extracted with 0 μg g^{-1} silver nanofibers (experimental controls) were 10.15%

Table 4.1. Results of lipid extraction (%, mass/mass based on dry biomass) using Folch's method with the addition of silver nanofibers (0, 50, 200, 500, 1000 μg g^{-1}, mass/mass based on the whole biomass/solvent mixture).

Solvent:Biomass, v:v	Nanofiber concentration (μg g^{-1})				
	1000	500	200	50	0
10:1	14.7±0.52^{b}	12.7±0.88^{bcd}	11.9±0.19^{cde}	11.4±0.93^{de}	10.2±0.23^{e}
20:1	22.2±1.19^{a}	14.4±0.71^{bc}	15.2±1.60^{b}	14.4±0.22^{bc}	14.2±0.86^{bc}

* mean±standard deviation (%) of triplicate samples

*$^{a-e}$ values with different superscript letters indicate a significant difference (p<0.05) between treatments, while values share same superscript letters indicate no significant difference

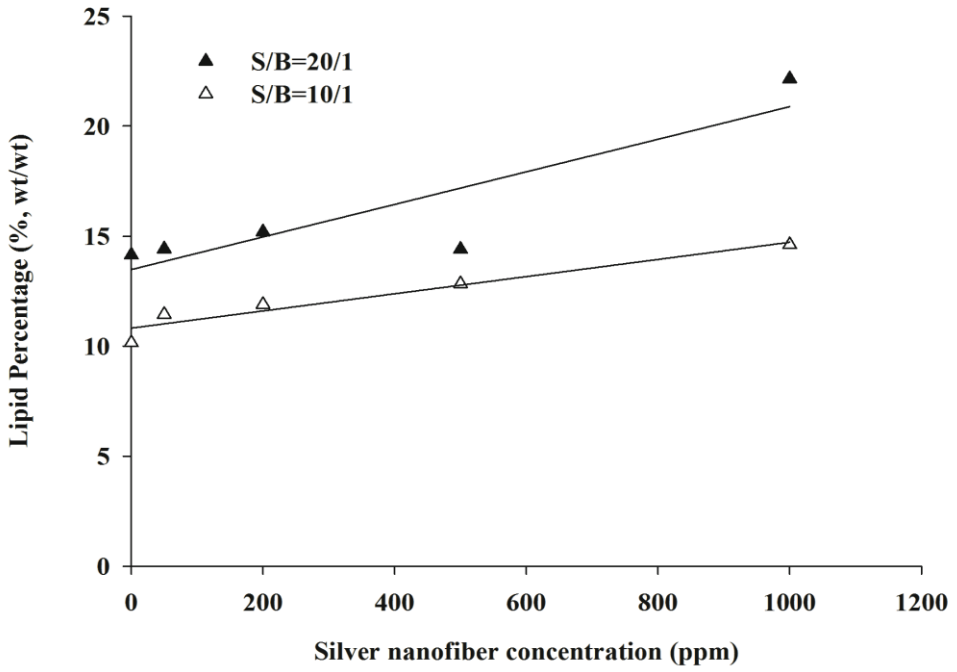

Figure 4.3. The linear relationships between the Ag nanofiber concentration (x, μg g^{-1}) and lipid percentage (y, mass/mass on dry biomass) for the Folch's method. (1) S/B=20/1 (solvent:biomass 20:1) y=13.48+0.0074x (R^2=0.886); (2) S/B=10/1, y=10.82+0.0039x (R^2=0.967).

and 14.14% (based on dry biomass, mass/mass) for solvent/biomass ratio of 10:1 and 20:1 (v:v) respectively (Table 4.1). For extraction with the solvent/biomass ratio of 10:1, 50 μg g^{-1} nanofibers had no significant effect on the lipid extraction efficiency compared to the control. When the silver nanofiber concentration was 200 to 1000 μg g^{-1}, the lipid content increased as the nanofiber concentration increased. Compared to the control samples, the lipid percentage of the microalgal paste increased about 40% with the 1000 μg g^{-1} silver nanofibers and 30% with the 500 μg g^{-1} nanofibers at solvent biomass ratio 10:1. As the solvent ratio doubled (20:1, solvent/biomass ratio, mass/mass), the lipid percentage of the microalgal biomass for each nanofiber concentration was higher than the samples with the solvent/biomass ratio of 10:1.

However, as the concentration of silver nanofibers increased, there was no significant increase (p>0.05) in lipid percentage until the nanofiber concentration reached 1000 μg g^{-1}. Approximately 22.2% of lipid percentage was attained for 1000 μg g^{-1} silver nanofibers, an almost 57% increase compared to extraction without silver nanofibers (Table 4.1).

The significant increase of lipid extraction efficiency compared to the control samples (no silver nanofibers added) was most likely attributed to disruptive effects of silver nanofibers on cell wall (Chwalibog et al., 2010; Nel et al., 2009). Chwalibog et al. (2010) described the possible mechanisms of the effects of silver nanoparticles on bacterial cell walls. The silver nanofibers anchored and attached to the surface of the cell wall (Chwalibog et al., 2010). Electrostatic forces and molecular interaction between the silver nanofibers and the cell wall caused the damages on the cell wall. The nanofibers then penetrated the cell wall through the damaged areas, perforating the cell membranes and releasing the intracellular material (Nel et al., 2009). It is possible that the similar interactions occurred for silver nanofiber and microalgal cell walls. Therefore, the lipids could directly interact with solvent without first having to diffuse through the cell wall, increasing the lipid extraction efficiency. The morphologic difference between microalgal cells extracted with and without silver nanofibers addition was shown in Figure 4.4. The cell wall structure disappeared and *Chlorella vulgaris* cell seemed lost part of its intracellular content after lipid extraction with 1000 μg g^{-1} silver nanofibers (Figure 4.4a) indicating efficient cell wall disruption by silver nanofibers, while for the extraction conducted without silver nanofibers, the cell wall was almost intact for the cell, keeping a complete microalgal cell structure (Figure 4.4b).

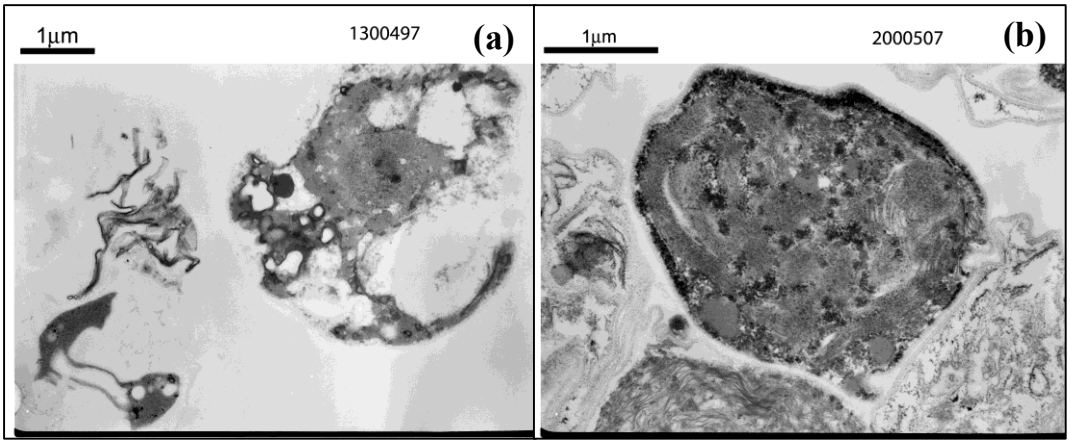

Figure 4.4. TEM photos of the microalgal cells from the *Chlorella vulgaris*/*Leptolyngbya sp.* co-culture after lipid extraction with Folch's method. (a) Folch's method with Ag nanofibers; (b) Folch's method without Ag nanofibers.

Zheng et al. (2011) investigated several methods to improve lipid extraction efficiency from *Chlorella vulgaris* via cell disruption, and found out that grinding in liquid nitrogenshowed the greatest improvement for lipid percentage, percentage from ~5% (Bligh and Dyer as control) to ~28% and indicated that extremely low temperature of liquid nitrogen (-196^{o}C) made the cell walls easy to crack under low-impact force (cryo-impacting), resulting higher lipid extraction efficiency. Lee et al. (2010b) microwave (100^{o}C for 5 minutes) had increased lipid percentage from ~5% to ~10% for *Chlorella vulgaris*. However, Prabakaran and Ravindran (2011) found that sonication for 15 minutes showed better lipid extraction efficiency than microwave assistant extraction (100^{o}C, 5 minutes) for *Chlorella sp.* The increase in lipid percentage with the addition of 1000 μg g^{-1} silver nanofibers is similar to 15 minutes of sonication pre-treatment in Prabakaran and Ryindran (2011), which is much more efficient than beads beating, osmotic shock and microwave (100^{o}C for 5 minutes). Nevertheless, cell disruption by silver nanofibers does not require extra energy and time for pretreatment, which could reduce significant amount of cost for lipid extraction process in an industrial size lipid extraction system. Although the cost

of producing silver nanofibers could be high due to the high temperature and expensive reagent (e.g. $AgNO_3$) needed for silver nanofibers synthesis, strategies to reuse the silver nanofibers could be developed to minimize the cost. One of the possible strategies involves taking advantage of the magnetic susceptibility of cobalt composition in the nanofibers. By increasing the cobalt composition, the magnetic susceptibility of the nanofibers should increase. When a magnetic field is applied, the nanofibers will most likely move toward the magnetic field, separating from the rest of the mixture. Another possible way to recover the silver nanofibers is to use silver nanoparticles fixed on bulk substrate (i.e. wafer, metal plates etc. Although the surface area of silver nanoparticles fixed on a bulk substrate could be relatively limited, the recover and reuse of the silver nanoparticles could be significantly improved compared to the silver nanoparticle suspension.

The lipid content (14.7%) of the 1000 μg g^{-1} sample and 10:1 solvent:biomass ratio was almost equal to the lipid content (14.2%) of the sample treated with twice the volume of solvent and no silver nanofibers. This result implies that the addition of 1000 μg g^{-1} silver nanofibers could save half of the solvent for the lipid extraction by using Folch's method. For the commercial scale lipid extraction process, although the solvent is usually reusable, the energy consumption for recovering the solvent is significant. The addition of the silver nanofibers could lower the energy consumption in the lipid extraction process.

The lipid extractions conducted with the addition of Ag^+ instead of silver nanofibers had no significant effects (p=0.9920) on the lipid extraction efficiency at any of the concentrations tested (0, 50, 200, 500, 1000 μg g^{-1}) (Table 4.2). It is most likely because silver ions do not have the mechanical strength that nanostructured metal silver possesses. To disrupt cell wall, the silver most likely has to first anchor on the surface of cell wall and induces damage on the cell wall by

electrostatic forces and molecular interactions (Chwalibog et al., 2010; Nel et al., 2009). High energy concentration on the surface of nanostructured metal silver (Adleman et al., 2006), other than Ag^+ , could also be another factor inducing strong interaction between the silver nanofibers and the cell wall, causing more damages on cell wall. Additionally, the silver has to penetrate through the damage areas of the cell wall to expand the damages. It is highly likely that the mechanical strength, which nanostructured metal silver other than Ag^+ possesses, is required to physically pierce through the strong semi-crystalline structures of the cell wall (Northcote, 1963).

Table 4.2. Results of lipid extraction (%, mass/mass based on dry biomass) using Folch's method with the addition of Ag^+ (0, 50, 200, 500, 1000 μg g^{-1}, mass/mass based on the whole biomass/solvent mixture).

Solvent:Biomass, v:v	Ag^+ concentration (μg g^{-1})				
	1000	500	200	50	0
10:1	10.2±0.25	10.4±1.20	10.3±0.47	10.4±0.60	10.4±1.29

* mean±standard deviation (%) of triplicate samples

4.3.3. Effects of Silver Nanofibers in Microwave Assisted Lipid Extraction

The highest lipid content (24.4%, based on the dry biomass, mass/mass) was achieved with 1000 μg g^{-1} of silver nanofibers, 70°C and 5 minutes of heating time. The addition of 1000 μg g^{-1} silver nanofibers improved the lipid percentage (mass/mass, based on dry biomass) by ~67% at 70°C for 5 minutes of heating. Compared to results obtained with Folch's method (without silver nanofibers), the lipid percentage (mass/mass, based on dry biomass) increased by more than 100%. (Table 4.3).

Three-way ANOVA analysis showed that temperature (p=0.1356) had no significant effects on the lipid content of the microalgal biomass. However, both heating time (p<0.0001)

Table 4.3. Results of lipid extraction using microwave assisted extraction method with the addition of silver nanofibers (0, 50, 200, 500, 1000 μg g^{-1}) at two temperatures (70 and 90°C with 3 heating durations (2, 5, 10 minutes). The solvent biomass ratio was 10:1 (v:v) for all the samples.

		Nanofiber Concentration /Total Lipid Percentage (%)				
T/°C	Heating time/min	1000 μg g^{-1}	500 μg g^{-1}	200 μg g^{-1}	50 μg g^{-1}	0 μg g^{-1}
70	2	22.9±3.89^{ab}	13.9±0.56^{fghij}	12.1±0.79^{ghi}	10.3±0.27^{ij}	9.68±0.24^{j}
	5	24.4±3.60^{a}	21.7±3.33^{abc}	19.9±2.27^{abcdef}	17.3±0.77^{bcdefgh}	15.6±2.49^{cdefghij}
	10	20.6±0.78^{abcd}	13.6±1.57^{ghij}	12.5±2.19^{hij}	12.3±1.88^{ghij}	11.3±3.25^{hij}
90	2	18.3±0.99^{abcdefg}	15.9±2.22^{cdefghi}	14.2±1.21^{efghij}	13.3±1.60^{ghij}	12.5±1.02^{ghij}
	5	21.3±0.40^{abc}	15.8±2.34^{cdefghij}	14.1±1.83^{fghij}	12.6±0.51^{ghij}	12.9±0.64^{ghij}
	10	20.3±3.66^{abcde}	16.0±1.52^{cdefghi}	14.6±1.85^{defghij}	13.4±0.72^{ghij}	13.8±0.50^{fghij}

* mean±standard deviation (%) of triplicate samples

*$^{a-j}$ values with different superscript letters indicate a significant difference (p<0.05) between treatments, while values share the same superscript letters indicate no significant difference

and silver nanofiber concentration (p<0.0001) had significant effects on the lipid content for microwave assisted lipid extraction from the Louisiana *Chlorella vulgaris*/*Leptolyngbya sp.* co-culture. The lipid extraction efficiency increased with the increased silver nanofiber concentration (Table 4.3) at all tested temperatures and heating durations. The more nanofibers were added in the biomass/solvent mixture, the more contact between the cell wall and silver nanofibers there might be. Thus more damage was likely caused on the cell wall by silver nanofibers through electrostatic forces, molecular interaction etc. (Nel et al., 2009). The diffusion rate of solvent and lipid would be expected increased with the more damaged cell wall, resulting higher lipid extraction efficiency.

The lipid percentage and the silver nanofiber concentrations follow linear relationship under each heating temperature and duration (Figures 4.5 and 4.6). These relationships enable the prediction of lipid percentage by applying the silver nanofibers within the range tested in this work (0-1000 μg g^{-1}). The lipid extraction efficiency was more responsive to the dose of nanofibers at lower temperatures and shorter heating times (Table 4.3). For example, at 70^{o}C and 2 minutes heating time, lipid extraction efficiency were significantly different for the five silver nanofiber When the heating temperature concentrations (9.68% for 0 μg g^{-1}, 10.26% for 50 μg g^{-1}, 12.52% for 200 μg g^{-1}, 13.94% for 500 μg g^{-1}, 22.87 for 1000 μg g^{-1}), but at 70^{o}C and 5 minutes, the lipid content for 0, 50, 200 μg g^{-1} of silver nanofibers had no significant difference (p>0.05). It is probably because of the overlap of the cell disruptive effects of the silver nanofibers and microwave.and heating duration were low. The cell disruption induced by microwave was limited. The majority of cell disruption was caused by silver nanofibers, the efficiency of lipid extraction was more sensitive to the dosage of silver nanofibers.

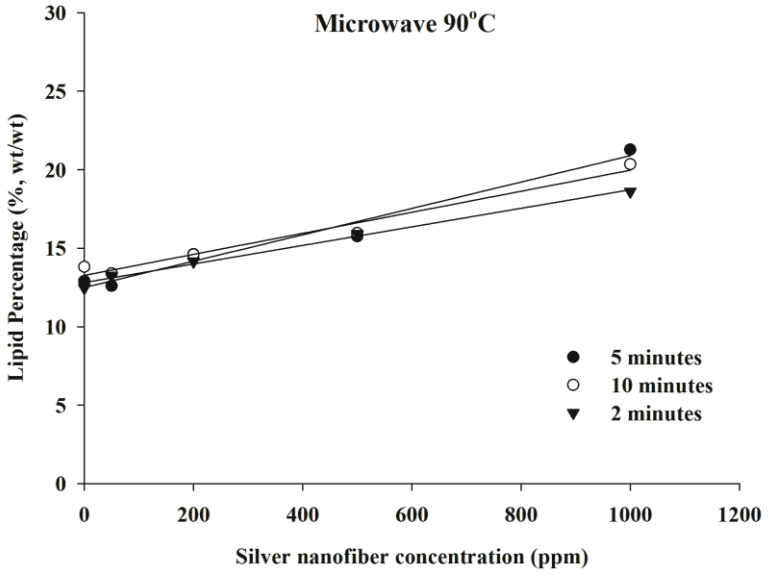

Figure 4.5. The linear relationships between Ag nanofiber concentration (μg g^{-1}, x) and total lipid percentage (y, mass/mass on biomass) with microwave assisted extraction at 90°C under different heating durations. (1) 5 minutes y=12.49+0.0084x (R^2=0.9698); (2) 10 minutes y=13.26+0.0067x (R^2=0.9710); (3) 2 minutes y= 12.81+0.0059x (R^2=0.9913).

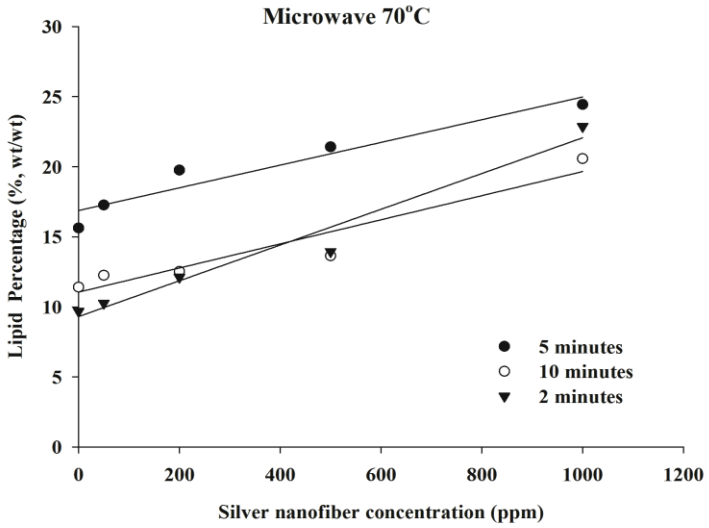

Figure 4.6. The linear relationships between Ag nanofiber concentration (μg g^{-1}, x) and total lipid percentage (y, mass/mass on dry biomass) with microwave assisted extraction at 70°C under different heating durations. (1) 5 minutes y=16.94+0.0081x (R^2=0.9112); (2) 10 minutes y=11.01+0.0086x (R^2=0.9651); (3) 2 minutes y=9.307+0.0128x (R^2=0.9651).

As the temperature and heating time increased, cells disruption caused by the microwave increased. Therefore, the low dosage of nanofibers did not exhibit a significant effect on cell disruption. Among the three heating time (2, 5, 10 minutes), 5 minutes proved to be the optimum for any given heating temperature and silver nanofiber concentration. For 2 minutes heating, the diffusion rate of solvent and lipids was limited and cell rupture caused by both microwave and silver nanofibers was reduced compared to 5 minutes heating, constraining the lipid extraction efficiency. The lower lipid extraction efficiency for 10 minutes heating duration was most likely attributed to the thermal oxidation of the lipids, which was caused by exposure to high temperature for prolonged heating duration (Anjum et al., 2006; Yoshida et al., 2006; Ramezanzadeh et al., 2000). Additionally, silver nanoparticles have been reported to be oxidative, especially under high temperatures (Govindasamy and Rahuman, 2012; Stevanovic et al., 2012; Kumari et al., 2009). In the oxidation process, unsaturated fatty acids reacted with oxygen in the ambient air and primarily converted to lipid hydroperoxide (Frankel, 1984). Pokorny et al. (1976) found that oxidized lipid could form chloroform-insoluble compounds with cellulose, protein etc. Thus, the lipid extraction efficiency at 10 minutes heating duration was lower than 5 minutes. When the temperature was increased from 70^{o}C to 90^{o}C, both the cell disruption and diffusion rate would be expected to improve significantly. However, similar to the effects of prolonged heating duration, the increase in lipids extracted at 90^{o}C was most likely eliminated due to the oxidative effects of microwave and silver nanofibers at higher temperature. Therefore, the lipid extraction efficiency had no significant difference between 70^{o}C and 90^{o}C (p>0.05).

The optimum condition for microwave and silver nanofibers assisted lipid extraction in this work was 1000 μg g^{-1} of silver nanofibers, at 70^{o}C and 5 minutes of heating. The lipid

percentage under these extraction conditions was much higher than in the work Lee et al. (2010b) reported for microwave assisted lipid extraction on *Chlorella vulgaris* (~24% in this work compared to 10% in Lee et al. (2010)).

4.3.4. Fatty Acid Analysis

In biodiesel production, chain length close to petrol diesel (C12) is preferred since the viscosity and gelling points of biodiesel are dependent on the chain lengths of the fatty acids. However, the dominant compositions of biodiesel are C16 and C18 (Bannister et al., 2011; Risher and Rhodes, 1995). Saturated fatty acids are desirable because saturated fatty acids give higher cetane numbers and higher oxidative stability than unsaturated fatty acids (Rasoul-Amini et al., 2011). Additionally, unsaturated content is more corrosive to metals, prohibiting the integration of biodiesel to the existing infrastructure (i.e. transportation pipe, tank, engine etc.) (Wang et al., 2011; Lee et al., 2010a; Kaul et al., 2007). Therefore, knowledge about the effects of extraction methods on the fatty acids profiles is imperative for microalgal based biodiesel production. There were 14 fatty acids detected in the lipids samples from this co-culture (Table 4.4). The majority of fatty acids were C16 and C18, similar to the fatty acids profiles of biodiesel (Bannister et al., 2011; Risher and Rhodes, 1995). However, the fatty acids profiles varied with extraction technique tested.

The optimal lipid extraction method based on fatty acid profiles was Folch's method without the addition of silver nanofibers, since it generated the highest content of short chain fatty acids (C14 and C16) and saturated fatty acids than other conditions tested (Table 4.4). However, considering lipid extraction efficiency and fatty acid profiles, microwave assisted lipid extraction with silver nanoparticles was the optimum.

Table 4.4. Fatty acids profiles under four lipid extraction conditions: Microwave assisted lipid extraction with silver nanofibers; Microwave assisted lipid extraction without silver nanofibers; Folch's method with silver nanofibers; Folch's method without silver nanofibers**.**

Fatty Acids	Microwave with AgNF	Microwave without AgNF	Folch with AgNF	Folch without AgNF
C14:0	17.4±0.62	11.8±0.66	15.1±2.89	21.1±0.56
C16:0	31.7±2.78	20.1±1.40	26.9±1.74	30.5±1.49
C16:1n7	0.56±0.09	0.63±0.13	0.69±0.09	0.52±0.03
C16:1n9	1.81±0.38	2.53±0.73	2.71±0.31	2.12±0.20
C16:2n10	2.39±0.65	3.70±0.77	2.80±0.20	2.15±0.11
C18:0	5.70±1.59	1.67±0.24	2.21±0.30	3.30±0.56
C18:3n9	4.69±1.04	7.44±1.02	5.78±0.50	4.62±0.21
C18:1n9c	4.51±1.34	5.37±1.85	5.95±0.28	5.20±0.16
C18:1n9t	1.21±0.06	1.17±0.18	1.29±0.08	1.10±0.06
C18:2	10.2±1.48	14.7±0.76	11.3±0.80	9.52±0.47
C20:0	1.55±0.19	1.98±0.14	2.07±0.33	1.57±0.11
C18:3n3	17.0±2.54	28.4±1.01	22.2±2.18	17.1±1.35
C20:1	0.66±0.31	0.42±0.04	0.61±0.09	0.72±0.13
C22:0	0.59±0.14	0.17±0.02	0.38±0.08	0.43±0.08
Saturated FA	56.9±5.32	35.7±2.46	46.7±5.34	56.9±2.80
FA≤ C16	53.9±4.52	38.8±3.69	48.2±5.32	56.4±2.39

** mean±standard error (%) of triplicate samples*
**AgNF stands for silver nanofibers*
** FA stands for fatty acids; FA≤ C16 stands for fatty acids that have less than 16 carbons*

For the Folch's method, the application of silver nanofibers increased the composition of C18 fatty acids (p<0.05). The solubility of fatty acids in chloroform decreases with an increase in the chain length (Charkrabarty, 2009). Most likely, C18 fatty acids were not completely extracted when the lipid extraction efficiency was relatively low. In the samples with the addition of silver nanofibers, more microalgal cell walls were ruptured and lipid extraction efficiency significantly increased. Therefore, the ratio of the less soluble C18 fatty acids to the total fatty acids increased. Since most of the C18 fatty acids of the lipid extracted from the

Louisiana co-culture were unsaturated fatty acids, an increase in C18 fatty acid content resulted in a higher portion of unsaturated fatty acids. However, the increase of C18 fatty acids and unsaturated fatty acids was not dramatic (difference<10%), the fatty acid profile still fit ASTM D 6751 standards with silver nanofibers added in the lipid extraction process.

However, for microwave assisted lipid extraction, the addition of the silver nanofibers lowered the C18 fatty acids content while simultaneously increasing overall lipid extraction efficiency. The majority of the C18 fatty acids in the co-culture were unsaturated. The silver nanofibers most likely enhanced the thermal oxidation effects on the lipid (Govindasamy and Rahuman, 2012; Stevanovic et al., 2012; Kumari et al., 2009), resulting in more C18 unsaturated fatty acids being oxidized. Therefore, the sample with silver nanofibers had less C18 fatty acids and more saturated shorter chain fatty acids. The addition of silver nanofibers for microwave assisted lipid extraction not only increased the lipid extraction efficiency but also improved the quality of the biodiesel. When silver nanofibers were not added, the microwave assisted extraction led to higher concentration of C18 fatty acids and unsaturated fatty acids than using Folch's method. Although microwaves may oxidize some C18 fatty acids, more C18 fatty acids were extracted thanks to improved lipid extraction efficiency resulting in a net increase in C18 fatty acids. On the contrary, the lipid extracted with the assistance of microwave and silver nanofibers had significantly lower content C18 fatty acids and unsaturated fatty acids. This is most likely because silver nanofibers could significantly enhance the thermal oxidative effects of microwave. The increase in the C18 fatty acids content by the improved efficiency of extraction could not compensate the loss of unsaturated C18 fatty acids by oxidation.

To use the biodiesel in current diesel engines, the fuel properties (cetane number, viscosity, cold filter plug point etc.) have to be meet the technical standards. However, the

technical standards for biodiesel did not provide the criteria for FAME composition. Ramos et al. (2009) demonstrated a relationship between fatty acid profile (%, mass/mass of saturated, monounsaturated, polyunsaturated fatty acids) and the EN 14214 standards. Based the study, the saturated fatty acids have to fall in the range of 30~60% of total fatty acids (mass/mass) and 50% of the unsaturated fatty acids have to be monounsaturated. However, the fatty acid profiles of Louisiana co-culture for all the lipid extraction methods exceeded the limit for polyunsaturated fatty acid. Therefore, the biodiesel produced from the Louisiana co-culture in these studies needs to be de-saturated or used by blending with petrol diesel. The methods to de-saturate fatty acid include distillation, catalytic hydrogenation, genetic engineering etc. (Pozdeev et al., 2012).

4.4. Conclusions

The silver nanofibers were able to rupture the cell walls of the microalgae and increase the lipid extraction efficiency for both Folch's method and microwave assisted lipid extraction. The addition of the silver nanofibers saved large amounts of solvent and energy consumption for the lipid extraction process. The silver nanofibers had significant impact on the fatty acids profile of the lipids. The optimal lipid extraction method for desirable fatty acids profile in this work was Folch's method without the addition of silver nanofibers. However, the lipid extraction with microwave and silver nanofibers should be the optimal extraction method for biodiesel production, considering the overall increase in lipid content.

Although the cost of silver nanofibers could be high, techniques to reuse the silver nanofibers could be developed to minimize the cost. By adjusting the synthesis conditions the cobalt composition could be increased to improve the magnetic susceptibility of nanofibers, and then magnetic force could be applied to separate nanofibers from the mixture. Another possible method is using silver nanofibers embedded on bulk substrate (silicon wafer, Teflon plate etc.). The silver nanofibers could be easily removed along with the substrate after lipid extraction

process. The reuse of silver nanofibers would be expected to significantly reduce the cost of this method, making it more competitive than the existing methods (sonication, freeze drying, grinding etc.).

5. MECHANISTIC MODEL FOR LIIPID PRODUCTIVITY IN HISTAR

5.1. Introduction

The climate change concerns caused by burning fossil fuels has sparked the interest in developing renewable energy resources. Over the last several decades, microalgae have received considerable interest as the third generation biofuel feedstock. The energy yield per unit area of microalgae are reported to be 1~100 times higher than other oil crops (DOE, 2010; Greenwell et al., 2010; Chisti, 2007). Researchers estimated only 1-3% of the arable land would be enough for microalgae to meet 50% of the transport fuel needs in the US (Chisti, 2008). However, mass production of microalgae in a large-scale culture system remains one of the principal challenges for microalgal biofuel production.

Large-scale microalgal culture is usually conducted in open ponds (Ghasemi et al., 2012). Most commonly used open ponds system include raceway ponds, unmixed ponds, circulate ponds and thin layer inclined ponds (Bhatnagar et al., 2011). Since the culture in open ponds is directly exposed to the environment, only a few strains such as *Chlorella*, *Spirulina*, *Haematococcus* and *Dunaliella* that can tolerate highly alkaline or saline conditions could be successfully cultivated in these types of systems (Chisti, 2007). Additionally, the productivity of open ponds is heavily dependent on the weather conditions including light intensity, temperature, precipitation, all of which vary throughout the year, resulting in the fluctuation of the productivity for microalgae (Ghasemi et al., 2012). Finally, it is difficult to maintain a monoalgal culture in open ponds due to contamination of invasive algal species, zooplankton, and virus etc. (DOE, 2010). Therefore, the reported productivity for microalgal culture in open ponds was in the range of 1-21 mg m^{-2} d^{-1} (Singh and Dhar, 2011).

To overcome the problems of open pond for microalgal culture, closed photobioreactors have been developed. Most commonly used photobioreactors, listed in Ghasemi et al. (2012), are plastic bag systems, bubble column photoreactors, flat plate photobioreactors etc. These reactors allowed the maximum control over the culture conditions (temperature, pH, irradiance etc.). They usually have high surface area to volume ratio, which is in the range of 25-125 m^{-1} compared to 3-10 m^{-1} for open ponds (Lee, 2001), resulting in high average irradiance level in the culture. In order to isolate the contamination (invasive algal species, zooplankton, bacteria etc.) in the environment, it is more likely to maintain monoalgal culture in closed photobioreactors. Therefore, the biomass concentration in these systems could reach 1-5 g L^{-1} and the harvest time is significantly reduced (Lee, 2001). However, there are still major challenges that keep closed photobioreactors from commercial availability (DOE, 2010). First, most closed systems require temperature maintenance since the evaporation cooling is limited. Second, periodical cleaning and sterilization of the whole system might significantly increase the production cost. Third, the scalability of closed photobioreactors is relatively limited compared to open pond systems. Currently, the cost of microalgal oil production is projected at \$2.25 L^{-1} (\$8.52 gal^{-1}) for open ponds and \$4.78 L^{-1} (\$18.10 gal^{-1}) for closed photobioreactors (Davis et al., 2011).

Rusch and Malone (1998) developed Hydraullically Integrated Serial Turbidostat Algal Reactor (HISTAR) for mass production of microalgae. HISTAR is comprised of two precisely controlled close-top turbidostats, which are hydraulically connected with eight serial continuous-flow stirred-tank reactors. A theoretical and physical description of the HISTAR system was done in early studies (Rusch and Christensen, 2003; Rusch and Malone, 1998). The turbidostats release high quality, contaminant-free algal culture into the first CFSTR every 10 minutes, and

water with nutrients is continuously flushed into the first CFSTR, driving the culture through the eight open topped CFSTRs.

Unlike most of the open pond culture systems, which are vulnerable to the contaminants, HISTAR is capable to contain and mitigate the contaminants (Theegala et al., 1999; Rusch and Malone, 1998). By adjusting the system flow rate, the local dilution rate (Gardner et al.) for each tank is maintained greater than the specific growth rate of any potential contaminants. Consequently, the contaminants can be flushed out before they reach a detrimental concentration. Theegala et al. (1999) demonstrated that the microalgae which had been invaded by 300 million live rotifers completely revived after simply increasing the local dilution rate by 6 times. Therefore, HISTAR system is highly promising for the commercial success of up-scaled microalgal mass production compared to traditional open pond culture systems.

To gain fundamental understanding of the HISTAR system, several studies on modeling of HISTAR system were conducted. Rusch and Malone (Rusch and Malone, 1998) established the first HISTAR model by coupling mass balance with Monod growth kinetics to provide foresights during the designing process. Theegala et al. (1999) improved the model by including the impact of contaminants on the system productivity.

Benson et al. (2006) investigated the light dynamics for microalgal culture in the HISTAR system using *Selenastrum capricornutum*. The study determined (1) the linear relationship between surface irradiance (I_{os}) and lamp evaluation (E); (2) the relationship between depth (z) and irradiance level at depth (z) (Lambert-Beer law); (3) light attenuation coefficient (k_0) as a linear partition of biomass and water attenuation; (4) the relationship between average scalar irradiance (I_a) and specific growth rate for microalgae followed Steele's model:

$$\mu = \mu_{max} \frac{I_a(PAR)}{I_{opt}(PAR)} e^{1-\frac{I_a(PAR)}{I_{opt}(PAR)}} \quad (1)$$

Where μ is the specific growth rate (d^{-1}), μ_{max} the maximum specific growth rate, I_{opt} the means internal scalar irradiance associated with μ_{max}, I_a average scalar irradiance level.

Gutierrez-Wing et al. (2011) studied the impact of different light sources (high-pressure sodium (HPS), metal halide (MH), Son Agro® and fluorescent light) on specific growth rate and contaminants growth on the wall of *Selenastrum capricornutum* in the HISTAR system. The results suggested that the HPS and MH lamps would be the most appropriate for HISTAR system, while fluorescent lamp results in low growth rate and Son Angro® lamps induce high contaminant wall growth.

Benson et al. (2007) developed a mechanistic model to investigate the impacts of light dynamics on biomass productivity in HISTAR using *Selenastrum capricornutum*. In the model, the relationship of instantaneous average irradiance and the specific growth rate was described by Steel's equation. The instantaneous average irradiance was calculated by integrating the Lambert–Beer Law over the depth of the culture in each CFSTR. Biorhythm of the microalgae was included in the model using Fourier series analysis. The model was then calibrated using four sets of experimental data in the HISTAR. The optimum areal biomass productivity (P_a) was predicted at 46.8 g m^{-2} d^{-1} under optimum dilution rate via multiple simulation runs.

The biomass productivity, photosynthetic efficiency and lighting cost for the HISTAR system were optimized under various management strategies, operational parameters and reactor design configurations via model simulations (Benson et al., 2009). The results suggested that using HPS lamps (instead of MH lamps) at 25.4 cm above the CFSTRs with six 1000 W and two 400 W lamps (instead of eight 400 W lamps) at system dilution rate of 0.641 d^{-1} would cut 13%

of production cost ($ (kg biomass)$^{-1}$) compared to the original configuration of HISTAR (Benson et al., 2009).

While the importance of irradiance on the biomass production for the HISTAR system has been demonstrated in these studies, the impact of nitrogen levels also should also be included. Nitrogen, which is the essential element for all structural and functional proteins in all algal cells (Richmond, 2004), has been reported for its significant effects on microalgal biomass productivity, lipid content and productivity (Pruvost et al., 2011; Widjaja et al., 2009; Chu and Alvarez-Cohen, 1998; Suen et al., 1987). Although nitrogen limitation can induce higher lipid content in microalgal cells, the increase may not compensate the loss of biomass productivity, which could result in lower lipid productivity (Bai et al., (under review); Gardner et al.; Pruvost et al., 2009; Li et al., 2008b). Furthermore, life-cycle analyses have shown that the consumption of fertilizers (mainly nitrogen and phosphorus) represents large part of energy cost for the whole microalgal biofuel production process (Clarens et al., 2010; Lardon et al., 2009), which could significantly limit the commercial feasibility of algal biofuels. Thus, understanding and being able to predict the effects of nitrogen and balancing the cost of nitrogen and microalgal productivity in the cultivation system is imperative for the overall interests of microalgal biofuels.

The effects of nutrients on microalgal growth have been described by either Monod equation or Droop equation (Bougaran et al., 2010; Li et al., 2010a; Levert and Xia, 2001; Sommer, 1991). In Monod model, the specific growth rate relies on ambient concentrations of limiting nutrients (Monod, 1949), while Droop model assumes that the growth rate depends on the intracellular nitrogen concentration (Droop, 1983). To establish the Droop model, the intracellular nutrients quotas in the microalgal cells have to be accurately measured. However,

for a multi-population culture, this could be technically challenging. Monod model has been reported to describe the effects of nitrogen in several studies (Li et al., 2010a; Rier and Stevenson, 2006; Levert and Xia, 2001). Thus, the Monod model was used in this research to describe the effects of nitrogen on microalgal growth and lipid productivity.

There are very few studies on the modeling of microalgal lipid production. Packer et al. (2011) explained the lipid accumulation in microalgal cells by separating the lipid and the rest of the biomass. However, the model is based on the assumption that the lipid was not produced at all when the nitrogen saturated. Hence, it is not suitable for the *Chlorella vulgaris*/*Leptolyngbya* co-culture in HISTAR system. Luedeking and Piret equation (Luedeking and Piret, 1959) was used to construct the microalgal lipid production models (Tevatia et al., 2012; Yang et al., 2011). In this equation, the instantaneous production rate of the bio-product is directly proportional to the instantaneous biomass production rate and biomass concentration. It is able to describe the relative constant lipid content in the exponential phase, and the increase in lipid content after the biomass growth slows down. Therefore, the Luedeking-Piret equation was applied in the model presented in this dissertation to describe the lipid production in HISTAR system.

5.2. HISTAR Descriptions and Data Acquisition

The experimental HISTAR system is comprised of two automated enclosed turbidostats and eight open-top continuous-flow stirred-tank reactors (CFSTR) (Figure 5.1). High Pressure Sodium (HPS) lamps (400 watt) are located approximately 26.6 cm over each CFSTR to provide continuous artificial illumination to the microalgal culture. The volume of each CFSTR (vertical cylinder) is 454 L with the depth of 0.52 m. Each turbidostat is active every other day. Approximately 227 L of inoculum culture was injected into the first CFSTR per day. After a day of running, the active turbidostat was refilled with culture media to the original volume (454 L) and the culture was grown in batch mode for one day to reach higher biomass concentration. The

inoculum culture was injected to the first CFSTR every 20 minutes (at the flow rate Q_{tb}=3.15 L min^{-1} for 1 minute). The biomass concentration increases to the final concentration of X_8, as the culture flows through the eight CFSTRs. Constant flow rate for culture media (make up water + nutrients) was maintained to assure a fixed system dilution rate (D_s) during each run.

The methods for estimation of irradiance parameters followed the previous light kinetics studies (Benson et al., 2007; Benson and Rusch, 2006), which provide the information of (1) surface irradiance I_{os} (PAR) as a function of lamp elevation; (2) scalar irradiance I_{zn} (PAR) as a function of culture depth z; (3) average irradiance I_{an} (PAR) in the CFSTR as a function of biomass concentration; (4) specific growth rate μ_n as a function of I_{an} (PAR) and optimum irradiance I_{opt} (PAR). The data for model calibration were collected from a series of studies on biomass and lipid productivity in HISTAR with the system dilution rates D_s of 0.360 and 0.459. A *Chlorella vulgaris/Leptolyngbya sp.* co-culure, which has been reported for high growth rate and lipid productivity (Bai et al., (under review); Silaban et al., (under reivew)) is used for all the experiments. F/2 media (Kent Marine, Inc.) was used for all the experiments in HISTAR.

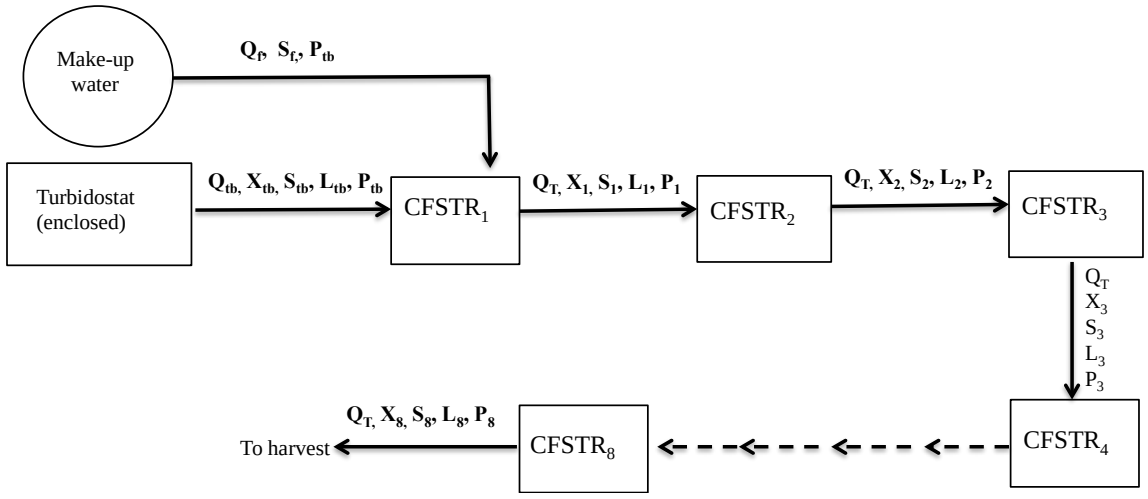

Figure 5.1. Schematic diagram of HISTAR system. The biomass was inoculated to $CFSTR_1$ from turbidostat and amplified through eight serial CFSTRs.

5.3. Model Expansion

The model from Benson et al. (2007), which mainly described the effects of instantaneous scalar irradiance level on biomass productivity, was expanded to include the impacts of nitrogen level on biomass and lipid productivity. Therefore, the module for impacts of irradiance on biomass productivity throughout this research followed Benson et al. (2007).

The expanded model mainly describes three state variables:

$X_n(t)$=algal biomass concentration in n^{th} CFSTR (g m^{-3})

$L_n(t)$=lipid concentration in n^{th} CFSTR (g m^{-3})

$S_n(t)$= nitrogen concentration in n^{th} CFSTR (g m^{-3}).

The effects of light dynamics (Lambert–Beer Law), average irradiance (Steele's equation) and nitrogen concentration (Monod equation) on biomass productivity, nitrogen consumption and lipid productivity (Luedeking-Piret equation) in the HISTAR system are included in the model. The model was coded in Matlab™ (2009b) platform. The simulations were run using 4^{th} order Runge-Kutta with a time step of 0.1 day.

5.3.1. Governing Equations

The same as Benson et al. (2007), the mass balance for algal biomass in the first CFSTR can be written as:

$$\frac{dX_1}{dt}V_n = Q_T X_i - Q_T X_1 + U_1 X_1 V_n \tag{2}$$

where Q_T is the combination of make-up water flow rate (Q_f) and inoculum flow rate (Q_{tb}). The biomass concentration of the input flow for the first CFSTR (X_i) was calculated as:

$$X_i = \frac{Q_{tb} X_{tb}}{Q_{tb} + Q_f} \tag{3}$$

In the experiment conducted for this study, the biomass concentration in the turbidostats (X_{tb}) was not constant, since the two turbidostats were alternatively active and operated in a batch mode. Therefore, the average X_i for each day was a graphical input for the model. The mass balance of algal biomass on the rest of the tanks was expressed as:

$$\frac{dx_n}{dt}V_n = Q_T X_{n-1} - Q_T X_n + U_n X_n V_n \quad (4)$$

Similarly, the governing equations for the nitrogen S_n (g m^{-3}) and lipid concentration L_n (g m^{-3}) in CFSTRs can then be written as:

$$\frac{dS_1}{dt}V_n = Q_T S_i - Q_T S_1 - W_{s1} S_1 V_n \quad (5)$$

$$\frac{dS_n}{dt}V_n = Q_T S_{n-1} - Q_T S_n - W_{sn} S_n V_n \quad (6)$$

$$\frac{dL_1}{dt}V_n = Q_T L_i - Q_T L + R_{P1} P_1 V_n \quad (7)$$

$$\frac{dL_n}{dt}V_n = Q_T L_{n-1} - Q_T L_n + R_{Pn} P_n V_n \quad (8)$$

Where R_{p1} is the lipid production rate (d^{-1}) in $CFSTR_1$ and R_{pn} is the lipid production rate of $CFSTR_n$.

5.3.2. Biomass Growth Kinetics and Nitrogen Consumption Kinetics

The last terms of the equations (2) and (4) represent the net growth rate of the biomass in the CFSTRs, which can be written as:

$$U_n X_n V_n = (\mu_n - k_{en}) X_n V_n \quad (9)$$

As Benson et al. (2007) stated, the decay rate of the biomass increases with the cell age. The decay rate and the system residence time in $CFSTR_n$ (τ_n) followed a linear relationship:

$$k_{en} = a\tau_n + b \quad (10)$$

Where a, b are coefficients obtained by fitting a set of data collected from the productivity experiment in HISTAR. However, the decay rate in this study on the Louisiana co-culture did

not follow this linear equation, most likely due to the culture shifts between *Chlorella vulgaris* and *Leptolyngbya sp.* observed in biomass productivity experiments in HISTAR. Thereby, the decay rate in this study was fitted by directly comparing the actual net specific growth rate with the results from simulation performed at k_{en}=0.

In Benson et al. (2007), the effects of mean internal scalar irradiance I_{an} on the specific growth rate of biomass were described by using Steele's model (Equation (1)). In the model presented in this research, the effects of both mean internal scalar irradiance and nitrogen concentration on the biomass productivity were included. Two common approaches are used to combine the effects. The first is "Blackman's law of the minimum", which uses the smaller of the fractional growth rates as the one in the growth model. The second approach multiples the two fractional growth rate to generate a combined growth rate (Haney and Jackson, 1996). Since the relationship (i.e. greater or smaller) between the two fractional growth rate depends on the biomass concentration and the nitrogen concentrations and may vary in different CFSTRs for HISTAR, the growth rate based on the second approach was used in this work. The specific growth rate for algal biomass was calculated by multiplying the fractional growth rate of Steele's equation and Monod equation for light and nutrient limitations, respectively:

$$\mu_n = \mu_{max} F_D \frac{I_{an}(PAR)}{I_{opt}(PAR)} e^{1-\frac{I_{an}(PAR)}{I_{opt}(PAR)}} \cdot \frac{S_n}{K_s + S_n} \cdot \frac{P_n}{K_p + P_n} \quad (11)$$

Where P_n is the phosphorus concentration (g m^{-3}) and K_p is the half saturation coefficient of phosphorus. Since the N:P ratio in this work (~6:1) was much lower than the Redfield ratio (~16:1) (Redfield, 1934) , only nitrogen is considered as rate limiting nutrient ($P_n/(K_p+P_n)$=1).

The nitrogen consumption rate ($W_{Sn}S_n$) was calculated by:

$$Y = \frac{U_n X_n}{W_{Sn} S_n} \quad (12)$$

where Y is the lipid yield on nitrogen (g g^{-1}N). The nitrogen content in dry biomass of *Chlorella* species was reported in the range of 6.2~7.7%, resulting in the Y value of 12.98~16.11 (Oh-Hama and Miyachi, 1988). Each of these parameters that have significant impact on the growth rate of algal biomass and consumption rate of nitrogen is discussed further in the following section.

5.3.3. Light Dynamics

As discussed in Benson et al. (2007), the average internal scalar irradiance I_{an} from Equation (11) can be determined by integrating the Lambert-Beer law over the culture depth d_n in $CFSTR_n$:

$$I_{an}(PAR) = \frac{I_{osn}(PAR)(1 - e^{-k_0(PAR)d_n}}{k_0(PAR)d_n} \tag{13}$$

The surface irradiance I_{osn} (PAR) in Equation (13) was estimated empirically by air attenuation coefficient studies following the method described in Benson et al. (2006):

$$I_{Os_n}(PAR) = I_{E0} - k_a E_n \tag{14}$$

The relationship between the surface irradiance levels (I_{os}) and elevation (E_n) of the lamps was explained by a simple linear equation. The surface irradiance level over six lamp elevations (25, 29, 33, 37, 41, 45 cm) was measured. Linear regression of surface irradiance levels versus the lamp elevations (E_n) was performed to calculate the hypothetic surface irradiance at E_n=0 (I_{E0}) and light diffusion constant (k_a) (Figure 5.2). The irradiance level (I_z)

was plotted against depth z (X=0, 50, 53, 56, 79, 105 g m^{-3}), and the data were fitted to Lambert-Beer equation to determine the light attenuation (k_0) at each biomass concentration (X=0, 50, 53, 56, 79, 105 g m^{-3}):

$$I_Z(PAR) = I_{OS}(PAR)e^{-k_0(PAR)z} \tag{15}$$

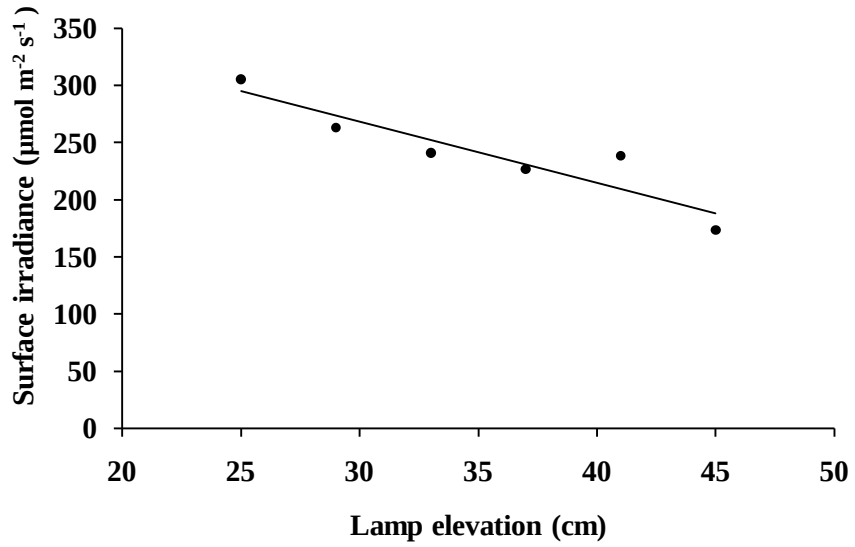

Figure 5.2. The relationship between surface irradiance levels and elevation (E_n) of the lamps explained by linear equation I_{OS}=-5.34E_n+428 (R^2=0.850).

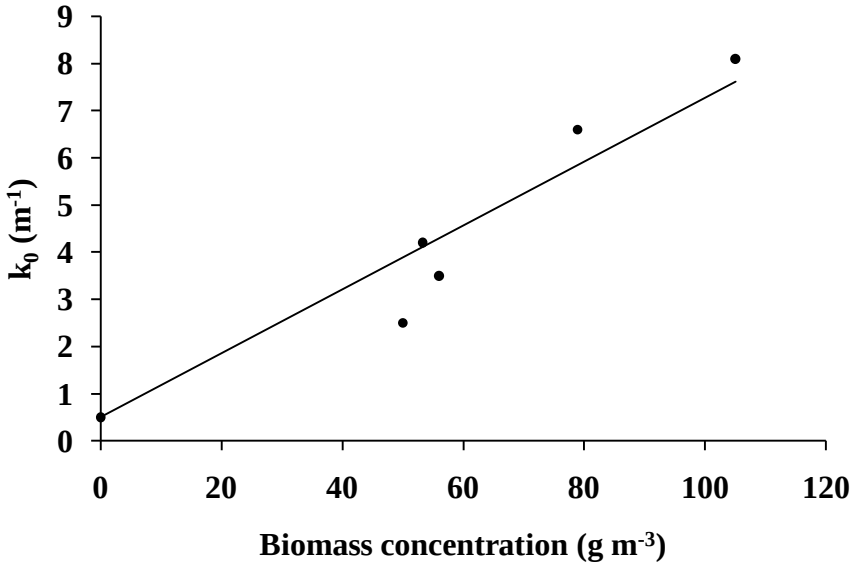

Figure 5.3. The relationship between biomass concentration (X, g m^{-3}) and light attenuation coefficient k_0 (m^{-1}) explained by linear equation: k_0=0.0678X+0.501 (R^2=0.911).

The k_0 for each study was then regressed against the respective biomass concentration (X), resulting in a linear partition of k_0 in terms of k_w and k_b (Figure 5.3):

$$k_0(PAR) = k_w + k_b X \tag{16}$$

5.3.4. Self-shading Effect

The factor F_D in Equation (12) represents the effects of self-shading on μ_n. As stated in Benson et al. (2007), the relationship between specific growth rate μ_n and average internal scalar irradiance I_{an} changes as the dilution rate D_s varies. In Benson et al. (2007), the effects of self-shading were represented by multiplying the relationship between μ_n and I_{an} by a factor (F_D). When the system is at steady state and D_s is less than optimum, μ_n would increase as D_s increases and self-shading decreases (F_D would increase until it reaches 1 as D_s increases to the optimum). When D_s values are greater than optimum, μ_n is limited by the intrisic biological growth capacity (μ_{max}) of the culture, but μ_n required to maintain the steady state continues to increase, resulting in washout of the culture (Benson et al., (2007). The self-shading factor was estimated by the ratio of average μ_s (hypothetic average system growth rate required to maintain steady state at the given D_s) and μ_{max}. μ_s was calculated as the average of μ_8 and μ_{max}, while μ_8 was estimated by the equation:

$$\mu_n = D_n \left[1 - \frac{X_i}{X_n}\left(\frac{1}{(\prod_{j=1,n\neq 1}^{n-1}(1 - U_j D_j^{-1})}\right)\right] + k_{en} \tag{17}$$

And F_D was calculated as:

$$F_D = \frac{\mu_s}{\mu_{max}} \tag{18}$$

5.3.5. Lipid Production Rate

Luedeking-Piret equation is capable of describing the relative constant metabolite (lipid) content in the exponential phase, and the increase in lipid content after the biomass growth slows

down (Luedeking and Piret, 1959). Several studies have reported this equation to be suitable to describe the lipid production kinetics for microalgal culture. (Tevatia et al., 2012; Yang et al., 2011). Thus Luedeking-Piret equation was selected for lipid production module in this model:

$$\gamma_p = U_{Pn} L_n = \alpha U_n X_n + \beta X_n \tag{19}$$

γ_p is the rate of lipid productivity (g m^{-3} d^{-1}). Therefore, mass balance equations for lipid in $CFSTR_n$ can be rewritten as:

$$\frac{dL}{dt} V_1 = Q_T L_i - Q_T L_1 + (\alpha U_1 X_1 + \beta X_1) V_n \tag{20}$$

$$\frac{dL_n}{dt} V_n = Q_T L_{n-1} - Q_T L_n + (\alpha U_n X_n + \beta X_n) V_n \tag{21}$$

Where α is lipid formation coefficient (g g^{-1}) and β is the non-growth correlation coefficient (g g^{-1} d^{-1}). In this study, the initial value of α and β were calculated using batch experiments conducted under the irradiance level of 180 μmol m^{-2} s^{-1} and nitrogen level of 20.6 g m^{-3}.

5.4. Model Calibration

A sensitivity analysis was conducted to determine which parameters had the greatest impact on the biomass and lipid concentrations in the HISTAR system. Based on the results, the F_D was selected as the primary calibration parameter for biomass concentration (X). Multiple simulations were conducted by varying the F_D in the range of ±50% of the calculated value to find the best fit for the minimum standard error of prediction, which was calculated as:

$$\text{Standard error of prediction} = \sqrt{\left[\frac{\sum_1^n \left(X_{8p} - X_{8a}\right)^2}{n_x - 1}\right]} \tag{22}$$

After adjusting the F_D, the standard error of prediction was 20.7% of the mean of the actual data. The biomass yield on nitrogen Y (g biomass $(g\ N)^{-1}$) was calibrated to match the experimental data for nitrogen levels in the HISTAR (Table 5.1). The predicted lipid percentage

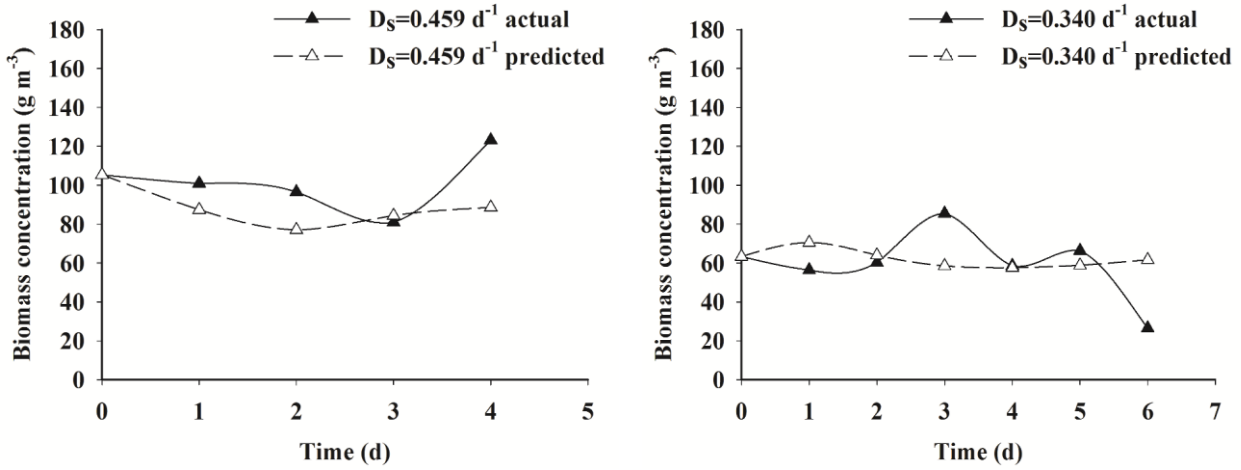

Figure 5.4. The model was calibrated using two biomass data sets collected from the HISTAR system operated at D_s levels of 0.459 and 0.340 d^{-1}.

was compared with the actual lipid percentage of dry biomass (Table 5.2). The results showed that the standard error of prediction was 54.8% for D_s=0.459 d^{-1} and 17.13% for D_s=0.340 d^{-1}. The error between actual data and predicted values is most likely attributed to the biological variance of the culture. Additionally, culture shift from *Chlorella vulgaris* dominant to *Leptolyngbya sp*. dominant, which was observed during the experiments, might be another factor that causing the error of prediction.

Table 5.1. The predicted value from simulations versus actual value for nitrogen concentration in HISTAR.

Conditions	Nitrogen concentration (g m^{-3})	
	Predicted	Actual
D_s=0.340 d^{-1}, Day 1	5.4	5.7
D_s=0.459 d^{-1}, Day1	10.56	10.4

Table 5.2. The predicted value from simulations versus actual value for lipid percentage of the Louisiana co-culture produced from HISTAR.

Conditions	Lipid Percentage (%, mass/mass)	
	Predicted	Actual
D_s=0.340 d^{-1}, Day 4	29.57	25.18
Ds=0.459 d^{-1}, Day 3	28.92	18.35

5.5 Simulation Results and Discussion

Simulations were conducted on the calibrated model to investigate and illustrate the impact of nitrogen levels on the system productivity for biomass and lipid. The system dilution rate was set at 0.459 d^{-1} (Q_f=1.0 L min^{-1}), since biomass concentration and productivity are higher at this dilution rate. Other operational conditions were listed in Table 5.3.

5.5.1 Basic HISTAR Dynamics

The changes/variations in the biomass, lipid, lipid percentage (mass/mass on dry biomass) and nitrogen concentration with respect to time and $CFSTR_n$ were demonstrated (Figure 5.5). The simulations were performed under the initial conditions X_{0n}=0, S_{0n}=12.3 g m^{-3} and L_{0n}=0. In the transition phase, the biomass concentrations in prior CFSTRs were higher than the latter ones (Figure 5.5a). The trend gradually reversed as the culture reached the steady state, where the biomass concentration of $CFSTR_{n+1}$ was incrementally higher than $CFSTR_n$. There was an approximate two-day lag period between the $CFSTR_1$ and $CFSTR_8$, which matches the 2.1 days system retention time at D_s= 0.459 d^{-1} (Q_f=1 L min^{-1}). As expected, the nitrogen levels (Figure 5.5b) in each CFSTR was inversely related to the biomass concentrations since microalgae consume nitrogen to produce biomass. Therefore, the lag time between $CFSTR_1$ and $CFSTR_8$ was also around 2 days.

As steady state is reached, $CFSTR_{n+1}$ shows incrementally higher lipid percentage than $CFSTR_n$ (Figure 5.5 c). This is most likely attributed to the lower nitrogen levels in $CFSTR_{n+1}$

Table 5.3. The estimated parameters of the productivity model for HISTAR.

Parameter	Calculated or experimental estimation	Final calibrated parameters	Literature values
Operational parameters			
Q_f (m^{-3} d^{-1})			
D_s=0.459	1.44	Not adjusted	Unique for HISTAR
D_s=0.340	1.08	Not adjusted	Unique for HISTAR
Q_{tb} (m^{-3} d^{-1})	0.227	Not adjusted	Unique for HISTAR
X_{tb} (g dry mass m^{-3})	unique for the data set	Not adjusted	
X_{n0} (g dry mass m^{-3})	unique for the data set	Not adjusted	
Light parameters			
I_{E0n} (μmol m^{-2} s^{-1})	428	Not adjusted	
k_a (μmol m^{-2} s^{-1} cm^{-1})	5.34	Not adjusted	
k_w (m^{-1})	0.501	Not adjusted	0.001; Grima et al. (1994)
k_b (m^2 g^{-1})	0.0678	Not adjusted	
Growth parameters			
μ_{max} (d^{-1})	1.51	Not adjusted	
I_{opt} (μmol m^{-2} s^{-1})	605	Not adjusted	
F_D (dimensionless)			
F_D (D_s=0.459)	0.416	0.624	
F_D (D_s=0.340)	0.545	0.709	
k_{en} (d^{-1})		Unique for each CFSTR	
Y	12.98-16.10	11.6	(Oh-Hama and Miyachi, 1988)
K_s (g m^{-3})	3.03	Not adjusted	
Lipid parameters			
α	0.24	Not adjusted	Unique for each culture
β	0.04	Not adjusted	Unique for each culture

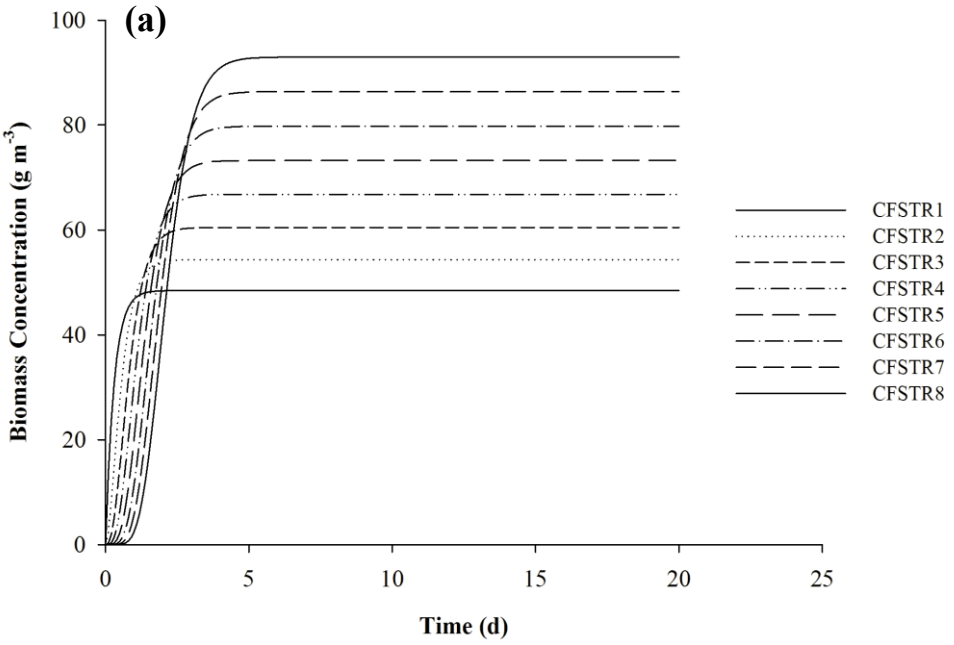
(a)
Biomass Concentration (g m-3)
Time (d)
CFSTR1
CFSTR2
CFSTR3
CFSTR4
CFSTR5
CFSTR6
CFSTR7
CFSTR8

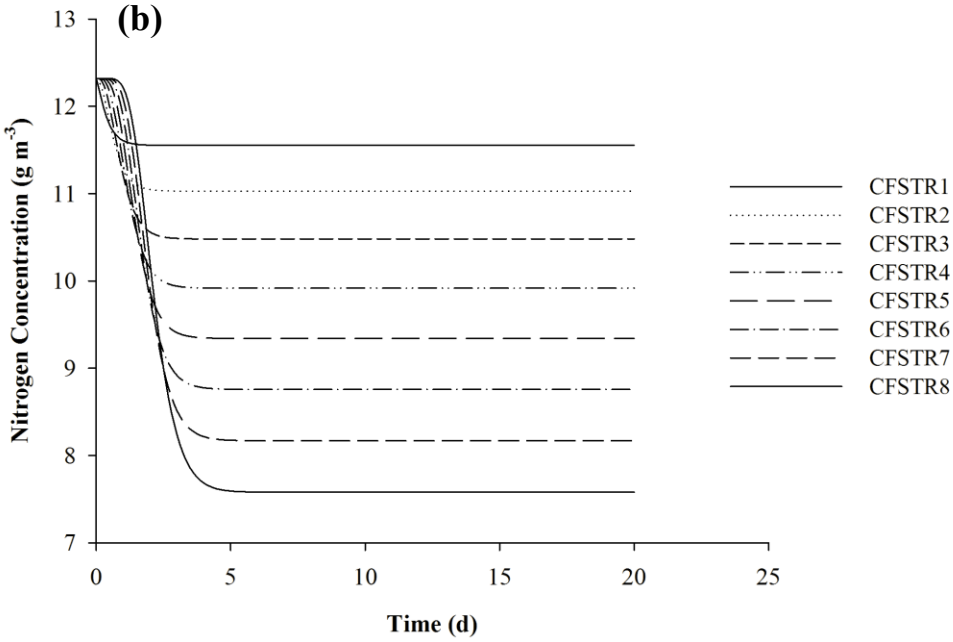
(b)
Nitrogen Concentration (g m-3)
Time (d)
CFSTR1
CFSTR2
CFSTR3
CFSTR4
CFSTR5
CFSTR6
CFSTR7
CFSTR8

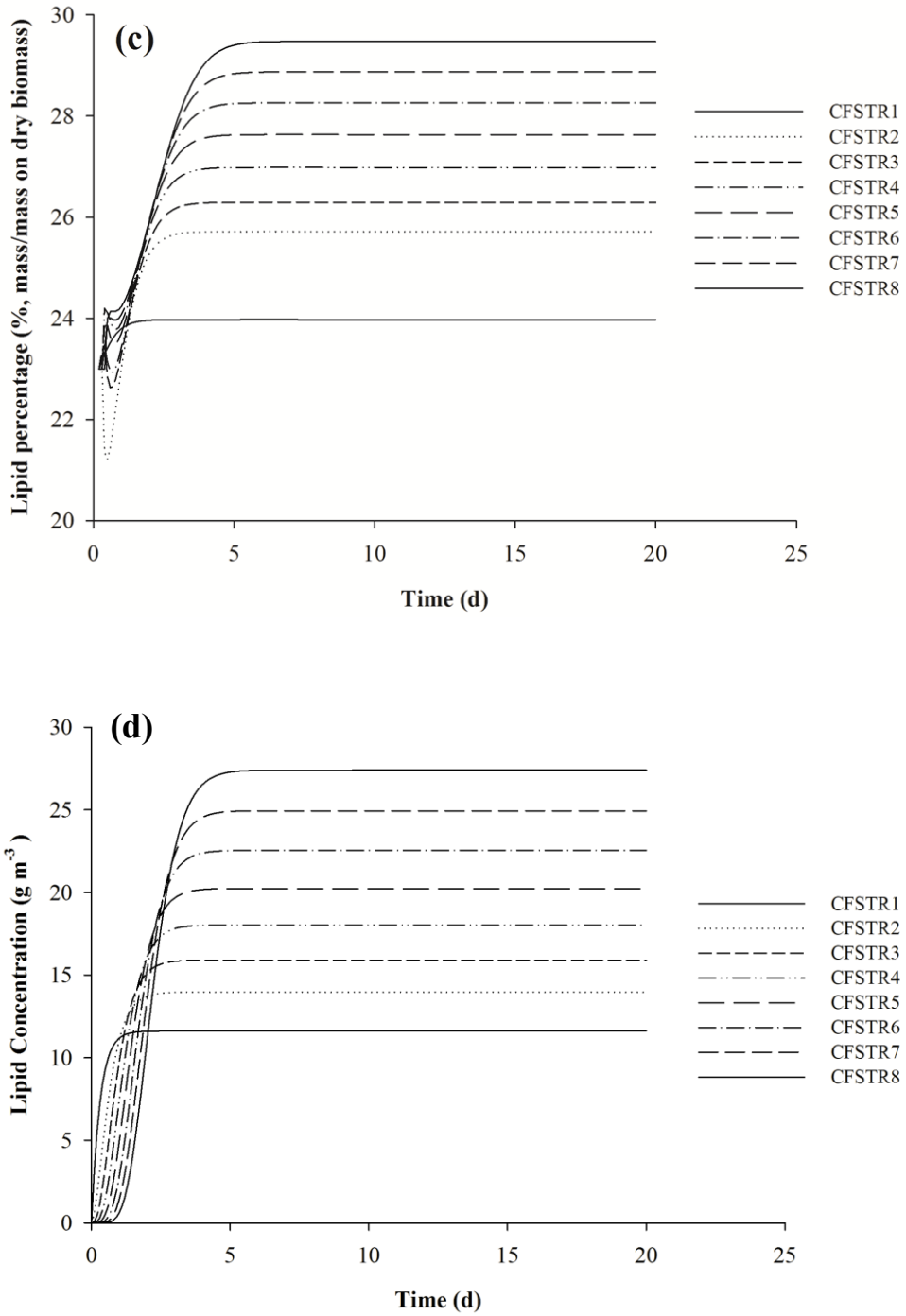

Figure 5.5. The change in a) biomass concentration; b) nitrogen concentration; c) lipid percentage; d) lipid concentration in each of the CFSTRs simulated to demonstrate the transitional state of the system from start-up to steady state.

than $CFSTR_n$, since many studies have reported that lower nitrogen levels induced increase in lipid percentage for microalgae (Pruvost et al., 2011; Widjaja et al., 2009; Chu and Alvarez-Cohen, 1998; Suen et al., 1987). When nitrogen is lower, the cell division and cell growth rates inevitably slow down due to the lack of nitrogen to support protein and enzyme synthesis (Sharma et al., 2012), resulting in the decrease of the demand for metabolic energy (the citric acid cycle), which competes with lipid synthesis for precursors. Therefore, lipid percentage in microalgal cells increases at lower nitrogen concentration (Deng et al., 2010). As a result of incrementally higher biomass and lipid percentage, the lipid concentration in $CFSTR_{n+1}$ is incrementally higher than $CFSTR_n$ (Figure 5.5d).

5.5.2 Impact of Nitrogen Level in the Input Flow on Biomass and Lipid Production

Nitrogen level can significantly affect the biomass and lipid production. The nitrogen consumption is also a major part of the production cost for microalgal biofuels according to several results of life-cycle analyses (Teixeira, 2012; Brentner et al., 2011; Lardon et al., 2009). Thus, it is critical to investigate the effects of nitrogen levels in the make-up water (the nitrogen level in the input flow of the system S_f) of the biomass and lipid production and find the optimal nitrogen level for the HISTAR system. Five nitrogen concentrations are 12.32 g m^{-3} for F/2 media, 41.2 g m^{-3} for Bold's Basal media, 20.6 g m^{-3} for 50% of Bold's basal media, and 4 g m^{-3} and 1 g m^{-3} for nitrogen limitation. The results showed that the lower nitrogen input level resulted in higher lipid percentage (mass/mass, on dry biomass) (Figure 5.6a), which matched the results reported in the literature (Chen et al., 2011b; Widjaja et al., 2009; Chu and Alvarez-Cohen, 1998; Suen et al., 1987). The highest lipid percentage (~32%) was obtained at the nitrogen concentration of 1 g m^{-3}. The biggest difference in the lipid percentages (mass/mass on

dry biomass) for all the tested nitrogen levels was less than 3%. However, the decrease in nitrogen level constrained the biomass concentration (Figure 5.6b), resulting in a decrease in the lipid concentration in $CFSTR_8$ (g lipid per m^3 culture, Figure 5.6c) and daily volumetric and areal lipid productivity (Figure 5.7). To obtain the maximum lipid productivity, the higher nitrogen levels (20.6 and 41.2 g m^{-3}) were preferred. However, the left over nitrogen level in the outlet flow of the system was higher in for the culture with higher nitrogen input concentrations (Figure 5.6d). Hence, the nitrogen reuse from the outlet flow of the system should be applied (Roesch et al., 2012).

The highest daily areal lipid productivity for these simulations was 5.76 g m^{-2} d^{-1} respectively (Figure 5.7), which was close to the baseline assumption for areal lipid productivity of 6.25 g m^{-2} d^{-1} in open ponds system in Davis et al. (2011). The maximum volumetric lipid productivity was 13.0 g m^{-3} d^{-1}, which was in the range of the volumetric lipid productivity of *Chlorella vulgaris* reported in Mata et al. (2010) (11.2-40.0 g m^{-3} d^{-1}). Both biomass and lipid productivity for HISTAR was lower than the closed photobioreactors (Carvalho et al., 2006), but the lower production cost would compensate the low lipid productivity for open pond systems. Therefore, when the media recycling is applied, nitrogen levels at 41.2 and 20.6 g m^{-3} is preferred to maximize the lipid productivity. These results were consistent with the batch experiments (Bai et al., (under review)) and other studies on the impacts of nitrogen limitation on microalgal lipid production, suggesting that this model is capable to simulate the effects of nitrogen levels on the lipid percentage and lipid productivity. Thus, the model can be a predicative tool for optimizing the nitrogen level for the HISTAR system.

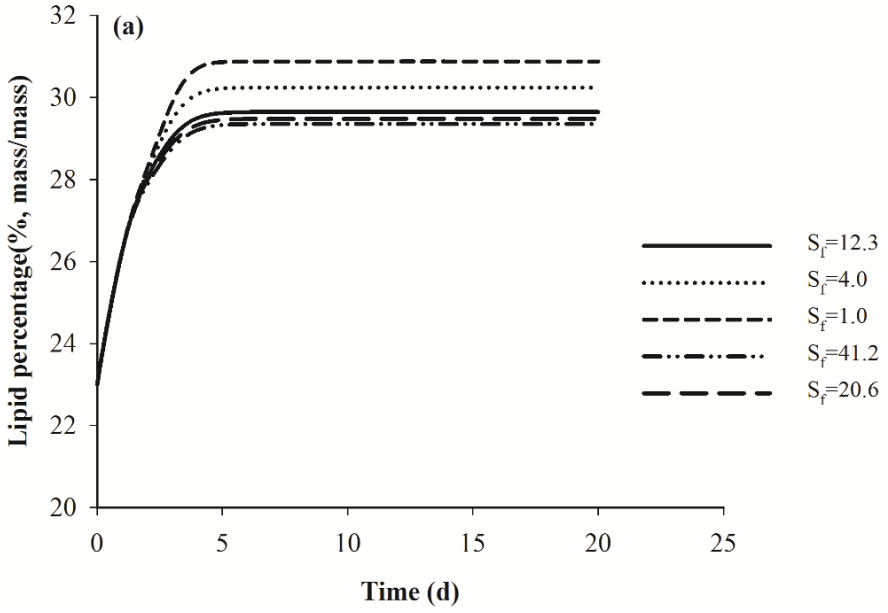
(a)
Lipid percentage(%, mass/mass)
32
30
28
26
24
22
20
0
5
10
15
20
25
Time (d)
S_f=12.3
S_f=4.0
S_f=1.0
S_f=41.2
S_f=20.6

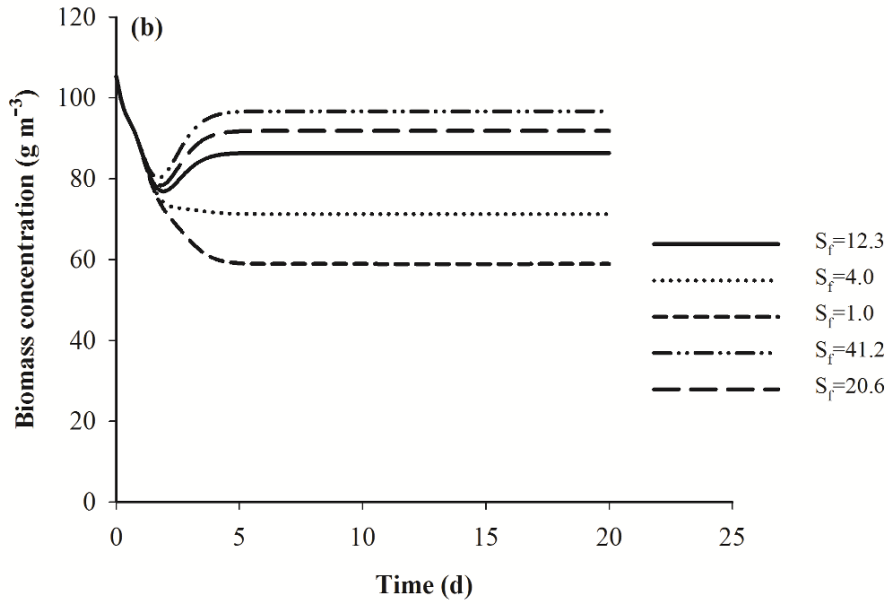
(b)
Biomass concentration (g m^{-3})
120
100
80
60
40
20
0
0
5
10
15
20
25
Time (d)
S_f=12.3
S_f=4.0
S_f=1.0
S_f=41.2
S_f=20.6

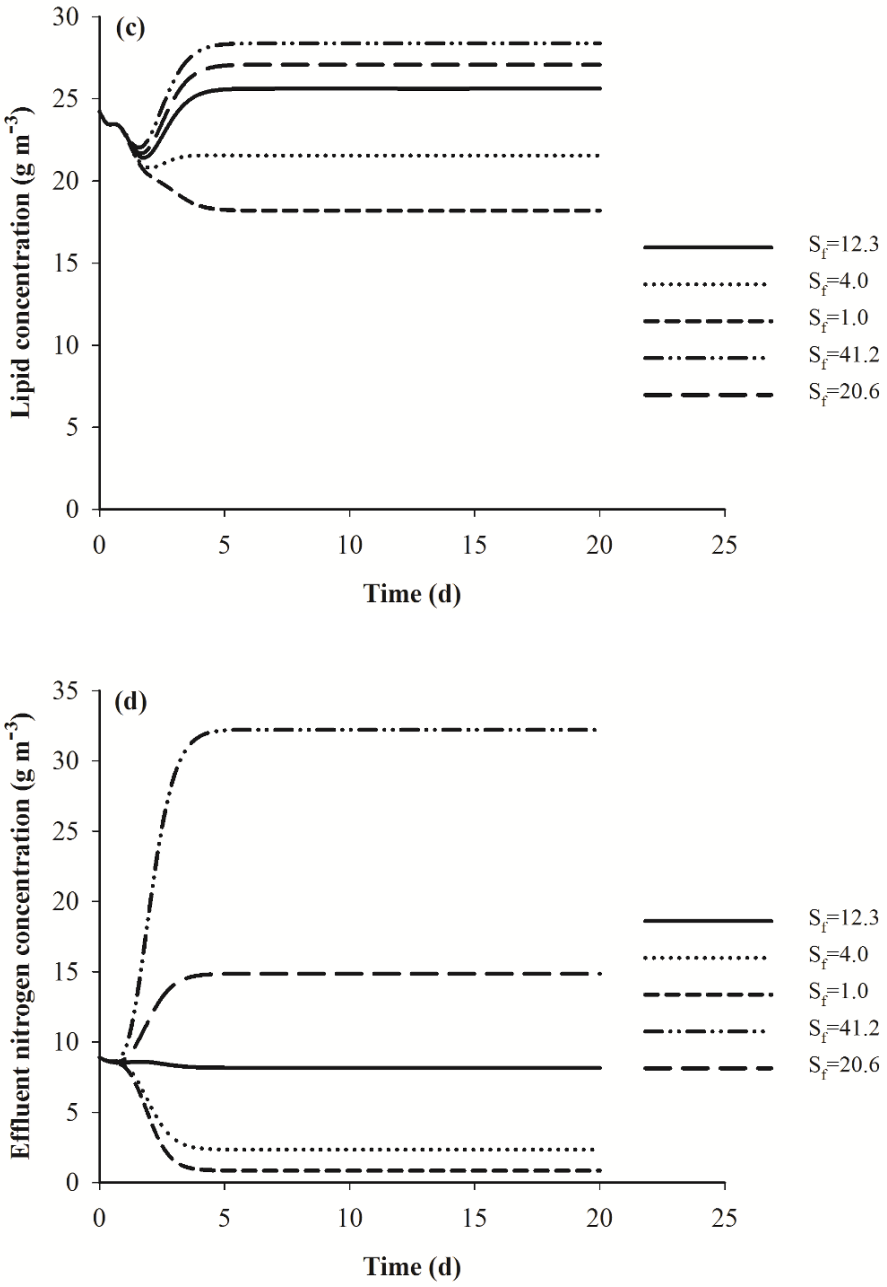

Figure 5.6. a) Lipid percentage (mass/mass on dry biomass), b) biomass concentration, c) lipid concentration, d) nitrogen level of the *Chlorella vulgaris*/ *Leptolyngbya sp.* co-culture in the $CFSTR_8$ of the HISTAR. S_f is the nitrogen concentration (g m^{-3}) of the input flow for the system. The system dilution rate D_s=0.459 d^{-1}.

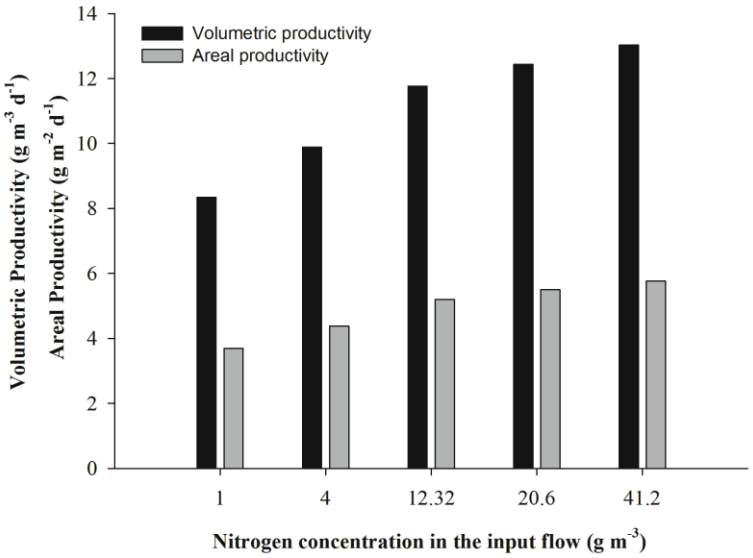

Figure 5.7. The volumetric and areal lipid productivity of the HISTAR under different nitrogen levels in make-up water (the input flow of the system). The system dilution rate D_s=0.495 d^{-1}.

5.5.3 Impact of Biomass Inoculum on System Productivity

The effect of the biomass inoculum (H_{tb}, g d^{-1}) from the first CFSTR, on the biomass and lipid harvested from the last CFSTR (H_s and L_s, g d^{-1}) were investigated via several simulations under different nitrogen levels in the make-up water of the system. The average H_{tb} and L_{tb} (the amount of lipid in the inoculated biomass) values (31, 62, 93, 124 g d^{-1}) in range typical for the HISTAR system were used in the simulations. The nitrogen levels in the make-up water for the system were 12.32, 4.0, 1.0, 41.2 and 20.6 g m^{-3}. The ratios of H_s/H_{tb} and L_s/L_{tb} under each condition were reported and compared. The highest values of both H_s/H_{tb} and L_s/L_{tb} were attained at 31 g d^{-1} inoculum biomass and 41.2 g m^{-3} nitrogen level (Figure 5.8). The H_s/H_{tb} and L_s/L_{tb} values were inversely correlated to H_{tb} and L_{tb} respectively, but they were directly related to the nitrogen level in the input flow of the system.

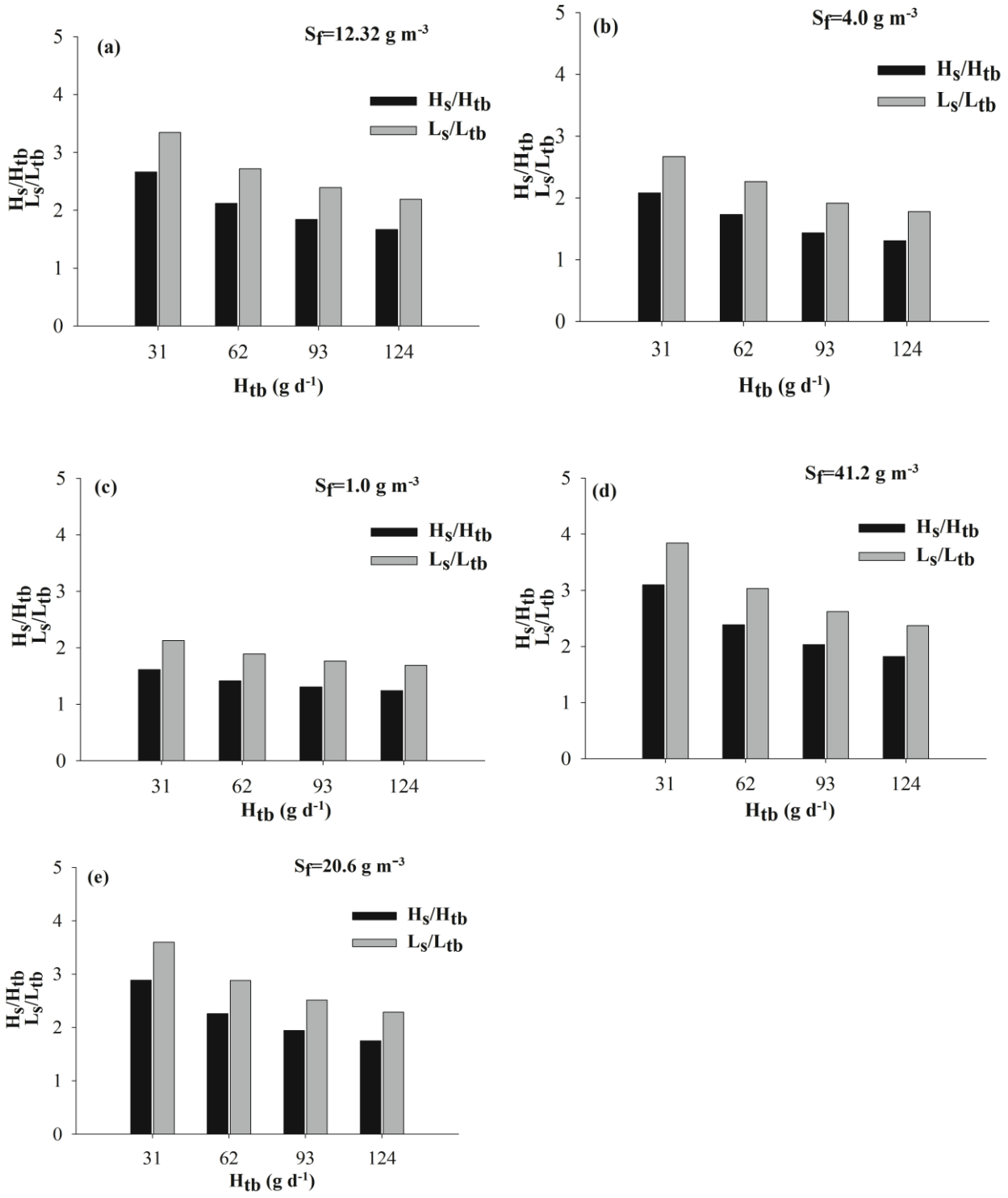

Figure 5.8. The daily harvest of biomass and lipid from the HISTAR system (H_s, L_s g d^{-1}) was compared to that harvested from the turbidostats (H_{tb}, L_{tb} g d^{-1}) for the five nitrogen levels (a) 12.32 g m^{-3}, (b) 4.0 g m^{-3}, (c) 1.0 g m^{-3}, (d) 41.2 g m^{-3}, (e) 20.6 g m^{-3} in the make-up water (the input flow of the system). The system dilution rate D_s=0.459 d^{-1}.

5.5.4 Impacts of Nitrogen Levels on the Cost of Lipid Production

Simulations were performed at five different nitrogen levels in the input flow (S_f) to investigate the nitrogen levels that would result in lowest lipid production cost ($ kg^{-1}) for the HISTAR. The production cost included the cost of electricity (lighting and aeration), water and chemicals for culture media. As the nitrogen levels increased, the lipid production cost decreased from $316 kg^{-1} for 1 g m^{-3} nitrogen to $208 kg^{-1} for 41.2 g m^{-3} nitrogen (Figure 5.9). These numbers were significantly higher than the cost reported by Davis et al. (2011). However, the lighting cost, which took around ~67% of the total production cost, could be minimized by using sun light in an outdoor system instead of artificial illuminations. The cost for mixing the culture by aeration, which took ~15% of the total production cost (using 746 W air blower), could be reduced by using pedal wheel. Additionally, up scaling the HISTAR from a pilot-scale system to an - the lipid production cost. Therefore, to obtain a realistic production cost of HISTAR system for industrial-scaled lipid production, an up scaled model that incorporate outdoor conditions such as natural lighting, temperature oscillation etc. will be needed.

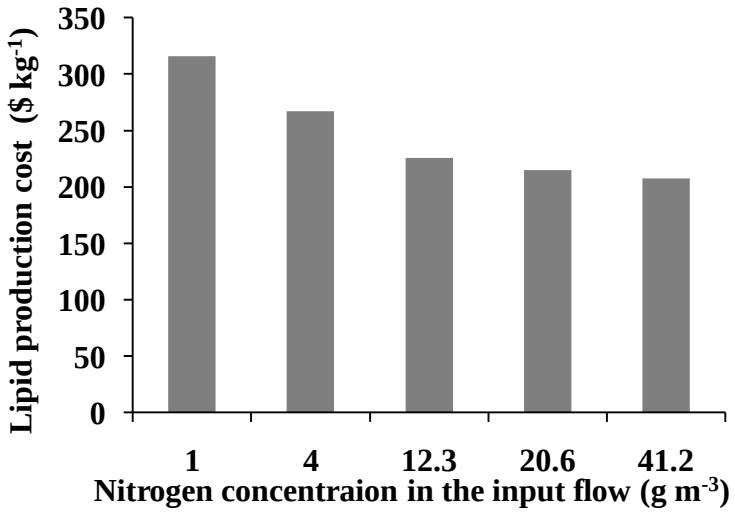

Figure 5.9. The lipid production cost ($ kg^{-1}) at five nitrogen levels (S_f) in the input flow.

5.6 Conclusions

The mechanistic model developed in this study included the effects of both nitrogen and average scalar irradiance on biomass production, lipid percentage (mass/mass, on dry biomass) and lipid production for the HISTAR system. The simulations demonstrated the trend for biomass, lipid and nitrogen levels in the HISTAR system. The results of the simulations indicated that the effects of nitrogen level described by this model were consistent with bench top studies and the other literature on nitrogen limitations. The lower nitrogen levels were able to increase the lipid percentage, but the increase could not compensate the loss of biomass productivity, resulting lower overall lipid productivity. The model was calibrated, but extra data sets are needed for further calibration and model validation. The results suggested that high nitrogen level (Bold's Basal medium, 41.2 g m^{-3}) is necessary for high lipid productivity (13.0 g m^{-2} d^{-1}) and low lipid production cost (\$208 kg^{-1}), although the residual nitrogen level flow out of the last CFSTR may be high. Therefore, nutrients recycle is needed to lower the cost of nitrogen.

Nomenclature

d_n	culture depth of $CFSTR_n$ (m)
D_n	local dilution rate for $CFSTR_n$ (d^{-1})
D_s	system dilution rate (d^{-1})
E_n	elevation of the light source over $CFSTR_n$
F_D	factor representing the effect of self-shading on growth rate
$I_{an}(PAR)$	average scalar irradiance in $CFSTR_n$ (μmol m^{-2} s^{-1})
$I_{opt}(PAR)$	optimum scalar irradiance (μmol m^{-2} s^{-1})
$I_{osn}(PAR)$	surface irradiance in $CFSTR_n$ (μmol m^{-2} s^{-1})
$I_{zn}(PAR)$	scalar irradiance (μmol m^{-2} s^{-1}) at z depth for $CFSTR_n$
$k_0(PAR)$	Overall scalar attenuation coefficient (m^{-1})=$k_w+k_bX_n$
k_a	light diffusion coefficient (μmol m^{-2} s^{-1} m^{-1})
k_b	biomass attenuation coefficient (μmol m^{-2} s^{-1} m^{-1})
k_{en}	decay rate for $CFSTR_n$ (d^{-1})
k_w	water attenuation coefficient (μmol m^{-2} s^{-1} m^{-1})
n	numerical position of the specific CFSTR in the series
n_x	number of samples included in the data set
N	total number of CFSTRs in HISTAR
L_i	the lipid concentration (g lipid (m^3 of culture)$^{-1}$) in inoculum
L_n	lipid concentration (g lipid (m^3 of culture)$^{-1}$) in $CFSTR_n$
S_f	nitrogen concentration (g m^{-3}) in the input flow
S_n	nitrogen concentration (g m^{-3}) in the in $CFSTR_n$
U_n	net specific growth rate for biomass in $CFSTR_n$ (d^{-1})
W_{sn}	net consumption rate for nitrogen in $CFSTR_n$ (d^{-1})
L_{pn}	net production rate for lipid in $CFSTR_n$ (d^{-1})
V_n	volume of $CFSTR_n$ (m^3)
X_{0n}	initial biomass concentration in $CFSTR_n$ (g dry mass m^{-3})
X_{8a}	actual biomass concentration in $CFSTR_8$ (g dry mass m^{-3})
X_{8p}	predicted biomass concentration in $CFSTR_8$ (g dry mass m^{-3})
X_n	concentration of biomass in $CFSTR_n$ (g dry mass m^{-3})
z_n	depth z of $CFSTR_n$ having a culture of d_n (m)

Greek symbols	
α	lipid formation coefficient (g lipid (g^{-}biomass)$^{-1}$)
β	non-growth correlation coefficient (g lipid (g biomass)$^{-1}$ d^{-1})
μ_{max}	maximum specific growth rate (d^{-1})
μ_n	specific growth rate in reactor n (d^{-1})
μ_s	hypothetical average system growth rate (d^{-1})

6. OVERALL DISCUSSION AND RECOMMENDATIONS

This work focused on lipid production from a Louisiana native *Chlorella vulgaris*/ *Leptolyngbya sp.* co-culture for biofuel applications. The ultimate goal for this research is to optimize the lipid production via cultivation design (nitrogen, irradiance, and aeration, CO_2), lipid extraction and pilot-scale culture (modeling), resulting in four stand-alone chapters (Chapter 2-5).

Chapters 2 and 3 investigated the impact of several culture conditions, including irradiance, nitrogen, aeration and CO_2 on lipid percentage (mass/mass on dry biomass), lipid productivity, neutral lipid percentage (mass/mass on total lipids) and fatty acid profiles. Although the experiments in Chapters 2 and 3 were conducted in a bench top scale, it could provide information on this co-culture for pilot-scale production. The research in Chapter 4 focused on improving the lipid production by increasing lipid extraction efficiency. In this chapter, silver nanofibers were investigated to disrupt the microalgal cell walls, which were considered the major factor limiting the lipid extraction process. Chapter 5 described the model development for the lipid production from the *Chlorella vulgaris*/*Leptolyngbya sp.* co-culture in the HISTAR system. The model added the lipid production and impact of nitrogen modules to the previous model that focused on effects of the irradiance. The final model was able to predict the biomass and lipid productivity under different nitrogen input levels.

The goal of this chapter is to unify the results and conclusions from each part of the research and provide recommendations for the future research regarding to cultivation design, lipid extraction and culture and modeling for HISTAR.

6.1. Overall Discussion

The experiment work done in Chapter 2, Lipid Productivity and Fatty Acid Composition of a Non-aerated Louisiana Co-culture under Different Irradiance and Nitrogen Levels, characterized the effects of irradiance and nitrate levels on lipid productivity, neutral lipid percentage and fatty acid profile for a non-aerated *Chlorella vulgaris/Leptolyngbya sp.*co-culture. The results indicate this Louisiana native co-culture exhibited high lipid productivity (maximum ~17 mg L^{-1} d^{-1}). Neutral lipids comprise ~75% of total lipids, 16- and 18-carbon components dominate the fatty acid profile and approximately 39% of the fatty acids are saturated.

The irradiance affected the lipid percentage (lipid/dry biomass; mass/mass), total lipid productivity and the neutral lipid percentage for this co-culture. For all tested conditions, the optimal irradiance levels were 400 and 800 μmol m^{-2} s^{-1}, corresponding to the highest lipid percentage, total lipid productivity and neutral lipid percentages. The lower lipid productivity for 180 μmol m^{-2} s^{-1} was due to the insufficient energy input while for 1200 μmol m^{-2} s^{-1}, the irradiance energy induced photoinhibition that prevent the lipid production for the Louisiana co-culture. Further study is needed to investigate the reason of lower lipid productivity at 600 μmol m^{-2} s^{-1} than 400 and 800 μmol m^{-2} s^{-1}. Based on these results, the optimal irradiance levels that could be applied in a large-scale culture system to maximize the biodiesel productivity from the biomass feedstock of this native co-culture are 400, 800 μmol m^{-2} s^{-1}. Nitrogen starvation promoted lipid percentage but decreased the total lipid productivity and thus should not be applied in the mass production system. The optimum nitrate nitrogen level was 100%.

Neither irradiance nor nitrate levels had significant effects on the fatty acid profile (all the *p*-values in Tukey test on all the FAMEs were greater than 0.05) of the co-culture, which implied the possible consistency of the biodiesel produced from the Louisiana co-culture.

Chapter 3, Lipid Productivity and Lipid Composition of an Aerated Co-culture under Different Irradaince and Nitrogen Levels, investigated the effects of scalar irradiance level and nitrogen level on the total lipid percentage, lipid productivity, neutral lipid percentage and fatty acid composition of a Louisiana native *Chlorella vulgaris/Leptolyngbya sp.* co-culture with controlled pH and continuous aeration.

The highest lipid productivity for this Louisiana co-culture was 116 g m^{-3} d^{-1} for 800 μmol m^{-2} s^{-1} with 100% nitrogen level and the lowest was 59.2 g m^{-1} d^{-1} for 800 μmol m^{-2} s^{-1} with 50% nitrogen level. In this work, scalar irradiance and nitrogen levels only had significant effect on lipid productivity. The low scalar irradiance (180, 400 μmol m^{-2} s^{-1}) and low nitrogen level (50% N) limited the productivity by constraining the biomass productivity. However, in large-scale production system, the cost of nitrogen and light energy must be taken into consideration along with lipid productivity. Wastewater with high nitrogen concentration could be used to lower the cost of nitrogen. For outdoor culture systems, the cost for light energy could be considered zero, but indoor culture systems should be designed to maximize the conversion efficiency of light energy (from irradiance to lipids).

The compositions of the fatty acids profile suggested that the biodiesel produced from this Louisiana co-culture needs to be blended with petrol diesel or desaturated to comply with the requirement of diesel engines. The stability of fatty acids for various scalar irradiance and nitrogen levels implied that the properties (gelling point, viscosity, acidity, oxidation stability

etc.) of the biodiesel produced from this Louisiana *Chlorella vulgaris/Leptolyngbya sp.*co-culture most likely will be relatively consistent.

The comparison of the results of this work and study in chapter 2 on the same Louisiana co-culture (Bai et al., (under review)) suggested that the aeration and excess CO_2 could significantly increase total and neutral lipid productivity and protect the cells from photoinhibition. However, aeration and excess CO_2 had little effects on the fatty acid composition.

Although all the experiments in this work were conducted on a bench top scale, the results can provide information for the design of a large culture system. According to the results obtained from this work, the aeration could significantly increase the lipid productivity for the Louisiana co-culture. However, in a large-scale culture system, pumping air through the whole culture can dramatically increase the production cost. Paddlewheels can be used instead of aeration. Although it might not be able to completely compensate the effects of aeration, paddlewheel can significantly lower energy cost. The use of CO_2 should be implemented for the large-scale culture since it had a drastic impact on lipid productivity of the co-culture and generally considered available at no cost (Chisti, 2007; Grima et al., 2003). Nevertheless, the cost of bubbling the CO_2 through the culture should be evaluated depending on the specific design of the culture system (culture depth, surface area etc.). The irradiance level can be adjusted by varying the depth of the culture. In a confined area for microalgal culture, the optimal irradiance for maximum lipid productivity (g m^{-3} d^{-1}) results in low energy conversion efficiency and limited culture volume as discussed earlier, however high energy conversion efficiency lowers the culture concentration and significantly increases the cost for dewater

process. Therefore, the optimal irradiance level should be able to balance lipid productivity and the conversion efficiency from solar energy to lipid.

According to Chapter 4, Silver Nanofiber Assisted Lipid Extraction from Biomass of a Louisiana *Chlorella vulgaris/Leptolyngbya sp.* co-culture, the silver nanofibers were able to rupture the cell walls of the microalgae and increase the lipid extraction efficiency for both Folch's method and microwave assisted lipid extraction. The addition of the silver nanofibers saved large amounts of solvent and energy consumption for the lipid extraction process. The silver nanofibers had significant impact on the fatty acids profile of the lipids. The optimal lipid extraction method for desirable fatty acids profile in this work was Folch's method without the addition of silver nanofibers. However, the lipid extraction with microwave and silver nanofibers should be the optimal extraction method for biodiesel production, considering the overall increase in lipid content.

Although the cost of silver nanofibers could be high, techniques to reuse the silver nanofibers could be developed to minimize the cost. By adjusting the synthesis conditions the cobalt composition could be increased to improve the magnetic susceptibility of nanofibers, and then magnetic force could be applied to separate nanofibers from the mixture. Another possible method is using silver nanofibers embedded on bulk substrate (silicon wafer, Teflon plate etc.). The silver nanofibers could be easily removed along with the substrate after lipid extraction process. The reuse of silver nanofibers would be expected to significantly reduce the cost of this method, making it more competitive than the existing methods (sonication, freeze drying, grinding etc.).

The mechanistic model developed in Chapter 5, A Mechanistic Model to Investigate the Impacts of Irradiance and Nitrogen Levels on the Biomass and Lipid Productivity of a Louisina *Chlorella vulgaris*/*Leptolyngbya sp.* Co-culture, included the effects of both nitrogen and average scalar irradiance on biomass production, lipid percentage (mass/mass, on dry biomass) and lipid production for the HISTAR system. The simulations well demonstrated the trend for biomass, lipid and nitrogen levels in the HISTAR system. The results of the simulations indicated that the effects of nitrogen level described by this model were consistent with bench top studies and other literature on nitrogen limitations. The lower nitrogen levels were able to increase the lipid percentage, but the increase could not compensate the loss of biomass productivity, resulting lower overall lipid productivity. The model was calibrated, but extra data sets are needed for further calibration and model validation. The results suggested that high nitrogen level (Bold's Basal medium, 41.2 g m^{-3}) is necessary for high lipid productivity, although the residual nitrogen level flow out of the last CFSTR may be high. Therefore, nutrients recycle is needed to lower the cost of nitrogen.

6.2. Recommendations

The recommendations of possible future work are presented here in the aspects of the work for each chapter (Chapters 2-5).

- The impact of light-dark cycle on biomass and lipid productivity should be investigated in both bench top scale and pilot scale cultures to simulate the natural light conditions for day and night. The irradiance fluctuation throughout the daytime could also be studied.
- The experiments on the effects of different CO_2 concentrations (on overall aeration rate) should be tested in both bench top and pilot scale cultures. The costs for CO_2 and aeration against the increase of biomass and lipid productivity should be evaluated.

- Research on by-products such as high-value pigments, omega-3 fatty acids and proteins from the Louisiana co-culture should be conducted.
- For silver nanofiber assisted lipid extraction, research on recover and reuse of the silver nanofibers is needed. Multiple methods could be tested. The composition of cobalt seeds could be increased to enhance the magnetic permeability for the nanofibers, so that magnetic force can be applied to recover the nanofibers.
- The effects of shape and size of the silver nanoparticles on lipid extraction efficiency can be investigated to further enhance the effects of silver nanoparticles. Nanoparticles of metals like copper should also be tested for increasing lipid extraction efficiency from the Louisiana co-culture.
- Up-scaled model for HISTAR system is needed to provide a predictive tool for microalgal biomass and lipid production in industrial scaled system. The industrial scaled model should be able to include the effects of non-ideal mixing, limited CO_2 supply and fluctuation of environmental conditions etc.

REFERENCES CITED

Abou-Shanab, R.A.I., Matter, I.A., Kim, S.N., Oh, Y.K., Choi, J., Jeon, B.H., 2011. Characterization and identification of lipid-producing microalgae species isolated from a freshwater lake. Biomass & Bioenergy 35, 3079-3085.

Adarme-Vega, T.C., Lim, D.K.Y., Timmins, M., Vernen, F., Li, Y., Schenk, P.M., 2012. Microalgal biofactories: a promising approach towards sustainable omega-3 fatty acid production. Microb. Cell. Fact. 11.

Adleman, J.R., Eggert, H.A., Buse, K., Psaltis, D., 2006. Holographic grating formation in a colloidal suspension of silver nanoparticles. Optics Letters 31, 447-449.

Ahmad, A.L., Yasin, N.H.M., Derek, C.J.C., Lim, J.K., 2011. Microalgae as a sustainable energy source for biodiesel production: A review. Renewable & Sustainable Energy Reviews 15, 584-593.

Anjum, F., Anwar, F., Jamil, A., Iqbal, M., 2006. Microwave roasting effects on the physico-chemical composition and oxidative stability of sunflower seed oil. Journal of the American Oil Chemists Society 83, 777-784.

Atsumi, S., Hanai, T., Liao, J.C., 2008. Non-fermentative pathways for synthesis of branched-chain higher alcohols as biofuels. Nature 451, 86-U13.

Ayala-Núñez, N., Lara Villegas, H., del Carmen Ixtepan Turrent, L., Rodríguez Padilla, C., 2009. Silver nanoparticles toxicity and bactericidal effect against methicillin-resistant *Staphylococcus aureus*: Nanoscale does matter. NanoBioTechnology 5, 2-9.

Bai, M.D., Cheng, C.H., Wan, H.M., Lin, Y.H., 2011. Microalgal pigments potential as byproducts in lipid production. J. Taiwan Inst. Chem. Eng. 42, 783-786.

Bai, R., Silaban, A., Gutierrez-Wing, M.T., Benton, M.G., Rusch, K.A., (under review). Effects of nitrogen and irradiance on lipid content and composition of a Louisiana native *Chlorella vulgaris/Leptolyngbya sp.* co-culture.

Bakshi, A., 2003. Potential adverse health effects of genetically modified crops. Journal of Toxicology and Environmental Health-Part B-Critical Reviews 6, 211-225.

Bannister, C.D., Chuck, C.J., Bounds, M., Hawley, J.G., 2011. Oxidative stability of biodiesel fuel. Proceedings of the Institution of Mechanical Engineers Part D-Journal of Automobile Engineering 225, 99-114.

Barbosa, M.J., Hadiyanto, Wijffels, R.H., 2004. Overcoming shear stress of microalgae cultures in sparged photobioreactors. Biotechnology and Bioengineering 85, 78-85.

Beer, L.L., Boyd, E.S., Peters, J.W., Posewitz, M.C., 2009. Engineering algae for biohydrogen and biofuel production. Current Opinion in Biotechnology 20, 264-271.

Ben-Amotz, A., 1995. New mode of Dunaliella biotechnology: two-phase growth for Œ≤-carotene production. Journal of Applied Phycology 7, 65-68.

Benamotz, A., Fishler, R., Schneller, A., 1987. Chemical composition of dietary species of marine unicellular algae and rotifers with emphasis on fatty acids. Marine Biology 95, 31-36.

Benson, B.C., 2003. Optimization of the light dynamics in the Hydraulically Integrated Serial Turbidostat Algal Reactor (HISTAR), Civil & Environmental Engineering Louisiana State Univerisity, Baton Rouge, p. 378.

Benson, B.C., Gutierrez-Wing, M.T., Rusch, K.A., 2007. The development of a mechanistic model to investigate the impacts of the light dynamics on algal productivity in a Hydraulically Integrated Serial Turbidostat Algal Reactor (HISTAR). Aquacultural Engineering 36, 198-211.

Benson, B.C., Gutierrez-Wing, M.T., Rusch, K.A., 2009. Optimization of the lighting system for a Hydraulically Integrated Serial Turbidostat Algal Reactor (HISTAR): Economic implications. Aquacultural Engineering 40, 45-53.

Benson, B.C., Rusch, K.A., 2006. Investigation of the light dynamics and their impact on algal growth rate in a hydraulically integrated serial turbidostat algal reactor (HISTAR). Aquacultural Engineering 35, 122-134.

Bhatnagar, A., Chinnasamy, S., Singh, M., Das, K.C., 2011. Renewable biomass production by mixotrophic algae in the presence of various carbon sources and wastewaters. Applied Energy 88, 3425-3431.

Bligh, E.G., Dyer, W.J., 1959. A rapid method of total lipid extraction and purification. Canadian Journal of Biochemistry and Physiology 37, 911-917.

Bonente, G., Pippa, S., Castellano, S., Bassi, R., Ballottari, M., 2012. Acclimation of *Chlamydomonas reinhardtii* to different growth irradiances. Journal of Biological Chemistry 287, 5833-5847.

Borthwick, K.A.J., Coakley, W.T., McDonnell, M.B., Nowotny, H., Benes, E., Groschl, M., 2005. Development of a novel compact sonicator for cell disruption. Journal of Microbiological Methods 60, 207-216.

Bougaran, G., Bernard, O., Sciandra, A., 2010. Modeling continuous cultures of microalgae colimited by nitrogen and phosphorus. Journal of Theoretical Biology 265, 443-454.

Brentner, L.B., Eckelman, M.J., Zimmerman, J.B., 2011. Combinatorial Life Cycle Assessment to Inform Process Design of Industrial Production of Algal Biodiesel. Environmental Science & Technology 45, 7060-7067.

Brown, M.R., 1991. The amino-acid and sugar composition of 16 species of microalgae used in mariculture. Journal of Experimental Marine Biology and Ecology 145, 79-99.

Bunt, J.S., 1971. Levels of dissolved oxygen and carbon fixation by marine microalgae. Limnology and Oceanography 16, 564-&.

Campbell, M.L., 2011. Assessing biosecurity risk associated with the importation of non-indigenous microalgae. Environmental Research 111, 989-998.

Cardone, M., Mazzoncini, M., Menini, S., Rocco, V., Senatore, A., Seggiani, M., Vitolo, S., 2003. Brassica carinata as an alternative oil crop for the production of biodiesel in Italy: agronomic evaluation, fuel production by transesterification and characterization. Biomass & Bioenergy 25, 623-636.

Carpita, N.C., 1985. Tensile-strength of cell-walls of living cells Plant Physiology 79, 485-488.

Carvalho, A.P., Malcata, F.X., 2000. Effect of culture media on production of polyunsaturated fatty acids by *Pavlova lutheri*. Cryptogamie Algologie 21, 59-71.

Carvalho, A.P., Meireles, L.A., Malcata, F.X., 2006. Microalgal reactors: A review of enclosed system designs and performances. Biotechnology Progress 22, 1490-1506.

Charkrabarty, M.M., 2009. Chemistry and Technology of Oils and Fats. Allied Publishers.

Chaumont, D., Thepenier, C., 1995. Carotenoid content in growing cells of *Haematococcus pluvialis* during a sunlight cycle. Journal of Applied Phycology 7, 529-537.

Chen, C.-Y., Yeh, K.-L., Aisyah, R., Lee, D.-J., Chang, J.-S., 2011a. Cultivation, photobioreactor design and harvesting of microalgae for biodiesel production: A critical review. Bioresource Technology 102, 71-81.

Chen, M., Tang, H., Ma, H., Holland, T.C., Ng, K.Y.S., Salley, S.O., 2011b. Effect of nutrients on growth and lipid accumulation in the green algae *Dunaliella tertiolecta*. Bioresource Technology 102, 1649-1655.

Chen, W., Zhang, C., Song, L., Sommerfeld, M., Hu, Q., 2009. A high throughput Nile red method for quantitative measurement of neutral lipids in microalgae. Journal of Microbiological Methods 77, 41-47.

Cheung, P.C.K., Leung, A.Y.H., Ang, P.O., 1998. Comparison of supercritical carbon dioxide and soxhlet extraction of lipids from a brown seaweed, *Sargassum hemiphyllum* (Turn.) C. Ag. Journal of Agricultural and Food Chemistry 46, 4228-4232.

Chi, Z.Y., Liu, Y., Frear, C., Chen, S.L., 2009. Study of a two-stage growth of DHA-producing marine algae Schizochytrium limacinum SR21 with shifting dissolved oxygen level. Appl. Microbiol. Biotechnol. 81, 1141-1148.

Chisti, Y., 2007. Biodiesel from microalgae. Biotechnology Advances 25, 294-306.

Chisti, Y., 2008. Biodiesel from microalgae beats bioethanol. Trends in Biotechnology 26, 126-131.

Chiu, S.Y., Kao, C.Y., Chen, C.H., Kuan, T.C., Ong, S.C., Lin, C.S., 2008. Reduction of CO2 by a high-density culture of Chlorella sp in a semicontinuous photobioreactor. Bioresource Technology 99, 3389-3396.

Chu, K.H., Alvarez-Cohen, L., 1998. Effect of nitrogen source on growth and trichloroethylene degradation by methane-oxidizing bacteria. Applied and Environmental Microbiology 64, 3451-3457.

Chwalibog, A., Sawosz, E., Hotowy, A., Szeliga, J., Mitura, S., Mitura, K., Grodzik, M., Orlowski, P., Sokolowska, A., 2010. Visualization of interaction between inorganic nanoparticles and bacteria or fungi. International Journal of Nanomedicine 5, 1085-1094.

Clarens, A.F., Resurreccion, E.P., White, M.A., Colosi, L.M., 2010. Environmental Life Cycle Comparison of Algae to Other Bioenergy Feedstocks. Environmental Science & Technology 44, 1813-1819.

Cohen, Z., Reungjitchachawali, M., Siangdung, W., Tanticharoen, M., Heimer, Y.M., 1993. Herbicide resistant lines of microalgae - growth and fatty acid composition. Phytochemistry 34, 973-978.

Converti, A., Casazza, A.A., Ortiz, E.Y., Perego, P., Del Borghi, M., 2009. Effect of temperature and nitrogen concentration on the growth and lipid content of *Nannochloropsis oculata* and *Chlorella vulgaris* for biodiesel production. Chemical Engineering and Processing: Process Intensification 48, 1146-1151.

Cooney, M., Young, G., Nagle, N., 2009. Extraction of bio-oils from microalgae. Separation and Purification Reviews 38, 291-325.

Cordero, B.F., Obraztsova, I., Couso, I., Leon, R., Angeles Vargas, M., Rodriguez, H., 2011. Enhancement of Lutein Production in *Chlorella sorokiniana* (Chorophyta) by Improvement of Culture Conditions and Random Mutagenesis. Marine Drugs 9, 1607-1624.

Courchesne, N.M.D., Parisien, A., Wang, B., Lan, C.Q., 2009. Enhancement of lipid production using biochemical, genetic and transcription factor engineering approaches. Journal of Biotechnology 141, 31-41.

Cravotto, G., Boffa, L., Mantegna, S., Perego, P., Avogadro, M., Cintas, P., 2008. Improved extraction of vegetable oils under high-intensity ultrasound and/or microwaves. Ultrasonics Sonochemistry 15, 898-902.

Davis, R., Aden, A., Pienkos, P.T., 2011. Techno-economic analysis of autotrophic microalgae for fuel production. Applied Energy 88, 3524-3531.

Davis, R., Fishman, D., Frank, E.D., Wigmosta, M.S., Aden, A., Coleman, A.M., Pienkos, P.T., Skaggs, R.J., Venteris, E.R., Wang, M.Q., 2012. Renewable diesel from algal lipids: an integrated baseline for cost, emissions, and resource potential from a harmonized model. Argonne National Laboratory, Argonne.

de la Vega, M., Diaz, E., Vila, M., Leon, R., 2011. Isolation of a new strain of *Picochlorum sp* and characterization of its potential biotechnological applications. Biotechnology Progress 27, 1535-1543.

de-Bashan, L.E., Bashan, Y., Moreno, M., Lebsky, V.K., Bustillos, J.J., 2002. Increased pigment and lipid content, lipid variety, and cell and population size of the microalgae Chlorella spp. when co-immobilized in alginate beads with the microalgae-growth-promoting bacterium Azospirillum brasilense. Can J Microbiol 48, 514-521.

Del Campo, J.A., Garcia-Gonzalez, M., Guerrero, M.G., 2007. Outdoor cultivation of microalgae for carotenoid production: current state and perspectives. Appl. Microbiol. Biotechnol. 74, 1163-1174.

Deng, X.D., Fei, X.W., Li, Y.J., 2011. The effects of nutritional restriction on neutral lipid accumulation in *Chlamydomonas* and *Chlorella*. African Journal of Microbiology Research 5, 260-270.

Díaz-Visurraga, J., Gutiérrez, C., von Plessing, C., Garcia, A., 2011. Metal nanostructures as antibacterial agents, in: Mendez-Vilas, A. (Ed.), Science against microbial pathogens: communicating current research and technological advances. Formatex Research Center, Badajoz, p. 691.

DOE, U.S., 2010. National algal biofuels technology roadmap.

Dote, Y., Sawayama, S., Inoue, S., Minowa, T., Yokoyama, S., 1994. Recovery of liquid fuel from hydrocarbon-rich microalgae by thermochemical liquefaction. Fuel 73, 1855-1857.

Doucha, J., Livansky, K., 2006. Productivity, CO2/O2 exchange and hydraulics in outdoor open high density microalgal (*Chlorella sp.*) photobioreactors operated in a Middle and Southern European climate. Journal of Applied Phycology 18, 811-826.

Doucha, J., Livansky, K., 2009. Outdoor open thin-layer microalgal photobioreactor: potential productivity. Journal of Applied Phycology 21, 111-117.

Droop, M.R., 1983. 25 years of algal growth-kinetics - a personal view. Botanica Marina 26, 99-112.

Falkowski, P.G., Raven, J.A., 1997. Quatic Photosynthesis. Blackwell Science, Malden, Massachusetts.

Fischer, C.R., Klein-Marcuschamer, D., Stephanopoulos, G., 2008. Selection and optimization of microbial hosts for biofuels production. Metabolic Engineering 10, 295-304.

Folch, J., Lees, M., Stanley, G.H.S., 1957. A simple method for the isolation and purification of total lipids from animal tissues. Journal of Biological Chemistry 226, 497-509.

Frankel, E.N., 1984. Lipid oxidation-mechanisms, products and biological significance. Journal of the American Oil Chemists Society 61, 1908-1917.

Fry, S.C., Miller, J.G., Dumville, J.C., 2002. A proposed role for copper ions in cell wall loosening. Plant and Soil 247, 57-67.

Gardner, R., Peters, P., Peyton, B., Cooksey, K.E., 2011. Medium pH and nitrate concentration effects on accumulation of triacylglycerol in two members of the chlorophyta. Journal of Applied Phycology 23, 1005-1016.

Gerde, J.A., Montalbo-Lomboy, M., Yao, L., Grewell, D., Wang, T., 2012. Evaluation of microalgae cell disruption by ultrasonic treatment. Bioresource Technology 125, 175-181.

Ghasemi, Y., Rasoul-Amini, S., Naseri, A.T., Montazeri-Najafabady, N., Mobasher, M.A., Dabbagh, F., 2012. Microalgae biofuel potentials (Review). Applied Biochemistry and Microbiology 48, 126-144.

Goldman, J.C., 1979. Outdoor algal mass-cultures. 2. photosynthetic yield limitations. Water Research 13, 119-136.

Gouveia, L., Oliveira, A.C., 2009. Microalgae as a raw material for biofuels production. Journal of Industrial Microbiology & Biotechnology 36, 269-274.

Govindasamy, R., Rahuman, A.A., 2012. Histopathological studies and oxidative stress of synthesized silver nanoparticles in Mozambique tilapia (*Oreochromis mossambicus*). Journal of Environmental Sciences-China 24, 1091-1098.

Graham, L.E., Wilcox, L.W., 2004. Algae. Prentice Hall, Upper Saddle River.

Greenwell, H.C., Laurens, L.M.L., Shields, R.J., Lovitt, R.W., Flynn, K.J., 2010. Placing microalgae on the biofuels priority list: a review of the technological challenges. Journal of the Royal Society Interface 7, 703-726.

Griffiths, M.J., Harrison, S.T.L., 2009. Lipid productivity as a key characteristic for choosing algal species for biodiesel production. Journal of Applied Phycology 21, 493-507.

Grima, E.M., Belarbi, E.H., Fernandez, F.G.A., Medina, A.R., Chisti, Y., 2003. Recovery of microalgal biomass and metabolites: process options and economics. Biotechnology Advances 20, 491-515.

Grima, E.M., Sevilla, J.M.F., Perez, J.A.S., Camacho, F.G., 1996. A study on simultaneous photolimitation and photoinhibition in dense microalgal cultures taking into account incident and averaged irradiances. Journal of Biotechnology 45, 59-69.

Guedes, A.C., Meireles, L.A., Amaro, H.M., Malcata, F.X., 2010. Changes in lipid class and fatty acid composition of cultures of *pavlova lutheri*, in response to light Intensity. Journal of the American Oil Chemists Society 87, 791-801.

Guschina, I.A., Harwood, J.L., 2006. Lipids and lipid metabolism in eukaryotic algae. Progress in Lipid Research 45, 160-186.

Gutierrez-Wing, M.T., Rusch, K.A., 2011. Methods of extracting lipids and pigments from microalgal biomass (Patent (Pending)).

Guven, B., Howard, A., 2011. Sensitivity Analysis of a Cyanobacterial Growth and Movement Model under Two Different Flow Regimes. Environmental Modeling & Assessment 16, 577-589.

Halim, R., Danquah, M.K., Webley, P.A., 2012. Extraction of oil from microalgae for biodiesel production: A review. Biotechnology Advances 30, 709-732.

Hallegreaff, G.M., Anderson, D.M., Cembella, A.D., 2003. Epidemiology and public health of human illnesses associated with harmful marine phytoplankton, Manual on harmful marine algae. UNESCO/WHO, Geneva, pp. 725-750.

Han, B.P., Virtanen, M., Koponen, J., Straskraba, M., 2000. Effect of photoinhibition on algal photosynthesis: a dynamic model. Journal of Plankton Research 22, 865-885.

Haney, J.D., Jackson, G.A., 1996. Modeling phytoplankton growth rates (vol 18, pg 63, 1996). Journal of Plankton Research 18, 1269-1269.

Hase, R., Oikawa, H., Sasao, C., Morita, M., Watanabe, Y., 2000. Photosynthetic production of microalgal biomass in a raceway system under greenhouse conditions in Sendai city. Journal of Bioscience and Bioengineering 89, 157-163.

Hempel, N., Petrick, I., Behrendt, F., 2012. Biomass productivity and productivity of fatty acids and amino acids of microalgae strains as key characteristics of suitability for biodiesel production. Journal of Applied Phycology 24, 1407-1418.

Hill, J., 2007. Environmental costs and benefits of transportation biofuel production from food- and lignocellulose-based energy crops. A review. Agronomy for Sustainable Development 27, 1-12.

Horton, H.R., Moran, L.A., Ochs, R.S., Rawn, J.D., Scrimgeour, K.G., 2002. Principles of Biomchemistry, Third ed. Prentice Hall, Upper Saddle River.

Hu, Q., Sommerfeld, M., Jarvis, E., Ghirardi, M., Posewitz, M., Seibert, M., Darzins, A., 2008. Microalgal triacylglycerols as feedstocks for biofuel production: perspectives and advances. Plant Journal 54, 621-639.

Huang, G., Chen, F., Wei, D., Zhang, X., Chen, G., 2010a. Biodiesel production by microalgal biotechnology. Applied Energy 87, 38-46.

Huang, G.H., Chen, F., Wei, D., Zhang, X.W., Chen, G., 2010b. Biodiesel production by microalgal biotechnology. Applied Energy 87, 38-46.

Huerlimann, R., de Nys, R., Heimann, K., 2010. Growth, Lipid Content, Productivity, and Fatty Acid Composition of Tropical Microalgae for Scale-Up Production. Biotechnology and Bioengineering 107, 245-257.

Huntley, M., Redalje, D., 2007. CO2 Mitigation and Renewable Oil from Photosynthetic Microbes: A New Appraisal. Mitig Adapt Strat Glob Change 12, 573-608.

Illman, A.M., Scragg, A.H., Shales, S.W., 2000. Increase in *Chlorella* strains calorific values when grown in low nitrogen medium. Enzyme and Microbial Technology 27, 631-635.

Imase, M., Watanabe, K., Aoyagi, H., Tanaka, H., 2008. Construction of an artificial symbiotic community using a Chlorella-symbiont association as a model. Fems Microbiology Ecology 63, 273-282.

Iqbal, J., 2012. Development of cost-effective and benign lipid extraction system for microalgae, Engineering Science. Louisiana State University, Baton Rouge, Louisiana, p. 140.

IUPAC, 1979. Standard Methods for the Analysis of Oils and Derivatives, 6th ed.

John Sheehan, T.D., John Benemann, Paul Roessler, 1998. A Look Back at the U.S. Department of Energy's Aquatic Species Program-Biodiesel from Algae. the National Renewable Energy Laboratory.

Johnson, M.B., Wen, Z.Y., 2010. Development of an attached microalgal growth system for biofuel production. Appl. Microbiol. Biotechnol. 85, 525-534.

Kaul, S., Saxena, R.C., Kumar, A., Negi, M.S., Bhatnagar, A.K., Goyal, H.B., Gupta, A.K., 2007. Corrosion behavior of biodiesel from seed oils of Indian origin on diesel engine parts. Fuel Processing Technology 88, 303-307.

Keri Carstens, J.A., Pamela Bachman, Adinda De Schrijver, Galen Dively, Brian Federici, Mick Hamer, Marco Gielkens, Peter Jensen , William Lamp , Stefan Rauschen , Geoff Ridley , Jo¨rg Romeis , Annabel Waggoner, 2011. Genetically modified crops and aquatic ecosystems: considerations for environmental risk assessment and non-target organism testing. Transgenic Research (in press).

Ketheesan, B., Nirmalakhandan, N., 2011. Development of a new airlift-driven raceway reactor for algal cultivation. Applied Energy 88, 3370-3376.

Khoeyi, Z.A., Seyfabadi, J., Ramezanpour, Z., 2012. Effect of light intensity and photoperiod on biomass and fatty acid composition of the microalgae, *Chlorella vulgaris*. Aquaculture International 20, 41-49.

Klimov, V.V., Baranov, S.V., Allakhverdiev, S.I., 1997. Bicarbonate protects the donor side of photosystem II against photoinhibition and thermoinactivation. Febs Letters 418, 243-246.

Klimov, V.V., Shafiev, M.A., Allakhverdiev, S.I., 1990. Photoinactivation of the reactivation capacity of photosystem-II in pea subchloroplast particles after complete removal of Manganese. Photosynth. Res. 23, 59-65.

Kora, A.J., Manjusha, R., Arunachalam, J., 2009. Superior bactericidal activity of SDS capped silver nanoparticles: Synthesis and characterization. Materials Science & Engineering C-Materials for Biological Applications 29, 2104-2109.

Kralova, I., Sjoblom, J., 2010. Biofuels-renewable energy sources: a review. Journal of Dispersion Science and Technology 31, 409-425.

Kumari, M., Mukherjee, A., Chandrasekaran, N., 2009. Genotoxicity of silver nanoparticles in *Allium cepa*. Science of the Total Environment 407, 5243-5246.

Lam, M.K., Lee, K.T., 2012. Microalgae biofuels: A critical review of issues, problems and the way forward. Biotechnology Advances 30, 673-690.

Lardon, L., Helias, A., Sialve, B., Steyer, J.P., Bernard, O., 2009. Life-Cycle Assessment of Biodiesel Production from Microalgae. Environmental Science & Technology 43, 6475-6481.

Lee, J.S., Ray, R.I., Little, B.J., 2010a. An assessment of alternative diesel fuels: microbiological contamination and corrosion under storage conditions. Biofouling 26, 623-635.

Lee, J.Y., Yoo, C., Jun, S.Y., Ahn, C.Y., Oh, H.M., 2010b. Comparison of several methods for effective lipid extraction from microalgae. Bioresource Technology 101, S75-S77.

Lee, Y.-K., 2001. Microalgal mass culture systems and methods: Their limitation and potential. Journal of Applied Phycology 13, 307-315.

Lehr, F., Posten, C., 2009. Closed photo-bioreactors as tools for biofuel production. Current Opinion in Biotechnology 20, 280-285.

Lesser, M.P., Falcon, L.I., Rodriguez-Roman, A., Enriquez, S., Hoegh-Guldberg, O., Iglesias-Prieto, R., 2007. Nitrogen fixation by symbiotic cyanobacteria provides a source of nitrogen for the scleractinian coral *Montastraea cavernosa*. Marine Ecology-Progress Series 346, 143-152.

Levert, J.M., Xia, J.L., 2001. Modeling the growth curve for *Spirulina (Arthrospira) maxima*, a versatile microalga for producing uniformly labelled compounds with stable isotopes. Journal of Applied Phycology 13, 359-367.

Lewis, T., Nichols, P.D., McMeekin, T.A., 2000. Evaluation of extraction methods for recovery of fatty acids from lipid-producing microheterotrophs. Journal of Microbiological Methods 43, 107-116.

Li, X., Hu, H.Y., Gan, K., Sun, Y.X., 2010a. Effects of different nitrogen and phosphorus concentrations on the growth, nutrient uptake, and lipid accumulation of a freshwater microalga *Scenedesmus sp*. Bioresource Technology 101, 5494-5500.

Li, Y., Horsman, M., Wu, N., Lan, C.Q., Dubois-Calero, N., 2008a. Biofuels from microalgae. Biotechnology Progress 24, 815-820.

Li, Y.Q., Horsman, M., Wang, B., Wu, N., Lan, C.Q., 2008b. Effects of nitrogen sources on cell growth and lipid accumulation of green alga *Neochloris oleoabundans*. Appl. Microbiol. Biotechnol. 81, 629-636.

Li, Y.T., Han, D.X., Hu, G.R., Sommerfeld, M., Hu, Q.A., 2010b. Inhibition of Starch Synthesis Results in Overproduction of Lipids in *Chlamydomonas reinhardtii*. Biotechnology and Bioengineering 107, 258-268.

Liang, Y.N., Sarkany, N., Cui, Y., 2009. Biomass and lipid productivities of *Chlorella vulgaris* under autotrophic, heterotrophic and mixotrophic growth conditions. Biotechnology Letters 31, 1043-1049.

Long, S.P., Humphries, S., Falkowski, P.G., 1994. Photoinhibition of photosynthesis in nature. Annual Review of Plant Physiology and Plant Molecular Biology 45, 633-662.

Luedeking, R., Piret, E.L., 1959. A kinetic study of the lactic acid fermentation - batch process at controlled pH. Journal of Biochemical and Microbiological Technology and Engineering 1, 393-412.

Luque-Garcia, J.L., de Castro, L., 2003. Ultrasound: a powerful tool for leaching. Trac-Trends in Analytical Chemistry 22, 41-47.

Lv, J.-M., Cheng, L.-H., Xu, X.-H., Zhang, L., Chen, H.-L., 2010. Enhanced lipid production of *Chlorella vulgaris* by adjustment of cultivation conditions. Bioresource Technology 101, 6797-6804.

Macfie, S.M., Tarmohamed, Y., Welbourn, P.M., 1994. Effects of cadmium, cobalt, copper and nickel on growth of the green-alga *Chlamydomonas-reinhardtii* - the influences of the cell wall and pH. Archives of Environmental Contamination and Toxicology 27, 454-458.

Majidi, V., Laude, D.A., Holcombe, J.A., 1990. Investigation of the metal algae binding-site with CD-113 nuclear-magnetic-resonance Environmental Science & Technology 24, 1309-1312.

Marcus, Y., Altman-Gueta, H., Snir, A., Wolff, Y., Gurevitz, M., 2008. Does Rubisco Limit the Rate of Photosynthesis?, in: Allen, J., Gantt, E., Golbeck, J., Osmond, B. (Eds.), Photosynthesis. Energy from the Sun. Springer Netherlands, pp. 863-866.

Martin, P.D., 1993. Sonochemistry in industry - progress and prospects Chemistry & Industry, 233-236.

Mata, T.M., Martins, A.A., Caetano, N.S., 2010. Microalgae for biodiesel production and other applications: A review. Renewable & Sustainable Energy Reviews 14, 217-232.

Medina, A.R., Grima, E.M., Gimenez, A.G., Gonzalez, M.J.I., 1998. Downstream processing of algal polyunsaturated fatty acids. Biotechnology Advances 16, 517-580.

Melis, A., 1999. Photosystem-II damage and repair cycle in chloroplasts: what modulates the rate of photodamage in vivo? Trends in Plant Science 4, 130-135.

Melis, A., 2012. Photosynthesis-to-fuels: from sunlight to hydrogen, isoprene, and botryococcene production. Energy & Environmental Science 5, 5531-5539.

Mercer, P., Armenta, R.E., 2011. Developments in oil extraction from microalgae. European Journal of Lipid Science and Technology 113, 539-547.

Monod, J., 1949. The growth of bacterial cultures. Annual Review of Microbiology 3, 371-394.

Morita, M., Watanabe, Y., Saiki, H., 2000. Investigation of photobioreactor design for enhancing the photosynthetic productivity of microalgae. Biotechnology and Bioengineering 69, 693-698.

Morita, M., Watanabe, Y., Saiki, H., 2002. Photosynthetic productivity of conical helical tubular photobioreactor incorporating *Chlorella sorokiniana* under field conditions. Biotechnology and Bioengineering 77, 155-162.

Mur, L.R., 1983. Some aspects of the ecophysiology of cyanobacteria. Annales De Microbiologie B134, 61-72.

Mur, L.R., Skulberg, O.M., Utkilen, H., 1999. Cyanobacteria in the environment, in: Bartram, J., Chorus, I. (Eds.), Toxic cyanobacteria in water. A guide to the public health consequences, monitoring and management. E&EN Spon, London & New York, pp. 15-40.

Mutanda, T., Ramesh, D., Karthikeyan, S., Kumari, S., Anandraj, A., Bux, F., 2011. Bioprospecting for hyper-lipid producing microalgal strains for sustainable biofuel production. Bioresource Technology 102, 57-70.

Nel, A.E., Madler, L., Velegol, D., Xia, T., Hoek, E.M.V., Somasundaran, P., Klaessig, F., Castranova, V., Thompson, M., 2009. Understanding biophysicochemical interactions at the nano-bio interface. Nature Materials 8, 543-557.

Nelson, N., Yocum, C.F., 2006. Structure and function of photosystems I and II, Annual Review of Plant Biology, pp. 521-565.

Nigam, S., Rai, M.P., Sharma, R., 2011. Effect of Nitrogen on Growth and Lipid Content of *Chlorella pyrenoidosa*. American Journal of Biochemistry and Biotechnology 7, 124-129.

Northcote, D.H., 1963. The biology and chemistry of the cell walls of higher plants, algae, and fungi. International Review of Cytology-a Survey of Cell Biology 14, 223-265.

Oh-Hama, T., Miyachi, S., 1988. *Chlorella*, in: Borowitzka, M.A., Borowitzka, L.J. (Eds.), Microalgal biotechnology,. Cambridge University Press, Cambridge, pp. 3-36.

Olson, G.J., Ingram, L.O., 1975. Eeffects of temperature and nutritional changes on fatty-acids of Agmenellum-Quadruplicatum. Journal of Bacteriology 124, 373-379.

Oltra, C., 2011. Stakeholder perceptions of biofuels from microalgae. Energy Policy 39, 1774-1781.

Onyeche, T.I., Schlafer, O., Bormann, H., Schroder, C., Sievers, M., 2002. Ultrasonic cell disruption of stabilised sludge with subsequent anaerobic digestion. Ultrasonics 40, 31-35.

Ortiz-Marquez, J.C.F., Do Nascimento, M., Dublan, M.D., Curatti, L., 2012. Association with an Ammonium-Excreting Bacterium Allows Diazotrophic Culture of Oil-Rich Eukaryotic Microalgae. Applied and Environmental Microbiology 78, 2345-2352.

Packer, A., Li, Y.T., Andersen, T., Hu, Q.A., Kuang, Y., Sommerfeld, M., 2011. Growth and neutral lipid synthesis in green microalgae: A mathematical model. Bioresource Technology 102, 111-117.

Park, Y., Je, K.-W., Lee, K., Jung, S.-E., Choi, T.-J., 2008. Growth promotion of *Chlorella ellipsoidea* by co-inoculation with Brevundimonas sp. isolated from the microalga. Hydrobiologia 598, 219-228.

Pearsall, R.V., Connelly, R.L., Fountain, M.E., Hearn, C.S., Werst, M.D., Hebner, R.E., Kelley, E.F., 2011. Electrically dewatering microalgae. Ieee Transactions on Dielectrics and Electrical Insulation 18, 1578-1583.

Pernet, F., Pelletier, C.J., Milley, J., 2006. Comparison of three solid-phase extraction methods for fatty acid analysis of lipid fractions in tissues of marine bivalves. Journal of Chromatography A 1137, 127-137.

Pernet, F., Tremblay, R., 2003. Effect of ultrasonication and grinding on the determination of lipid class content of microalgae harvested on filters. Lipids 38, 1191-1195.

Pienkos, P.T., Darzins, A., 2009. The promise and challenges of microalgal-derived biofuels. Biofuels Bioproducts & Biorefining-Biofpr 3, 431-440.

Piorreck, M., Baasch, K.-H., Pohl, P., 1984. Biomass production, total protein, chlorophylls, lipids and fatty acids of freshwater green and blue-green algae under different nitrogen regimes. Phytochemistry 23, 207-216.

Pokorny, J., Kocourek, V., Zajic, J., 1976. Reactions of oxidized lipids with protein. XIII. Interactions of polar groups of lipids with nonlipidic substances. Die Nahrung 20, 707-714.

Posten, C., 2009. Design principles of photo-bioreactors for cultivation of microalgae. Engineering in Life Sciences 9, 165-177.

Pozdeev, V.A., Safronov, S.P., Levanova, S.V., Krasnykh, E.L., 2012. Catalytic hydrogenation of fatty acid methyl esters. Russian Journal of Applied Chemistry 85, 261-266.

Prabakaran, P., Ravindran, A.D., 2011. A comparative study on effective cell disruption methods for lipid extraction from microalgae. Letters in Applied Microbiology 53, 150-154.

Pruvost, J., Van Vooren, G., Cogne, G., Legrand, J., 2009. Investigation of biomass and lipids production with *Neochloris oleoabundans* in photobioreactor. Bioresource Technology 100, 5988-5995.

Pruvost, J., Van Vooren, G., Le Gouic, B., Couzinet-Mossion, A., Legrand, J., 2011. Systematic investigation of biomass and lipid productivity by microalgae in photobioreactors for biodiesel application. Bioresource Technology 102, 150-158.

Pulz, O., Scheibenbogen, K., 1998. Photobioreactors: Design and performance with respect to light energy input. Bioprocess and Algae Reactor Technology, Apoptosis. Springer Berlin / Heidelberg, pp. 123-152.

Rai, M., Yadav, A., Gade, A., 2009. Silver nanoparticles as a new generation of antimicrobials. Biotechnology Advances 27, 76-83.

Ramezanzadeh, F.M., Rao, R.M., Prinyawiwatkul, W., Marshall, W.E., Windhauser, M., 2000. Effects of microwave heat, packaging, and storage temperature on fatty acid and proximate compositions in rice bran. Journal of Agricultural and Food Chemistry 48, 464-467.

Ramos, M.J., Fernández, C.M., Casas, A., Rodríguez, L., Pérez, Á., 2009. Influence of fatty acid composition of raw materials on biodiesel properties. Bioresource Technology 100, 261-268.

Rasmussen, U., Nilsson, M., 2003. Cyanobacterial Diversity and Specificity in Plant Symbioses. Cyanobacteria in Symbiosis, in: Rai, A.N., Bergman, B., Rasmussen, U. (Eds.). Springer Netherlands, pp. 313-328.

Rasoul-Amini, S., Montazeri-Najafabady, N., Mobasher, M.A., Hoseini-Alhashemi, S., Ghasemi, Y., 2011. *Chlorella sp.*: A new strain with highly saturated fatty acids for biodiesel production in bubble-column photobioreactor. Applied Energy 88, 3354-3356.

Redfield, A., 1934. On the proportions of organic derivations in sea water and their relation to the composition of plankton, in: Daniel, R.J. (Ed.), James Johnstone Memorial Volume. University Press of Liverpool, pp. 177-192.

Renaud, S.M., Parry, D.L., Thinh, L.V., Kuo, C., Padovan, A., Sammy, N., 1991. Effect of light-intensity on the proximate biochemical and fatty acid composition of *Isochrysis sp.* and *Nannochloropsis oculata* for use in tropical aquaculture. Journal of Applied Phycology 3, 43-53.

Richmond, A., 2004. Handbook of Microalgal culture: Biotechnology and Applied Phycology, 1st ed. Blackwell Science.

Rier, S.T., Stevenson, R.J., 2006. Response of periphytic algae to gradients in nitrogen and phosphorus in streamside mesocosms
Advances in Algal Biology: A Commemoration of the Work of Rex Lowe, in: Stevenson, R.J., Pan, Y., Kociolek, J.P., Kingston, J.C. (Eds.). Springer Netherlands, pp. 131-147.

Risher, J., Rhodes, S., 1995. Toxicological profile for fuel oils.

Rittmann, B.E., 2008. Opportunities for renewable bioenergy using microorganisms. Biotechnology and Bioengineering 100, 203-212.

Rodolfi, L., Zittelli, G.C., Bassi, N., Padovani, G., Biondi, N., Bonini, G., Tredici, M.R., 2009. Microalgae for oil: strain selection, induction of lipid synthesis and outdoor mass cultivation in a low-cost photobioreactor. Biotechnology and Bioengineering 102, 100-112.

Roesch, C., Skarka, J., Wegerer, N., 2012. Materials flow modeling of nutrient recycling in biodiesel production from microalgae. Bioresource Technology 107, 191-199.

Roncarati, A., Meluzzi, A., Acciarri, S., Tallarico, N., Melotti, P., 2004. Fatty acid composition of different microalgae strains (*Nannochloropsis sp., Nannochloropsis oculata* (Droop) Hibberd, *Nannochloris atomus Butcher* and *Isochrysis sp.)* according to the culture phase and the carbon dioxide concentration. Journal of the World Aquaculture Society 35, 401-411.

Ruparelia, J.P., Chatteriee, A.K., Duttagupta, S.P., Mukherji, S., 2008. Strain specificity in antimicrobial activity of silver and copper nanoparticles. Acta Biomaterialia 4, 707-716.

Rusch, K.A., Christensen, J.M., 2003. The hydraulically integrated serial turbidostat algal reactor (HISTAR) for microalgal production. Aquacultural Engineering 27, 249-264.

Rusch, K.A., Malone, R.F., 1998. Microalgal production using a hydraulically integrated serial turbidostat algal reactor (HISTAR): a conceptual model. Aquacultural Engineering 18, 251-264.

Ryckebosch, E., Muylaert, K., Foubert, I., 2012a. Optimization of an Analytical Procedure for Extraction of Lipids from Microalgae. J Am Oil Chem Soc 89, 189-198.

Ryckebosch, E., Muylaert, K., Foubert, I., 2012b. Optimization of an Analytical Procedure for Extraction of Lipids from Microalgae. Journal of the American Oil Chemists Society 89, 189-198.

Samantaray, S., Mallick, N., 2012. Production and characterization of poly-beta-hydroxybutyrate (PHB) polymer from Aulosira fertilissima. Journal of Applied Phycology 24, 803-814.

Scholin, C.A., Gulland, F., Doucette, G.J., Benson, S., Busman, M., Chavez, F.P., Cordaro, J., DeLong, R., De Vogelaere, A., Harvey, J., Haulena, M., Lefebvre, K., Lipscomb, T., Loscutoff, S., Lowenstine, L.J., Marin, R., Miller, P.E., McLellan, W.A., Moeller, P.D.R., Powell, C.L., Rowles, T., Silvagni, P., Silver, M., Spraker, T., Trainer, V., Van Dolah, F.M., 2000. Mortality of sea lions along the central California coast linked to a toxic diatom bloom. Nature 403, 80-84.

Sharma, K.K., Schuhmann, H., Schenk, P.M., 2012. High lipid induction in microalgae for biodiesel production. Energies 5, 1532-1553.

Sharma, L., Singh, A.K., Panda, B., Mallick, N., 2007. Process optimization for poly-beta-hydroxybutyrate production in a nitrogen fixing cyanobacterium, *Nostoc muscorum* using response surface methodology. Bioresource Technology 98, 987-993.

Sheehan, J., Dunahay, T., Benemann, J., Roessler, P., 1998. A look back at the U.S. Department of Energy's aquatic species program-biodiesel from algae. National Renewable Energy Laboratory, Golden Colorado.

Siddiquee, M.N., Rohani, S., 2011. Lipid extraction and biodiesel production from municipal sewage sludges: A review. Renewable & Sustainable Energy Reviews 15, 1067-1072.

Silaban, A.G., Bai, R., Gutierrez-Wing, M.T., Rusch, K.A., (under reivew). Impact of culture conditions on the growth of a Louisiana native *Chlorella vulgaris/Leptolyngbya sp.* co-culture.

Simionato, D., Sforza, E., Carpinelli, E.C., Bertucco, A., Giacometti, G.M., Morosinotto, T., 2011. Acclimation of *Nannochloropsis gaditana* to different illumination regimes: Effects on lipids accumulation. Bioresource Technology 102, 6026-6032.

Singh, J., Cu, S., 2010. Commercialization potential of microalgae for biofuels production. Renewable & Sustainable Energy Reviews 14, 2596-2610.

Singh, N.K., Dhar, D.W., 2011. Microalgae as second generation biofuel. A review. Agronomy for Sustainable Development 31, 605-629.

Singh, S., Kate, B.N., Banerjee, U.C., 2005. Bioactive compounds from cyanobacteria and microalgae: An overview. Critical Reviews in Biotechnology 25, 73-95.

Sommer, U., 1991. A comparison of the Droop and the Monod models of nutrient limited growth applied to natrual-populations of phytoplankton. Functional Ecology 5, 535-544.

Souza, B.S., Pinho, D.M.M., Leopoldino, E.C., Suarez, P.A.Z., Nome, F., 2012. Selective partial biodiesel hydrogenation using highly active supported palladium nanoparticles in imidazolium-based ionic liquid. Applied Catalysis A: General 433¸Äì434, 109-114.

Spoehr, H.A., Milner, H.W., 1949. The chemical composition of *Chlorella* - effect of environmental conditions. Plant Physiology 24, 120-149.

Steele, J.H., 1965. Notes on some theoretical problems in production ecology, Primary productivity in aquatic environments. University of California Press, Berkely pp. 213-235.

Stevanovic, M.M., Skapin, S.D., Bracko, I., Milenkovic, M., Petkovic, J., Filipic, M., Uskokovic, D.P., 2012. Poly(lactide-co-glycolide)/silver nanoparticles: Synthesis, characterization, antimicrobial activity, cytotoxicity assessment and ROS-inducing potential. Polymer 53, 2818-2828.

Su, C.H., Chien, L.J., Gomes, J., Lin, Y.S., Yu, Y.K., Liou, J.S., Syu, R.J., 2011. Factors affecting lipid accumulation by *Nannochloropsis oculata* in a two-stage cultivation process. Journal of Applied Phycology 23, 903-908.

Suen, Y., Hubbard, J.S., Holzer, G., Tornabene, T.G., 1987. Total lipid production of the green-algae *Nannochloropsis sp.* QII under different nitrogen regimes. Journal of Phycology 23, 289-296.

Sukenik, A., Levy, R.S., Levy, Y., Falkowski, P.G., Dubinsky, Z., 1991. Optimizing algal biomass production in an outdoor pond- a simulation-model. Journal of Applied Phycology 3, 191-201.

Sun, Y., Gates, B., Mayers, B., Younan, X., 2002. Crystalline silver nanowires by soft solution processing. Nanno Letters 2, 4.

Takagi, M., Watanabe, K., Yamaberi, K., Yoshida, T., 2000. Limited feeding of potassium nitrate for intracellular lipid and triglyceride accumulation of *Nannochlorpsis sp* UTEX LB1999. Appl. Microbiol. Biotechnol. 54, 112-117.

Tedesco, M., Duerr, E., 1989. Light, temperature and nitrogen starvation effects on the total lipid and fatty acid content and composition of *Spirulina platensis* UTEX 1928. Journal of Applied Phycology 1, 201-209.

Teixeira, R.E., 2012. Energy-efficient extraction of fuel and chemical feedstocks from algae. Green Chemistry 14, 419-427.

Tevatia, R., Demirel, Y., Blum, P., 2012. Kinetic modeling of photoautotropic growth and neutral lipid accumulation in terms of ammonium concentration in *Chlamydomonas reinhardtii*. Bioresource Technology 119, 419-424.

Theegala, C.S., Malone, R.F., Rusch, K.A., 1999. Contaminant washout in a hydraulically integrated serial turbidostat algal reactor (HISTAR). Aquacultural Engineering 19, 223-241.

Thimijan, R.W., Heins, R.D., 1983. Photometric, radiometric, and quantatum light units of measure -a review of procudures for interconversion. Hortscience 18, 818-822.

Tran, H.L., Kwon, J.S., Lee, C.G., 2009. Optimization for the growth and the lipid productivity of *Botryococcus braunii* LB572. Journal of Bioscience and Bioengineering 108, S55-S55.

Trotta, P., 1981. A simple and inexpensive system for continuous monoxenic mass-culture of marine microalgae. Aquaculture 22, 383-387.

Tsuzuki, M., Ohnuma, E., Sato, N., Takaku, T., Kawaguchi, A., 1990. Effects of CO2 concentration during growth on fatty acid composition in microalgae. Plant Physiology 93, 851-856.

Tyson, K.S., 2001. Biodiesel handling and use guidelines. National Renewable Energy Laboratory, Glolden, CO.

Uduman, N., Qi, Y., Danquah, M.K., Forde, G.M., Hoadley, A., 2010. Dewatering of microalgal cultures: A major bottleneck to algae-based fuels. Journal of Renewable and Sustainable Energy 2.

Vandamme, D., Pontes, S.C.V., Goiris, K., Foubert, I., Pinoy, L.J.J., Muylaert, K., 2011. Evaluation of electro-coagulation-flocculation for harvesting marine and freshwater microalgae. Biotechnology and Bioengineering 108, 2320-2329.

Vivekananda Mandal, Y.M., S. Hemalatha, 2007. Microwave assisted extraction – an innovative and promising extraction tool for medicinal plant research. Pharmacognosy Reviews 1, 7-18.

Vyas, D., Kumar, H.D., 1995. Nitrogen-fixation and hydrogen uptake in 4 cyanobacteria. International Journal of Hydrogen Energy 20, 163-168.

Walls, W.D., Rusco, F., Kendix, M., 2011. Biofuels policy and the US market for motor fuels: Empirical analysis of ethanol splashing. Energy Policy 39, 3999-4006.

Walters, R.G., 2005. Towards an understanding of photosynthetic acclimation. Journal of Experimental Botany 56, 435-447.

Wang, C.H., Sun, Y.Y., Xing, R.L., Sun, L.Q., 2005. Effect of liquid circulation velocity and cell density on the growth of *Parietochloris incisa* in flat plate photobioreactors. Biotechnology and Bioprocess Engineering 10, 103-108.

Wang, W., Jenkins, P.E., Ren, Z.Y., 2011. Heterogeneous corrosion behaviour of carbon steel in water contaminated biodiesel. Corrosion Science 53, 845-849.

Wang, Z.T., Ullrich, N., Joo, S., Waffenschmidt, S., Goodenough, U., 2009. Algal Lipid Bodies: Stress Induction, Purification, and Biochemical Characterization in Wild-Type and Starchless *Chlamydomonas reinhardtii*. Eukaryotic Cell 8, 1856-1868.

Widjaja, A., Chien, C.C., Ju, Y.H., 2009. Study of increasing lipid production from fresh water microalgae *Chlorella vulgaris*. J. Taiwan Inst. Chem. Eng. 40, 13-20.

Wijffels, R.H., Barbosa, M.J., 2010. An Outlook on Microalgal Biofuels. Science 329, 796-799.

Wolf, R.B., Cavins, J.F., Kleiman, R., Black, L.T., 1982. Effect of temperature on soybean seed constituents - oil, protein, moisture, fatty-acids, amino-acids and sugars. Journal of the American Oil Chemists Society 59, 230-232.

Wolkers, H., Barbosa, M.J., Kleinegris, D.M.M., Bosma, R., Wijffels, R.H., Harmsen, P.F.H., 2011. Microalgae: the green gold of the future? : large-scale sustainable cultivation of microalgae for the production of bulk commodities. Wageningen UR Food & Biobased Research, Wageningen, p. 34.

Wollman, F.A., 2001. State transitions reveal the dynamics and flexibility of the photosynthetic apparatus. Embo Journal 20, 3623-3630.

Wu, G.F., Shen, Z.Y., Wu, Q.Y., 2002. Modification of carbon partitioning to enhance PHB production in Synechocystis sp PCC6803. Enzyme and Microbial Technology 30, 710-715.

Xia, J.R., Gao, K.S., 2003. Effects of doubled atmospheric CO2 concentration on the photosynthesis and growth of *Chlorella pyrenoidosa* cultured at varied levels of light. Fisheries Science 69, 767-771.

Xu, L., Wang, F., Guo, C., Liu, C.Z., 2012. Improved algal oil production from *Botryococcus braunii* by feeding nitrate and phosphate in an airlift bioreactor. Engineering in Life Sciences 12, 171-177.

Yang, J.S., Rasa, E., Tantayotai, P., Scow, K.M., Yuan, H.L., Hristova, K.R., 2011. Mathematical model of *Chlorella minutissima* UTEX2341 growth and lipid production under photoheterotrophic fermentation conditions. Bioresource Technology 102, 3077-3082.

Yeh, K.L., Chang, J.S., Chen, W.M., 2010. Effect of light supply and carbon source on cell growth and cellular composition of a newly isolated microalga Chlorella vulgaris ESP-31. Engineering in Life Sciences 10, 201-208.

Yoo, C., Jun, S.Y., Lee, J.Y., Ahn, C.Y., Oh, H.M., 2010. Selection of microalgae for lipid production under high levels carbon dioxide. Bioresource Technology 101, S71-S74.

Yoshida, H., Tomiyama, Y., Hirakawa, Y., Mizushina, Y., 2006. Microwave roasting effects on the oxidative stability of oils and molecular species of triacylglycerols in the kernels of pumpkin (*Cucurbita spp*.) seeds. Journal of Food Composition and Analysis 19, 330-339.

Yusof, Y.A.M., Basari, J.M.H., Mukti, N.A., Sabuddin, R., Muda, A.R., Sulaiman, S., Makpol, S., Ngah, W.Z.W., 2011. Fatty acids composition of microalgae *Chlorella vulgaris* can be modulated by varying carbon dioxide concentration in outdoor culture. African Journal of Biotechnology 10, 13536-13542.

Zehr, J.P., 2011. Nitrogen fixation by marine cyanobacteria. Trends in Microbiology 19, 162-173.

Zharmukhamedov, S.K., Shirshikova, G.N., Maevskaya, Z.V., Antropova, T.M., Klimov, V.V., 2007. Bicarbonate protects the water-oxidizing complex of photosystem II against thermoinactivation in intact *Chlamydomonas reinhardtii* cells. Russian Journal of Plant Physiology 54, 302-308.

Zheng, H., Yin, J., Gao, Z., Huang, H., Ji, X., Dou, C., 2011. Disruption of *Chlorella vulgaris* Cells for the Release of Biodiesel-Producing Lipids: A Comparison of Grinding, Ultrasonication, Bead Milling, Enzymatic Lysis, and Microwaves. Appl Biochem Biotechnol 164, 1215-1224.

Zhou, W.G., Li, Y.C., Min, M., Hu, B., Chen, P., Ruan, R., 2011. Local bioprospecting for high-lipid producing microalgal strains to be grown on concentrated municipal wastewater for biofuel production. Bioresource Technology 102, 6909-6919.

Zhu, C.J., Lee, Y.K., Chao, T.M., 1997. Effects of temperature and growth phase on lipid and biochemical composition of *Isochrysis galbana* TK1. Journal of Applied Phycology 9, 451-457.

Zijffers, J.W.F., Schippers, K.J., Zheng, K., Janssen, M., Tramper, J., Wijffels, R.H., 2010. Maximum Photosynthetic Yield of Green Microalgae in Photobioreactors. Marine Biotechnology 12, 708-718.

Zimmerman, W.B., Zandi, M., Tesar, V., Gilmour, D.J., Ying, K.Z., 2011. Design of an airlift loop bioreactor and pilot scales studies with fluidic oscillator induced microbubbles for growth of a microalgae *Dunaliella salina*. Applied Energy 88, 3357-3369.

APPENDIX A. DATA FOR LIPID PRODUCTION FROM NON-AERATED STUDIES OF THE LOUISIANA CO-CULTURE

The purpose of this part of research was to evaluate the lipid productivity, lipid percentage (mass/mass, dry biomass), neutral lipid percentage (mass/mass, total lipids) and fatty acid profile of the co-culture under five irradiance (180, 400, 600, 800, 1200 μmol m^{-2} s^{-1}) and two nitrogen levels (2.94 mM and 1.47 mM). The light source used in this experiment was from high pressure sodium lamps. The culture was not continuously aerated. Carbon dioxide was bubbled into the culture daily at the rate of 0.24 L min^{-1} for 15 seconds. Triplicates were done for each treatment.

The biomass productivity was calculated by averaging the daily biomass increment (g m^{-3} d^{-1}) throughout the exponential growth phase. The collection of biomass data and biomass productivity calculations were done by Athens Silaban. Before the lipid extraction, dry biomass was measured (g). Lipid percentage was calculated dividing the mass of total lipid by the mass of dry biomass used for extraction. The lipid productivity was calculated by multiplying biomass productivity by lipid percentage.

Replicate #1	Louisiana co-culture				
Irradiance (μmol m^{-2} s^{-1})	Nitrate Level	biomass (g m^{-3})	Lipid/Biomass	Biomass productivity (g m^{-3} d^{-1})	Lipid Productivity (g m^{-3} d^{-1})
180	50%	609	25.85%	38	9.82
	100%	990	23.74%	44	10.4
400	50%	748	33.18%	37	12.3
	100%	1139	30.07%	60	18.0
600	50%	549	33.54%	36	12.1
	100%	875	28.00%	51	14.3
800	50%	729	29.83%	40	11.9
	100%	1192	30.84%	59	18.2
1200	50%	463	20.18%	26	5.25
	100%	786	20.36%	37	7.53

Replicate #2	Louisiana co-culture				
Irradiance level (µmol m^{-2} s^{-1})	Nitrate Level	biomass (g m^{-3})	Lipid/Biomass	Biomass productivity (g m^{-3} d^{-1})	Lipid productivity (g m^{-3} d^{-1})
180	50%	618	26.01%	33	8.58
	100%	949	22.96%	44	10.1
400	50%	815	39.33%	37	14.6
	100%	1143	31.66%	56	17.7
600	50%	544	31.31%	45	14.1
	100%	865	21.93%	44	9.60
800	50%	853	39.06%	22	8.59
	100%	1193	33.54%	49	16.4
1200	50%	447	19.54%	34	6.64
	100%	721	16.45%	40	6.58

Replicate #3	Louisiana co-culture				
Irradiance (µmol m^{-2} s^{-1})	Nitrate Level	biomass (g m^{-3})	Lipid/Biomass	Biomass productivity (g m^{-3} d^{-1})	Lipid productivity (g m^{-3} d^{-1})
180	50%	538	22.48%	47	10.6
	100%	926	18.09%	59	10.7
400	50%	780	40.02%	36	14.4
	100%	1098	30.22%	50	15.1
600	50%	538	28.79%	37	10.7
	100%	853	26.56%	45	12.0
800	50%	774	35.95%	33	11.9
	100%	1420	27.46%	50	13.7
1200	50%	430	19.11%	34	6.50
	100%	655	12.21%	30	3.66

Neutral lipid percentage (mass/mass, based on total lipid)

The protocol of neutral lipid percentage analysis followed Pernet et al. (2006) using solid phase extraction. The total lipid was loaded on the Si-NH_2 column. The neutral lipids were eluted by chloroform:isopropanol 2:1 into a pre-weighed test tube. After the solvent was evaporated, the mass of neutral lipids was calculated by mass of tube plus neutral lipids minus the mass of test tube. The neutral lipid percentage was then calculated by dividing the neutral lipid mass by mass of total lipids.

Replicate #1	Louisiana co-culture					
Irradiance level (μmol m^{-2} s^{-1})	Nitrogen	Tube (g)	Tube+Neutral (g)	Neutral (g)	Total lipid (g)	Neutral lipid (%)
180	50%	8.0551	8.0674	0.0123	0.0157	78.34%
	100%	8.0144	8.0236	0.0092	0.0122	75.41%
400	50%	7.994	8.022	0.028	0.0349	80.23%
	100%	8.0533	8.0862	0.0329	0.042	78.33%
600	50%	7.9413	7.9566	0.0153	0.0204	75.00%
	100%	8.0489	8.0688	0.0199	0.027	73.70%
800	50%	8.0325	8.0603	0.0278	0.0369	75.34%
	100%	7.9931	8.0289	0.0358	0.0465	76.99%
1200	50%	8.0171	8.0238	0.0067	0.01	67.00%
	100%	7.9793	7.9918	0.0125	0.0177	70.62%

Replicate #2	Louisiana co-culture					
Irradiance level (μmol m^{-2} s^{-1})	Nitrogen	Tube (g)	Tube+Neutral (g)	Neutral (g)	total lipid (g)	Neutral lipid (%)
180	50%	8.0395	8.0476	0.0081	0.0118	68.64%
	100%	8.0514	8.0642	0.0128	0.0187	68.45%
400	50%	8.038	8.0512	0.0132	0.0177	74.58%
	100%	7.9805	8.0006	0.0201	0.0279	72.04%
600	50%	5.1575	5.1798	0.0223	0.0308	72.40%
	100%	5.2616	5.2683	0.0067	0.0092	72.83%
800	50%	7.9673	7.9915	0.0242	0.0316	76.58%
	100%	7.9966	8.0313	0.0347	0.0448	77.46%
1200	50%	8.0002	8.0061	0.0059	0.0088	67.05%
	100%	7.9966	8.0008	0.0042	0.0076	55.26%

Replicate #3	Louisiana co-culture					
Irradiance level ($\mu mol\ m^{-2}\ s^{-1}$)	Nitrogen	Tube (g)	Tube Neutral (g)	Neutral (g)	Total lipid (g)	Neutral lipid (%)
180	50%	7.9883	8.0014	0.0131	0.0171	76.61%
	100%	7.9976	8.0186	0.021	0.0268	78.36%
400	50%	7.9558	7.9775	0.0217	0.028	77.50%
	100%	7.9679	7.9976	0.0297	0.0397	74.81%
600	50%	7.9465	7.9542	0.0077	0.0105	73.33%
	100%	7.9913	8.0018	0.0105	0.0138	76.09%
800	50%	7.9773	7.9952	0.0179	0.0253	70.75%
	100%	7.9881	8.0188	0.0307	0.0422	72.75%
1200	50%	8.0477	8.0516	0.0039	0.0056	69.64%
	100%	7.9999	8.0038	0.0039	0.0065	60.00%

Energy return of lipid on light energy (%)

To evaluate the efficiency of the Louisiana co-culture to convert light energy into lipid energy, the energy return (lipid energy) on energy input (light energy) was calculated. The calculation was adapted from the Zijffers et al. (2010), which was used for biomass yield on light energy:

$$Y_{lipid\ ,E} = \frac{P_L}{I_s \times 10^{-6} \times 8.64 \times 10^4} \times \frac{V}{A} \quad (1)$$

where $Y_{lipid,\ E}$ is the lipid per mole photons, P_L (g m^{-3} d^{-1}) is the lipid productivity, I_s is scalar irradiance level (µmol m^{-2} s^{-1}, culture concentration x=0), V/A is the volume to wetted surface area ratio of the culture. For 1.0 L culture in a 2.0 L Erlenmeyer flask used in this work, V/A is 0.023 m^3 m^{-2}.

The lipid caloric content (C_L, kJ g^{-1}) was determined with a Parr 6200 isoperibol calorimeter. The sample of 0.5 g of total lipid in sample cup was installed into the caloric bomb, and a platinum ignition wire was attached to the lipid sample. The caloric bomb was charged with O_2 till the pressure reached 10-35 atm. The platinum wire then was ignited. After the run finished, the caloric content of the lipid was automatically calculated. Duplicates were done. The energy return of lipid on light energy was calculated following the equation:

$$\eta = Y_{\boldsymbol{Lipid,E}} \times \frac{C_L}{E} \quad (2)$$

Where η (%) is the energy return of lipid on the light energy for each irradiance level. E (kJ (mole photon)$^{-1}$) is a parameter to convert the scalar irradiance to energy. For HPS lamps, E is estimated to be 201 kJ (mole photon)$^{-1}$ as reported by Thimijan and Heins (1983). The calculated

η was plotted against each internal scalar irradiance level (where the culture concentration x=0) to investigate the effects of irradiance levels on the energy return (lipid energy) on light energy input.

Irradiance ($\mu mol\ m^{-2}\ s^{-1}$)	Nitrate	Replicate #	Lipid Productivity	Lipid energy/irradiance energy	Lipid yield per mole photon
180	50%	1	9.82	0.22%	0.0145
180		2	10.6	0.23%	0.0157
180		3	8.58	0.19%	0.0127
180	100%	1	10.4	0.23%	0.0154
180		2	10.7	0.24%	0.0158
180		3	10.1	0.22%	0.0149
400	50%	1	12.3	0.12%	0.0082
400		2	14.4	0.14%	0.0096
400		3	14.6	0.14%	0.0097
400	100%	1	18.0	0.18%	0.0120
400		2	15.1	0.15%	0.0100
400		3	17.7	0.18%	0.0118
600	50%	1	12.1	0.08%	0.0054
600		2	10.7	0.07%	0.0047
600		3	14.1	0.09%	0.0063
600	100%	1	14.3	0.09%	0.0063
600		2	9.60	0.06%	0.0043
600		3	12.0	0.08%	0.0053
800	50%	1	11.9	0.06%	0.0040
800		2	11.9	0.06%	0.0040
800		3	8.59	0.04%	0.0029
800	100%	1	18.2	0.09%	0.0061
800		2	13.7	0.07%	0.0046
800		3	16.4	0.08%	0.0055
1200	50%	1	5.25	0.02%	0.0012
1200		2	6.50	0.02%	0.0014
1200		3	6.64	0.02%	0.0015
1200	100%	1	7.53	0.02%	0.0017
1200		2	3.66	0.01%	0.0008
1200		3	6.58	0.02%	0.0015

Fatty acid profiles (% of total fatty acids)

The fatty acids were determined using gas chromatography (HP 5890 Series II) equipped with an SP^{TM}-2330 column (30 m, 0.25mm ID, 0.20 μm film). The initial oven temperature was kept at 80 ^{o}C for 1 minute and then increased to 220 ^{o}C at the ramp of 4 ^{o}C min^{-1} and maintained at 220 ^{o}C for 5 minutes. Helium was kept at 2.0 mL min^{-1} as the carrier gas. The gas chromatography data were analyzed with Chemstation^{TM} software, and the mass percentage of each fatty acid component was reported.

The first number in the first column is the number of replicate, second number is the nitrogen level and the last number in the first column is the irradiance level. There were three samples for each treatment, and triplicates were done for each sample. Therefore, there were totally nine runs for each culture condition.

Fatty acid							
C14:0				C16:0			
1 50%N 180 μmol	0.504	0.485	0.67	1 50%N 180 μmol	26.576	26.792	26.979
1 100%N 180 μmol	0.5	0.478	0.612	1 100%N 180 μmol	26.235	26.227	26.234
1 50%N 400 μmol	0.47	0.409	0.395	1 50%N 400 μmol	28.216	28.979	29.025
1 100%N 400 μmol	0.497	0.451	0.514	1 100%N 400 μmol	27.76	27.521	28.748
1 50%N 800 μmol	0.443	0.444	0.427	1 50%N 800 μmol	28.736	29.085	28.417
1 100%N 800μmol	0.393	0.36	0.445	1 100%N 800 μmol	27.76	26.847	26.847
2 50%N 180 μmol	0.58	0.501	0.448	2 50%N 180 μmol	27.772	28.446	27.282
2 100%N 180 μmol	1.003	1.035	0.934	2 100%N 180 μmol	29.245	30.143	29.771
2 50%N 400 μmol	0.364	0.366	0.337	2 50%N 400 μmol	26.895	26.731	27.117
2 100%N 400 μmol	0.383	0.309	0.337	2 100%N 400 μmol	29.083	28.553	27.117
2 50%N 800 μmol	0.353	0.351	0.342	2 50%N 800 μmol	30.112	28.489	28.488
2 100%N 800 μmol	0.316	0.403	0.32	2 100%N 800 μmol	28.733	32.311	28.862
3 50%N 180 μmol	0.492	0.575	0.554	3 50%N 180 μmol	27.646	27.285	27.281
3 100%N 180 μmol	0.55	0.65	0.648	3 100%N 180 μmol	27.305	27.369	28.084
3 50%N 400 μmol	0.492	0.575	0.554	3 50%N 400 μmol	30.01	30.019	30.58
3 100%N 400 μmol	0.397	0.395	0.7	3 100%N 400 μmol	29.142	28.911	28.513
3 50%N 800 μmol	0.607	0.405	0.342	3 50%N 800 μmol	27.443	27.727	27.851
3 100%N 800 μmol	0.316	0.361	0.407	3 100%N 800 μmol	28.733	29.338	28.788
1 50%N 600 μmol	0.614	0.569	0.483	1 50%N 600 μmol	35.219	34.597	33.451

1 100%N 600 µmol	0.953	0.955	0.928	1 100%N 600 µmol	33.14	33.23	32.556
2 50%N 600 µmol	0.419	0.442	0.444	2 50%N 600 µmol	33.285	33.403	33.237
2 100%N 600 µmol	0.5	0.49	0.506	2 100%N 600 µmol	31.979	31.83	31.67
3 50%N 600 µmol	0.506	0.529	0.632	3 50%N 600 µmol	31.176	35.328	33.757
3 100%N 600 µmol	0.497	0.515	0.601	3 100%N 600 µmol	35.415	31.166	32.616
1 50%N 1200 µmol	0.456	0.447	0.447	1 50%N 1200 µmol	31.864	32.225	32.011
1 100%N1200 µmol	0.539	0.637	0.529	1 100%N1200 µmol	28.772	29.074	28.48
2 50%N 1200 µmol	0.497	0.515	0.56	2 50%N 1200 µmol	31.166	35.415	32.031
2 100%N1200 µmol	0.419	0.442	0.444	2 100%N 1200µmol	33.285	33.403	33.237
3 50%N 1200 µmol	0.524	0.447	0.407	3 50%N 1200 µmol	34.337	32.015	33.011
3 100%N1200 µmol	0.5	0.49	0.506	3 100%N1200µmol	31.979	31.83	31.67
1 50%N 800 µmol	0.655	0.638	0.61	1 50%N 800 µmol	36.569	36.73	35.714
1 100%N 800 µmol	0.632	0.596	0.63	1 100%N 800 µmol	35.98	34.89	36.35
2 50%N 800 µmol	0.462	0.461	0.474	2 50%N 800 µmol	30.345	30.58	30.331
2 100%N 800 µmol	0.506	0.456	0.543	2 100%N 800 µmol	31.117	31.4	31.671
3 50%N 800 µmol	0.462	0.461	0.474	3 50%N 800 µmol	30.345	30.58	30.331
3 100%N 800 µmol	0.506	0.456	0.543	3 100%N 800 µmol	31.117	31.4	31.671

C16:1 n7				C16:1 n9			
1 50%N 180 µmol	0.785	0.814	0.753	1 50%N 180 µmol	1.877	1.911	1.973
1 100%N 180 µmol	1.048	1.108	1.137	1 100%N 180 µmol	2.086	2.124	2.146
1 50%N 400 µmol	0.796	0.834	0.832	1 50%N 400 µmol	1.656	1.847	1.668
1 100%N 400 µmol	0.905	0.918	0.942	1 100%N 400 µmol	1.825	1.855	1.917
1 50%N 800 µmol	0.854	0.866	0.874	1 50%N 800 µmol	2.061	2.12	2.063
1 100%N 800µmol	0.889	0.87	0.97	1 100%N 800µmol	2.189	2.185	2.27
2 50%N 180 µmol	0.522	0.695	0.63	2 50%N 180 µmol	2.194	2.331	2.403
2 100%N 180 µmol	0.71	0.76	0.753	2 100%N 180 µmol	2.028	2.191	2.18
2 50%N 400 µmol	0.732	0.725	0.743	2 50%N 400 µmol	1.861	1.834	1.99
2 100%N 400 µmol	0.648	0.713	0.743	2 100%N 400 µmol	1.93	2.104	1.49
2 50%N 800 µmol	0.775	0.778	0.778	2 50%N 800 µmol	1.935	1.842	1.846
2 100%N 800 µmol	0.803	0.912	0.805	2 100%N 800 µmol	1.907	2.153	1.899
3 50%N 180 µmol	0.677	0.727	0.707	3 50%N 180 µmol	1.654	1.721	1.729
3 100%N 180 µmol	0.634	0.673	0.774	3 100%N 180 µmol	2.152	2.413	2.278
3 50%N 400 µmol	0.961	0.948	0.936	3 50%N 400 µmol	1.862	1.715	1.649
3 100%N 400 µmol	0.765	0.746	0.855	3 100%N 400 µmol	1.389	1.513	1.564
3 50%N 800 µmol	0.87	0.771	0.807	3 50%N 800 µmol	2.134	1.713	1.807
3 100%N 800 µmol	0.803	0.877	0.843	3 100%N 800 µmol	1.907	1.709	1.771
1 50%N 600 µmol	1.172	1.148	0.856	1 50%N 600 µmol	1.846	1.81	1.623
1 100%N 600 µmol	0.928	0.96	0.91	1 100%N 600 µmol	1.585	1.631	1.573
2 50%N 600 µmol	0.818	0.847	0.825	2 50%N 600 µmol	1.574	1.616	1.594
2 100%N 600 µmol	1.076	1.057	1.079	2 100%N 600 µmol	1.608	1.59	1.606
3 50%N 600 µmol	0.966	1.011	0.961	3 50%N 600 µmol	1.624	1.891	0.639
3 100%N 600 µmol	0.982	1.169	0.939	3 100%N 600 µmol	1.826	2.104	1.608
1 50%N 1200 µmol	0.967	0.962	0.938	1 50%N 1200 µmol	1.377	1.431	1.368
1 100%N 1200µmol	1.099	1.158	1.095	1 100%N 1200 µmol	2.769	3.017	2.67
2 50%N 1200 µmol	0.982	1.169	1.036	2 50%N 1200 µmol	1.826	2.104	1.916
2 100%N 1200µmol	0.818	0.847	0.825	2 100%N 1200 µmol	1.574	1.616	1.594
3 50%N 1200 µmol	0.965	0.962	0.938	3 50%N 1200 µmol	1.377	1.431	1.368
3 100%N1200 µmol	1.076	1.057	1.079	3 100%N 1200 µmol	1.608	1.59	1.606
1 50%N 800 µmol	1.129	1.121	1.051	1 50%N 800 µmol	1.526	1.539	1.496
1 100%N 800 µmol	0.949	0.907	0.938	1 100%N 800 µmol	1.397	1.347	1.402
2 50%N 800 µmol	1.22	1.226	1.247	2 50%N 800 µmol	1.514	1.531	1.538
2 100%N 800 µmol	1.056	1.055	1.094	2 100%N 800 µmol	1.293	1.256	1.276
3 50%N 800 µmol	1.22	1.226	1.247	3 50%N 800 µmol	1.514	1.531	1.538
3 100%N 800 µmol	1.056	1.055	1.094	3 100%N 800 µmol	1.293	1.256	1.276

C16:2 n10				C18:0			
1 50%N 180 µmol	1.877	1.911	1.973	1 50%N 180 µmol	3.711	3.716	3.824
1 100%N 180 µmol	2.086	2.124	2.146	1 100%N 180 µmol	4.247	4.277	4.344
1 50%N 400 µmol	1.656	1.847	1.668	1 50%N 400 µmol	4.042	3.947	3.94
1 100%N 400 µmol	1.825	1.855	1.917	1 100%N 400 µmol	4.653	4.698	4.546
1 50%N 800 µmol	2.061	2.12	2.063	1 50%N 800 µmol	4.281	4.272	4.541
1 100%N 800µmol	2.189	2.185	2.27	1 100%N 800µmol	3.935	3.493	3.963
2 50%N 180 µmol	2.194	2.331	2.403	2 50%N 180 µmol	3.855	4.038	3.984
2 100%N 180 µmol	2.028	2.191	2.18	2 100%N 180 µmol	6.852	6.804	6.972
2 50%N 400 µmol	1.861	1.834	1.99	2 50%N 400 µmol	4.275	4.313	4.243
2 100%N 400 µmol	1.93	2.104	1.49	2 100%N 400 µmol	4.336	4.321	4.243
2 50%N 800 µmol	1.935	1.842	1.846	2 50%N 800 µmol	3.855	4.038	3.984
2 100%N 800 µmol	1.907	2.153	1.899	2 100%N 800 µmol	3.935	3.493	3.963
3 50%N 180 µmol	1.654	1.721	1.729	3 50%N 180 µmol	3.896	3.653	3.761
3 100%N 180 µmol	2.152	2.413	2.278	3 100%N 180 µmol	3.817	3.721	3.729
3 50%N 400 µmol	1.862	1.715	1.649	3 50%N 400 µmol	4.372	4.707	4.556
3 100%N 400 µmol	1.389	1.513	1.564	3 100%N 400 µmol	4.655	4.43	4.676
3 50%N 800 µmol	2.134	1.713	1.807	3 50%N 800 µmol	4.152	4.081	4.073
3 100%N 800 µmol	1.907	1.709	1.771	3 100%N 800 µmol	4.167	4.607	4.656
1 50%N 600 µmol	2.392	1.947	2.281	1 50%N 600 µmol	5.402	5.6	6.064
1 100%N 600 µmol	2.386	2.339	2.338	1 100%N 600 µmol	7.259	7.099	7.233
2 50%N 600 µmol	2.205	2.244	2.213	2 50%N 600 µmol	5.338	5.389	5.675
2 100%N 600 µmol	2.177	2.142	2.168	2 100%N 600 µmol	5.308	6.023	5.787
3 50%N 600 µmol	4.01	4.612	2.213	3 50%N 600 µmol	6.871	5.929	5.675
3 100%N 600 µmol	1.946	1.984	1.311	3 100%N 600 µmol	5.341	4.637	7.079
1 50%N 1200 µmol	2.112	2.134	2.083	1 50%N 1200 µmol	5.567	5.423	5.444
1 100%N1200µmol	2.455	2.732	2.512	1 100%N 1200µmol	5.394	5.385	5.634
2 50%N 1200µmol	1.946	1.984	2.078	2 50%N 1200 µmol	5.341	4.637	5.28
2 100%N1200µmol	2.205	2.244	2.213	2 100%N 1200µmol	5.338	5.389	5.675
3 50%N 1200µmol	2.112	2.275	2.083	3 50%N 1200 µmol	6.218	5.378	5.444
3 100%N1200µmol	2.177	2.142	2.168	3 100%N1200 µmol	5.308	6.023	5.787
1 50%N 800µmol	1.806	1.836	1.757	1 50%N 800 µmol	5.667	5.995	5.678
1 100%N 800µmol	1.943	1.869	1.955	1 100%N 800 µmol	4.902	5.204	5.037
2 50%N 800µmol	2.033	2.068	2.1	2 50%N 800 µmol	4.078	4.41	5.446
2 100%N 800µmol	1.896	1.906	1.956	2 100%N 800 µmol	4.748	4.735	4.02
3 50%N 800µmol	2.033	2.068	2.1	3 50%N 800 µmol	4.078	4.41	5.446
3 100%N 80 µmol	1.896	1.906	1.956	3 100%N 800 µmol	4.748	4.735	4.02

C18:3n9				C18:1n9C			
1 50%N 180 µmol	6.135	6.733	6.245	1 50%N 180µmol	18.471	18.227	18.188
1 100%N 180 µmol	7.328	7.471	7.423	1 100%N 180µmol	18.256	18.21	19.299
1 50%N 400 µmol	6.9	6.464	6.643	1 50%N 400µmol	18.932	19.587	19.477
1 100%N 400 µmol	6.118	6.039	6.358	1 100%N 400µmol	17.945	18.08	17.64
1 50%N 800 µmol	5.766	5.875	5.45	1 50%N 800 µmol	17.164	17.008	17.358
1 100%N 800 µmol	5.619	5.272	5.592	1 100%N 800µmol	16.414	16.288	16.193
2 50%N 180 µmol	5.471	5.423	5.127	2 50%N 180 µmol	19.423	19.792	20.089
2 100%N 180 µmol	4.814	5.499	5.115	2 100%N 180µmol	18.046	19.55	18.132
2 50%N 400 µmol	4.674	4.583	4.73	2 50%N 400µmol	20.556	19.658	19.462
2 100%N 400 µmol	5.365	5.273	4.73	2 100%N 400µmol	18.459	18.475	22.462
2 50%N 800 µmol	4.88	4.585	4.546	2 50%N 800µmol	20.257	20.676	20.692
2 100%N 800 µmol	4.858	5.711	4.851	2 100%N 800µmol	20.067	18.229	19.995
3 50%N 180 µmol	6.417	6.468	6.503	3 50%N 180 µmol	19.375	19.165	19.254
3 100%N 180 µmol	7.237	7.242	7.635	3 100%N 180µmol	19.63	20.564	19.208
3 50%N 400 µmol	6.272	6.582	6.274	3 50%N 400µmol	20.598	20.073	20.12
3 100%N 400 µmol	6.013	5.851	6.032	3 100%N 400µmol	19.804	20.171	20.037
3 50%N 800 µmol	5.912	5.774	5.98	3 50%N 800 µmol	17.515	17.641	17.53
3 100%N 800 µmol	4.858	4.954	4.808	3 100%N 800µmol	20.067	20.821	21.06
1 50%N 600 µmol	5.109	5.08	7.297	1 50%N 600µmol	16.961	17.246	15.728
1 100%N 600 µmol	4.019	4.319	4.394	1 100%N 600µmol	18.047	17.988	18.016
2 50%N 600 µmol	8.004	7.94	7.617	2 50%N 600µmol	16.176	15.968	15.95
2 100%N 600 µmol	6.003	5.362	5.508	2 100%N 600µmol	18.839	18.786	18.97
3 50%N 600 µmol	5.835	7.167	6.413	3 50%N 600µmol	19.026	18.598	16.294
3 100%N 600 µmol	5.062	5.904	2.466	3 100%N 600µmol	21.542	19.89	21.259
1 50%N 1200 µmol	5.378	5.456	5.471	1 50%N 1200µmol	21.406	20.981	21.079
1 100%N 1200µmol	7.025	7.448	6.604	1100%N1200µmol	16.997	16.015	17.489
2 50%N 1200 µmol	5.062	5.904	5.141	2 50%N 1200µmol	21.542	19.89	21.259
2 100%N 1200µmol	8.004	7.94	7.617	2100%N1200µmol	16.176	15.968	15.95
3 50%N 1200 µmol	5.378	5.456	5.471	3 50%N 1200µmol	21.406	18.989	21.079
3 100%N 1200µmol	6.003	5.362	5.508	3100%N1200µmol	18.839	18.786	18.97
1 50%N 800µmol	5.499	5.156	5.509	1 50%N 800µmol	16.195	16.079	16.303
1 100%N 800µmol	5.586	5.328	5.448	1 100%N 800µmol	18.726	18.873	18.357
2 50%N 800µmol	4.952	4.78	3.499	2 50%N 800µmol	23.267	23.056	23.362
2 100%N 800µmol	5.03	5.074	5.685	2 100%N 800µmol	23.09	22.975	23.056
3 50%N 800µmol	4.952	4.78	3.499	3 50%N 800µmol	23.267	23.056	23.362
3 100%N 800µmol	5.03	5.074	5.685	3 100%N 800µmol	23.09	22.975	23.056

C18:1n9t				C18:2			
1 50%N 180 µmol	3.903	3.945	3.874	1 50%N 180 µmol	17.358	17.152	17.363
1 100%N 180 µmol	2.657	2.636	2.632	1 100%N 180 µmol	17.185	17.107	17.065
1 50%N 400 µmol	3.15	2.899	2.839	1 50%N 400 µmol	16.325	15.734	15.715
1 100%N 400 µmol	2.71	2.726	2.63	1 100%N 400 µmol	17.245	17.332	16.882
1 50%N 800 µmol	3.218	3.148	3.194	1 50%N 800 µmol	17.358	17.152	17.363
1 100%N 800 µmol	3.63	3.771	3.628	1 100%N 800 µmol	19.115	19.571	19.611
2 50%N 180 µmol	4.225	4.472	4.534	2 50%N 180 µmol	18.653	18.325	18.494
2 100%N 180 µmol	4.114	3.803	4.008	2 100%N 180 µmol	15.211	15.059	15.567
2 50%N 400 µmol	3.712	3.731	3.755	2 50%N 400 µmol	19.036	19.035	18.848
2 100%N 400 µmol	4.307	4.386	3.755	2 100%N 400 µmol	18.056	17.96	18.848
2 50%N 800 µmol	3.723	3.854	3.863	2 50%N 800 µmol	18.482	18.696	18.684
2 100%N 800 µmol	3.63	3.771	3.62	2 100%N 800 µmol	18.248	17.527	18.172
3 50%N 180 µmol	4.654	4.718	4.75	3 50%N 180 µmol	15.102	15.267	14.998
3 100%N 180 µmol	3.63	3.333	3.371	3 100%N 180µmol	15.324	15.168	14.753
3 50%N 400 µmol	3.219	3.031	2.694	3 50%N 400 µmol	14.711	14.385	14.858
3 100%N 400 µmol	3.433	3.426	3.374	3 100%N 400 µmol	15.62	15.89	15.779
3 50%N 800 µmol	4.126	4.278	4.259	3 50%N 800 µmol	17.324	17.374	17.173
3 100%N 800 µmol	3.63	3.333	3.371	3 100%N 800 µmol	18.248	16.599	16.818
1 50%N 600 µmol	2.74	2.877	2.671	1 50%N 600 µmol	13.278	13.582	11.409
1 100%N 600 µmol	2.267	2.261	2.365	1 100%N 600 µmol	13.252	13.16	13.276
2 50%N 600 µmol	2.55	2.479	2.582	2 50%N 600 µmol	11.534	11.434	11.512
2 100%N 600 µmol	2.766	2.817	2.685	2 100%N 600 µmol	13.701	13.625	13.722
3 50%N 600 µmol	2.096	1.96	2.582	3 50%N 600 µmol	12.418	11.826	11.512
3 100%N 600 µmol	3.181	2.94	2.997	3 100%N 600 µmol	12.728	11.909	12.481
1 50%N 1200 µmol	2.84	2.949	3.115	1 50%N 1200 µmol	12.322	12.24	12.376
1 100%N 1200 µmol	3.008	3.07	2.862	1 100%N1200µmol	12.472	11.943	12.62
2 50%N 1200 µmol	3.181	2.94	2.997	2 50%N 1200 µmol	12.728	11.909	12.481
2 100%N 1200 µmol	2.55	2.479	2.582	2 100%N1200µmol	11.534	11.434	11.512
3 50%N 1200 µmol	2.84	2.141	3.115	3 50%N 1200µmol	12.322	12.24	12.288
3 100%N 1200 µmol	2.766	2.817	2.685	3 100%N1200µmol	13.701	13.625	13.722
1 50%N 800 µmol	2.501	2.612	2.766	1 50%N 800 µmol	12.942	12.955	13.144
1 100%N 800 µmol	2.262	2.409	2.464	1 100%N 800 µmol	13.659	13.778	13.528
2 50%N 800 µmol	2.779	2.918	2.773	2 50%N 800 µmol	15.441	15.355	13.437
2 100%N 800 µmol	2.342	2.407	2.235	2 100%N 800 µmol	14.971	14.957	14.8
3 50%N 800 µmol	2.779	2.918	2.773	3 50%N 800 µmol	15.441	15.355	13.437
3 100%N 800 µmol	2.342	2.407	2.235	3 100%N 800 µmol	14.971	14.957	14.8

C20:0				C18:3n3			
1 50%N 180 µmol	2.747	2.421	2.596	1 50%N 180 µmol	15.082	14.992	14.52
1 100%N 180 µmol	3.137	3.203	3.276	1 100%N 180 µmol	17.045	16.84	16.74
1 50%N 400 µmol	2.793	2.518	2.529	1 50%N 400 µmol	14.892	14.936	15.047
1 100%N 400 µmol	3.22	3.211	3.047	1 100%N 400 µmol	14.569	14.617	14.178
1 50%N 800 µmol	3.107	3.111	3.239	1 50%N 800 µmol	14.583	14.437	14.641
1 100%N 800 µmol	3.606	3.597	3.675	1 100%N 800 µmol	14.738	15.454	14.588
2 50%N 180 µmol	1.582	1.383	2.135	2 50%N 180 µmol	12.389	12.096	12.173
2 100%N 180 µmol	3.828	3.388	3.521	2 100%N 180 µmol	12.484	12.273	12.083
2 50%N 400 µmol	2.004	2.107	2.042	2 50%N 400 µmol	12.123	12.344	12.098
2 100%N 400 µmol	2.131	2.334	2.042	2 100%N 400 µmol	12.975	13.345	12.098
2 50%N 800 µmol	1.598	2.224	2.197	2 50%N 800 µmol	11.997	12.359	12.397
2 100%N 800 µmol	2.287	1.179	2.344	2 100%N 800 µmol	12.791	12.115	12.747
3 50%N 180 µmol	1.648	1.617	1.702	3 50%N 180 µmol	14.717	14.831	14.859
3 100%N 180 µmol	2.022	2.258	1.997	3 100%N 180 µmol	17.124	16.834	16.652
3 50%N 400 µmol	2.004	2.107	2.042	3 50%N 400 µmol	13.968	13.981	14.172
3 100%N 400 µmol	2.51	1.982	1.995	3 100%N 400 µmol	17.124	16.834	16.652
3 50%N 800 µmol	2.116	2.219	2.21	3 50%N 800 µmol	15.761	15.849	15.717
3 100%N 800 µmol	2.287	2.326	2.414	3 100%N 800 µmol	12.791	12.804	12.843
1 50%N 600 µmol	2.884	3.273	3.22	1 50%N 600 µmol	11.42	11.791	14.472
1 100%N 600 µmol	3.986	3.982	4.192	1 100%N 600 µmol	11.623	11.433	11.615
2 50%N 600 µmol	3.352	3.305	3.323	2 50%N 600 µmol	14.295	14.461	14.551
2 100%N 600 µmol	3.845	3.991	4.048	2 100%N 600 µmol	11.642	11.666	11.625
3 50%N 600 µmol	6.268	3.175	3.323	3 50%N 600 µmol	13.783	12.96	14.551
3 100%N 600 µmol	2.976	1.62	2.475	3 100%N 600 µmol	12.505	11.675	12.256
1 50%N 1200 µmol	2.918	3.014	2.868	1 50%N 1200 µmol	12.268	12.217	12.291
1 100%N 1200 µmol	3.001	2.823	3.262	1 100%N1200µmol	15.948	16.215	15.687
2 50%N 1200 µmol	2.709	1.62	2.475	2 50%N 1200 µmol	12.505	11.675	12.256
2 100%N 1200 µmol	3.352	3.305	3.323	2 100%N1200µmol	14.295	14.461	14.551
3 50%N 1200 µmol	2.918	2.275	2.868	3 50%N 1200 µmol	15.599	12.217	12.291
3 100%N 1200 µmol	3.845	3.991	4.048	3 100%N1200µmol	11.642	11.666	11.625
1 50%N 800 µmol	3.266	3.073	3.427	1 50%N 800 µmol	11.766	11.815	12.038
1 100%N 800 µmol	3.215	3.768	3.169	1 100%N 800 µmol	10.301	10.462	10.281
2 50%N 800 µmol	3.463	3.298	3.431	2 50%N 800µmol	9.822	9.73	9.75
2 100%N 800 µmol	3.451	3.368	3.416	2 100%N 800µmol	9.855	9.836	9.643
3 50%N 800 µmol	3.463	3.298	3.431	3 50%N 800µmol	9.822	9.73	9.75
3 100%N 800 µmol	3.451	3.368	3.416	3 100%N 800µmol	9.855	9.836	9.643

C20:1				C22:0			
1 50%N 180 µmol	0.201	0.176	0.245	1 50%N 180 µmol	0.266	0.225	0.243
1 100%N 180 µmol	0.185	0.256	0.191	1 100%N 180 µmol	0.311	0.255	0.289
1 50%N 400 µmol	0.21	0.244	0.238	1 50%N 400 µmol	0.207	0.203	0.215
1 100%N 400 µmol	0.207	0.233	0.169	1 100%N 400 µmol	0.284	0.289	0.283
1 50%N 800 µmol	0.193	0.2	0.208	1 50%N 800 µmol	0.306	0.297	0.32
1 100%N 800 µmol	0.204	0.157	0.17	1 100%N 800 µmol	0.361	0.339	0.255
2 50%N 180 µmol	0.307	0.199	0.224	2 50%N 180 µmol	0.148	0.178	0.276
2 100%N 180 µmol	0.748	0.725	0.191	2 100%N 180 µmol	0.583	0.495	0.343
2 50%N 400 µmol	0.35	0.266	0.334	2 50%N 400 µmol	0.221	0.214	0.271
2 100%N 400 µmol	0.222	0.248	0.334	2 100%N 400 µmol	0.207	0.23	0.271
2 50%N 800 µmol	0.197	0.247	0.283	2 50%N 800 µmol	0.102	0.233	0.286
2 100%N 800 µmol	0.211	0.135	0.234	2 100%N 800 µmol	0.253	0.086	0.266
3 50%N 180 µmol	0.236	0.32	0.32	3 50%N 180 µmol	0.204	0.205	0.238
3 100%N 180 µmol	0.205	0.216	0.229	3 100%N 180 µmol	0.245	0.259	0.207
3 50%N 400 µmol	0.297	0.292	0.231	3 50%N 400 µmol	0.209	0.387	0.101
3 100%N 400 µmol	0.231	0.246	0.344	3 100%N 400 µmol	0.203	0.133	0.334
3 50%N 800 µmol	0.236	0.32	0.32	3 50%N 800 µmol	0.276	0.284	0.303
3 100%N 800 µmol	0.211	0.297	0.304	3 100%N 800 µmol	0.253	0.284	0.289
1 50%N 600 µmol	0.147	0.166	0.147	1 50%N 600 µmol	0.439	0.314	0.297
1 100%N 600 µmol	0.14	0.161	0.102	1 100%N 600 µmol	0.419	0.424	0.465
2 50%N 600 µmol	0.147	0.151	0.115	2 50%N 600 µmol	0.304	0.332	0.322
2 100%N 600 µmol	0.166	0.182	0.191	2 100%N 600 µmol	0.389	0.439	0.435
3 50%N 600 µmol	0.085	0.069	0.115	3 50%N 600 µmol	0.782	0.181	0.322
3 100%N 600 µmol	0.102	0.12	0.197	3 100%N 600 µmol	0.307	0.299	0.291
1 50%N 1200 µmol	0.205	0.227	0.221	1 50%N 1200 µmol	0.321	0.296	0.289
1 100%N 1200µmol	0.21	0.142	0.185	1 100%N 1200 µmol	0.361	0.35	0.37
2 50%N 1200 µmol	0.209	0.12	0.197	2 50%N 1200 µmol	0.307	0.118	0.291
2 100%N 1200 µmol	0.147	0.151	0.115	2 100%N 1200 µmol	0.304	0.332	0.322
3 50%N 1200 µmol	0.157	0.237	0.221	3 50%N 1200µmol	0.206	0.296	0.289
3 100%N 1200 µmol	0.166	0.182	0.191	3 100%N 1200µmol	0.389	0.439	0.435
1 50%N 800 µmol	0.153	0.16	0.161	1 50%N 800 µmol	0.325	0.292	0.346
1 100%N 800 µmol	0.166	0.172	0.152	1 100%N 800 µmol	0.282	0.398	0.281
2 50%N 800 µmol	0.232	0.243	0.253	2 50%N 800 µmol	0.393	0.344	0.357
2 100%N 800 µmol	0.266	0.243	0.25	2 100%N 800 µmol	0.379	0.333	0.354
3 50%N 800 µmol	0.232	0.243	0.253	3 50%N 800 µmol	0.393	0.344	0.357
3 100%N 800 µmol	0.266	0.243	0.25	3 100%N 800 µmol	0.379	0.333	0.354

APPENDIX B. DATA FOR LIPID PRODUCTION FOR THE LOUISIANA CO-CULTURE WITH AERATION

The purpose of this part of research was to evaluate the lipid productivity, lipid percentage (mass/mass, on dry biomass), neutral lipid percentage (mass/mass, total lipids) and fatty acid profile of the co-culture under five irradiance (180, 400, 600, 800, 1200 μmol m^{-2} s^{-1}) and two nitrogen levels (2.94 mM and 1.47 mM). The light source used in this experiment was from high pressure sodium lamps. The culture was not continuously aerated. Carbon dioxide was bubbled into the culture daily at the rate of 0.24 L min^{-1} for 15 seconds. Triplicates were done for each treatment.

The biomass productivity was calculated by averaging the daily biomass increment (g m^{-3} d^{-1}) throughout the exponential growth phase. The collection of biomass data and biomass productivity calculations were done by Athens Silaban. Before the lipid extraction, dry biomass was measured (g). Lipid percentage was calculated dividing the mass of total lipid by the mass of dry biomass used for extraction. The lipid productivity was calculated by multiplying biomass productivity by lipid percentage.

Replicate#1	Louisiana co-culture				
Irradiance level (μmol m^{-2} s^{-1})	Nitrogen Level	Biomass (g/m^{-3})	Biomass productivity (g m^{-3} d^{-1})	Lipid percentage (%)	Lipid productivity (g m^{-3} d^{-1})
180	50%	1720	256	35.28%	90.32
	100%	1840	260	34.94%	90.84
400	50%	1920	251	36.96%	92.77
	100%	2860	325	30.43%	98.90
600	50%	1660	278	39.78%	110.6
	100%	1700	247	38.48%	95.05
800	50%	1700	213	36.48%	77.70
	100%	2980	387	34.91%	135.1
1200	50%	1780	220	36.62%	80.56
	100%	2900	364	34.22%	124.6

Replicate#2	Louisiana co-culture				
Irradiance level (μmol m^{-2} s^{-1})	Nitrogen Level	Biomass (g m^{-3})	Biomass productivity (g m^{-3} d^{-1})	Lipid percentage (%)	Lipid productivity (g m^{-3} d^{-1})
180	50%	1160	193	36.42%	70.29
	100%	1660	267	28.31%	75.59
400	50%	1440	215	33.79%	72.65
	100%	2040	304	30.61%	93.05
600	50%	1420	238	38.46%	91.53
	100%	1720	238	36.42%	86.68
800	50%	1400	175	28.24%	49.42
	100%	2480	336	33.92%	114.0
1200	50%	1420	192	32.37%	62.15
	100%	2240	307	29.70%	91.18

Replicate#3	Louisiana co-culture				
Irradiance level (μmol m^{-2} s^{-1})	Nitrate Level	Biomass (g m^{-3})	Biomass productivity(g m^{-3} d^{-1})	Lipid percentage (%)	Lipid productivity (mg d^{-1} L^{-1})
180	50%	1220	144	39.64%	57.08
	100%	1920	222	28.67%	63.65
400	50%	1300	163	31.95%	52.08
	100%	2220	240	40.19%	96.46
600	50%	1930	225	38.09%	85.70
	100%	2450	402	37.47%	150.6
800	50%	1240	146	34.53%	50.41
	100%	2100	245	40.00%	98.00
1200	50%	1200	155	40.80%	63.24
	100%	2180	244	33.37%	81.42

Neutral lipid percentage (mass/mass, based on total lipid)

The protocol of neutral lipid percentage analysis followed Pernet et al. (2006) using solid phase extraction. The total lipid was loaded on the Si-NH_2 column. The neutral lipids were eluted by chloroform:isopropanol 2:1 into a pre-weighed test tube. After the solvent was evaporated, the mass of neutral lipids was calculated by mass of tube plus neutral lipids minus the mass of test tube. The neutral lipid percentage was then calculated by dividing the neutral lipid mass by mass of total lipids.

Replicate #1	Louisiana co-culture					
Irradiance level (μmol m^{-2} s^{-1})	Nitrogen	Tube (g)	Tube Neutral (g)	Neutral (g)	total lipid (g)	Neutral lipid (%)
180	50%	8.0494	8.0769	0.0275	0.0322	85.40%
	100%	7.9709	7.9936	0.0227	0.027	84.07%
400	50%	7.9748	8.0037	0.0289	0.0324	89.20%
	100%	7.9749	8.0053	0.0304	0.0358	84.92%
600	50%	7.9798	7.9978	0.018	0.0204	88.24%
	100%	7.9914	8.0023	0.0109	0.0129	84.50%
800	50%	8.0024	8.0257	0.0233	0.0262	88.93%
	100%	8.0192	8.047	0.0278	0.0312	89.10%
1200	50%	7.992	8.0205	0.0285	0.0329	86.63%
	100%	7.9947	8.0255	0.0308	0.0341	90.32%

Replicate#2	Louisiana co-culture					
Irradiance level (μmol m^{-2} s^{-1})	Nitrogen	Tube (g)	Tube Neutral (g)	Neutral (g)	Total lipid (g)	Neutral lipid (%)
180	50%	8.0152	8.036	0.0208	0.0247	84.21%
	100%	7.9839	8.0039	0.02	0.0237	84.39%
400	50%	7.9858	8.0083	0.0225	0.0257	87.55%
	100%	7.9799	8.0064	0.0265	0.0296	89.53%
600	50%	7.9998	8.0148	0.015	0.0173	86.71%
	100%	7.9897	8.0009	0.0112	0.0133	84.21%
800	50%	7.9525	7.9702	0.0177	0.02	88.50%
	100%	8.0246	8.0613	0.0367	0.0414	88.65%
1200	50%	7.9808	7.9996	0.0188	0.0217	86.64%
	100%	7.9755	8.0048	0.0293	0.0323	90.71%

Replicate #3	Louisiana co-culture					
Irradiance level ($\mu mol\ m^{-2}\ s^{-1}$)	Nitrogen	Tube (g)	Tube Neutral (g)	Neutral (g)	total lipid (g)	Neutral lipid (%)
180	50%	7.9941	8.0134	0.0193	0.021	91.90%
	100%	7.9733	8.0047	0.0314	0.0345	91.01%
400	50%	8.0268	8.0487	0.0219	0.0245	89.39%
	100%	8.0113	8.0421	0.0308	0.0346	89.02%
600	50%	7.9476	7.9676	0.02	0.0221	90.50%
	100%	8.0001	8.0251	0.025	0.028	89.29%
800	50%	7.9471	7.9573	0.0102	0.0118	86.44%
	100%	7.9893	8.0187	0.0294	0.0325	90.46%
1200	50%	7.9927	8.0176	0.0249	0.0283	87.99%
	100%	8.0488	8.0834	0.0346	0.0389	88.95%

Energy return of lipid on light energy (%)

To evaluate the efficiency of the Louisiana co-culture to convert light energy into lipid energy, the energy return (lipid energy) on energy input (light energy) was calculated. The calculation was adapted from the Zijffers et al. (2010), which was used for biomass yield on light energy:

$$Y_{lipid\ ,E} = \frac{P_L}{I_s \times 10^{-6} \times 8.64 \times 10^4} \times \frac{V}{A} \quad (1)$$

where $Y_{lipid,\ E}$ is the lipid per mole photons, P_L (g m^{-3} d^{-1}) is the lipid productivity, I_s is scalar irradiance level (µmol m^{-2} s^{-1}, culture concentration x=0), V/A is the volume to wetted surface area ratio of the culture. For 1.0 L culture in a 2.0 L Erlenmeyer flask used in this work, V/A is 0.023 m^3 m^{-2}.

The lipid caloric content (C_L, kJ g^{-1}) was determined with a Parr 6200 isoperibol calorimeter. The sample of 0.5 g of total lipid in sample cup was installed into the caloric bomb, and a platinum ignition wire was attached to the lipid sample. The caloric bomb was charged with O_2 till the pressure reached 10-35 atm. The platinum wire then was ignited. After the run finished, the caloric content of the lipid was automatically calculated. Duplicates were done. The energy return of lipid on light energy was calculated following the equation:

$$\eta = Y_{\boldsymbol{Lipid,E}} \times \frac{C_L}{E} \quad (2)$$

Where η (%) is the energy return of lipid on the light energy for each irradiance level. E (kJ (mole photon)$^{-1}$) is a parameter to convert the scalar irradiance to energy. For HPS lamps, E is estimated to be 201 kJ (mole photon)$^{-1}$ as reported by Thimijan and Heins (1983). The calculated

η was plotted against each internal scalar irradiance level (where the culture concentration x=0) to investigate the effects of irradiance levels on the energy return (lipid energy) on light energy input. .

Irradiance (μmol m^{-2} s^{-1})	Nitrate	Replicate #	Lipid Productivity	Lipid energy/irradiance energy	Lipid yield per mole photon
180	50%	1	90.32	1.99%	0.134
180		2	70.29	1.55%	0.104
180		3	57.08	1.26%	0.084
180	100%	1	90.84	2.00%	0.134
180		2	75.59	1.66%	0.112
180		3	63.65	1.40%	0.094
400	50%	1	92.77	0.92%	0.062
400		2	72.65	0.72%	0.048
400		3	52.08	0.52%	0.035
400	100%	1	98.90	0.98%	0.066
400		2	93.05	0.92%	0.062
400		3	96.46	0.96%	0.064
600	50%	1	110.6	0.73%	0.049
600		2	91.53	0.60%	0.041
600		3	85.70	0.57%	0.038
600	100%	1	95.05	0.63%	0.042
600		2	86.68	0.57%	0.038
600		3	150.6	0.99%	0.067
800	50%	1	77.70	0.38%	0.026
800		2	49.42	0.24%	0.016
800		3	50.41	0.25%	0.017
800	100%	1	135.1	0.67%	0.045
800		2	114.0	0.56%	0.038
800		3	98.00	0.49%	0.033
1200	50%	1	80.56	0.27%	0.018
1200		2	62.15	0.21%	0.014
1200		3	63.24	0.21%	0.014
1200	100%	1	124.6	0.41%	0.028
1200		2	91.18	0.30%	0.020
1200		3	81.42	0.27%	0.018

Fatty acid profiles (%,mass/mass on total fatty acids)

The fatty acids were determined using gas chromatography (HP 5890 Series II) equipped with an SP^{TM}-2330 column (30 m, 0.25mm ID, 0.20 μm film). The initial oven temperature was kept at 80 ^{o}C for 1 minute and then increased to 220 ^{o}C at the ramp of 4 ^{o}C min^{-1} and maintained at 220 ^{o}C for 5 minutes. Helium was kept at 2.0 mL min^{-1} as the carrier gas. The gas chromatography data were analyzed with Chemstation^{TM} software, and the mass percentage of each fatty acid component was reported.

The first number in the first column is the number of replicate, second number is the nitrogen level and the last number in the first column is the irradiance level. There were three samples for each treatment, and triplicates were done for each sample. Therefore, there were totally nine runs for each culture condition

C14:0				C16:0			
1 50%N 180μmol	0.16	0.164	0.181	1 50%N 180μmol	24.544	24.531	24.539
1 100%N 180μmol	0.244	0.25	0.228	1 100%N 180μmol	23.884	24.027	24.028
1 50%N 400μmol	0.185	0.186	0.187	1 50%N 400μmol	25.793	25.783	25.838
1 100%N 400μmol	0.213	0.176	0.183	1 100%N 400μmol	26.325	24.12	23.157
1 50%N 600μmol	0.251	0.269	0.268	1 50%N 600μmol	26.862	27.116	27.081
1 100%N 600μmol	0.241	0.204	0.22	1 100%N 600μmol	25.718	25.7	25.721
1 50%N 800μmol	0.219	0.217	0.203	1 50%N 800μmol	23.158	25.286	25.456
1 100%N 800μmol	0.242	0.231	0.233	1 100%N 800μmol	26.644	26.874	26.847
1 50%N 1200μmol	0.206	0.182	0.138	1 50%N 1200μmol	25.551	25.539	25.714
1 100%N 1200μmol	0.233	0.236	0.229	1 100%N1200μmol	27.019	27.087	27.032
2 50%N 180μmol	0.207	0.226	0.17	2 50%N 180μmol	23.497	23.483	23.548
2 100%N 180μmol	0.254	0.199	0.274	2 100%N 180μmol	25.656	25.609	25.595
2 50%N 400μmol	0.232	0.242	0.221	2 50%N 400μmol	23.476	23.521	23.486
2 100%N 400μmol	0.211	0.246	0.222	2 100%N 400μmol	25.444	25.44	25.45
2 50%N 600μmol	0.252	0.263	0.245	2 50%N 600μmol	26.162	26.041	24.569
2 100%N 600μmol	0.228	0.157	0.231	2 100%N 600μmol	25.694	25.475	25.246
2 50%N 800μmol	0.208	0.27	0.22	2 50%N 800μmol	25.12	25.116	25.12
2 100%N 800μmol	0.198	0.239	0.207	2 100%N 800μmol	25.353	25.244	25.253
2 50%N 1200μmol	0.289	0.303	0.222	2 50%N 1200μmol	24.662	24.612	24.588
2 100%N 1200μmol	0.331	0.296	0.255	2 100%N1200μmol	25.566	25.511	25.522
3 50%N 180μmol	0.159	0.216	0.174	3 50%N 180μmol	24.997	24.993	24.96

3 100%N 180µmol	0.197	0.204	0.187	3 100%N 180µmol	24.552	24.586	24.585
3 50%N 400µmol	0.204	0.207	0.191	3 50%N 400µmol	25.16	25.162	25.217
3 100%N 400µmol	0.204	0.211	0.234	3 100%N 400µmol	25.368	25.315	25.329
3 50%N 600µmol	0.256	0.234	0.265	3 50%N 600µmol	27.203	27.224	27.41
3 100%N 600µmol	0.24	0.233	0.196	3 100%N 600µmol	25.201	25.141	25.167
3 50%N 800µmol	0.177	0.266	0.157	3 50%N 800µmol	26.94	26.627	26.511
3 100%N 800µmol	0.212	0.217	0.217	3 100%N 800µmol	26.962	26.98	27.024
3 50%N 1200µmol	0.195	0.183	0.184	3 50%N 1200µmol	25.485	25.524	25.487
3 100%N 1200µmol	0.200	0.187	0.19	3 100%N1200µmol	25.205	25.225	25.224

C16:1 n7				C16:1 n9			
1 50%N 180µmol	0.308	0.31	0.309	1 50%N 180µmol	0.451	0.452	0.451
1 100%N 180µmol	0.437	0.445	0.446	1 100%N 180µmol	0.667	0.647	0.66
1 50%N 400µmol	0.324	0.327	0.329	1 50%N 400µmol	0.542	0.546	0.551
1 100%N 400µmol	0.319	0.29	0.278	1 100%N 400µmol	0.566	0.511	0.495
1 50%N 600µmol	0.444	0.443	0.421	1 50%N 600µmol	0.658	0.746	0.698
1 100%N 600µmol	0.436	0.427	0.45	1 100%N 600µmol	0.636	0.594	0.612
1 50%N 800µmol	0.321	0.352	0.362	1 50%N 800µmol	0.498	0.565	0.555
1 100%N 800µmol	0.305	0.33	0.337	1 100%N 800µmol	0.602	0.618	0.622
1 50%N 1200µmol	0.383	0.381	0.387	1 50%N 1200µmol	0.564	0.573	0.573
1 100%N 1200µmol	0.339	0.365	0.36	1 100%N 1200µmol	0.633	0.645	0.638
2 50%N 180µmol	0.376	0.397	0.376	2 50%N 180µmol	0.443	0.501	0.474
2 100%N 180µmol	0.507	0.528	0.537	2 100%N 180µmol	0.521	0.578	0.541
2 50%N 400µmol	0.435	0.423	0.422	2 50%N 400µmol	0.694	0.698	0.695
2 100%N 400µmol	0.368	0.365	0.362	2 100%N 400µmol	0.586	0.586	0.588
2 50%N 600µmol	0.452	0.395	0.421	2 50%N 600µmol	0.659	0.64	0.638
2 100%N 600µmol	0.33	0.328	0.365	2 100%N 600µmol	0.519	0.49	0.519
2 50%N 800µmol	0.483	0.476	0.508	2 50%N 800µmol	0.756	0.755	0.758
2 100%N 800µmol	0.422	0.418	0.418	2 100%N 800µmol	0.669	0.657	0.655
2 50%N 1200µmol	0.518	0.517	0.518	2 50%N 1200µmol	0.803	0.805	0.81
2 100%N 1200µmol	0.442	0.462	0.448	2 100%N 1200µmol	0.643	0.717	0.801
3 50%N 180µmol	0.349	0.293	0.316	3 50%N 180µmol	0.445	0.43	0.43
3 100%N 180µmol	0.379	0.378	0.38	3 100%N 180µmol	0.547	0.547	0.547
3 50%N 400µmol	0.301	0.295	0.299	3 50%N 400µmol	0.518	0.518	0.542
3 100%N 400µmol	0.294	0.309	0.312	3 100%N 400µmol	0.498	0.496	0.504
3 50%N 600µmol	0.428	0.41	0.434	3 50%N 600µmol	0.794	0.263	0.804
3 100%N 600µmol	0.424	0.425	0.369	3 100%N 600µmol	0.641	0.67	0.571
3 50%N 800µmol	0.409	0.321	0.377	3 50%N 800µmol	0.431	0.427	0.542
3 100%N 800µmol	0.345	0.349	0.367	3 100%N 800µmol	0.654	0.667	0.65
3 50%N 1200µmol	0.349	0.36	0.381	3 50%N 1200µmol	0.601	0.614	0.603
3 100%N 1200µmol	0.364	0.361	0.364	3 100%N 1200µmol	0.633	0.629	0.633

C16:2 n10				C18:0			
1 50%N 180µmol	1.353	1.354	1.352	1 50%N 180µmol	6.224	6.225	6.234
1 100%N 180µmol	2.257	2.311	2.304	1 100%N 180µmol	4.197	4.209	4.253
1 50%N 400µmol	0.952	0.951	0.96	1 50%N 400µmol	5.029	5.033	5.037
1 100%N 400µmol	1.438	1.324	1.271	1 100%N 400µmol	5.384	4.955	4.75
1 50%N 600µmol	1.081	1.076	1.061	1 50%N 600µmol	5.733	5.752	5.787
1 100%N 600µmol	0.923	0.856	0.895	1 100%N 600µmol	5.091	5.018	5.099
1 50%N 800µmol	0.847	0.924	0.86	1 50%N 800µmol	6.133	6.682	6.69
1 100%N 800µmol	1.138	1.097	1.131	1 100%N 800µmol	4.778	4.805	4.872
1 50%N 1200µmol	0.812	0.817	0.825	1 50%N 1200µmol	5.002	4.996	4.99
1 100%N 1200µmol	0.949	0.977	0.957	1 100%N 1200µmol	4.827	4.844	4.839
2 50%N 180µmol	1.44	1.448	1.447	2 50%N 180µmol	5.343	5.33	5.339
2 100%N 180µmol	1.443	1.435	1.434	2 100%N 180µmol	5.25	5.242	5.265
2 50%N 400µmol	1.112	1.128	1.124	2 50%N 400µmol	4.662	4.656	4.661
2 100%N 400µmol	1.215	1.215	1.217	2 100%N 400µmol	5.137	5.14	5.138
2 50%N 600µmol	0.906	0.943	0.91	2 50%N 600µmol	5.207	5.227	5.371
2 100%N 600µmol	0.891	0.967	0.93	2 100%N 600µmol	5.341	5.495	5.557
2 50%N 800µmol	1.079	1.056	1.064	2 50%N 800µmol	5.199	5.195	5.198
2 100%N 800µmol	1.052	1.051	1.066	2 100%N 800µmol	4.879	4.877	4.885
2 50%N 1200µmol	1.085	1.083	1.076	2 50%N 1200µmol	4.822	4.831	4.829
2 100%N 1200µmol	1.038	0.977	1.062	2 100%N 1200µmol	4.838	4.876	4.872
3 50%N 180µmol	1.133	1.162	1.133	3 50%N 180µmol	6.478	6.481	6.488
3 100%N 180µmol	1.23	1.231	1.243	3 100%N 180µmol	5.282	5.271	5.278
3 50%N 400µmol	0.938	0.939	0.952	3 50%N 400µmol	6.09	6.077	6.079
3 100%N 400µmol	1.003	0.989	0.996	3 100%N 400µmol	6.624	6.613	6.62
3 50%N 600µmol	1.015	1.114	1.053	3 50%N 600µmol	5.979	5.964	5.918
3 100%N 600µmol	1.134	1.154	1.155	3 100%N 600µmol	6.13	6.18	6.188
3 50%N 800µmol	1.613	1.592	1.582	3 50%N 800µmol	6.106	6.031	6.057
3 100%N 800µmol	0.897	0.915	0.925	3 100%N 800µmol	5.463	5.454	5.457
3 50%N 1200µmol	0.776	0.779	0.779	3 50%N 1200µmol	5.562	5.553	5.561
3 100%N 1200µmol	0.917	0.917	0.917	3 100%N 1200µmol	5.019	5.014	5.017

C18:3n9				C18:1n9C			
1 50%N 180µmol	2.463	2.459	2.469	1 50%N 180µmol	32.519	32.536	32.503
1 100%N 180µmol	4.792	4.845	4.825	1 100%N 180µmol	21.558	20.753	20.701
1 50%N 400µmol	3.157	3.148	3.143	1 50%N 400µmol	29.661	29.646	29.668
1 100%N 400µmol	3.829	3.522	3.377	1 100%N 400µmol	25.291	23.245	22.277
1 50%N 600µmol	2.822	2.824	2.817	1 50%N 600µmol	31.063	30.98	31.004
1 100%N 600µmol	3.158	3.176	3.149	1 100%N 600µmol	31.526	31.591	31.607
1 50%N 800µmol	2.875	3.144	3.133	1 50%N 800µmol	28.666	31.17	31.148
1 100%N 800µmol	4.258	4.301	4.33	1 100%N 800µmol	25.155	25.172	24.589
1 50%N 1200µmol	2.889	2.89	2.909	1 50%N 1200µmol	31.885	31.861	31.862
1 100%N 1200µmol	3.882	3.88	3.884	1 100%N1200µmol	25.682	25.684	25.692
2 50%N 180µmol	3.043	3.038	3.042	2 50%N 180µmol	31.846	31.824	31.848
2 100%N 180µmol	3.832	3.828	3.832	2 100%N 180µmol	23.146	23.111	23.105
2 50%N 400µmol	3.611	3.615	3.613	2 50%N 400µmol	32.081	32.076	32.106
2 100%N 400µmol	3.378	3.375	3.381	2 100%N 400µmol	28.614	28.604	28.613
2 50%N 600µmol	3.307	3.286	3.373	2 50%N 600µmol	30.719	30.929	31.77
2 100%N 600µmol	3.146	3.19	3.157	2 100%N 600µmol	32.115	32.176	32.008
2 50%N 800µmol	3.758	3.747	3.742	2 50%N 800µmol	30.281	30.29	30.285
2 100%N 800µmol	3.854	3.854	3.855	2 100%N 800µmol	28.775	28.803	28.823
2 50%N 1200µmol	3.992	3.988	3.973	2 50%N 1200µmol	29.458	29.451	29.495
2 100%N 1200µmol	3.995	3.976	3.979	2 100%N1200µmol	28.003	27.894	28.019
3 50%N 180µmol	2.701	2.717	2.697	3 50%N 180µmol	29.512	29.461	29.505
3 100%N 180µmol	3.32	3.325	3.326	3 100%N 180µmol	30.503	30.501	30.502
3 50%N 400µmol	2.649	2.645	2.651	3 50%N 400µmol	32.855	32.785	32.813
3 100%N 400µmol	2.522	2.519	2.521	3 100%N 400µmol	31.792	31.699	31.685
3 50%N 600µmol	2.669	2.714	2.718	3 50%N 600µmol	30.378	30.282	30.284
3 100%N 600µmol	2.742	2.756	2.755	3 100%N 600µmol	31.109	31.133	31.211
3 50%N 800µmol	3.257	3.229	3.225	3 50%N 800µmol	25.166	24.906	24.76
3 100%N 800µmol	2.994	2.995	2.998	3 100%N 800µmol	31.379	31.321	31.309
3 50%N 1200µmol	2.569	2.579	2.572	3 50%N 1200µmol	33.793	33.734	33.771
3 100%N 1200µmol	3.188	3.192	3.199	3 100%N1200µmol	31.432	31.396	31.418

C18:1n9t				C18:2			
1 50%N 180µmol	1.435	1.418	1.435	1 50%N 180µmol	19.785	19.787	19.774
1 100%N 180µmol	1.482	1.405	1.459	1 100%N 180µmol	24.225	24.416	24.52
1 50%N 400µmol	1.4	1.411	1.399	1 50%N 400µmol	18.857	18.846	18.846
1 100%N 400µmol	1.368	1.364	1.313	1 100%N 400µmol	20.957	19.226	18.423
1 50%N 600µmol	1.459	1.498	1.465	1 50%N 600µmol	17.381	17.318	17.295
1 100%N 600µmol	1.484	1.359	1.419	1 100%N 600µmol	17.683	17.831	17.777
1 50%N 800µmol	1.358	1.496	1.48	1 50%N 800µmol	15.663	17.045	17.028
1 100%N 800µmol	1.469	1.025	1.489	1 100%N 800µmol	19.637	19.763	19.853
1 50%N 1200µmol	1.553	1.552	1.653	1 50%N 1200µmol	17.493	17.466	17.474
1 100%N 1200µmol	1.576	1.517	1.586	1 100%N 1200µmol	18.945	18.996	18.985
2 50%N 180µmol	1.32	1.308	1.319	2 50%N 180µmol	20.033	20.006	20.03
2 100%N 180µmol	1.426	1.322	1.422	2 100%N 180µmol	22.066	22.131	22.099
2 50%N 400µmol	1.557	1.557	1.566	2 50%N 400µmol	17.313	17.299	17.306
2 100%N 400µmol	1.499	1.499	1.497	2 100%N 400µmol	19.336	19.321	19.333
2 50%N 600µmol	1.649	1.629	1.282	2 50%N 600µmol	17.07	17.262	17.644
2 100%N 600µmol	1.496	1.451	1.435	2 100%N 600µmol	17.926	17.961	17.905
2 50%N 800µmol	1.626	1.629	1.619	2 50%N 800µmol	15.935	15.937	15.935
2 100%N 800µmol	1.61	1.619	1.607	2 100%N 800µmol	17.049	17.07	17.073
2 50%N 1200µmol	1.65	1.668	1.669	2 50%N 1200µmol	16.278	16.256	16.282
2 100%N 1200µmol	1.693	1.556	1.684	2 100%N 1200µmol	16.944	17.004	16.983
3 50%N 180µmol	1.421	1.432	1.346	3 50%N 180µmol	20.471	20.465	20.492
3 100%N 180µmol	1.358	1.361	1.359	3 100%N 180µmol	19.289	19.284	19.282
3 50%N 400µmol	1.342	1.349	1.36	3 50%N 400µmol	17.459	17.419	17.44
3 100%N 400µmol	1.441	1.353	1.456	3 100%N 400µmol	19.105	19.085	19.057
3 50%N 600µmol	1.509	1.585	1.51	3 50%N 600µmol	17.493	17.383	17.304
3 100%N 600µmol	1.383	1.352	1.368	3 100%N 600µmol	18.74	18.734	18.782
3 50%N 800µmol	1.684	1.005	1.142	3 50%N 800µmol	22.705	22.445	22.373
3 100%N 800µmol	1.585	1.576	1.592	3 100%N 800µmol	17.03	17.003	17
3 50%N 1200µmol	1.62	1.624	1.625	3 50%N 1200µmol	15.977	15.956	15.974
3 100%N 1200µmol	1.59	1.596	1.57	3 100%N 1200µmol	17.565	17.557	17.567

C20:0				C18:3n3			
1 50%N 180µmol	2.365	2.369	2.363	1 50%N 180µmol	7.931	7.934	7.925
1 100%N 180µmol	2.833	2.825	2.867	1 100%N 180µmol	12.158	12.266	12.317
1 50%N 400µmol	2.231	2.236	2.233	1 50%N 400µmol	11.253	11.266	11.212
1 100%N 400µmol	2.572	2.352	2.24	1 100%N 400µmol	11.114	18.606	21.997
1 50%N 600µmol	2.637	2.615	2.614	1 50%N 600µmol	8.861	8.748	8.784
1 100%N 600µmol	2.372	2.428	2.411	1 100%N 600µmol	10.021	10.083	10.049
1 50%N 800µmol	1.893	2.069	2.052	1 50%N 800µmol	18.224	10.344	10.331
1 100%N 800µmol	2.174	2.193	2.185	1 100%N 800µmol	13.073	13.158	13.183
1 50%N 1200µmol	2.252	2.246	2.242	1 50%N 1200µmol	10.608	10.604	10.601
1 100%N 1200µmol	2.163	2.195	2.189	1 100%N 1200µmol	13.387	13.009	12.908
2 50%N 180µmol	2.122	2.111	2.114	2 50%N 180µmol	9.759	9.73	9.744
2 100%N 180µmol	2.801	2.813	2.831	2 100%N 180µmol	11.653	11.678	11.663
2 50%N 400µmol	1.923	1.924	1.917	2 50%N 400µmol	12.315	12.297	12.302
2 100%N 400µmol	2.28	2.274	2.278	2 100%N 400µmol	11.338	11.33	11.336
2 50%N 600µmol	2.445	2.521	2.505	2 50%N 600µmol	10.404	10.307	10.562
2 100%N 600µmol	2.216	2.109	2.251	2 100%N 600µmol	10.009	10.073	9.986
2 50%N 800µmol	1.944	1.943	1.949	2 50%N 800µmol	12.964	12.962	12.953
2 100%N 800µmol	2.035	2.052	2.051	2 100%N 800µmol	12.853	12.869	12.863
2 50%N 1200µmol	2.076	2.077	2.068	2 50%N 1200µmol	13.843	13.821	13.848
2 100%N 1200µmol	1.987	1.991	2.015	2 100%N 1200µmol	13.602	13.657	13.637
3 50%N 180µmol	2.338	2.339	2.339	3 50%N 180µmol	9.625	9.614	9.632
3 100%N 180µmol	2.016	2.013	2.015	3 100%N 180µmol	10.764	10.754	10.346
3 50%N 400µmol	2.341	2.329	2.324	3 50%N 400µmol	9.526	9.502	9.506
3 100%N 400µmol	2.613	2.599	2.6	3 100%N 400µmol	8.255	8.245	8.243
3 50%N 600µmol	2.809	2.893	2.883	3 50%N 600µmol	8.755	8.748	8.702
3 100%N 600µmol	3.115	3.105	3.11	3 100%N 600µmol	8.425	8.422	8.443
3 50%N 800µmol	2.648	2.652	2.645	3 50%N 800µmol	9.997	9.894	9.867
3 100%N 800µmol	2.216	2.217	2.214	3 100%N 800µmol	9.666	9.65	9.643
3 50%N 1200µmol	2.304	2.298	2.301	3 50%N 1200µmol	10.039	10.017	10.025
3 100%N 1200µmol	2.062	2.049	2.058	3 100%N 1200µmol	11.235	11.265	11.244

C20:1				C22:0			
1 50%N 180µmol	0.365	0.362	0.362	1 50%N 180µmol	0.298	0.302	0.301
1 100%N 180µmol	0.261	0.29	0.262	1 100%N 180µmol	0.306	0.312	0.33
1 50%N 400µmol	0.386	0.383	0.359	1 50%N 400µmol	0.231	0.238	0.238
1 100%N 400µmol	0.356	0.247	0.237	1 100%N 400µmol	0.269	0.163	0.101
1 50%N 600µmol	0.314	0.313	0.313	1 50%N 600µmol	0.335	0.303	0.332
1 100%N 600µmol	0.331	0.363	0.34	1 100%N 600µmol	0.379	0.361	0.252
1 50%N 800µmol	0.064	0.368	0.374	1 50%N 800µmol	0.081	0.339	0.329
1 100%N 800µmol	0.304	0.298	0.211	1 100%N 800µmol	0.22	0.136	0.119
1 50%N 1200µmol	0.432	0.431	0.429	1 50%N 1200µmol	0.27	0.36	0.203
1 100%N 1200µmol	0.232	0.244	0.351	1 100%N 1200µmol	0.135	0.122	0.25
2 50%N 180µmol	0.351	0.345	0.356	2 50%N 180µmol	0.219	0.254	0.193
2 100%N 180µmol	0.317	0.268	0.277	2 100%N 180µmol	0.33	0.36	0.321
2 50%N 400µmol	0.367	0.373	0.369	2 50%N 400µmol	0.222	0.19	0.211
2 100%N 400µmol	0.362	0.362	0.364	2 100%N 400µmol	0.231	0.243	0.221
2 50%N 600µmol	0.394	0.273	0.432	2 50%N 600µmol	0.373	0.283	0.276
2 100%N 600µmol	0.315	0.316	0.412	2 100%N 600µmol	0.275	0.311	0.286
2 50%N 800µmol	0.384	0.341	0.333	2 50%N 800µmol	0.263	0.283	0.317
2 100%N 800µmol	0.37	0.367	0.366	2 100%N 800µmol	0.882	0.881	0.879
2 50%N 1200µmol	0.315	0.355	0.375	2 50%N 1200µmol	0.208	0.234	0.247
2 100%N 1200µmol	0.362	0.399	0.408	2 100%N 1200µmol	0.356	0.287	0.215
3 50%N 180µmol	0.359	0.361	0.358	3 50%N 180µmol	0.21	0.237	0.231
3 100%N 180µmol	0.349	0.349	0.346	3 100%N 180µmol	0.214	0.195	0.195
3 50%N 400µmol	0.342	0.361	0.328	3 50%N 400µmol	0.277	0.413	0.299
3 100%N 400µmol	0.373	0.371	0.372	3 100%N 400µmol	0.109	0.295	0.272
3 50%N 600µmol	0.382	0.336	0.344	3 50%N 600µmol	0.33	0.35	0.373
3 100%N 600µmol	0.33	0.321	0.302	3 100%N 600µmol	0.386	0.385	0.393
3 50%N 800µmol	0.343	0.346	0.367	3 50%N 800µmol	0.172	0.258	0.396
3 100%N 800µmol	0.33	0.351	0.322	3 100%N 800µmol	0.267	0.305	0.281
3 50%N 1200µmol	0.43	0.405	0.406	3 50%N 1200µmol	0.2	0.273	0.23
3 100%N 1200µmol	0.387	0.408	0.388	3 100%N 1200µmol	0.205	0.204	0.212

APPENDIX C. BIOMASS AND LIPID PRODUCTIVITY MODEL FOR HISTAR SYSTEM

Light attenuation study

Biomass attenuation coefficient

Date:	7/13/12	Type of lighting:	High Pressure Sodium
Time:	10:00	Distance from light to surface:	26.6 cm
Sensor:	Bulb quantum sensor	Depth of water/culture:	52 cm
Tank:	CFSTR 8	Tank Diameter:	114.3 cm
		Culture density:	**56 g m^{-3}**

Depth	Distance from the center			
cm	0.00	21.43	35.72	50.01
0	630.7	357.6	232.5	156.4
3.25	516.6	313.4	219	150.1
9.75	358.8	248.6	183.6	135.2
16.25	251	192.4	139.7	115.2
22.75	181.3	146.8	113.5	95.79
29.25	126.8	111.1	94.3	77.38
35.75	93.2	82.9	71.7	61.51
42.25	72.4	68.6	58.86	50.78
48.75	59.1	53.4	49.25	39.97

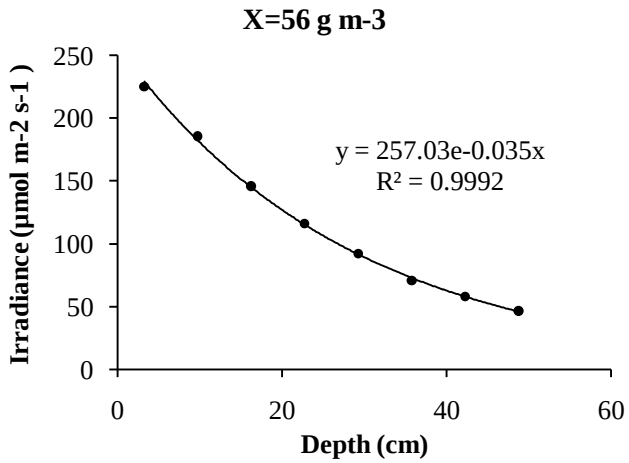

Depth	Distance from center				
cm	0.00	21.43	35.72	50.01	SUM
*weighted**	*0.06*	*0.19*	*0.31*	*0.44*	1.00
0	39.4	67.1	72.7	68.4	247.6
3.25	32.3	58.8	68.4	65.7	225.2
9.75	22.4	46.6	57.4	59.2	185.6
16.25	15.7	36.1	43.7	50.4	145.8
22.75	11.3	27.5	35.5	41.9	116.2
29.25	7.9	20.8	29.5	33.9	92.1
35.75	5.8	15.5	22.4	26.9	70.7
42.25	4.5	12.9	18.4	22.2	58.0
48.75	3.7	10.0	15.4	17.5	46.6
	Avg Irradiance (Ia):			117.5	µmol m^{-2} s^{-1}

Date:	7/13/12	Type of lighting:	High Pressure Sodium
Time:	10:00	Distance from light to surface:	26.6 cm
Sensor:	Bulb quantum sensor	Depth of water/culture:	52 cm
Tank:	CFSTR 8	Tank Diameter:	114.3 cm
		Culture density:	**0 g m^{-3}**

Depth	Distance from center			
	0.00	21.43	35.72	50.01
0	997	696	516	362
3.25	680	469	403	320
9.75	598	440	395	312
16.25	515	431	374	327
22.75	473	408	370	323
29.25	413	383	356	322
35.75	381	362	350	317
42.25	355	344	344	312
48.75	315	321	319	288

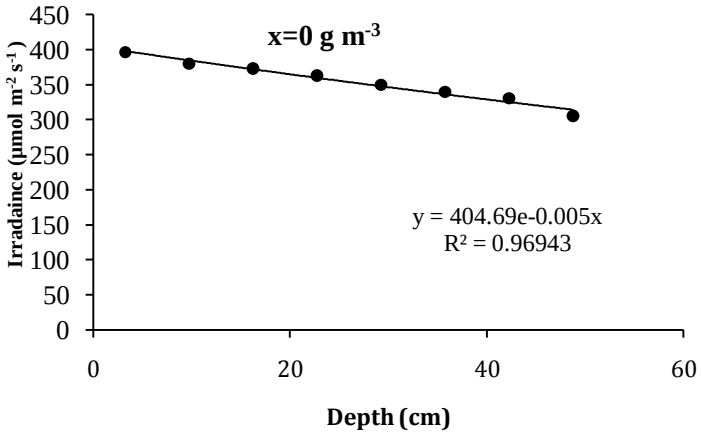

Depth	Distance from center				
cm	0.00	21.43	35.72	50.01	SUM
*weighted**	*0.06*	*0.19*	*0.31*	*0.44*	1.00
0	62.3	130.5	161.3	158.4	512.4
3.25	42.5	87.9	125.9	140.0	396.4
9.75	37.4	82.5	123.4	136.5	379.8
16.25	32.2	80.8	116.9	143.1	372.9
22.75	29.6	76.5	115.6	141.3	363.0
29.25	25.8	71.8	111.3	140.9	349.8
35.75	23.8	67.9	109.4	138.7	339.8
42.25	22.2	64.5	107.5	136.5	330.7
48.75	19.7	60.2	99.7	126.0	305.6
	Avg Irradiance (I_a):			372.3	µmol m^{-2} s^{-1}

Date:	8/2/12	Type of lighting:	HPS		
Time:	10:00AM	Distance from light to surface:	26.6	cm	
Sensor:	Bulb quantum sensor	Depth of water/culture:	52	cm	
Tank:	CFSTR 8	Tank Diameter:	114.3	cm	
		Culture density:	**105**	**g m^{-3}**	

Depth	Distance from the center			
cm	0.00	21.43	35.72	50.01
0	547.4	315.4	120.6	75.1
3.25	367	207.9	115	67.8
9.75	192.5	128.1	68.9	54.89
16.25	99.88	70.6	43.3	30.6
22.75	61.5	37.9	26	21
29.25	29	25.6	14	10.3
35.75	15.7	12.4	9.8	6.5
42.25	9.8	7.2	5.5	4.8
48.75	6	5.4	3.54	2.1

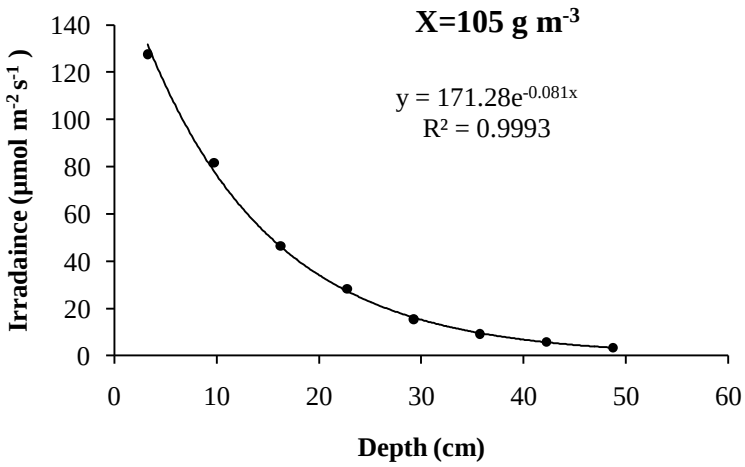

Depth	Distance from center				
cm	0.00	21.43	35.72	50.01	SUM
*weighted**	*0.06*	*0.19*	*0.31*	*0.44*	1.00
0	34.2	59.1	37.7	32.9	163.9
3.25	22.9	39.0	35.9	29.7	127.5
9.75	12.0	24.0	21.5	24.0	81.6
16.25	6.2	13.2	13.5	13.4	46.4
22.75	3.8	7.1	8.1	9.2	28.3
29.25	1.8	4.8	4.4	4.5	15.5
35.75	1.0	2.3	3.1	2.8	9.2
42.25	0.6	1.4	1.7	2.1	5.8
48.75	0.4	1.0	1.1	0.9	3.4
	Avg Irradiance (I_a):			39.7	µmol m^{-2} s^{-1}

Date:	8/3/12	Type of lighting:	HPS
Time:		Distance from light to surface:	26.6 cm
Sensor:	Bulb quantum sensor	Depth of water/culture:	52 cm
Tank:	CFSTR 8	Tank Diameter:	114.3 cm
		Culture density:	**78 g m^{-3}**

Depth	Distance from the center			
cm	0.00	21.43	35.72	50.01
0	475.3	475.1	177.9	108.8
3.25	419.6	239.2	150.2	97.94
9.75	250.4	161.2	100.6	79.44
16.25	138.3	97.31	66.7	51.58
22.75	90.6	62.29	42.1	34.62
29.25	51.29	40.07	27.32	19.87
35.75	31.49	24.51	19.15	13.64
42.25	20.82	14.3	12.27	10.07
48.75	14.25	11.9	8.387	6.707

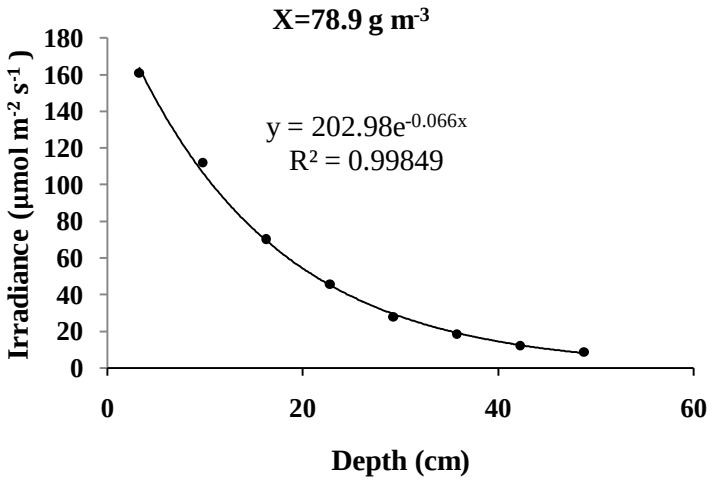

Depth	Distance from center				
cm	0.00	21.43	35.72	50.01	SUM
*weighted**	*0.06*	*0.19*	*0.31*	*0.44*	1.00
0	29.7	89.1	55.6	47.6	222.0
3.25	26.2	44.9	46.9	42.8	160.9
9.75	15.7	30.2	31.4	34.8	112.1
16.25	8.6	18.2	20.8	22.6	70.3
22.75	5.7	11.7	13.2	15.1	45.6
29.25	3.2	7.5	8.5	8.7	27.9
35.75	2.0	4.6	6.0	6.0	18.5
42.25	1.3	2.7	3.8	4.4	12.2
48.75	0.9	2.2	2.6	2.9	8.7
	Avg Irradiance (I_a):			57.0	µmol m^{-2} s^{-1}

Date:	8/3/12	Type of lighting:	HPS
Time:		Distance from light to surface:	26.6 cm
Sensor:	Bulb quantum sensor CFSTR	Depth of water/culture:	52 cm
Tank:	5	Tank Diameter:	114.3 cm
		Culture density:	**53.3 g m^{-3}**

Depth	Distance from the center			
cm	0.00	21.43	35.72	50.01
0	505.4	327.4	233.7	179.4
3.25	413.4	292.1	214.4	155.6
9.75	303.7	218.4	162.7	133.9
16.25	200.9	148.3	122.6	104.1
22.75	144.4	114.3	93.34	81.84
29.25	92.87	79.69	69.11	61.53
35.75	65.4	59.58	55.79	47.41
42.25	51.54	44.7	44.19	33.2
48.75	39.52	39.79	36.18	28.89

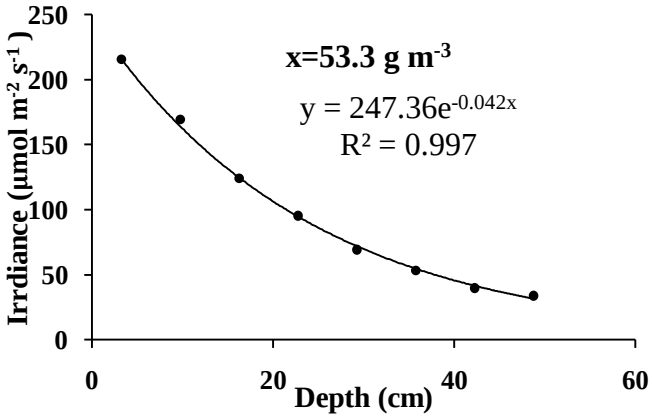

Depth	Distance from center				
cm	0.00	21.43	35.72	50.01	SUM
*weighted**	*0.06*	*0.19*	*0.31*	*0.44*	1.00
0	31.6	61.4	73.0	78.5	244.5
3.25	25.8	54.8	67.0	68.1	215.7
9.75	19.0	41.0	50.8	58.6	169.4
16.25	12.6	27.8	38.3	45.5	124.2
22.75	9.0	21.4	29.2	35.8	95.4
29.25	5.8	14.9	21.6	26.9	69.3
35.75	4.1	11.2	17.4	20.7	53.4
42.25	3.2	8.4	13.8	14.5	39.9
48.75	2.5	7.5	11.3	12.6	33.9
	Avg Irradiance (I_a):			100.1	µmol m^{-2} s^{-1}

Date:	8/3/12		Type of lighting:	HPS	
Time:			Distance from light to surface:	26.6	cm
Sensor:	Bulb quantum sensor		Depth of water/culture:	52	cm
Tank:	CFSTR 1		Tank Diameter:	114.3	cm
			Culture density:	**50**	**g m^{-3}**

Depth	Distance from the center			
cm	0.00	21.43	35.72	50.01
0	547.4	364.4	230.4	175.4
3.25	394.9	249.9	175.5	149.4
9.75	288.8	197.3	152.5	130.6
16.25	218.8	164.8	124.4	114.6
22.75	164.4	136.2	104.4	101.3
29.25	117.6	110.6	86.49	83.84
35.75	81.47	88.2	75.43	71.4
42.25	79.26	74.42	64.55	60.99
48.75	73.24	73.29	66.02	63.55

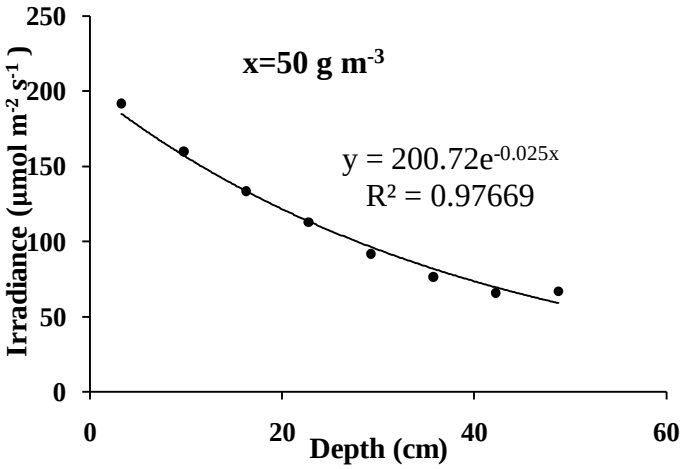

Depth	Distance from center				
cm	0.00	21.43	35.72	50.01	SUM
*weighted**	*0.06*	*0.19*	*0.31*	*0.44*	1.00
0	34.2	68.3	72.0	76.7	251.3
3.25	24.7	46.9	54.8	65.4	191.7
9.75	18.1	37.0	47.7	57.1	159.8
16.25	13.7	30.9	38.9	50.1	133.6
22.75	10.3	25.5	32.6	44.3	112.8
29.25	7.4	20.7	27.0	36.7	91.8
35.75	5.1	16.5	23.6	31.2	76.4
42.25	5.0	14.0	20.2	26.7	65.8
48.75	4.6	13.7	20.6	27.8	66.8
	Avg Irradiance (I_a):			112.3	µmol m^{-2} s^{-1}

X (g m^{-3})	K_0 (m^{-1})
0	0.5
50	2.5
53.3	4.2
56	3.5
78.9	6.6
105	8.1

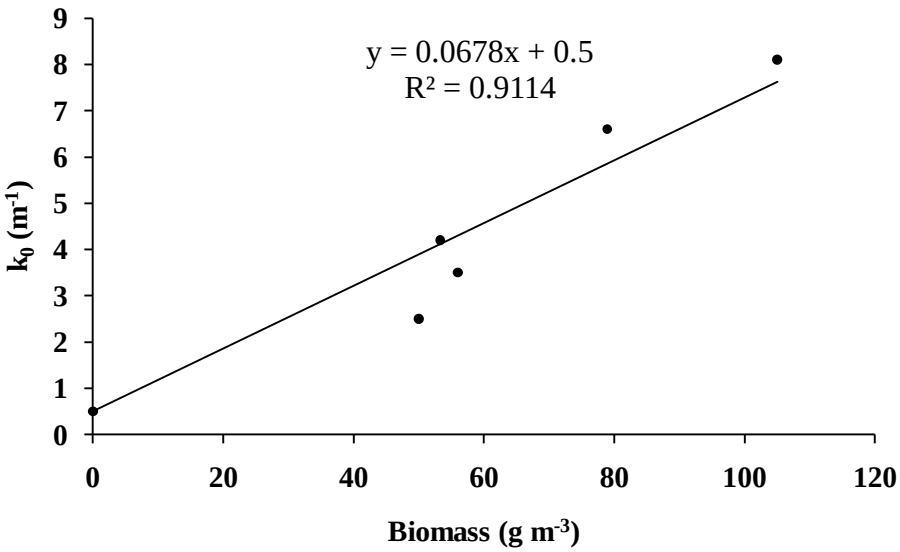

- Air attenuation coefficient

Elevation	Distance from the center				
cm	0	8.7	15.2	21	Sum
Weight	0.0484	0.182	0.3	0.47	
45	357	275	166	120	173.53
41	450	380	225	170	238.34
37	600	380	240	120	226.6
33	640	380	280	121	241.01
29	780	440	290	124	263.11
25	800	550	356	127	305.31

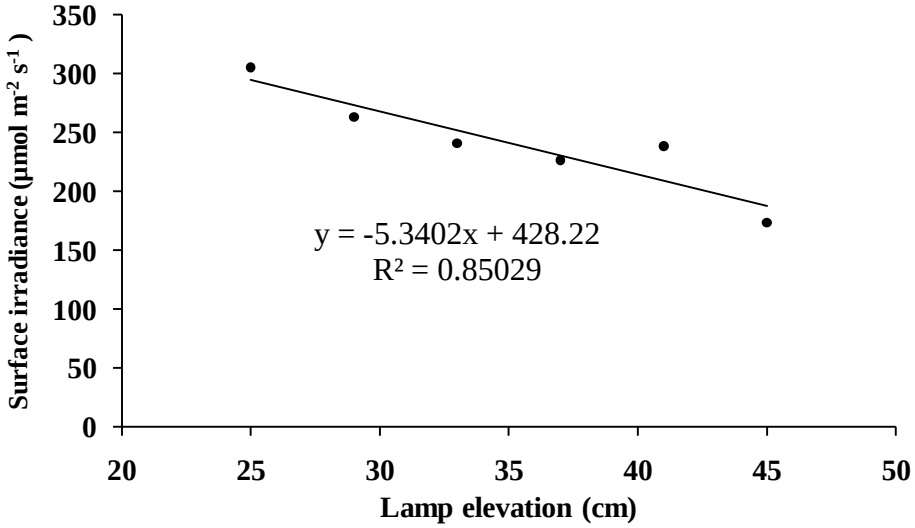

- Actual experimental data from HISTAR run

Q_f=1.0 L min^{-1}	Day	CFSTR1	CFSTR2	CFSTR3	CFSTR4	CFSTR5	CFSTR6	CFSTR7	CFSTR8
Biomass g m^{-3}	0	42.1	54.3	76.5	86.5	113.1	92.1	155.3	129.8
Nitrogen g m^{-3}		10.3	9.9	9.5	9.2	8.7	8.2	7.7	7.2
Biomass g m^{-3}	1	25.5	33.3	76.5	85.4	82.1	78.7	92.1	138.6
Nitrogen g m^{-3}		10.1			8.8				7.5
Biomass g m^{-3}	2	27.7	23.3	42.1	78.7	84.3	69.9	92.1	105.4
Nitrogen g m^{-3}		12.2	11.2	11.1	10.7	10.2	9.4	9.2	8.9
		6.4	5.4	9.7	18.1	19.4	16.1	21.2	24.2
Biomass g m^{-3}	3	28.8	25.5	44.4	64.3	64.3	58.8	82.1	100.9
Nitrogen g m^{-3}		11.0			10.4				
Biomass g m^{-3}	4	35.5	21.1	33.3	63.2	38.8	58.8	66.5	96.5
Biomass g m^{-3}	5	25.5	13.3	12.2	49.9	43.3	62.1	75.4	81.0
Biomass g m^{-3}	6	39.9	32.2	36.6	74.3	57.7	64.3	85.4	123.1

Q_f=0.75 L min^{-1}	Day	CFSTR1	CFSTR2	CFSTR3	CFSTR4	CFSTR5	CFSTR6	CFSTR7	CFSTR8
Biomass g m^{-3}	0	30.4	38.5	38.5	41.9	42.3	47.5	52.2	41.9
Nitrogen g m^{-3}	0	7.7			7.0				6.9
Biomass g m^{-3}	1	26.9	38.9	51.3	62.9	56.0	49.6	46.6	68.0
Nitrogen g m^{-3}	1	7.1			6.5				5.7
Biomass g m^{-3}	2	18.4	24.4	34.2	48.8	53.9	57.7	59.9	63.3
Lipid g m^{-3}	2	4.2	5.6	7.9	11.2	12.4	13.3	13.8	14.6
Nitrogen g m^{-3}	2	7.9	7.3	7.5	7.2	7.1	7.0	6.9	6.6
Biomass g m^{-3}	3	23.1	29.1	38.1	41.9	47.0	52.6	56.9	56.5
Biomass g m^{-3}	4	21.0	21.4	32.1	42.3	49.2	56.0	61.2	60.3
Biomass g m^{-3}	5	37.6	38.9	49.6	49.6	66.3	59.0	61.6	85.5
Biomass g m^{-3}	6	19.2	9.8	22.2	34.6	47.0	17.1	49.6	58.6
Biomass g m^{-3}	7	12.8	9.8	10.7	14.1	21.8	39.4	54.7	66.3
Biomass g m^{-3}	8	3.4	2.6	3.4	9.8	9.4	18.8	16.3	26.5

- Simulations for lipid percentage (mass/mass on dry biomass) in $CFSTR_8$ with 5 different nitrogen concentrations in the make-up water for the HISTAR

* Sf ($g\ m^{-3}$) is the nitrogen level in the make-up water

Day	Sf=12.32	Sf=4	Sf=1	Sf=41.2	Sf=20.58
0	23.00%	23.00%	23.00%	23.00%	23.00%
0.1	23.37%	23.37%	23.37%	23.37%	23.37%
0.2	23.73%	23.73%	23.73%	23.73%	23.73%
0.3	24.07%	24.07%	24.07%	24.07%	24.07%
0.4	24.41%	24.41%	24.41%	24.41%	24.41%
0.5	24.73%	24.73%	24.73%	24.73%	24.73%
0.6	25.04%	25.04%	25.04%	25.04%	25.04%
0.7	25.35%	25.35%	25.35%	25.34%	25.35%
0.8	25.63%	25.64%	25.64%	25.63%	25.63%
0.9	25.91%	25.91%	25.91%	25.90%	25.91%
1	26.17%	26.17%	26.17%	26.16%	26.16%
1.1	26.41%	26.42%	26.42%	26.39%	26.40%
1.2	26.63%	26.65%	26.65%	26.60%	26.62%
1.3	26.84%	26.86%	26.87%	26.79%	26.82%
1.4	27.03%	27.06%	27.08%	26.97%	27.01%
1.5	27.20%	27.25%	27.27%	27.12%	27.17%
1.6	27.36%	27.42%	27.46%	27.25%	27.32%
1.7	27.50%	27.59%	27.64%	27.38%	27.45%
1.8	27.64%	27.75%	27.82%	27.49%	27.57%
1.9	27.76%	27.91%	28.00%	27.59%	27.69%
2	27.88%	28.06%	28.19%	27.69%	27.79%
2.1	27.99%	28.21%	28.37%	27.79%	27.90%
2.2	28.10%	28.36%	28.56%	27.88%	27.99%
2.3	28.21%	28.51%	28.76%	27.97%	28.09%
2.4	28.31%	28.65%	28.95%	28.06%	28.18%
2.5	28.40%	28.79%	29.15%	28.14%	28.26%
2.6	28.49%	28.93%	29.35%	28.23%	28.35%
2.7	28.58%	29.06%	29.55%	28.31%	28.43%
2.8	28.67%	29.19%	29.75%	28.39%	28.51%
2.9	28.75%	29.32%	29.94%	28.46%	28.59%
3	28.83%	29.43%	30.12%	28.53%	28.66%
3.1	28.90%	29.54%	30.29%	28.60%	28.73%
3.2	28.97%	29.64%	30.45%	28.67%	28.79%
3.3	29.03%	29.74%	30.59%	28.73%	28.85%
3.4	29.09%	29.82%	30.72%	28.78%	28.91%
3.5	29.14%	29.90%	30.83%	28.83%	28.96%
3.6	29.19%	29.97%	30.94%	28.88%	29.01%

3.7	29.24%	30.04%	31.03%	28.93%	29.05%
3.8	29.28%	30.09%	31.11%	28.97%	29.09%
3.9	29.32%	30.15%	31.18%	29.01%	29.13%
4	29.36%	30.20%	31.25%	29.04%	29.17%
4.1	29.39%	30.25%	31.31%	29.08%	29.20%
4.2	29.43%	30.29%	31.36%	29.11%	29.23%
4.3	29.46%	30.33%	31.42%	29.13%	29.26%
4.4	29.48%	30.36%	31.46%	29.16%	29.29%
4.5	29.51%	30.40%	31.50%	29.18%	29.31%
4.6	29.53%	30.42%	31.54%	29.20%	29.33%
4.7	29.54%	30.44%	31.57%	29.21%	29.35%
4.8	29.56%	30.46%	31.59%	29.22%	29.36%
4.9	29.56%	30.47%	31.60%	29.23%	29.36%
5	29.57%	30.48%	31.61%	29.23%	29.37%
5.1	29.57%	30.48%	31.61%	29.23%	29.37%
5.2	29.56%	30.47%	31.61%	29.23%	29.36%
5.3	29.56%	30.47%	31.60%	29.22%	29.36%
5.4	29.55%	30.45%	31.58%	29.22%	29.35%
5.5	29.54%	30.44%	31.57%	29.21%	29.34%
5.6	29.52%	30.42%	31.54%	29.19%	29.33%
5.7	29.51%	30.41%	31.52%	29.18%	29.31%
5.8	29.50%	30.39%	31.50%	29.17%	29.30%
5.9	29.48%	30.37%	31.47%	29.16%	29.29%
6	29.47%	30.35%	31.45%	29.14%	29.27%
6.1	29.45%	30.33%	31.42%	29.13%	29.26%
6.2	29.44%	30.32%	31.40%	29.12%	29.25%
6.3	29.43%	30.30%	31.38%	29.11%	29.24%
6.4	29.42%	30.29%	31.36%	29.10%	29.23%
6.5	29.41%	30.27%	31.34%	29.10%	29.22%
6.6	29.40%	30.26%	31.33%	29.09%	29.22%
6.7	29.40%	30.25%	31.31%	29.08%	29.21%
6.8	29.39%	30.25%	31.30%	29.08%	29.21%
6.9	29.39%	30.24%	31.30%	29.08%	29.20%
7	29.39%	30.24%	31.29%	29.08%	29.20%
7.1	29.39%	30.24%	31.29%	29.08%	29.20%
7.2	29.39%	30.24%	31.29%	29.08%	29.21%
7.3	29.39%	30.24%	31.29%	29.08%	29.21%
7.4	29.40%	30.25%	31.29%	29.08%	29.21%
7.5	29.40%	30.25%	31.30%	29.09%	29.21%
7.6	29.40%	30.26%	31.30%	29.09%	29.22%
7.7	29.41%	30.26%	31.31%	29.10%	29.22%
7.8	29.41%	30.27%	31.31%	29.10%	29.23%
7.9	29.42%	30.27%	31.32%	29.10%	29.23%

8	29.42%	30.28%	31.33%	29.11%	29.23%
8.1	29.43%	30.28%	31.33%	29.11%	29.24%
8.2	29.43%	30.29%	31.34%	29.12%	29.24%
8.3	29.43%	30.29%	31.34%	29.12%	29.25%
8.4	29.44%	30.30%	31.35%	29.12%	29.25%
8.5	29.44%	30.30%	31.35%	29.13%	29.25%
8.6	29.44%	30.30%	31.36%	29.13%	29.26%
8.7	29.45%	30.31%	31.36%	29.13%	29.26%
8.8	29.45%	30.31%	31.36%	29.13%	29.26%
8.9	29.45%	30.31%	31.37%	29.13%	29.26%
9	29.45%	30.31%	31.37%	29.14%	29.26%
9.1	29.45%	30.32%	31.37%	29.14%	29.26%
9.2	29.46%	30.32%	31.37%	29.14%	29.27%
9.3	29.46%	30.32%	31.37%	29.14%	29.27%
9.4	29.46%	30.32%	31.38%	29.14%	29.27%
9.5	29.46%	30.32%	31.38%	29.14%	29.27%
9.6	29.46%	30.32%	31.38%	29.14%	29.27%
9.7	29.46%	30.32%	31.38%	29.14%	29.27%
9.8	29.46%	30.32%	31.38%	29.14%	29.27%
9.9	29.46%	30.32%	31.38%	29.14%	29.27%
10	29.46%	30.32%	31.38%	29.14%	29.27%
10.1	29.46%	30.33%	31.38%	29.14%	29.27%
10.2	29.46%	30.33%	31.38%	29.15%	29.27%
10.3	29.46%	30.33%	31.38%	29.15%	29.27%
10.4	29.46%	30.33%	31.38%	29.15%	29.27%
10.5	29.46%	30.33%	31.38%	29.15%	29.27%
10.6	29.46%	30.33%	31.38%	29.15%	29.27%
10.7	29.46%	30.33%	31.38%	29.15%	29.27%
10.8	29.46%	30.33%	31.38%	29.15%	29.27%
10.9	29.46%	30.33%	31.38%	29.15%	29.27%
11	29.46%	30.33%	31.38%	29.15%	29.27%
11.1	29.46%	30.33%	31.38%	29.15%	29.27%
11.2	29.46%	30.33%	31.38%	29.15%	29.27%
11.3	29.46%	30.33%	31.38%	29.15%	29.27%
11.4	29.46%	30.33%	31.38%	29.15%	29.27%
11.5	29.46%	30.33%	31.38%	29.15%	29.27%
11.6	29.46%	30.33%	31.38%	29.15%	29.27%
11.7	29.46%	30.33%	31.39%	29.15%	29.27%
11.8	29.46%	30.33%	31.39%	29.15%	29.27%
11.9	29.46%	30.33%	31.39%	29.15%	29.27%
12	29.46%	30.33%	31.39%	29.15%	29.27%
12.1	29.46%	30.33%	31.39%	29.15%	29.27%
12.2	29.46%	30.33%	31.39%	29.15%	29.27%

12.3	29.46%	30.33%	31.39%	29.15%	29.28%
12.4	29.46%	30.33%	31.39%	29.15%	29.28%
12.5	29.46%	30.33%	31.39%	29.15%	29.28%
12.6	29.46%	30.33%	31.39%	29.15%	29.28%
12.7	29.47%	30.33%	31.39%	29.15%	29.28%
12.8	29.47%	30.33%	31.39%	29.15%	29.28%
12.9	29.47%	30.33%	31.39%	29.15%	29.28%
13	29.47%	30.33%	31.39%	29.15%	29.28%
13.1	29.47%	30.33%	31.39%	29.15%	29.28%
13.2	29.46%	30.33%	31.39%	29.15%	29.28%
13.3	29.46%	30.33%	31.39%	29.15%	29.28%
13.4	29.46%	30.33%	31.39%	29.15%	29.28%
13.5	29.46%	30.33%	31.39%	29.15%	29.27%
13.6	29.46%	30.33%	31.39%	29.15%	29.27%
13.7	29.46%	30.33%	31.39%	29.15%	29.27%
13.8	29.46%	30.33%	31.39%	29.15%	29.27%
13.9	29.46%	30.33%	31.39%	29.15%	29.27%
14	29.46%	30.33%	31.39%	29.15%	29.27%
14.1	29.46%	30.33%	31.39%	29.15%	29.27%
14.2	29.46%	30.33%	31.38%	29.15%	29.27%
14.3	29.46%	30.33%	31.38%	29.15%	29.27%
14.4	29.46%	30.33%	31.38%	29.15%	29.27%
14.5	29.46%	30.33%	31.38%	29.15%	29.27%
14.6	29.46%	30.33%	31.38%	29.15%	29.27%
14.7	29.46%	30.33%	31.38%	29.15%	29.27%
14.8	29.46%	30.33%	31.38%	29.15%	29.27%
14.9	29.46%	30.33%	31.38%	29.15%	29.27%
15	29.46%	30.33%	31.38%	29.15%	29.27%
15.1	29.46%	30.33%	31.38%	29.15%	29.27%
15.2	29.46%	30.33%	31.38%	29.15%	29.27%
15.3	29.46%	30.33%	31.38%	29.15%	29.27%
15.4	29.46%	30.33%	31.38%	29.15%	29.27%
15.5	29.46%	30.33%	31.38%	29.15%	29.27%
15.6	29.46%	30.33%	31.38%	29.15%	29.27%
15.7	29.46%	30.33%	31.38%	29.15%	29.27%
15.8	29.46%	30.33%	31.38%	29.15%	29.27%
15.9	29.46%	30.33%	31.38%	29.15%	29.27%
16	29.46%	30.33%	31.38%	29.15%	29.27%
16.1	29.46%	30.33%	31.38%	29.15%	29.27%
16.2	29.46%	30.33%	31.38%	29.15%	29.27%
16.3	29.46%	30.33%	31.38%	29.15%	29.27%
16.4	29.46%	30.33%	31.38%	29.15%	29.27%
16.5	29.46%	30.33%	31.38%	29.15%	29.27%

16.6	29.46%	30.33%	31.38%	29.15%	29.27%
16.7	29.46%	30.33%	31.38%	29.15%	29.27%
16.8	29.46%	30.33%	31.38%	29.15%	29.27%
16.9	29.46%	30.33%	31.38%	29.15%	29.27%
17	29.46%	30.33%	31.38%	29.15%	29.27%
17.1	29.46%	30.33%	31.38%	29.15%	29.27%
17.2	29.46%	30.33%	31.38%	29.15%	29.27%
17.3	29.46%	30.33%	31.38%	29.15%	29.27%
17.4	29.46%	30.33%	31.38%	29.15%	29.27%
17.5	29.46%	30.33%	31.38%	29.15%	29.27%
17.6	29.46%	30.33%	31.38%	29.15%	29.27%
17.7	29.46%	30.33%	31.38%	29.15%	29.27%
17.8	29.46%	30.33%	31.38%	29.15%	29.27%
17.9	29.46%	30.33%	31.38%	29.15%	29.27%
18	29.46%	30.33%	31.38%	29.15%	29.27%
18.1	29.46%	30.33%	31.38%	29.15%	29.27%
18.2	29.46%	30.33%	31.38%	29.15%	29.27%
18.3	29.46%	30.33%	31.38%	29.15%	29.27%
18.4	29.46%	30.33%	31.38%	29.15%	29.27%
18.5	29.46%	30.33%	31.38%	29.15%	29.27%
18.6	29.46%	30.33%	31.38%	29.15%	29.27%
18.7	29.46%	30.33%	31.38%	29.15%	29.27%
18.8	29.46%	30.33%	31.38%	29.15%	29.27%
18.9	29.46%	30.33%	31.38%	29.15%	29.27%
19	29.46%	30.33%	31.38%	29.15%	29.27%
19.1	29.46%	30.33%	31.38%	29.15%	29.27%
19.2	29.46%	30.33%	31.38%	29.15%	29.27%
19.3	29.46%	30.33%	31.38%	29.15%	29.27%
19.4	29.46%	30.33%	31.38%	29.15%	29.27%
19.5	29.46%	30.33%	31.38%	29.15%	29.27%
19.6	29.46%	30.33%	31.38%	29.15%	29.27%
19.7	29.46%	30.33%	31.38%	29.15%	29.27%
19.8	29.46%	30.33%	31.38%	29.15%	29.27%
19.9	29.46%	30.33%	31.38%	29.15%	29.27%
20	29.46%	30.33%	31.38%	29.15%	29.27%

VITA

Rong Bai was born and raised in Taiyuan, Shanxi Province, China. He attended high school in Taiyuan No. 5 middle school and received his diploma in 2003. He went to Dalian University of Technology and graduated with a degree in Bachelor of Science in Chemical Engineering in June 2007. In August following his graduation, he joined in the Department of Chemical Engineering, Louisiana State University-Baton Rouge to pursue a degree in Doctor of Philosophy in chemical engineering.